FINAL REPORT

NASA CR-
147504

RESPIRABLE PARTICULATE MONITORING WITH REMOTE SENSORS PUBLIC HEALTH ECOLOGY: AIR POLLUTION

(NASA-CR-147504) RESPIRABLE PARTICULATE MONITORING WITH REMOTE SENSORS. (PUBLIC HEALTH ECOLOGY: AIR POLLUTION) Final Report, 1 Jul. 1971 - 31 Oct. 1973 (Texas Univ. Health Science Center, Houston.)

N76-19597
HC $9.25
G3/45
Unclas
22657

Contract Number NAS 9-12041
Johnson Spacecraft Center
National Aeronautics
and Space Administration

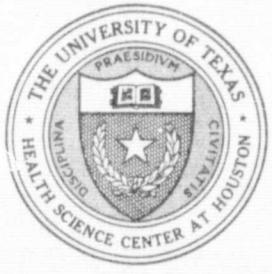

The University of Texas Health Science Center at Houston
School of Public Health

"RESPIRABLE PARTICULATE MONITORING WITH REMOTE SENSORS"

PUBLIC HEALTH ECOLOGY: AIR POLLUTION

by

Richard K. Severs, Ph.D.

Institute of Environmental Health

The University of Texas

Health Sciences Center at Houston

NAS 9-12041

Final Report: 1 July 71 - 31 October 73

National Aeronautics and Space Administration

Johnson Space Center

January, 1974

HOUSTON, TEXAS - Test Site 175

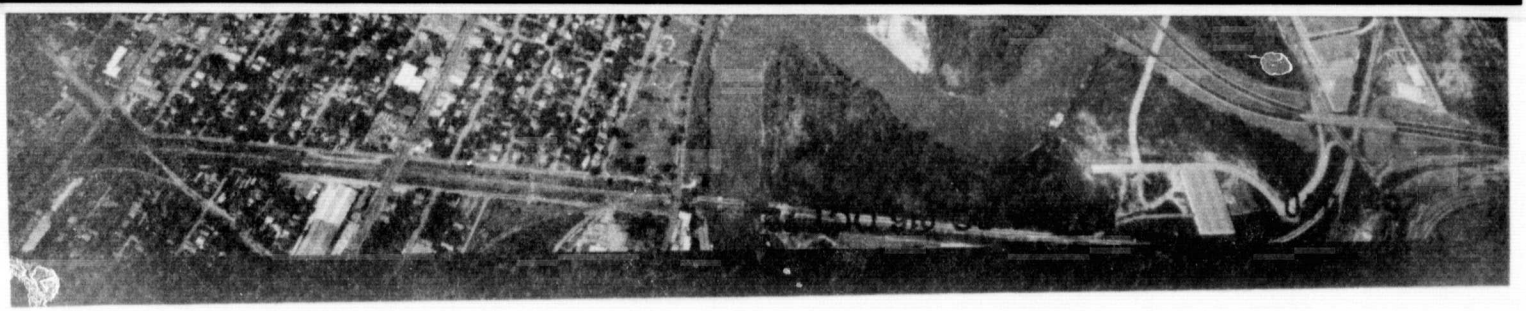

Abstract

The feasibility of monitoring atmospheric aerosol characteristics in the respirable range from air or space platforms was explored and demonstrated. The research plan included elements from contrast theory, Mie aerosol characteristics, and a vertical path length, limited by the altitude of the remote sensor platform, an aircraft, or the height of the inversion layer.

Secondary reflectance targets were located in the industrial area and near Galveston Bay. These approximated areas of high and low ambient air aerosol loadings. Film/filter channels were used to limit bandwidths. Multi-channel remote sensor data was processed and utilized to calculate the aerosol extinction coefficient, and thus determine the aerosol size distribution.

Houston and Texas air sampling network high-volume suspended particulate data were utilized to generate computer isopleth maps (SYMAPS) of suspended particulates over the test site areas. On-site 5-hour high-volume measurements were also conducted to establish the mass loading of the atmosphere. In addition a 5-channel nephelometer, and a multi-stage particulate air sampler were used to collect data at the site. After demonstrating the data best fit the Junge distribution, linear regression analyses were used to calculate the extinction coefficient.

The empirical models in the literature were utilized to predict ambient air mass loadings. The extinction coefficient determined from remote sensor data proved more representative of wide areal phenomena than that calculated from on-site measurements. It was also demonstrated

that a significant reduction in the standard deviation of the extinction coefficient could be achieved by reduction in the size of the bandwidths used in remote sensors. This technology and software may be transferable to use with satellite information.

Acknowledgements

This research could not have been accomplished without the cooperation and support of the following organizations:

Department of Public Health, State of Texas

Texas Air Control Board, State and Regional Offices

Department of Public Health, Houston, Texas

Pollution Control Division

Exxon Corporation, Baytown, Texas

General American Tank Storage Company, Pasadena,Texas

In particular I wish to express gratitude to the following individuals: Dr. Al Randall, Mr. V. Howard, and Mrs. M. Elliott of the Houston Pollution Control Division; Mr. C. Barden, Mr. R. Wallis, and Mr. J. Menke of the Texas Air Control Board. Further, I wish to acknowledge the help of my assistants, Dr. C.T. Chen during the first phase of the work and Mr. Jack Peng throughout the project.

Table of Contents

	PAGE
Abstract	iii
Acknowledgement	v
List of Tables	viii
List of Figures	x
Section	
I. Introduction	1
II. Public Health Considerations	2
III. Literature Review	3
IV. Remote Sensor Data: Considerations	21
V. Experimental Design	30
VI. Experimental Results - 1	31
VII. Mission HATS-175	50
VIII. Mission 216-175	79
XI. Miscellaneous Ground Truth Data	94
X. Conclusions and Recommendations	103
Appendix	105
A. Typical Flight Log	106
B. Mission LSF#2 - 28 September, 71 Microdensitometry Traces	110
C. Mission HATS-175	136
Microdensitometry Traces	139
Linear Regression Analysis	180
D. Mission 216 - 175	217
Microdensitometry Traces	218
Linear Regression Analyses	230

Table of Contents (Con't)

	PAGE
E. ERTS Ground Truth, 27 November 72	243
F. Mission 227 - 175, 27 April 73	253
Linear Regression Analyses	254
References	275

LIST OF TABLES

TABLE		PAGE
1	Microdensitometry Analyses	27
2	Suspended Particulate Data, $\mu g/M^3$ of Air Sept., 27, 1971	33
3	Data on Particle Size Range Distribution	35
4	Calculations of Extinction Coefficients, q_1, q_2	46
5	Comparisons of Mass Measurements, $\mu g/m^3$	49
6	Film and Filter Data	49
7	High-Volume Air Sampling Data - Sept. 8, 1972	52
8	Ground-Truth Data From Target Sites, Sept. 8, 1973	54
9	Air Temperature (°C) at Selected Altitudes	55
10	Particulate Size Distributions on Sept. 8, 1972	56
11	Details of Electron Microphotographs	60
12	Data Sets for Photographic Comparisons, Sept. 8, 1972	67
13	Densitometry Data From Heliocopter Flight (Ship Channel, Sept. 8, 1972)	69-74
14	Extinction Coefficients vs Altitude, HATS-175	75
15	Extinction Coefficients from Nephelometer Data, HATS-175	76
16	Suspended Particulates, $\mu g/m^3$, Oct. 3, 1972	80
17	Particulate Size Distributions on Oct. 3, 1972	81
18	Suspended Particulates, $\mu g/m^3$, at Targets, Oct. 3, 1972	82
19	Microdensitometry Data, Mission #216-175, Oct. 3, 1972	83
20	Extinction Coefficients from Film/Filter Combinations #216-175, Oct. 3, 1972	85

LIST OF TABLES (CON'T)

TABLE		PAGE
21	Extinction Coefficients q, Mission 216-175, Oct. 3, 1972 Remote Sensor Data	86
22	Extinction Coefficients, q, Mission 216-175, Oct. 3, 1972 Ground-truth Data	87
23	Mass Prediction from Extinction Coefficients	91
24	Suspended Particulates, $\mu g/m^3$, Nov. 27, 1972	94
25	Particle Size Distributions on Nov. 27, 1972	95
26	Extinction Coefficients from Ground-Truth, Nov. 27, 1972	97
27	Ground-Truth Data, April 27, 1973	98
28	Extinction Coefficients, q, from Ground-Truth Data, April 27, 1973	99

LIST OF FIGURES

FIGURE		PAGE
1	Volume/b_s^a Ratio vs Exponent β of Power Law	19
2	Visual Range vs Mass Conc.[14]	20
3	Wratten Filter 47B	23
4	Wratten Filter 57	24
5	Wratten Filter 25	25
6	Wratten Filter 89B	26
7	Infrared Color Print, Baytown Reflectance Target	28
8	Infrared Color Print, Ship Channel Reflectance Target	29
9	Particle Size Range Distribution	37
10	Suspended Particulate Concentration, $\mu g/M^3$ of Air September 27, 1971	38
11	Isodensity Recording, Ship Channel, WR25	40
12	Isodensity Recording, Ship Channel, WR89B	41
13	Isodensity Recording, Baytown, WR25	42
14	Isodensity Recording, Baytown, WR29B	43
15	Particle Scattering Coef. vs Mass Conc.[14]	44
16	Particle Scattering Coefficient vs Mass Concentration - Urban Environment[21]	45
17	Pasadena Site	57
18	Baytown Site	58
19	Suspended Particulates, $\mu g/M^3$ 12-24 O'Clock Samples, September 8, 1972	59
20	Electron Microphotograph #20	61
21	Electron Microphotograph #21	62

LIST OF FIGURES (Con't)

FIGURE		PAGE
22	Electron Microphotograph #22	63
23	Electron Microphotograph #23	64
24	Electron Microphotograph #24	65
25	Particle Size Distribution, Pasadena Site September 8, 1972	68
26	Ship Channel Site Area (a)	84
27	Ship Channel Site Area (b)	85
28	Suspended Particulates, ug/m^3, 12-24 O'clock samples, October 3, 1972	91

I. INTRODUCTION

SCOPE

This represents the first report of activities and progress on the research project entitled "Public Health Ecology: Air Pollution" (NAS 9-12041) supported by funds from the National Aero Space Administration, Manned Spacecraft Center (NASA-MSC). The period covered by this report is July 1, 1971 to October 30, 1973. The purpose of this research is to determine the feasibility of monitoring respirable particulates from air or space platforms.

Respirable particulates are generally considered to be those in the size range of 0.4 to about 2.0 microns in diameter with specific concern over those in the 0.4 to 0.7 μ diameter which may reach the alveolar region of the respiratory system.

During the first year of this contract, the initial experiments were designed, personnel were trained to make the ground truth measurements, the type of data desired from remote sensors was determined, a mission was requested and flown by NASA-MSC support groups, the data were processed and recommendations were made concerning future activities. During the second contract year missions were flown, data processed, and planned research was conducted.

This report includes a literature review, a description of the experiment, collected data, processed data results, and conclusions and recommendations.

FACILITIES

No special facilities were needed since the particle size determinations were made from samples collected at the target sites. Film

processing, microdensitometry tracings and isodensity plots were conducted at NASA-MSC, Houston, laboratories. Computer trend-surface maps were made at the Common Research Computer Facility located in the Medical Center, Houston, Texas

PERSONNEL

The following individuals were associated with the project during the period covered in this report.

Principal Investigator	Dr. R.K. Severs, Assistant Professor of Environmental Health
Research Assistant	Dr. Chia T. Chen, Mr. Jack Peng
Photo Interpreter	Mr. C. Olsen

AGENCIES

The Pollution Control Division of the City of Houston, Dept. of Public Health and the Air Pollution Control Services Division of the State of Texas, Dept. of Public Health cooperated generously with collection of high-volume air samples of suspended particulates.

II. PUBLIC HEALTH CONSIDERATIONS

Suspended particulates in air have been associated with high positive correlation coefficients to ill-health states of community populations. As a result of epidemiological, clinical, and toxicological investigations as well as occupational accidental data, environmental exposure standards have been promulgated which require communities to maintain a clean ambient air environment. The air quality standard for particulate matter is based on a 24 hour average sample. The annual maximum for any one sample is less than 260 $\mu g/m^3$ of air while the annual geometric mean to be obtained is 75 $\mu g/m^3$ or less. These air quality standards are considered to be safe for human health.

A build-up of suspended particulate concentration generally occurs

under two sets of conditions: (1) the stagnant air mass is trapped under an inversion layer thus allowing the pollutants to accumulate; (2) the ventilation rate of the city is lower than necessary to disperse the quantities of pollutants exhausted into the atmosphere thus resulting in a net gain of pollutant loading of the atmosphere during the week. In either case rain generally relieves the situation.

Because of the above considerations monitoring the atmosphere for respirable particulates by remote sensors is not critical when the winds have a high velocity or when rain storms are present.

New ambient air quality standards are being considered for respirable particulates rather than total suspended particulate mass since it is now evident that the latter mass contains particles of a diameter size range, > 2 μ, which have little health significance but bias the data toward the increased importance of that size (Lee, 1972). This is because the mass increase is proportional to the square of the radius of the particle. The respirable aerosol diameter range is considered to be between 0.2 μ to 2.0 μ.

Remote sensing of respirable particulates in ambient air by light-scattering sensitive collectors could be utilized on a worldwide basis. Present ground-truth methods are cumbersome, expensive, require trained personnel, and are difficult to deploy on an areal basis. If the feasibility of detecting respirable particulates with remote sensors can be demonstrated, one of the most useful applications of the observation of the earth will have been accomplished.

III. LITERATURE REVIEW

The feasibility of correlation of respirable particulates suspended in ambient air with data from remote sensors hopefully can be demonstrated

if approaches are utilized which embody theory from visibility and light scattering, concepts of quantitative data retrieval from film, properties of the atmosphere, and the particle size distribution found in ambient air.

Visibility and light scatter have been studied along a horizontal path by Horvath, Noll, Charlson, Middleton, Junge, and Koschmieder among others. Thus the optical properties of small particles have become known.

LIGHT SCATTERING THEORY

The particles or aerosols with a diameter between 0.3 and 0.7 μ are primarily responsible for the optical characteristics observed, i.e., seen or viewed, in the atmosphere. The only available rigorous theoretical treatment of particulates, by Mie, hypothesizes that all particulates are spherical in nature and then uses Maxwell's equations of electrodynamics to solve for interference and diffraction effects. When a decrease in luminosity along a light beam is noted (attenuation of path luminance) it is not known whether the reduction is due to scattering or absorption on the particles. But the Lambert-Beer Law can be used to describe the light extinction irregardless of the cause. Thus,

$$J = J_o \cdot \exp(-b \cdot x)$$

where J, J_o are respectively the light intensities before and after a path x, while b is the extinction coefficient of the aerosol. The extinction coefficient b can be further resolved into four different quantities

$$b = b_a^a + b_s^a + b_a^g + b_s^g$$

which are respectively: the absorbtion coefficient of the aerosol, scattering coefficient of the aerosol, absorption of the gas medium, scattering coefficient of the gas medium. In the case of the normal atmosphere with aerosol or particles in the diameter size range of 0.2 to 1.0 μ b_a^a, b_a^g, b_s^g

are small in comparison to b_s^a by integration over all scattered intensities in all angular directions. Q, the scattering efficiency is equal to a decrease in the luminous flux divided by the flux incident upon the particle cross section. Thus Q is a function of the light wavelength λ, the particle radius r, and the refractive index m of the particle or if α is set equal to $2\pi r/\lambda$, then Q is a function of α and m ($Q=Q(\alpha, m)$).

An aerosol which contained N particles of size r would have an extinction coefficient described by

$$b = Nr^2\pi Q(\alpha, m)$$

whereas if the aerosol possessed particles of different sizes between r and r + dr, then n(r)dr particles are present and the scattering coefficient is given by

$$b = \int_0^\infty n(r)r^2\pi Q(\alpha, m)dr.$$

Contrast exists when one object can be distinguished from another. Thus it is defined as

$$C = (I_b - I_o)/I_b$$

where I is the reflectance or luminous flux from (I_b) the background and from (I_o) the object. The contrast threshold ε is defined as the difference in background and object flux which is just noticeable.

When visibility is calculated, the radiation from the sun, clouds, sky, and earth's surface must be included as each volume element of length dx scatters light toward the observer. The amount of scattered light dB is proportional to dx, the original incident light H_o and the coefficient of extinction b

$$dB = H_o k b dx$$

where k is a proportionality factor. Since dB is also attenuated in the atmosphere by an amount exp (-bx), the contribution to brightness of dB of the element along dx at the site of the observer is

$$dB = kH_o b \exp(-b \cdot x)dx.$$

In the simplest case, a black body against the horizon, the distance is infinite so the brightness of the horizon is calculated by integration of 0 to ∞.

$$B_H = H_o k \int_0^{\infty} b\, e^{-bx} dx$$

$$B_H = kH_o$$

A black body becomes brighter due to the light scattered by the atmosphere into the visual path. Since the original brightness or intensity of luminous flux from a black body is zero (0), at a distance x the brightness of the black body B_o can be written

$$B_o = H_o k \int_0^{\infty} b\, e^{-bx} dx - k\, H_o\, (1-e^{-bx}).$$

Thus the contrast of the object against a background as detected by an observer is given by

$$C = (B_H - B_o)/B_H$$

where $C = \exp^{(-bx)}$

also, if one object is perfectly black. Otherwise with the inherent contrast, C(0), present we have

$$C = C(0) \exp(-bx).$$

The characteristics of film are such that a film response number, the film constant α, has to be determined by exposure to known quantities of light. Thus all film data include α determined from the grey scale. The density (D) of color (black and white) developed by exposure to luminous flux is measured with a microdensitometer. Thus

$$\frac{B_o}{B_H} = \log^{-1} \frac{D_2 - D_1}{\alpha}$$

where α again is determined from the grey scale. If x is the distance from the target and T is the light transmission then

$$\frac{B_o}{B_H} = \frac{1}{T}$$

$$C = \frac{1}{T} - 1$$

This assumes no loss of contrast due to dB if it is directly correlated with I_B and I_o, i.e., if secondary scattering is neglected, no significant external light source is present, and the suspension itself does not contribute to the luminous flux transmitted. Then

$$\ln C = -bx.$$

From light transmission theory developed by Steffens where the perfect light source or perfectly reflecting object (white) is contrasted with the first object which is black ($I(0) = 0$),

$$C = -\exp(-bx).$$

The minus sign indicates that object 1 is darker than its background. Then

$$b = -\frac{1}{x} \ln T.$$

Otherwise,

$$C = C(0) \exp(-bx).$$

The above calculations also assume that the target or object is of such size that it does not affect the light path by shading and is such that visual acuity is not significantly greater for large objects. Fortunately, the attenuation coefficient and the meteorological range are quite insensitive to many conditions that are expected from theory to affect the resultant luminous flux measurements.

The original arguments as presented by Koshmeider, Duntley, Middleton, and Steffens stress that the path must be homogenous in character. However, Horvath, Knoll, Mueller, Ahlquist, and Charlson have all found high positive correlations with visibility, mass, and particle size distributions over extended periods of time (up to 24 hours) and distance in polluted atmospheres which are not the "aged", homogenous atmosphere required by theory.

Since the theory was developed with a black object such that I_b= 0 or B_o=0 at x=0, it is of interest to know the fractional error resulting from this assumption. It has been shown by Steffens that "I(0)/dB or $I(0)/\tau$ ranges from 0.02 at $I(x)/\tau = 0.9$ to 0.1 at $I(x)/\tau = 0.4$, if $I(0)/\tau$ is really 0.05. I(x) is the intensity of the horizon at some distance x from the target. The objects that are viewed must evidently be quite dark if this term is to be neglected...The visual range, under a clear sky, of a grey object of abledo 0.25, in the shade, against the horizon sky is over 98 percent of that of a black object. $I(0)/\tau$ seems likely, therefore, to be about one-quarter to two-thirds of the albedo for objects that are not in direct sunlight." The albedo of dry grass is 15-25%, bare ground is 10-20%, black mold(wet) is 8%.

Junge in his studies assumed that the particle size distribution in the atmosphere could be fit to a power law mathematical model. This

has since been shown not to be true by Curcio, Whitby, and others for the complete range of particle sizes. However, for the particle size range between 0.2 to 1.0 μ most observers have found the model to be a good approximation. Only Quenzel (1970) found that the size distribution of atmospheric aerosols did not fit the Bouquer-Lambert Law(power-law) as well as a distribution described by a log-normal distribution. However, the aerosols were measured over the tropical ocean and represent a skewed distribution of aerosols. Thus for purposes of this experiment

$$n(r) = n_o r^{-q}$$

where n(r) is the number of particles of radius r per cubic centimeter and q is a characteristic of the distribution, empirically determined. Then substituting into one of the earlier equations we have

$$b = \int_o^\infty \pi r^2 \, Q(\alpha,m) n_o r^{-q} dr.$$

Let $\alpha = 2\pi r/\lambda$, then

$$b = \pi n_o \left(\frac{\lambda}{2\pi}\right)^{3-q} \int_o^\infty \alpha^{2-q} \, Q(\alpha) d\alpha$$

where $Q(\alpha)$ is not now a function of wavelengths for dielectrics and hence

$$b = \pi n_o K_s \left(\frac{\lambda}{2\pi}\right)^{3-q}$$

and K_s can be calculated for Mie theory. For light of two different wavelengths

$$\frac{b_2}{b_1} = \left(\frac{\lambda_2}{\lambda_1}\right)^{3-q}$$

$$q = 3 - \frac{\log(b_2/b_1)}{\log(\lambda_2/\lambda_1)}$$

where b_2 and b_1 are the scattering coefficients b_{s2}^{a2} and b_{s1}^{a1} respectively for the aerosols, identified as aerosol 2 and aerosol 1, of different

diameters. Thus, the scattering coefficient $b_{s_1}^{a_1}$ for aerosols with a diameter size range 0.3 to 0.5 μ can be measured using a frequency band with wavelengths of 0.3 to 0.5 μ. If a second scattering coefficient $b_{s_2}^{a_2}$ for the aerosols with a diameter size range from 0.5 to 0.7 μ is measured in a similar manner then let

$$b_{s_1}^{a_1} = b_1 \quad \text{and} \quad b_{s_2}^{a_2} = b_2, \text{ approximately.}$$

Then, for example, let

$$\lambda_1 = \lambda_{0.4} \text{ and } \lambda_2 = \lambda_{0.6}$$

where the subscripts refer to the average wavelength of the frequency band. In this manner frequency bands can be utilized to determine the extinction coefficients, b_1 and b_2, of different diameter aerosols. Then these can be used to calculate the characteristic q of the model which represents the particle size distribution measured in the transmission path.

Steffens and Rubin (1949) determined b_s^a at different wavelengths by photographing black targets on panchromatic film through filters such as these:

Wratten A (No. 25) = .62 μ
Wratten B (No. 58) = .54 μ
Wratten C5(No. 47) = .45 μ.

In one series of experiments q had a mean value of 4.5.

Yamamoto and Tanaka (1969) utilized spectral attenuation measurements in studies of the aerosol size distribution in the atmosphere. They concluded that the power law model was a valid representation of the measured

distribution but found that the fit was best when near infrared wavelengths were included. Some of their work successfully related Mie scattering, suspended mass, visibility, etc.

The vertical attenuation of the light transmission or luminous flux due to scattering by or absorption by the gaseous atmosphere can realistically be considered negligible at less than 6000 feet. Horvath, Brathwaite and Polcyn (1969) found little difference in the apparent spectral radiance of mature corn, wilting soybeans, or other crops using the multispectral analyzer to make the measurements. On hazy days the shorter (0.4 μ) wavelength radiance began to deviate with altitude above 4000 feet. Nalepka confirmed this with flights over large objects (a portion of the asphalt ramp, concrete in front of a hanger, and asphalt covered roof of the hanger) which had previously been designated as secondary reflectance standards. Thus the equivalent reflectance was known and could be extracted from flight data.

For applications utilizing space platforms the beam transmittance can be calculated utilizing the concept of equivalent attenuation length I_x developed by Boileau (1964). Thus,

$$\tau(x,\theta) = \exp\{-[x/Ix]\ \sec\theta\}$$

where τ is the atmospheric beam transmittance between sea level and altitude x for a path of sight inclined $\theta°$ from the vertical. Since the apparent luminance of targets and the apparent contrast are also affected a contrast transmittance nomogram has been constructed to determine the contrast transmittance.

$$C_r/C_o = [1 + b_x/\tau b_o]$$

where C_r, C_o, b_x, b_o are functions of distance x, and spherical angles θ, ϕ. τ is a function of x, θ. At least a body of knowledge is available

on which to build if higher altitudes than a mile are employed.

OPTICAL PROPERTIES OF AIR POLLUTION

The particle size distribution of respirable aerosols, grossly named suspended particulates, has only recently begun to be of interest to health authorities (Lee, 1972). In the past, measures of suspended particulates included mainly a soiling index (COHs) and total mass in $\mu g/m^3$ based on samples taken by high volume air samples being drawn through filters, equilibrated, and weighed. Burt concluded that the visibility index could not be used to predict or calculate visibility. Visibility has been characterized as meteorological range, L_v, by Koshmieder (1924) as the greatest distance at which a black object of a certain sufficiently large size could be seen against the horizon sky by an observer who can perceive a contrast difference of 2%. The scattering coefficient b_s^a can be related empirically to L_v by the following equation.

$$L_v = 3.91\ m/b_s^a = \frac{2.4 \times 10^{-3}}{b_s^a} \text{ miles}$$

Steffens (1956) suggested a relationship between mass concentration and visibility.

$$M = \frac{0.22\alpha}{BL_v}$$

where M is pollution in mg m^{-3} of air, α is 2π times the radius of particles divided by the wavelength of light; and B is a function of α and the optical properties of the particles. Charlson, Horvath, and Pueschel (1967) suggested that a simplified equation would lead to

$$V = \frac{K}{M}$$

where V is the prevailing visibility and K is a proportionality constant. Noll, et al., found the overall K average = 900 μg mile m^{-3}. The U.S. Weather Bureau defines prevailing visibility as the greatest visibility which is attained or surpassed around at least half of the horizon circle, but not necessarily in continuous sectors. It was recommended that V be the time weighted average of frequent readings V_1, $V_2 \ldots V_n$ taken during the time of the high-volume air sample.

Tombach (1971) using data published by every one else in the field indicated that where

$$J(x) = J_o\, e^{-bx}$$

as measured by an integrating nepheolometer, $b = b_s^a$ measured in visibility studies.

Thus $$L_v = \frac{1.8\ ^{+1.8}_{-0.9}}{M}$$

when L_v is in miles and M is in gm^{-3}.

Charlson, Ahlquist, Selvidge and MacCready (1969) showed that nephelometer output data could be correlated with visual range. Because the instrument is also dependent on the scattering component of the extinction coefficient, the nephelometer is wavelength dependent. Thus:

$$L_v = \frac{3.9}{b_s^a}\ (550\text{nm}) \simeq \frac{4.7}{b_s^a}\ (500\text{nm}).$$

Junge (1963) showed the same dependence as: $B_s^a \propto \lambda^{-\alpha}$. Horvath (1969) found a correlation coefficient of 0.9 between visual range and meteorological range calculated from the measured scattering coefficient at several locations. The three-way relationship between visual range, light scattering

coefficient and mass concentration has been tested. Since Charlson, et al. (1969) and Noll, et al. (1968) both found that

$$L_v \times \text{Mass} = 1.8 \text{ g/m}^2$$

then the ratio of Mass/b_s^a, measured by a nephelometer, can be related to the above product by using the Koshmeider visibility theory corrected to the effective wavelength of the instrument

$$L_v \times \text{Mass} = \frac{4.7 \text{ Mass}}{b_s^a},$$

Since it was also found that when a nephelometer is used

$$\text{Mass } (\text{g/m}^3) = 3.8 \, {}^{+3.8}_{-1.9} \times 10^5 \, b_s^a \, \text{m}^{-1}$$

then $L_v \times \text{Mass} = 1.8 \text{ g/m}^2$.

In actual practice, this constant has been shown to be exceedingly stable. From measurements made in Seattle, Washington, Altadena, California and Denver, Colorado in about 90% of the cases

$$\alpha = 1.8 \pm 0.5$$

The nephelometer calibrations only have to be considered when the high-volume air sampling data are correlated to the visual range. The vertical luminous path data will not be treated in the same manner.

HUMIDITY

The effects of humidity on light scattering have been well noted. The dramatic increase in light scattering from aerosols occurs when the relative humidity (RH) is increased above 65%. Sea-salt aerosols or NaCl

particles are transformed into droplets of salt solution above this RH and continue to increase in size as the RH increases thereby causing a tremendous drop in visibility. Other urban pollutants that respond in a similar manner include Na_2SO_4, H_2SO_4, and $(NH_4)_2SO_4$. The shape of the curve is characteristic of the salt or aerosol sample. As a general rule it can be assumed that all empirically derived constants are invalid at RH above 70%.

VERTICAL PROFILES

The vertical profiles of the atmosphere with relation to temperature and number of particles per cubic meter of air have shown that the inversion layer mixes well during the afternoon (Charlson, et al., 1969). Generally, this layer can be detected by a sharp change in the temperature profile of the atmosphere. Thus, the hypothesis (that the particles are uniformly mixed and present throughout all the elements of the light transmittance path) is reasonable if only a path length equivalent to the inversion layer height is used in the calculations. The size distribution of atmospheric aerosol particles has been determined by Quenzel (1970) from direct solar radiation measured in eight spectral bands at ground level. As usual the refractive index m of the aerosol particles was 1.50. The scattering coefficients most dependent on height were those determined from 0.45 to 0.6 μm wavelengths. This was anticipated by the theoretical plot of backscattered spectral radiance as a function of altitude by Nalepka (1970). The multispectral data reported by Horvath, Braithwaite and Polcyn (1960) reveal the same altitude, wavelength dependence.

Taylor (1964) calculated the size of the target diameter in minutes that can be seen for various contrast thresholds. These provide an index with which target sizes for various altitudes and film sensitivity can be chosen.

In addition Porch, et al. (1971) have devised another method to calculate the optical depth (vertical) x for scattering above observatories. Using Charlson's data for extinction coefficients (zenith)k, they report that

$$b_s = \frac{0.92k}{X} .$$

Thus several methods are available for estimating the optical depth or light transmittance path length.

PARTICULATES IN AMBIENT AIR

Suspended particulates in air "age" at different rates. There seems to be a tendency for small particles to agglomerate or coalesce until a diameter size of about 1.0 μ is achieved while larger particles tend to fall out of the atmosphere or disintegrate to a smaller size. Thus, the aerosols less than 1.0 μ in diameter have the longest life in the atmosphere and constitute the largest fraction by number of the aerosols in the atmosphere.

The meteorological phenomenon, the inversion, occurs nightly over most areas. This effectively blocks vertical mixing into the stratosphere above the altitude of the inversion layer such that in most models only horizontal mixing is considered. With velocities of less than seven miles per hour local eddies tend to keep the particulates from dispersing. Indeed, even in the most extreme cases laminar flow of the atmosphere over a city is not achieved. Generally, as the solar radiation heats the ground the vertical mixing of air increases until the inversion is dissipated. This results in a well mixed aerosol distribution in the atmosphere. It most probably isn't the ideal homogenous optical path assumed in light transmittance calculations but at least approaches the condition on a daily basis.

Most of the empirical statements relating visibility (or meteorological range, L_v) to the suspended particulate mass loading of the atmosphere have assumed a linear model. Noll, Mueller, and Amada (1968), Charlson, Ahlquist, and Horvath (1968), Charlson (1969), and Tombach (1971) use the form suggested by the Koshmieder visibility theory.

$$L_v = \frac{3.9}{b_s^a} \quad \text{and} \quad M = 0.39 \times b_s^a$$

where L_v is in meters and M is in g/m^3 of air and where b is the atmospheric extinction coefficient. It is then noted that the constant 3.9 in reality is 3.9 ± 0.5. Several factors suggest the relationship may in fact not be linear.

First, the extinction coefficient can be given by:

$$b_s^a = \int_o^\infty Q[\frac{2\pi r}{\lambda}], \; m(r)] \; \pi r^2 n(r) dr$$

and the mass is given by:

$$M = \int_o^\infty \frac{4\pi \rho(r) r^3 \; n(r) dr}{3}$$

Where M(r) is the scattering efficiency for light of wavelength λ and $\rho(r)$ is the density of the particle or aerosol. Then the ratio of mass concentration to the scattering coefficient is a function of several variables:

$$\frac{\text{Mass}}{b_s^a} = f[\rho(r), \; m(r), \; n(r), \lambda].$$

Further, if volume is calculated rather than mass and an index of refraction of 1.50 is assumed then:

$$\frac{V}{b_s^a} = f[n(r), \; \lambda]$$

if a uniform density is also assumed. If a power law size frequency distribution $n(r) = kr^{-\beta}$ is utilized with upper and lower size limits of 2 μ and 0.04 μ, Charlson, et al. (1968) calculate the curve shown in Figure 1, Volume / b_s^a ratio vs exponent β of size frequency curve. These are no more linear than the distribution of energy by frequency is in solar radiation.

Secondly, Ettinger and Royer (1972) found the following relationship between visual range (L_v) and mass concentration in a nonurban environment:

$$L_v = \frac{24.}{0.2 + (0.01 \pm^{0.01}_{.003}) M} \text{ miles}$$

Particle size was not related to the visual range because of the sampling time scale. Using this model the data of Charlson and Noll are presented in Figure 2, Visual Range vs Mass concentration.

Figure 1 Volume/b_s^a ratio vs Exponent β of Power Law

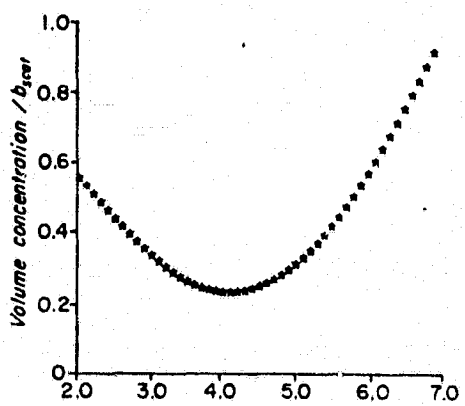

Calculated ratio of volume concentration to extinction coefficient due to scatter vs. the exponent of a power law size distribution function. Ordinate units are $cm^3\ m^{-3}$ per m^{-1} (10)

FIGURE 2: VISUAL RANGE vs MASS CONC.[14]

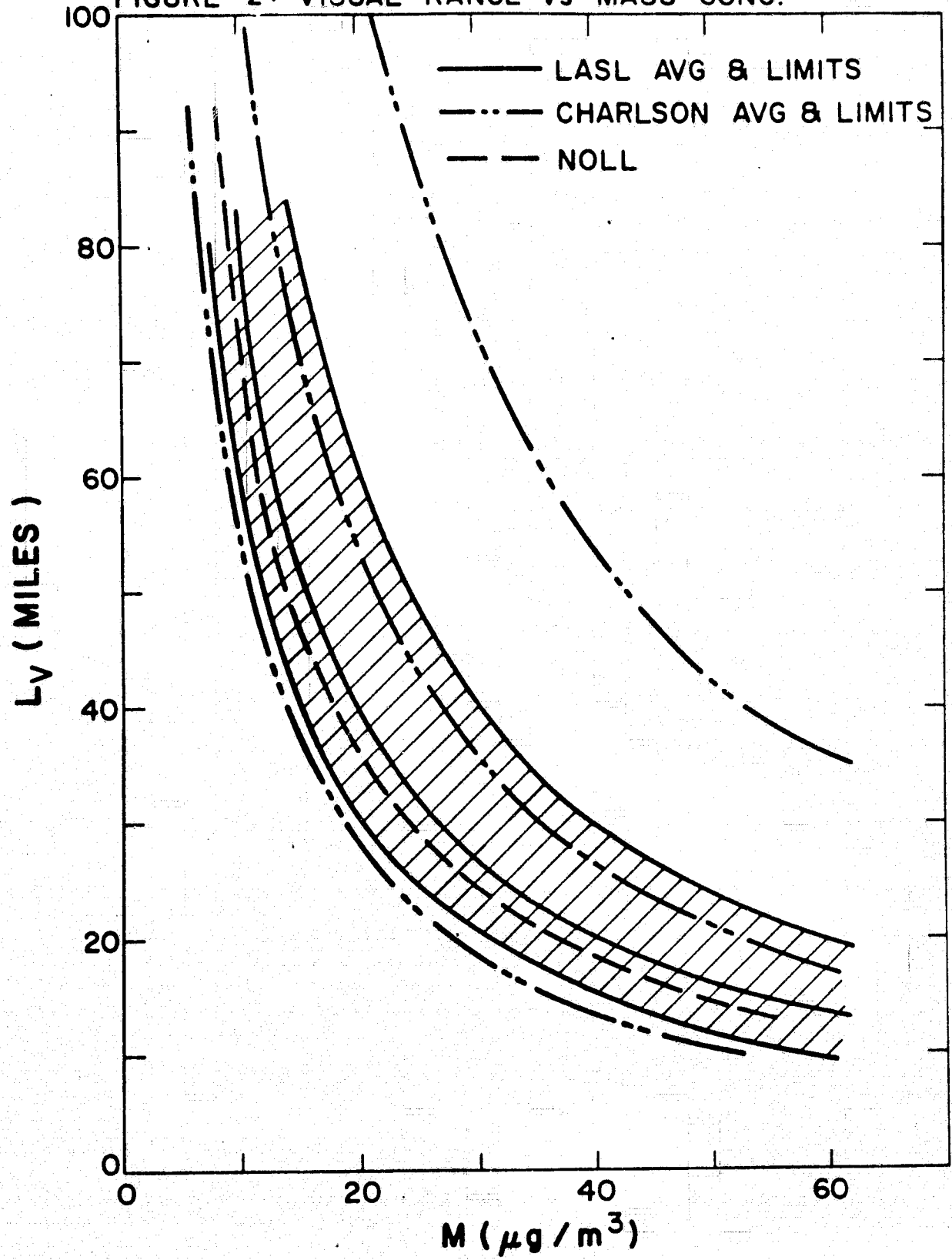

IV. REMOTE SENSOR DATA: CONSIDERATIONS AND ANALYSIS

Photogrammetry was utilized in lieu of the multi-spectral analyzer developed by Bendix and tested at the University of Michigan. The original request for proposal had specified correlation of ground-truth data with that collected with the multi-channel analyzer. When that was unavailable it was suggested that the principle could still be tested by utilizing filters and film. Specifics of the flight and equipment selected are presented in the flight request in the Appendix. The requested spectral reflectance measurements of the targets to be made by the Applied Physics Branch were not made. And in fact, the entire mission can be best treated as a shake-down run in which all efforts are analyzed to find what must be done to improve the experiment and its execution. Therefore, only two of the film channels were chosen for analysis.

Microdensitometry tracings were made at NASA-MSC along lines indicated on positive negatives developed after the flight. These are included in the Appendix. Inspection of the film from the four channels indicated that several of the frequency channels, simulated with filters, had been exposed improperly. The data processing requested (see Flight Request, Appendix) had been impossible to obtain due to the use of uncalibrated lenses and filters and other matters as yet unknown to the author. Since no precision step wedges were available after film processing, the microdensitometrist provided one from a "similar" film for type Plus X but none for the B&E infrared film. Thus the following

analysis is at best approximate.

The following filters were chosen to simulate frequency bands of those central wavelengths:

WR47B	----	0.43μ
WR57	----	0.53μ
WR25	----	0.66μ
WR89B	----	0.90μ

The Figures 3 through 6 are representative of the wavelengths passed by the various filters.

The microdensitometry analysis of the film data is presented in Table 1. The secondary reflectance standards are white gas storage tanks at the Humble Refining Companies Baytown, Texas location and white gas storage tanks located only at the Houston ship channel at the General American Tank Storage Company in Pasadena, Texas. These are shown in the photographs presented as Figures 7 and 8.

Figure 3 Wratten Filter 47B

47B

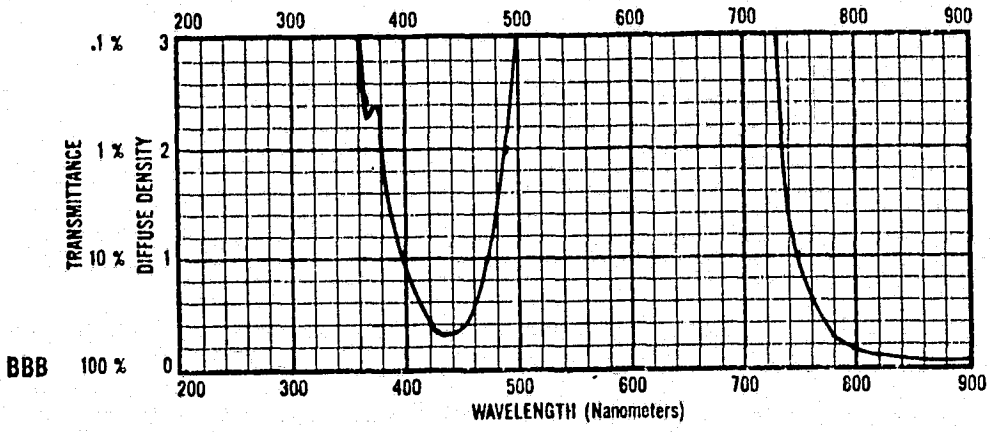

Deep Blue Tricolor. Used for color separation and tricolor printing work.

WAVELENGTH	PERCENT TRANSMITTANCE No. 47B	No. 48	No. 48A
400	16.0	0.96	4.51
10	29.5	3.16	9.32
20	43.6	8.25	16.9
30	50.0	15.0	22.4
40	47.2	22.6	25.9
50	36.0	30.3	27.1
60	25.0	33.2	23.2
70	13.2	29.6	16.6
80	4.5	22.4	9.78
90	1.3	14.1	4.57
500	0.17	7.30	1.62
10	—	2.64	0.26
20	—	0.50	—
30	—	—	—
40	—	—	—
50	—	—	—
60	—	—	—
70	—	—	—
80	—	—	—
90	—	—	—
600	—	—	—
10	—	—	—
20	—	—	—
30	—	—	—
40	—	—	—
50	—	—	—
60	—	—	—
70	—	—	—
80	—	—	—
90	—	—	—
700	—	—	—

Figure 4 Wratten Filter 57

57

WAVELENGTH	PERCENT TRANSMITTANCE No. 55	No. 56	No. 57
400	—	—	—
10	—	—	—
20	—	—	—
30	—	—	—
40	—	—	—
50	—	—	—
60	0.20	0.36	0.44
70	2.90	2.9	3.10
80	13.1	12.5	13.1
90	34.2	32.2	31.9
500	56.0	55.2	50.5
10	67.0	71.5	60.6
20	69.3	78.8	63.3
30	65.1	80.3	61.0
40	56.7	77.6	55.0
50	45.0	72.4	47.1
60	33.1	65.7	37.3
70	20.7	56.9	26.5
80	9.00	44.7	16.6
90	2.70	32.0	8.69
600	0.40	23.1	3.70
10	—	18.1	1.60
20	—	12.9	0.49
30	—	7.0	—
40	—	2.9	—
50	—	1.7	—
60	—	2.3	—
70	—	6.7	—
80	0.66	20.0	—
90	6.90	42.2	—
700	27.8	63.3	—

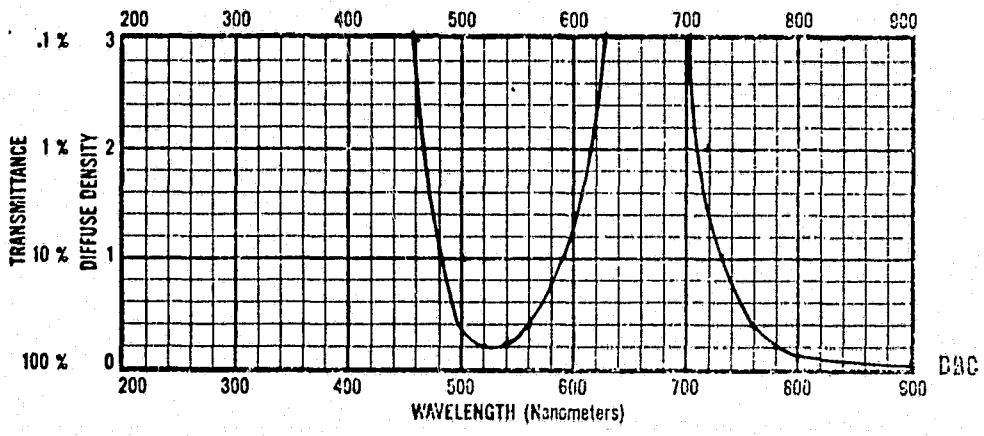

Green. Formerly used for "two-color photography" (daylight) with No. 24 (red). Often used with a No. 15 in tricolor printing from EASTMAN Color Negative Films.

75

Figure 5 Wratten Filter 25

WAVELENGTH	PERCENT TRANSMITTANCE No. 23A	No. 24	No. 25
400	—	—	—
10	—	—	—
20	—	—	—
30	—	—	—
40	—	—	—
50	—	—	—
60	—	—	—
70	—	—	—
80	—	—	—
90	—	—	—
500	—	—	—
10	—	—	—
20	—	—	—
30	—	—	—
40	—	—	—
50	—	—	—
60	—	—	—
70	11.0	—	—
80	47.0	4.55	—
90	69.6	37.3	12.6
600	82.7	72.3	50.0
10	85.8	82.9	75.0
20	87.2	86.4	82.6
30	87.9	87.8	85.5
40	88.5	88.5	86.7
50	89.0	89.0	87.6
60	89.4	89.3	88.2
70	89.6	89.7	88.5
80	89.8	89.9	89.0
90	90.0	90.2	89.3
700	90.2	90.3	89.5

25

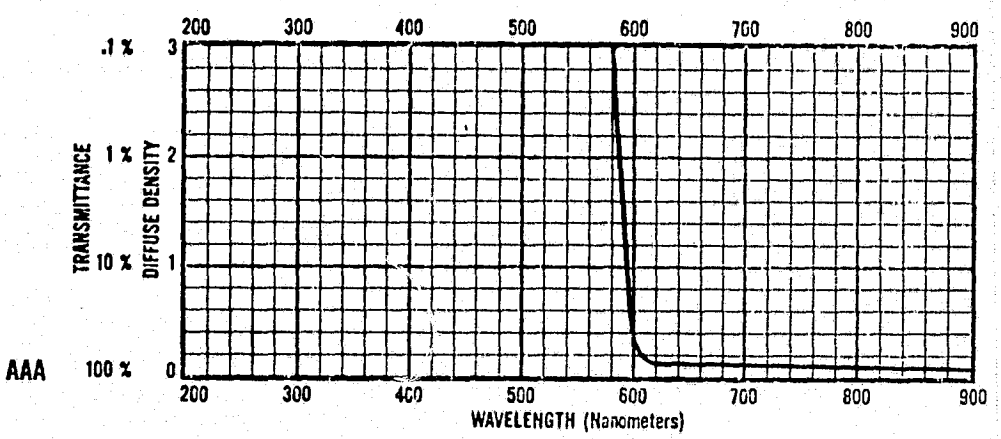

AAA

Red Tricolor. Used for color separation work and tricolor printing. Two-color general viewing. Contrast effects in commercial and outdoor black-and-white photography. Haze penetration in aerial work and removes blue in infrared photography.

64

Figure 6 Wratten Filter 89B

89B

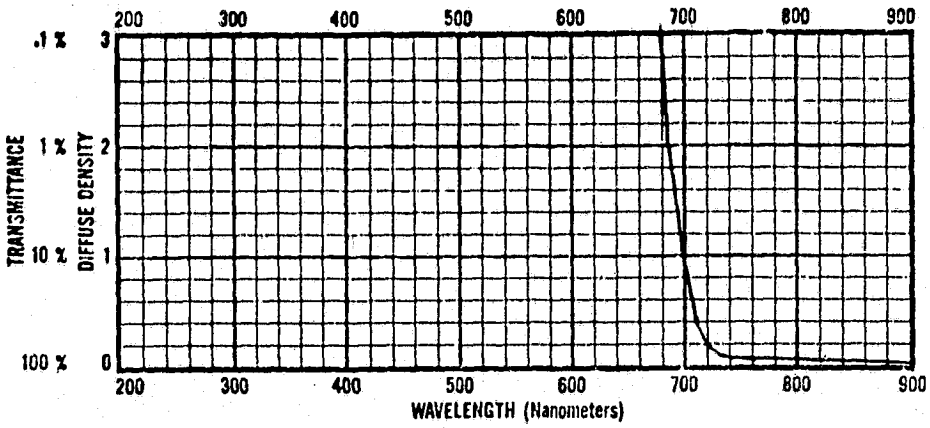

AAA

Visibly Opaque. Used for infrared photography, especially aerial.
See page 33 for infrared data.

WAVELENGTH	PERCENT TRANSMITTANCE No. 89B*	No. 90
400	—	—
10	—	—
20	—	—
30	—	—
40	—	—
50	—	—
60	—	—
70	—	—
80	—	—
90	—	—
500	—	—
10	—	—
20	—	—
30	—	—
40	—	—
50	—	0.7
60	—	13.5
70	—	32.5
80	—	33.0
90	—	23.0
600	—	14.9
10	—	10.4
20	—	6.7
30	—	2.8
40	—	0.7
50	—	0.2
60	—	0.2
70	—	1.7
80	0.10	10.3
90	1.58	28.5
700	11.2	53.2

Table 1, Microdensitometry Analyses

Tracing	Secondary Reflectance Target, d_2	Shadow or Limb, d_1	(d_1-d_2)	Darkest Nearby Measure, d_3	(d_3-d_2)	Description & Film Type
Baytown						Roll 3, WR 25 plus X
3-A	1.5 cm	6.4 cm	4.9 cm	10.4 cm	8.9 cm	
3-D	2.0	4.0	2.0	11.8	9.8	
3-F	1.7	5.3	3.6	11.6	9.9	
Ship Channel						Roll 3, WR 25 plus X
1-1	0.6	4.8	4.2	10.0	9.4	
1-2	0.5	5.3	4.8	10.1	9.6	
1-3	0.4	5.6	5.2	10.0	9.9	
1-4	0.3	5.3	5.0	9.6	9.3	
1-5	0.3	5.3	5.0	9.6	9.3	
Baytown						Roll 6, WR 89B B & E IR
4-A	1.7	3.4	1.7	11.0	9.3	
4-C	1.6	4.2	2.6	10.8	9.2	
4-D	1.0	4.3	3.3	10.3	9.3	
4-E	0.9	4.5	3.6	9.4	8.5	
Ship Channel						Roll 6, WR 89B B & E IR
2-1	2.4	5.0	2.6	8.0	5.6	
2-2	2.4	5.3	2.9	7.8	5.4	
2-3	2.0	4.6	2.6	8.5	6.5	
2-5	2.1	4.2	2.1	9.5	7.4	
2-6	2.0	4.8	2.8	10.3	8.3	

1. film gamma was 1.4 on each film

Figure 7 Infrared Color Print, Baytown Reflectance Target

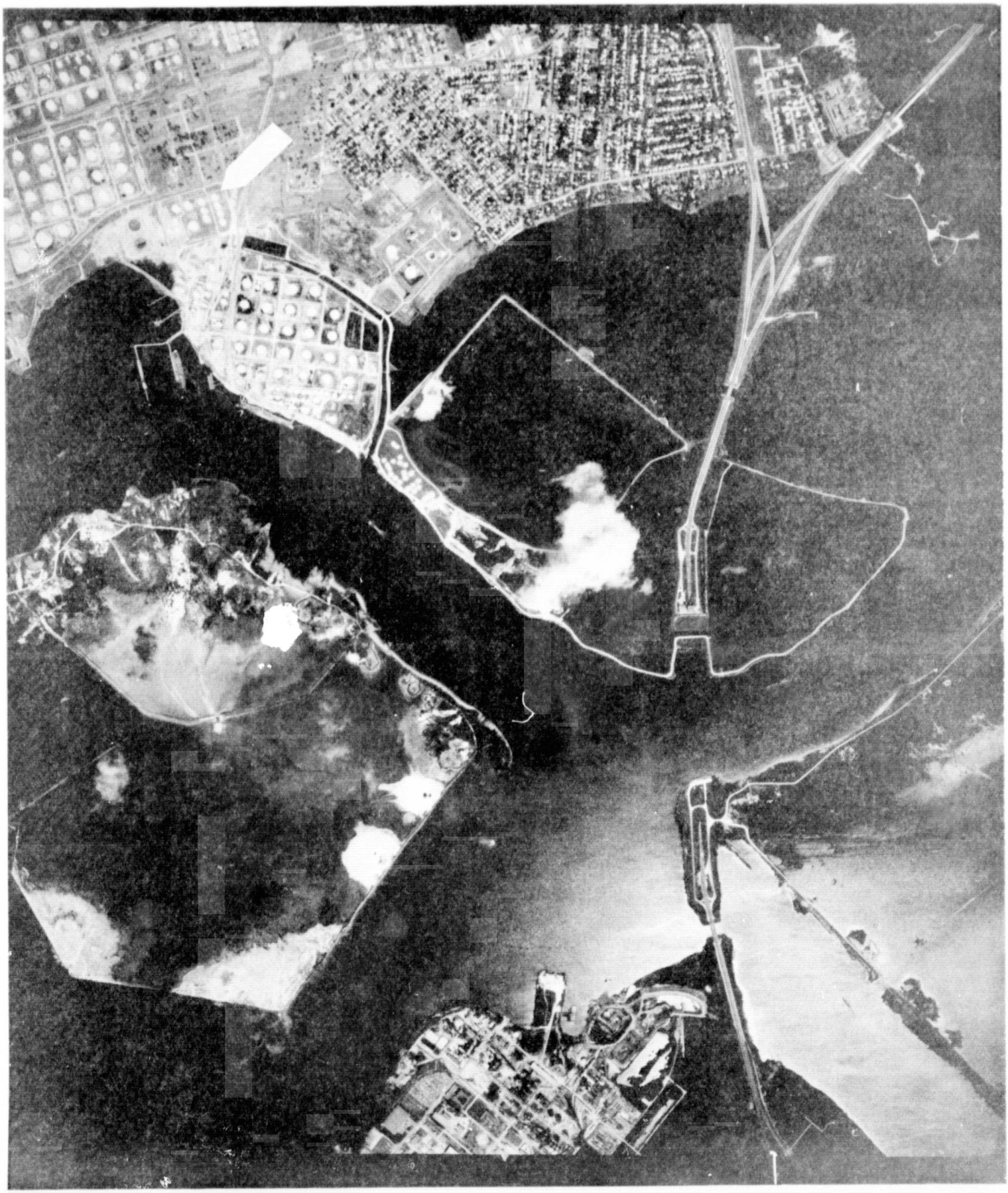

Figure 8 Infrared Color Print, Ship Channel Reflectance Target

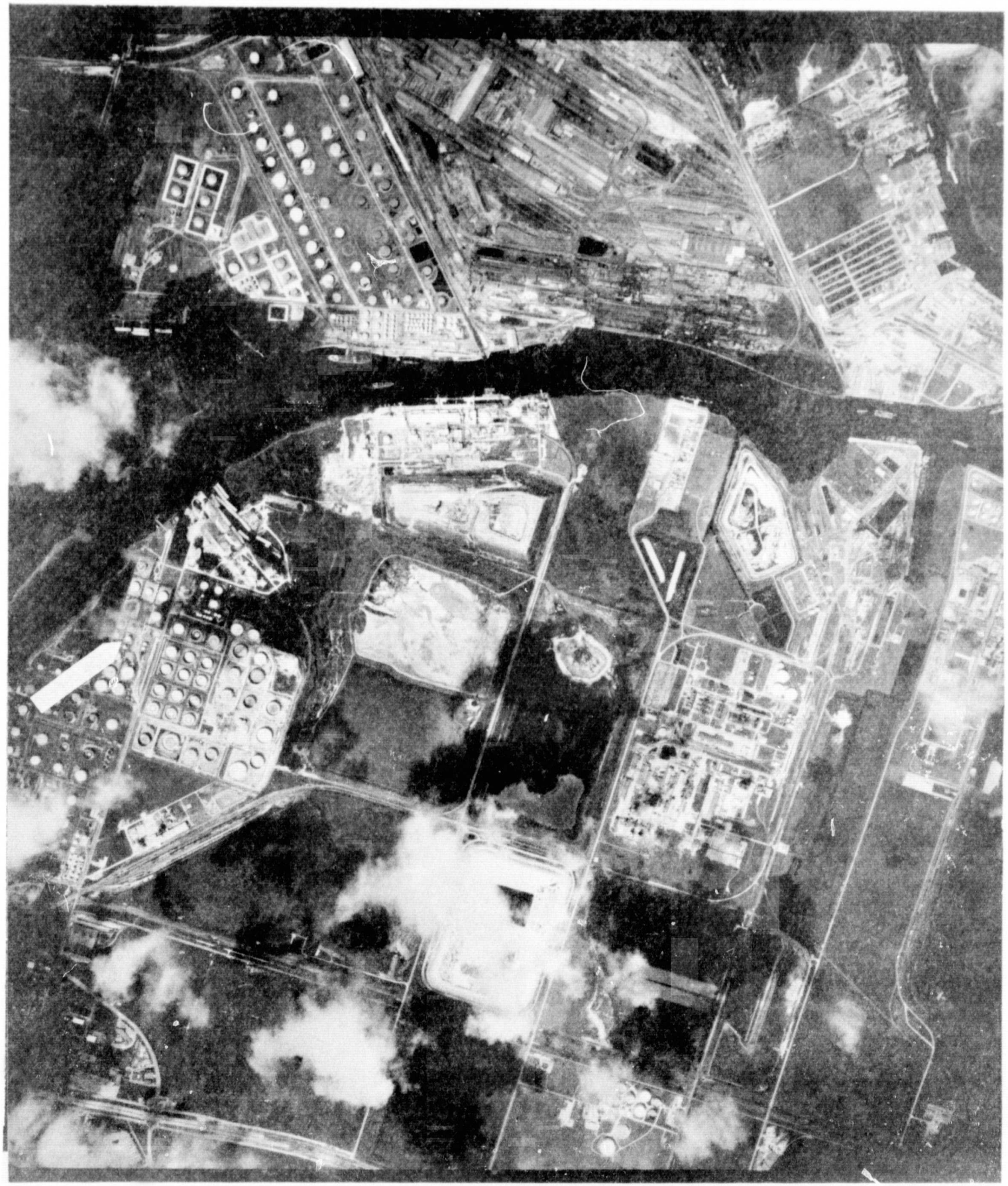

V. EXPERIMENTAL DESIGN

The hypothesis that emerged from the study of the foregoing sections was that the electromatic wave extinction measurements, that is the transmission both in the visible and the near infrared portion of the spectrum measured with passive remote sensors along a verticle path, would have a high positive correlation with extinction coefficients calculated from measurements of particle size distributions measured at ground level. It was first suggested that the multi-spectral analyzer be mounted in an airplane and used as the passive remote sensor since the frequency bands were far more discrete in that particular instrument than they were when such bands were defined by the use of filters and cameras. However, difficulties were encountered in scheduling the multi-spectral analyzer (it also seemed to be difficult to get it mounted in an airplane) so that the initial experiment utilized filters on a camera. The targets that were chosen for spectral reflectance were white petroleum products storage tanks. These offered the best opportunity to compare the white reflectance spectrum with a nearby supposedly black body reflectance in order to determine a contrast ratio. Balck was chosen initially to be the grass in the shadow of the storage tank which appeared as a limb on film.

Particle size distribution measurements can be made at the site with several techniques. It would appear possible from foregoing sections to relate particle size distribution to total mass measurements made with high volume air samplers, by counting the number of particles in a particular size range as is done with nephlometers, by optical sizing

of deposited particulates on slides utilizing electrostatic precipitation, followed by optical sizing, and also by the use of an Anderson air sampler (which divides the mass particles by inertial and aerodynamic consideration into various weight measurements). The ground-truth data to be correlated with remote sensing imagery should be collected by that method which best approximates the same situation, i.e. short sampling time with the sample sensed by electromagnetic radiation sensitive devices. Thus, the first choice would be a nephlometer. However, for this first study a nephlometer was not yet available.

VI. THE EXPERIMENTAL RESULTS

The high volume air sampling network of the city of Houston was utilized at the time of the overflight. The state regional office of the Air Pollution Control Services section of the Texas Department of Public Health was also very cooperative in taking additional high volume air samples in the Baytown area on the same date. In both cases, instructions were given to sample from about 10:00 to about 1600 o'clock. Some high volume air samples were also taken by staff members of the Exxon Company located in Baytown. These data are summarized in Table 2. This data can only be regarded as representative since the mission scheduled for the 27th of September, 1971 actually occurred the 28th of September, 1971. It is impossible to reschedule ground-truth activities of this complexity in that short a time span. However, the meteorological conditions were similar on both days. The wind was from the southeast at 2 to 6 miles per hour and the relative humidity was

less than 70 during the time period of interest.

Data from Table 2 were examined for compatibility and reduced to the computer input format. The base map of the Houston area was used as an additional input to the SYMAP Computer Program. Figure 10 indicates the best approximation of suspended particulate values present in the Houston-Baytown area on the 27th of September, 1971. This map was utilized in the correlation of the film densitometry data with ground-truth data.

The second type of ground-truth data that was needed for this correlation was the particle size diameter distribution. Although no nephlometry data were available from the time of the flight, a series of such measurements were made following that date in order to hypothesize what the distribution function might have been. Table 3 represents a summary of the data taken in the following months near the secondary reflectance targets located along the Houston Ship Channel near Galena Park in the city of Houston, Department of Public Health. It was assumed that the particle size distribution is best described by a power function. This assumption was arrived at after a careful examination of first, the literature and second, the data which was plotted on 4 x 6 cycle log/log paper. The constants a and q prime were determined from the plot of the data. In other words if S= the particle size diameter, N= the number of particles of that diameter, q prime equals the power of the distribution, and a equals the intercept, then $S= aN^{-q}$. The plot in Figure 9 indicates the relationship of the symbols.

A history of particle size distribution data such as these makes

Table 2. Suspended Particulate Data, ug/m^3 of Air September 27, 1971.

Site No.	Location	Time	ug/m^3
B 1	Humble Oil Company	1000 to 1400	39
B 2	Humble Oil Company	"	49
B 3	Park Street Pump Station	"	50
B 4	Bayway Fire Station	"	59
B 5	Roseland Park	"	20
B 6	Regional Office T.S.A.C.P.	"	126
H 2	811 N. San Jacinto	800 to 2000	122.2
H 3	824 San Antonio	"	67.2
H 4	10343 Hartsook	"	42.2
H 5	11212 Cullen	"	88.6
H 6	3801 Cullen	"	53.6
H 7	1115 N. MacGregor	"	43.5
H 8	3828 Aberdeen	"	32.0
H 9	6902 Bellaire	"	50.5
H 10	3735 W. Alabama	"	61.0
H 11	4420 Bingle	"	44.2
H 12	10413 Fulton	"	61.2
H 13	7330 N. Wayside	"	65.3
H 15	12759 Market St.	"	106.9
H 16	13349 Vicksburg	"	143.8
DP 1	1301 Center	"	58.6
P 2	112 N. Walter	"	73.5

B = Baytown
H = Houston
DP = Deer Park
P = Pasadina

it possible to postulate the particle size distribution at the secondary reflectance target sites if the mission is accomplished at a time other than that time when ground-truth data is collected.

The critical factors were delineated for analysis of film densitometry data and the flight request initiated is shown in the Appendix. With reference to the mission (LSF #2) conducted on September 28, 1971 with the MP3A for Drs. Fuller and Severs, the following information was requested:

a. The field irradiance of lenses as a function of wavelength at flight f number.

b. The calibrated shutter speeds.

c. The window transmission values.

d. The field irradiance of lenses in filters is flown as a function of wavelength in flight f numbers.

e. The spectral transmittance of filters.

f. The sensitometry reduced for the flight film to convert density of film to exposure in terms of energy per unit area (ergs/cm^2). Accuracy of energy should be traced to NBS standards.

Optionally item d. could replace items a. and e. The above information was impossible to obtain since lenses had not been calibrated before the flight and sensitometry wedges were not included in the film processing. However, one can make the assumption that any errors not accounted for in the above manner are less than the differences one is trying to measure. Thus, sources of transmission loss in the optical system were neglected.

The flight log lists Roll 3 from the KA62 camera, Plus X film in position one as being used with the WR25 filter. Roll 6 in position

Table 3. Data on Particle Size Range Distribution

Location	Date	Time	A	S	q
H 7	10-22-71	1020	13	0.5	1.29×10^{-5}
		1530	20	0.2	1.98×10^{-5}
	10-23-71	1010	12	0.3	1.20×10^{-5}
		1627	19	0.2	1.91×10^{-5}
	10-24-71	0913	12	0.4	1.12×10^{-5}
		1535	11	0.3	1.10×10^{-5}
	10-25-71	0837	18	0.5	1.78×10^{-5}
		1615	13	0.3	1.27×10^{-5}
	10-26-71	0840	22	0.3	2.13×10^{-5}
		1600	25	0.2	2.45×10^{-5}
	10-27-71	0800	22	0.3	2.17×10^{-5}
		1640	20	0.2	1.98×10^{-5}
	10-28-71	0845	15	0.3	1.47×10^{-5}
		1813	18	0.2	1.74×10^{-5}
Manchester Avenue, G.P.					
	11-15-71	0845	43	0.2	4.31×10^{-5}
		1610	38	0.2	3.98×10^{-5}

Table 3. Data on Particle Size Range Distribution (cont'd)

Location	Date	Time	A	S	q
	11-16-71	0907	21	0.4	2.02×10^{-5}
		1615	26	0.3	2.60×10^{-5}
	11-17-71	0855	30	0.3	2.97×10^{-5}
		1800	22	0.3	2.10×10^{-5}
	11-19-71	0915	15	0.3	1.47×10^{-5}
		1820	21	0.2	2.05×10^{-5}

Figure 9: Particle Size Range Distribution

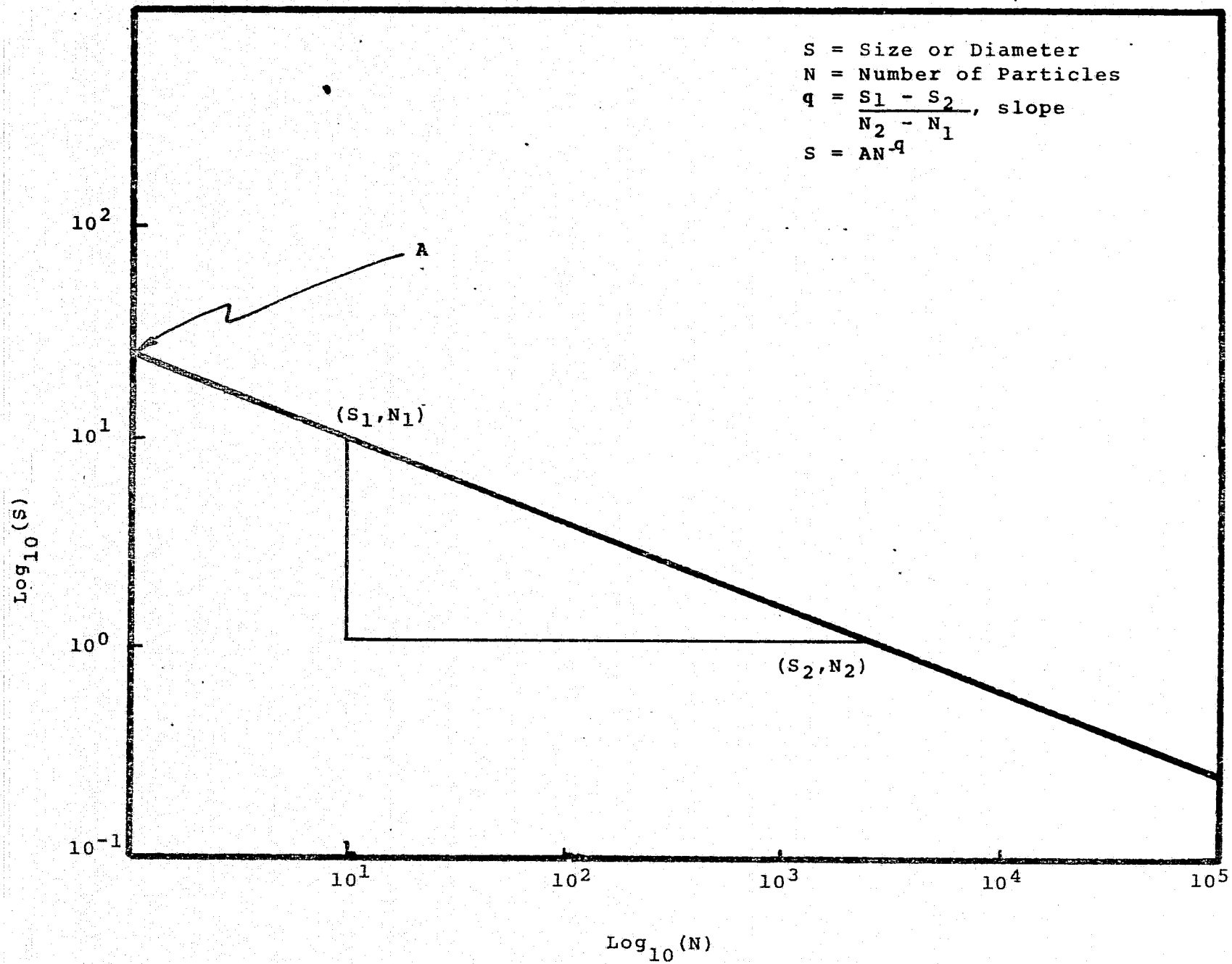

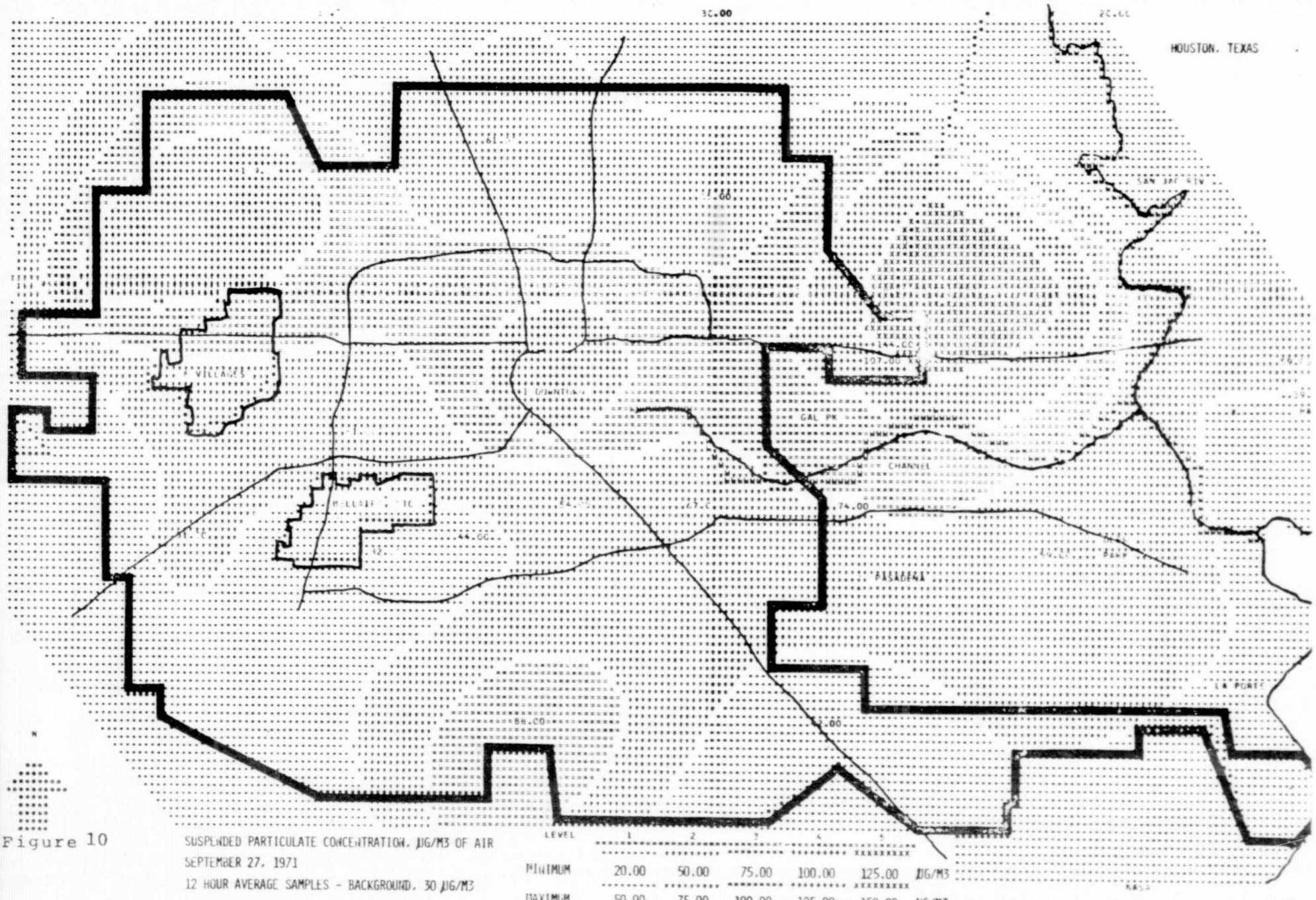

Figure 10

SUSPENDED PARTICULATE CONCENTRATION, UG/M3 OF AIR
SEPTEMBER 27, 1971
12 HOUR AVERAGE SAMPLES - BACKGROUND, 30 UG/M3

4, B&E IR film was used with the WR89B filter. Each roll was exposed to both reflectance targets. Isodensity recordings (I^2S) of these frames are presented in Figures 11 through 14 Table 1 includes the microdensitometry values for specific lines indicated on the isodensity recordings. In two of the I^2S recordings these indications were not made thus making it virtually impossible to identify and match the reflectance targets with their associated microdensitometry values.

From the two I^2S recordings which had indications of locations for microdensitometric tracings it was evident that the tops of the storage tanks were excellent reflectance targets and were the brightest objects in the field. The shadow of the tank was not as dark as other features of the scene. Thus values for the darkest elements and brightest elements were chosen to represent B_0 and B_H in the calculations. It was possible to obtain such values from the unidentified microdensitometry tracings as well. These are the values presented in Table 4. The film gamma reported was 1.40. The transmission distance was 10,000 ft. or 3.048 km. At 10,000 feet with a sun zenith angle of 0°, the sky luminance has been reported to be 420 ft.-lumens.

The extinction coefficients calculated from the film densitometry data are presented in Table 4. Alternate values may be obtained if either the transmission distance or the effective wavelength are thought to have different values, e.g. if Wratten Filter 89B is considered to have an effective average wavelength of 0.80 μ then the extinction coefficient q at the Baytown site equals 5.20 and that at the ship channel site equals 6.11.

Figure 11, Isodensity Recording, Ship Channel, WR25

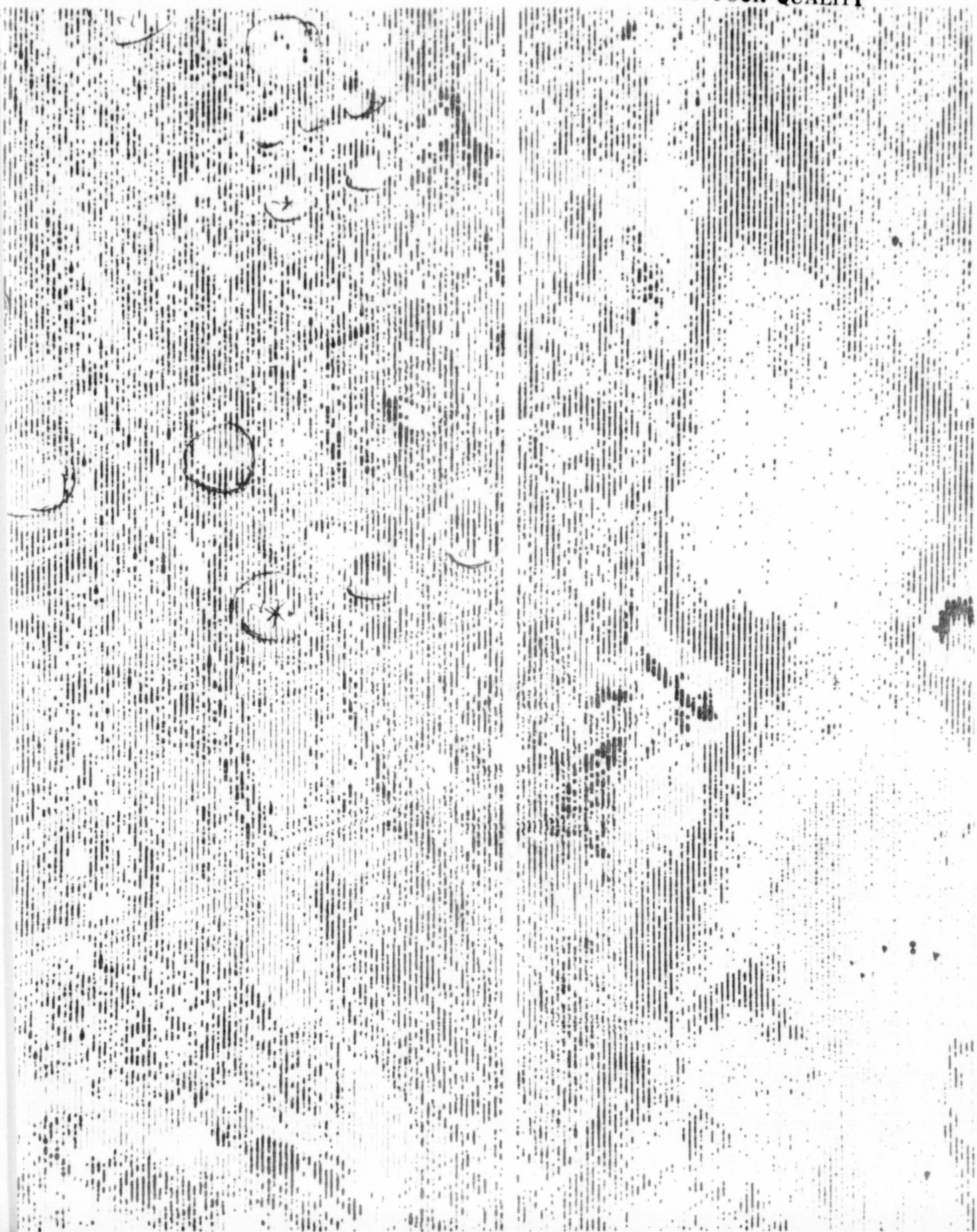

Figure 12 Isodensity Recording, Ship Channel, WR 89B

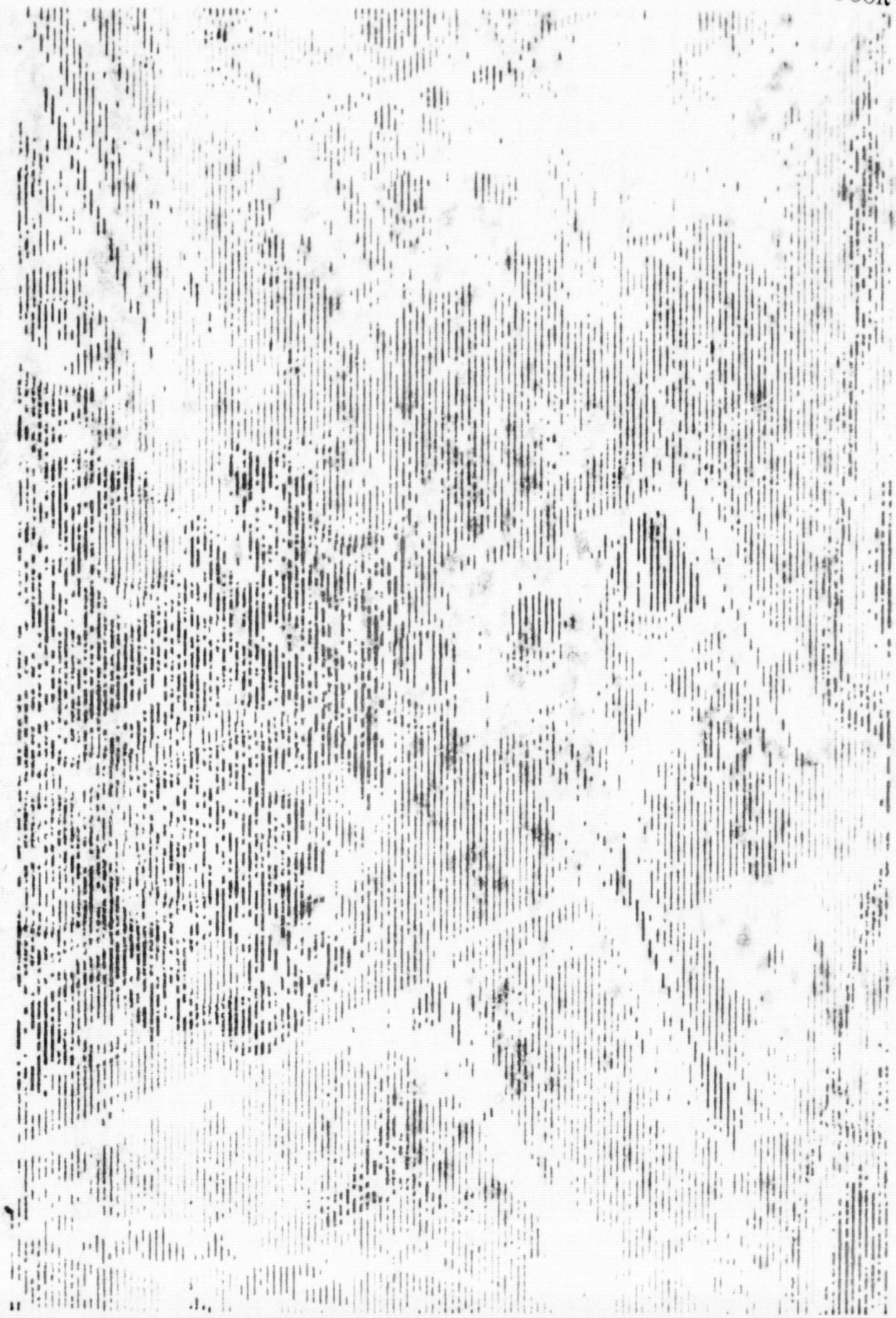

Figure 13, Isodensity Recording, Baytown, HH25

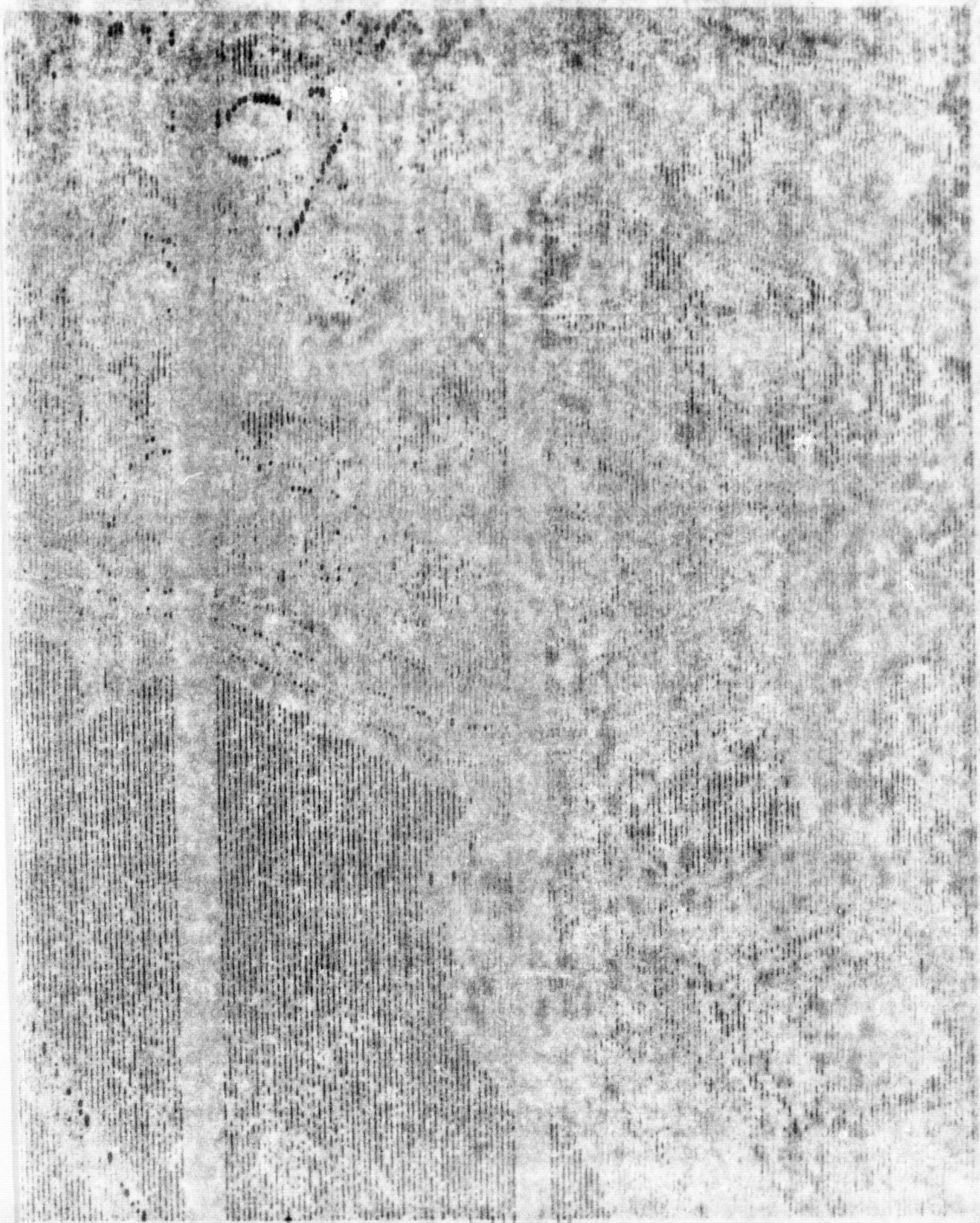

Figure 14 Isodensity Recording, Baytown, WR 89B

RURAL ENVIRONMENT

FIGURE 15: PARTICLE SCATTERING COEF. vs MASS CONC.[14]

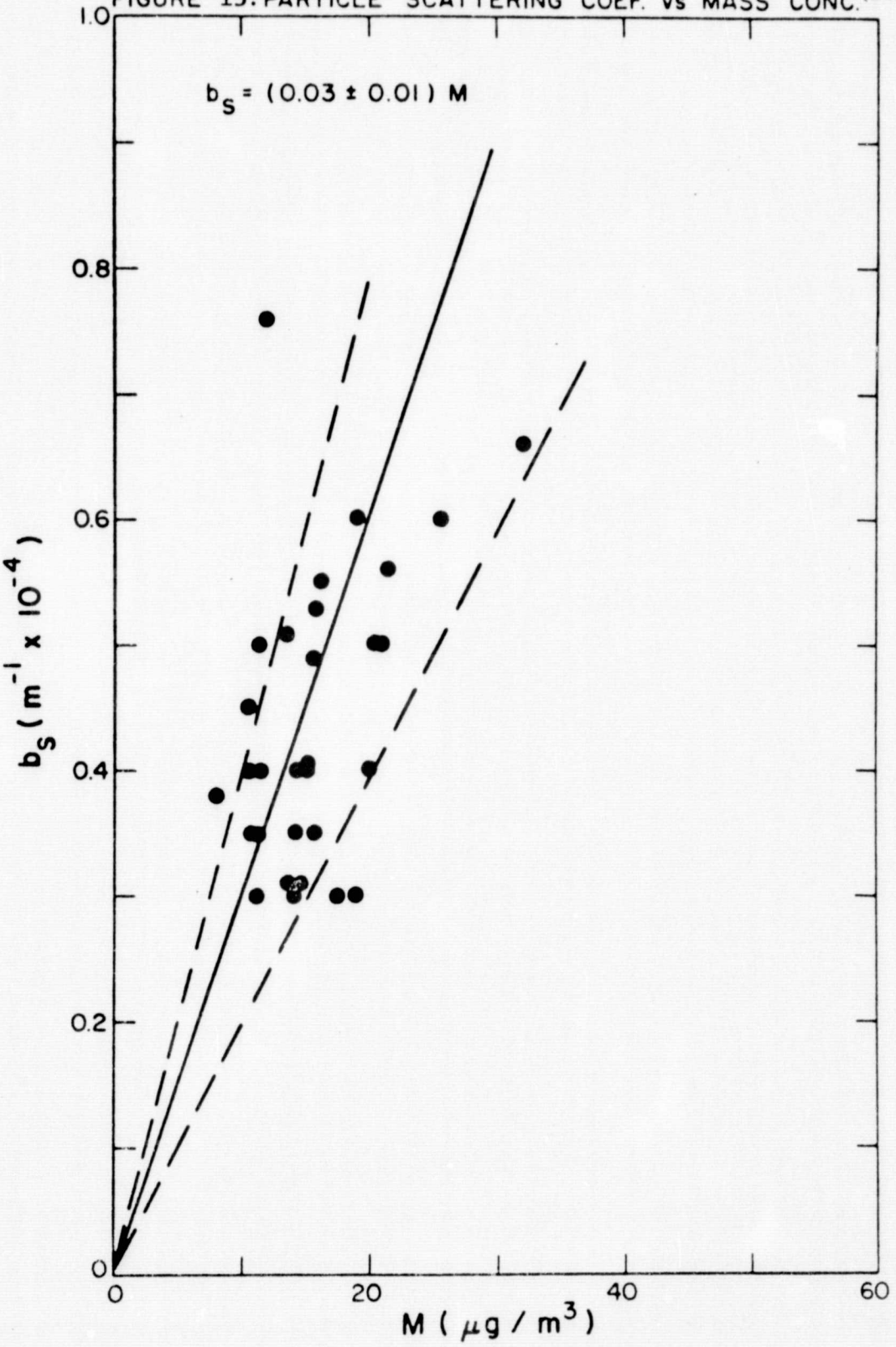

Figure 16, Particle Scattering Coefficient vs Mass Concentration - Urban Environment (21)

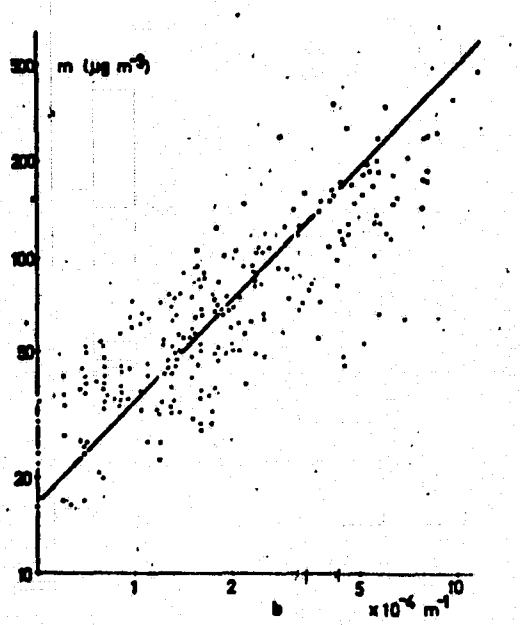

FIGURE 15. Measured mass concentration and light-scattering coefficient for atmospheric aerosols at different locations.

Table 4: Calculations of Extinction Coefficients, q_1, q_2

No.	$\log^{-1}\frac{D_3-D_2}{\gamma}$	T	$\frac{1}{T}$	$C=\frac{1}{T}-1$	$\ln C = -bx$	$b(10^{-4} \times m^{-1})$	$\frac{\log(\bar{b}_2/\bar{b}_1)}{\log(\lambda_2/\lambda_1)}$	q_x	Film Type	Location
1	$\log^{-1}6.38$	0.8048	1.2425	0.2425	-1.4168	4.648	$-\frac{0.2436}{0.1675}$	4.45	WR25*	Baytown
2	$\log^{-1}7.00$	0.8451	1.1833	0.1833	-1.6966	5.566			WR25	Baytown
3	$\log^{-1}7.09$	0.8507	1.1755	0.1755	-1.7401	3.028			WR25	Baytown
4	$\log^{-1}6.70$	0.8261	1.2105	0.2105	-1.5583	2.7116	$-\frac{0.3447}{0.1675}$		WR25	Ship Channel
5	$\log^{-1}6.87$	0.8369	1.1949	0.1949	-1.6353	2.8456		5.06	WR25	Ship Channel
6	$\log^{-1}7.09$	0.8507	1.1755	0.1755	-1.7401	3.0279			WR25	Ship Channel
7	$\log^{-1}6.64$	0.8222	1.2162	0.2162	-1.5316	2.6651			WR25	Ship Channel
8	$\log^{-1}6.64$	0.8222	1.2162	0.2162	-1.5316	2.6651			WR25	Ship Channel
9	$\log^{-1}6.64$	0.8222	1.2162	0.2162	-1.5316	2.6651			WR89B**	Baytown
10	$\log^{-1}6.57$	0.8176	1.2231	0.2231	-1.5001	2.6103			WR89B	Baytown
11	$\log^{-1}6.64$	0.8222	1.2162	0.2162	-1.5316	2.6651			WR89B	Baytown
12	$\log^{-1}6.07$	0.7732	1.2933	0.2933	-1.2266	2.1344			WR89B	Baytown
13	$\log^{-1}4.00$	0.6021	1.6609	0.6609	-0.4142	0.7207			WR89B	Baytown
14	$\log^{-1}3.85$	0.5854	1.7082	0.7082	-0.3450	0.6003			WR89B	Ship Channel
15	$\log^{-1}4.64$	0.6665	1.5004	0.5004	-0.6923	1.2047			WR89B	Ship Channel
16	$\log^{-1}5.28$	0.7226	1.3839	0.3839	-0.9432	1.6413			WR89B	Ship Channel
17	$\log^{-1}5.92$	0.7723	1.2948	0.2948	-1.2215	2.1255			WR89B	Ship Channel

*WR25 = 0.62μ

**WR89B = 0.90μ

The comparisons of respirable particulate mass from ground truth data with that calculated from remote sensor data are presented in Table 5. The first two values (m_1,m_2) were arrived at by a use of q calculated in Table 4 from the contrast remote sensor measurements and the formula derived from Figure 15.

$$\ln m = kq$$

where m is in $\mu g/m^3$ of air, q is the particle scattering coefficient and k is an empirical constant.

The second set of values are deduced in the same manner as the first set but the effective wavelength of Wratten Filter 89B was considered to be 0.80 microns instead of 0.90 microns as in the first case.

The third set of values ($\bar{m}_5$,$\bar{m}_6$) were estimated from ground truth data collected using high volume air samplers. These data points represent average values over time and can not be compared directly with the values calculated from remote sensor data. The data are shown in Figure 3 as represented by trend-surface analysis of the ground truth data. From computer calculated isopleths the average values ($\bar{m}_5$,$\bar{m}_6$) in the vicinity of the sites can be deduced.

The effective wavelength (λ_e) of the film/filter channels, necessary for all remaining calculations of the respirable particle size distribution, was established in the following manner. It was assumed that the film had a uniform response or sensitivity to light energy from 2500-7000A for plus X type 2402 and 6900-8400A for type 2424. Then let

$$\lambda_e = \lambda_a + \frac{1}{n} \int_a^b T_s(\lambda) I(\lambda) T_F(\lambda) d\lambda$$

where $E_T = \int_a^b T(\lambda) I(\lambda) T_F(\lambda) d\lambda$

E_T = the energy transmission factor

T_s = Transmittance of the atmosphere with a solar angle of 40°

I = Solar Spectral Irradiance outside the atmosphere in micro-watts x 10^2

T_F = percent efficiency of filter transmittance and a and b are the frequency limits set by each filter transmittance

$$\lambda_{ea} = E_T/n$$

where n = the number of incremental equal intervals. Then

$$\lambda_e = \lambda_{ea} + \lambda_a$$

where λ_a = the wavelength at which energy transmission begins. This expression was evaluated with a Taylor series expansion at intervals of 100A between 4000 to 4000 A, 250 A between 5000 to 7000 A, and 500 A between 8000 to 9000 A. The effective wavelengths for the filter/film combinations used in the remainder of the report are listed in Table 6.

Table 5: Comparisons of Mass Measurements, $\mu g/m^3$

Source	Ref.	Baytown Site	Ship Channel Site
Remote Sensing	$M_{1'2}$	210	305
Remote Sensing	$M_{3'4}$	150	200
Ground Truth	$\bar{M}_{5'6}$	50	100

$M_{1'2}$ = Calculated using Table 4 and Figure 15

$M_{3'4}$ = Calculated using 0.80 μ for WR89B and Figure 15

$\bar{M}_{5'6}$ = Estimated from computer isopleth values of 4 to 12 hour average high volume air sampler values, Table 2 and Figure 3.

Table 6: Film and Filter Data

Film Type Combination	b+w plus x 2402	2402	2402	2424	2402	2402
with filter	47B	57	25	89B	2A	29
Calculated mean Effective λ	4326A	5201A	6443A	7890A	5602	6550

VII. Mission HATS-175

On September 8, 1972, a heliocopter was utilized as the airborne sensor platform for Mission HATS-175. It was hypothesized that a hand-held, Hasselblad camera could be utilized as a remote sensor to determine through a vertical path the respirable particle size distribution of the atmospheric loading. The relationship of the scattering coefficient to altitude was also investigated. A comparison of the secondary target reflectance to the known reflectance spectrum of primary targets was also scheduled.

The heliocopter was instructed to hover at the positions shown in Table 8. Primary reflectance targets had been deployed at the Pasadena site. An individual in the heliocopter photographed the targets twice at each position, once using filter 2A, and once using filter 29. Sensitometry was requested on all imagery and is presented in Appendix C with the microdensitometry traces.

GROUND-TRUTH ACTIVITIES

Cooperative ground-truth activities were accomplished with the City of Houston, Pollution Control Section, Texas Air Control Services, Baytown Regional Office, and the Humble Refinery at Baytown. High-volume air samples were taken throughout the region by the above agencies and company. These samples make it possible to determine the total suspended particulate mass throughout the test site areas. The data are presented in Table 7.

Primary reflectance targets were deployed at the Pasadena target site and the Baytown target site. At the Pasadena site the white reflector was 20 ft. x 24 ft. and the black reflector was 15 ft. x 20 ft. These

were deployed on each side of the target storage tank.

At the Baytown site an 8 ft. x 6 ft. white target was deployed adjacent to the target tank. At that site a high-volume air sample was taken and several nephelometer measurements were made. These are presented in Table 8, Ambient Air Site Measurements.

At the Pasadena site a high-volume air sample, Anderson air sample, electrostatic precipitated aerosol sample, and nephelometer data were collected. The data from these samples are presented in Table 7, 8, and 10.

The Holmes Road Incinerator was chosen as a third target for remote sensing because the plume of smoke from the stack is usually in evidence. The helicopter was able to photograph plume just as the incinerator began to emit an effluent. It had been shut-down during the lunch hour.

The tank farms used for the secondary reflectance targets are shown in Figures 17 and 18. Accessory data taken from the heliocopter are presented in Table 9. The inversion layer was estimated to be at an altitude of 2,000 ft. from this data.

DATA PROCESSING

The frames from HATS-175 were identified and marked for microdensitometry. These traces appear in Appendix C. Data from ground-truth activities on September 8, 1972, were reviewed and made compatible with the computer format requirements. A trend-surface map of the suspended particulate concentration was then printed in the computer output (Figure 19).

The electron micrographs shown in Figures 20-24 were prepared by Mr. Wm. O'Hare under the direction of Dr. Ong of the UT Cancer Research

Table 7: High-Volume Air Sampling Data - Sept. 8, 1972

Suspended Particulates, $\mu g/m^3$

12 Noon to Midnight, 12-24 O'clock

Site		Mass
Deer Park		80.9
Pasadena		106.3
Houston	2	166.0
	3	142.0
	4	67.0
	5	91.0
	6	68.0
	7	87.0
	8	63.0
	9	90.0
	10	84.0
	12	153.0
	13	127.0
	14	111.0
	15	145.0
	16	199.0
	17	90.0
	18	66.0
	19	146.0
	20	75.0
	21	149.0
	22	48.0
	23	39.0
Baytown	Roseland Park	59.0
	1200 Park Street	123.0
	7200 Bayway	128.0
	Exxon Refinery, W. Side (5 hr.) 10:00 - 15:00	56.0

Institute. The samples had been taken as part of the previous ground-truth activities utilizing the electrostatic precipitator sampler. The necessary sample grids were prepared at the above laboratory and the electron micrographs were made. These were extremely difficult to obtain but could not be shown to be representative of air samples for technical reasons. Pertinent details are included in Table 11.

Table 8: Ground-Truth Data from Target Sites, Sept. 8, 1973

Pasadena (1) Anderson Air Sample, µg

Stage	
0	0.0005
1	0.0005
2	0.0003
3	0.0002
4	0.0007
5	0.0011
6	0.0007
7	0.0014

(2) Hi-Volume Air Sample, $\mu g/m^3$

10:00 to 15:35 (5 hrs., 35 min.)

$$\frac{0.0404g}{587m^3} = 67\mu g/m^3$$

(3) Electrostatic Aerosol Precipitator

13:20 to 15:35

Baytown (1) Hi-Volume Air Sample, $\mu g/m^3$*

10:00 to 14:00 (6 hrs., 0 min.)

$$\frac{0.2324g}{579.9m^3} = 400.8\mu g/m^3$$

*Road construction in vicinity

Table 9: Air Temperature (°C) at Selected Altitudes†

Site	Altitude in Feet					
	5000	2000	1500	1000	500	200
Baytown	20	27	29	28	29	31
Pasadena	20	27	--	30.5	31	32
Holmes Rd.	20	28	29.5	30	32*	**

*at 400 feet

**Below the stack plume

†Altimeter setting 31.10, EAFB = 40 MSL

Table 10: Particulate Size Distributions on Sept. 8, 1972

		number of particles per ft.^{3}, Royco #225				
Place	Time	0.3-0.5 μm	0.5-0.7 μm	0.7-1.4 μm	1.4-3.0 μm	3.0-10 μm
Baytown	11:20 a.m.	154,990	81,340	73,920	50,310	6,200
		138,260	109,780	68,490	101,170	12,460
		159,630	90,990	42,530	65,930	8,850
	3:07 p.m.	161,050	105,060	53,320	80,530	4,580
		158,140	87,250	39,490	74,340	5,300
		149,120	76,290	40,330	65,710	12,010
		131,860	84,680	42,950	69,380	6,500
Pasadena	10:12 a.m.	70,000	51,990	42,290	46,270	4,110
		69,770	53,490	41,090	51,250	4,680
		65,160	50,530	40,060	50,410	3,890
	1:00 p.m.	237,080	153,770	62,860	71,220	7,470
		533,340	136,110	57,240	59,250	5,580
		320,850	151,130	56,830	55,340	5,300
	1:20 p.m.	207,450	118,190	48,460	64,240	39,030
		285,230	137,980	69,580	6,490	2,220
		184,440	52,980	16,760		
	1:40 p.m.	134,690	76,360	29,350	2,210	990
		152,750	89,600	46,490	5,240	2,130
		137,700	42,930			
	2:00 p.m.	158,180	61,420	29,730	2,820	1,510
	Flight	221,980	134,440	56,060	5,010	1,530
	overhead			11,220	3,080	1,350
		193,610	98,150	30,340	4,180	2,260
	2:20 p.m.	214,560	163,770	70,190	6,770	2,410

Figure 17 Pasadena Site

Figure 18 Baytown Site

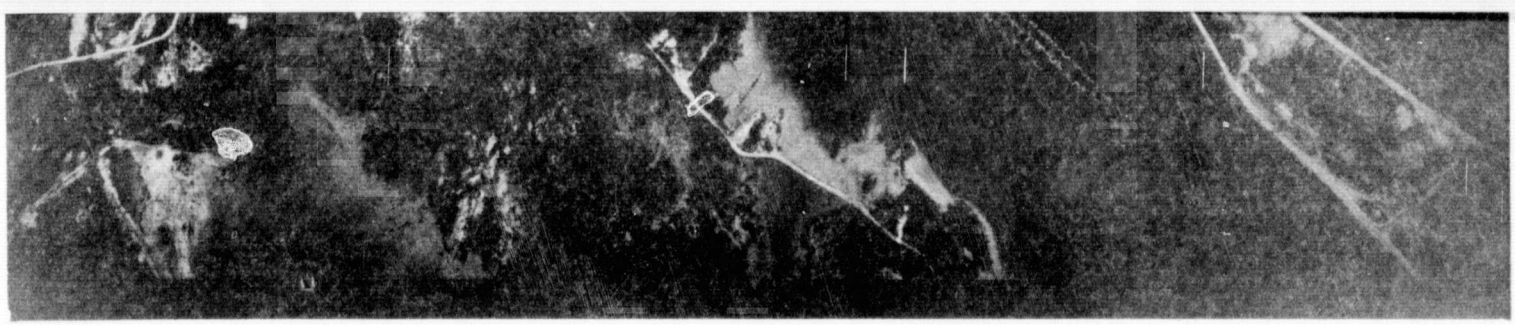

FIGURE 19

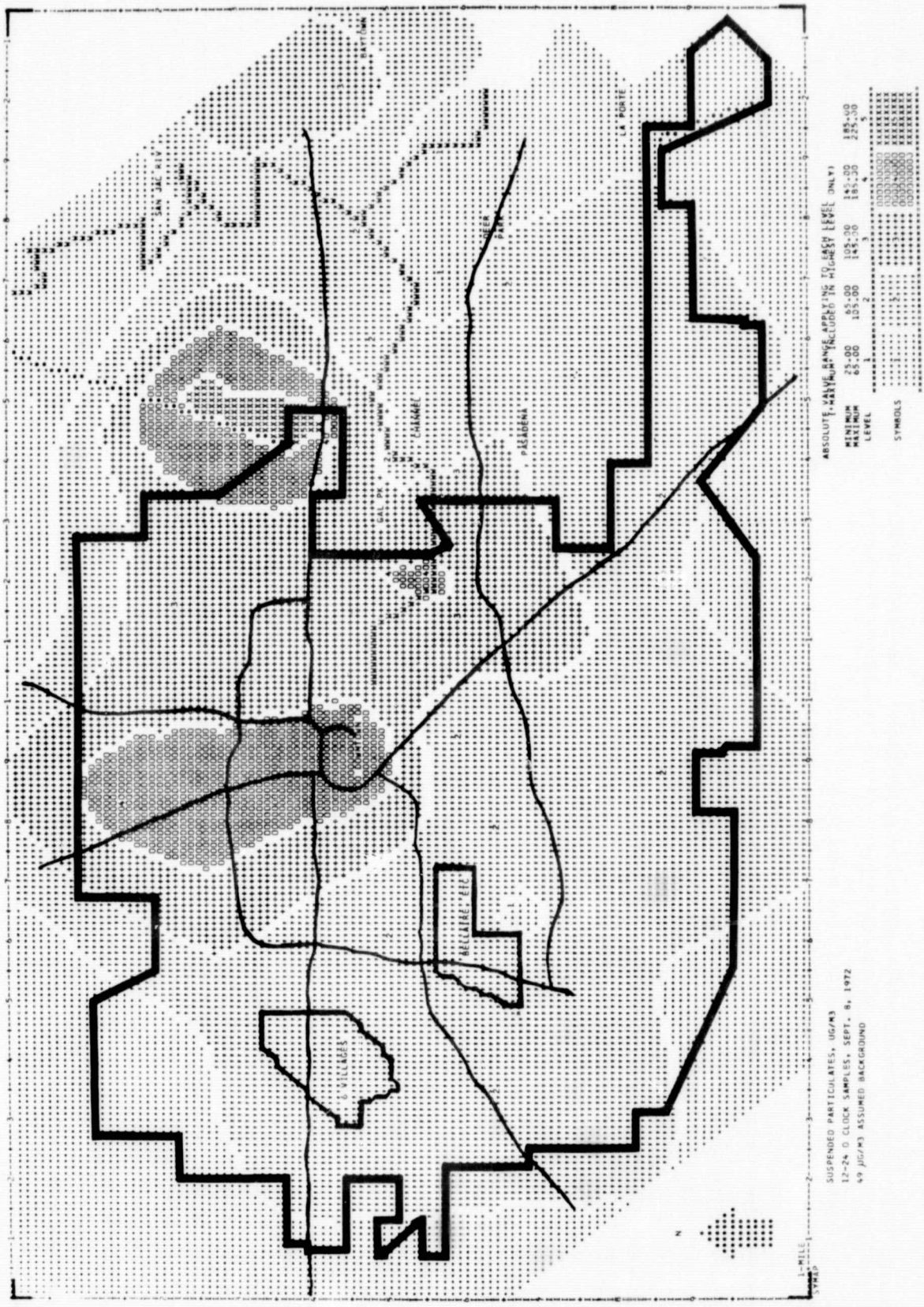
SUSPENDED PARTICULATES, UG/M3
12-24 O CLOCK SAMPLES, SEPT. 8, 1972
49 UG/M3 ASSUMED BACKGROUND
ABSOLUTE VALUE RANGE APPLYING TO EACH LEVEL (ONLY)
MINIMUM 23.00 65.00 105.00 145.00 185.00
MAXIMUM 65.00 105.00 145.00 185.00 225.00
LEVEL 1 2 3 4 5
SYMBOLS
1-MILE
N
LA PORTE
PASADENA
BELLAIRE
SAN JAC RIV
GAL PK
CHANNEL

Table 11: Details of Electron Microphotographs

Figure	Field	Sample Time	Magnification	Scale/cm
20	2/3	2 hours,	3,000 x	1.2 µm
21	4/3	4 hours,	3,000 x	1.2 µm
22	4	6 hours,	3,000 x	1.2 µm
23	7(same field as 4)	6 hours,	10,000 x	0.34 µm
24	11	6 hours,	10,000 x	0.34 µm

FIGURE 20

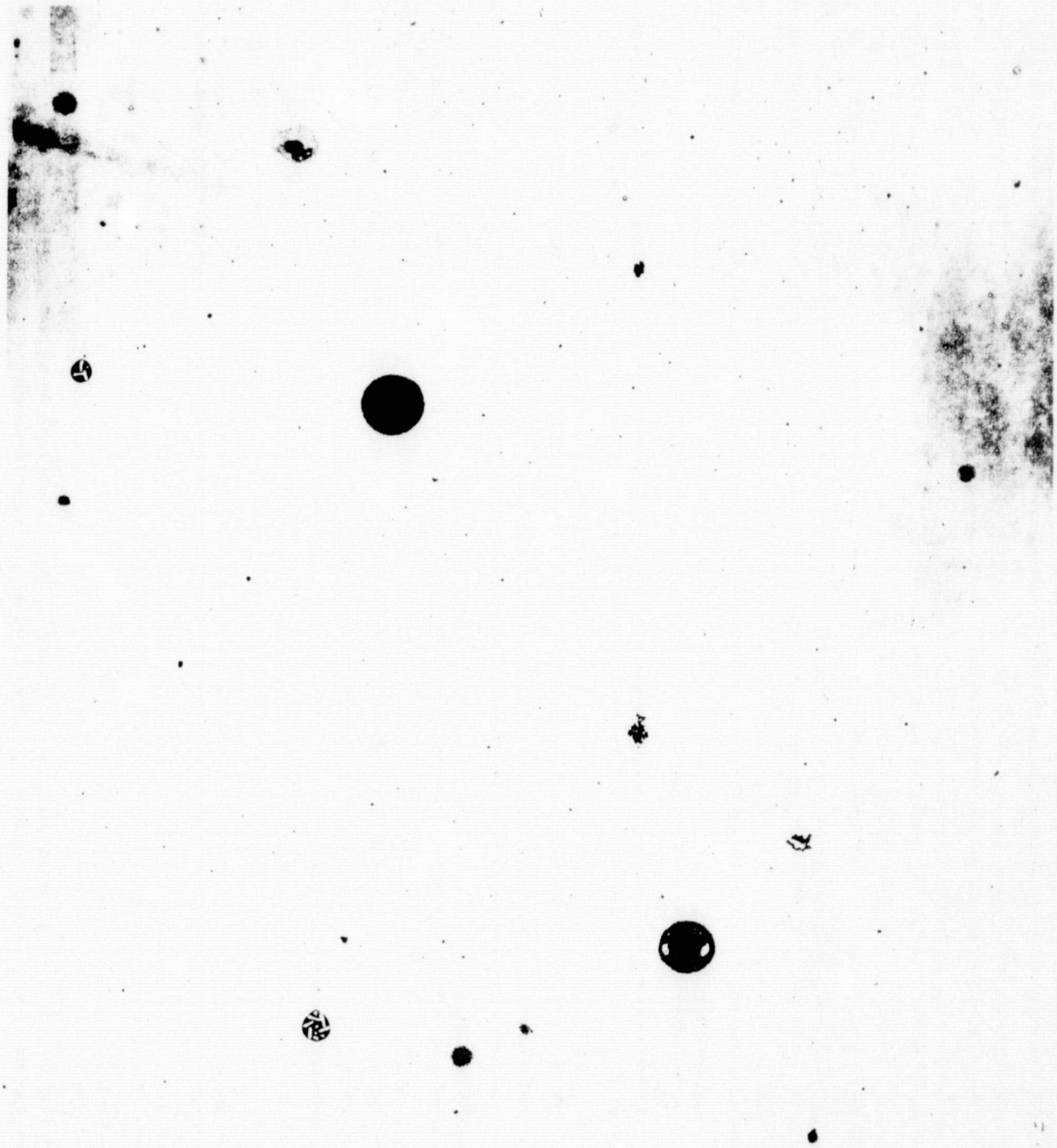

FIGURE 22

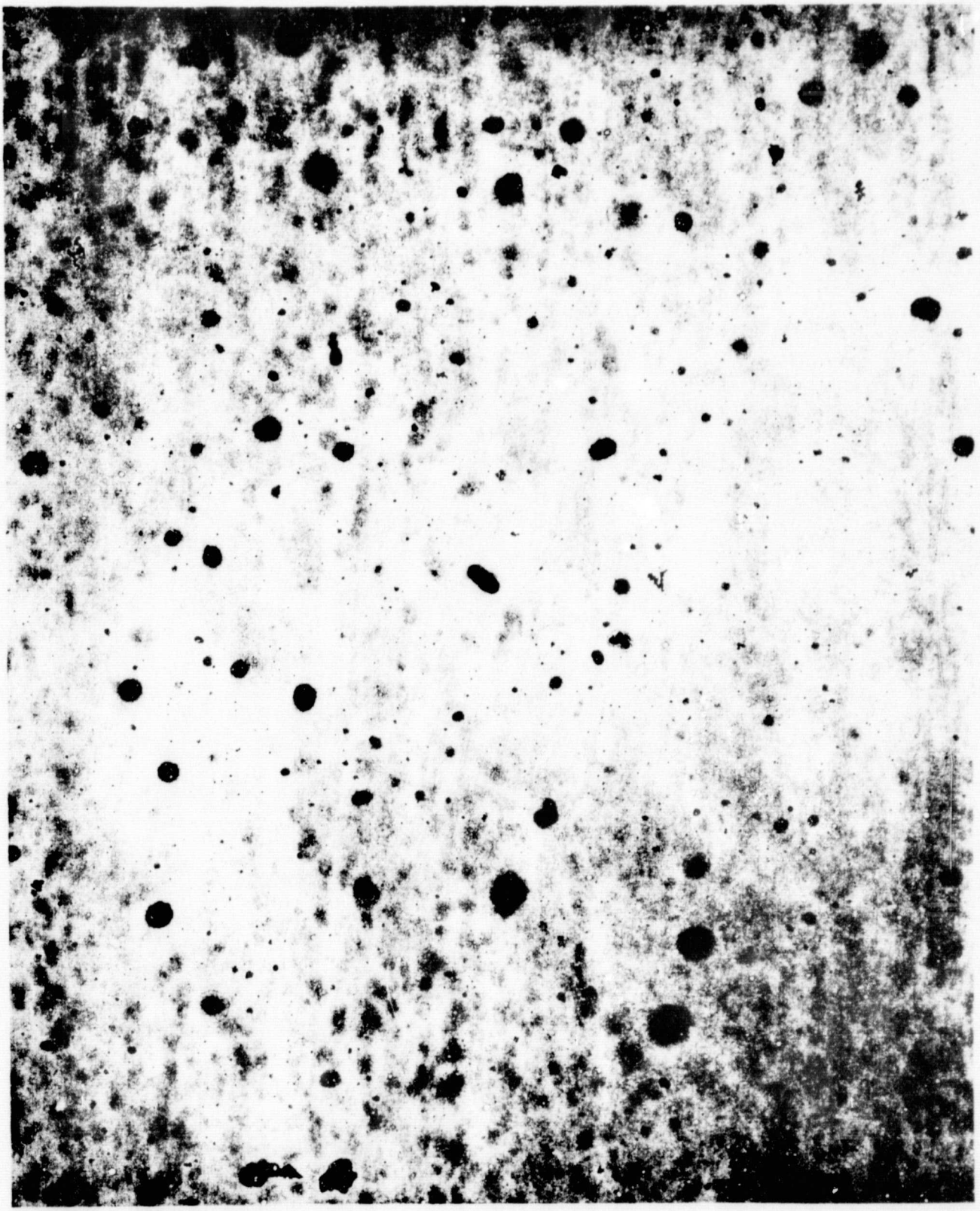

FIGURE 23

FIGURE 24

DATA ANALYSES

The principal investigator and Mr. Jack Peng began the data analyses when the densitometry traces were delivered. According to the plan shown in Table 12 the contrast imagery as photographed with the two types of filters could be compared.

The particle size distribution was established using a linear regression program on a Wang calculator with nephelometer data collected during the heliocopter flight of September 8, 1972. These regression analyses are presented in Appendix C. Of much interest was the particle size distribution determined by weight which was somewhat different (Figure 25).

The densitometry traces were compared with the photographs to identify the targets traced. Calibration curves were prepared for each series from the accompanying step-wedge densities. The target film densities were then measured as centimeters on the densitometry traces and converted to comparable density numbers with the use of the calibration curves. This data is presented in Table 13.

The overall extinction coefficient of the aerosol distribution was calculated using the two different film/filter combinations. The extinction coefficients and the corresponding altitudes are presented in Table 14. The extinction coefficients calculated from nephelometry data are presented in Table 15.

All primary reduction of remote sensor data was accomplished through the coordinating efforts of the Public Health Ecology Section at NASA. These records, enclosed in the appendix, were interpreted by the principal investigator. This procedure was followed throughout the research project.

TABLE 12: DATA SETS FOR PHOTOGRAPHIC COMPARISONS, SEPT. 8, 1972

	ALTITUDES			
PLACE	2000'	1000'	500'	200'
Baytown		45,44	51,52 46,47	53,54
Pasadena	(15,16), (13,14)	(11,12), (10,9)	(5,6), (7,8)	(1,2), (3,4)

FIGURE 25 . Particle Size Distribution

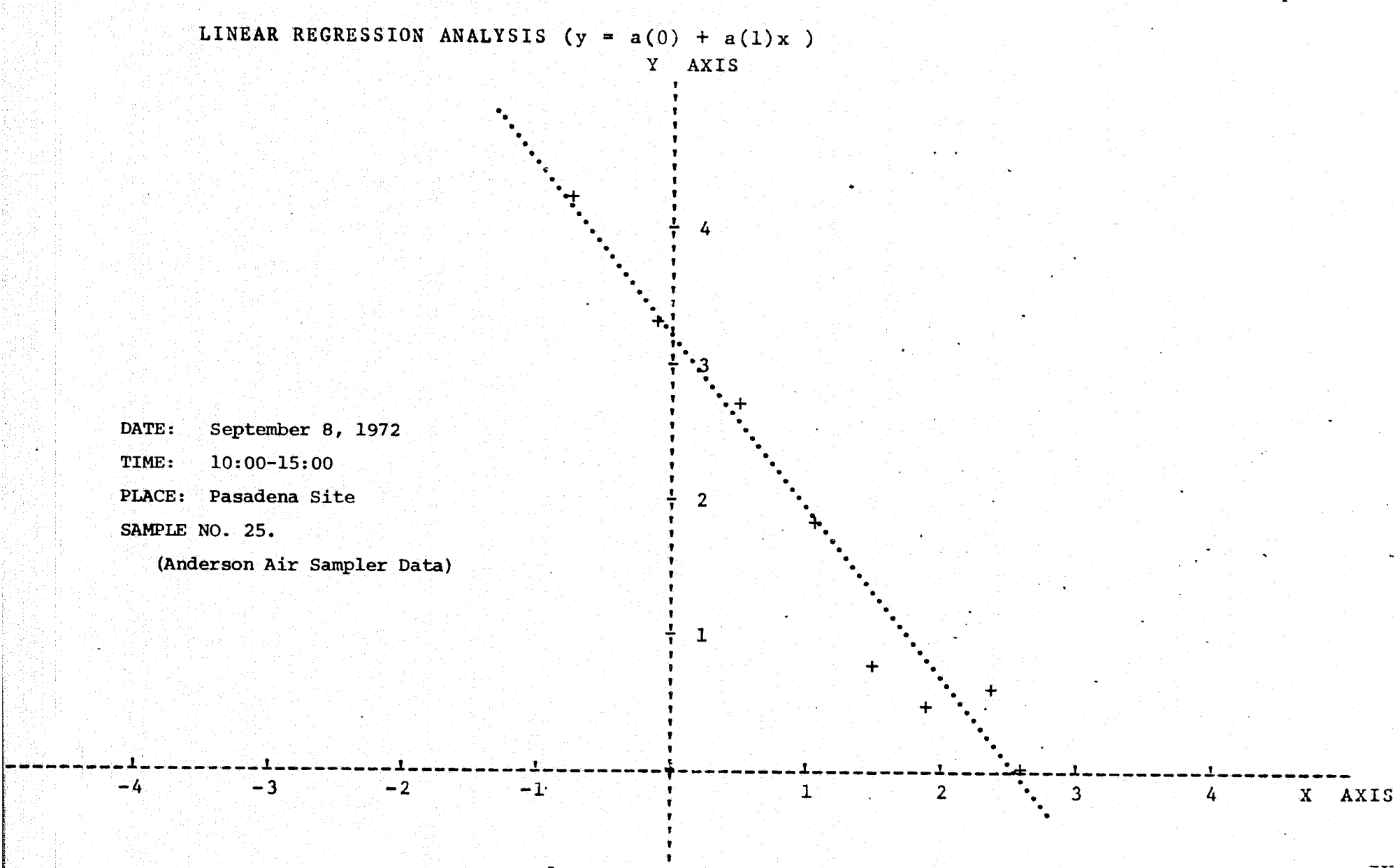

TABLE 13 DENSITOMETRY DATA FROM HELIOCOPTER FLIGHT

(Ship Channel, Sept. 8, 1972)

FRAME	RATIO	TARGET	cm.	LOG E	D	PAIRS
1	5:1	Tank Shadow	13.3-0.3	1.57	2.275	(1,2), (3,4)
		Grass	4.5	0.51	1.35	
2	5:1	Tank Top	1.3	0.18	0.87	
		Tank Side	6.0 ± 1	0.65	1.46	
		Shadow	14.3-0.3	1.66	2.85	
		White SQ	2.1	0.30	1.12	
3	5:1	Tank Top	1.6	0.21	0.97	
		Tank Side	6.0 ± 1	0.65	1.46	
		Shadow	14.3-0.3	1.66	2.85	
4	5:1	Black Sq	11.0	1.28	1.87	
		Grass	4.0	0.46	1.30	
		Top Tank	1.6	0.21	0.96	
5	10:1	Black Sq	11.5	1.35	1.93	(5,6), (7,8)
		Grass	7.0	0.81	1.54	
		White Sq	1.3	0.21	0.96	
6	10:1	Tank Top	1.3	0.21	0.96	
		"Side"	5.3	0.63	1.45	
		Shadow	13.0	1.60	2.36	
		White Sq	1.4	0.22	0.98	
7	10:1	Tank Top	1.2	0.20	0.94	(5,6), (8,7)
		Shadow	14.0 ± 0.3	1.66	2,85	
		White Sq	1.3	0.21	0.97	

TABLE 13: (CON'T) DENSITOMETRY DATA FROM HELIOCOPTER FLIGHT

(Ship Channel, Sept. 8, 1972)

FRAME	RATIO	TARGET	cm.	LOG E	D	PAIRS
8	10:1	Black SQ	12.5 ± 1.0	1.47	2.08	
		Grass	7.0 ± 1.0	0.81	1.54	
		White SQ	1.5	0.23	1.00	
9	10:1	Tank Top	0.9	0.19	0.90	
		Shadow	13.3	1.60	2.36	
		Grass	10.0 ± 0.5	1.19	1.80	
		White SQ	1.1	0.22	0.98	
10	10:1	Black SQ	11.5 - 0.5	1.37	1.95	
		Grass	6.5 ± 1.0	0.55-0.63	1.4-1.46	
		White SQ	1.3	0.23	1.00	
11	10:1	Black SQ	10.5	1.25	1.84	
		Grass	6.5 ± 0.5	0.63-0.73	1.4-1.5	
		White SQ	1.0	0.20	0.94	
12	10:1	Tank Top	0.9	0.19	0.90	(11,12), (10,9)
		Tank Shadow	12.0	1.43	2.02	
		White SQ	0.9	0.19	0.90	
13	50:1	Tank Top	0.6	0.15	0.77	
		Grass	3.5	0.42	1.26	
		White SQ	0.8	0.17	0.83	
		Tank Shadow	[10.4 (11.7 Peak max.)]	[1.19 (1.35)]	[1.79 (1.93)]	
14	50:1	Black SQ	8.5	0.94	1.63	
		White SQ	0.7	0.16	0.80	
		Grass	5.0	0.55	1.39	

TABLE 13:(CON'T) DENSITOMETRY DATA FROM HELIOCOPTER FLIGHT

(Ship Channel, Sept. 8, 1972)

FRAME	RATIO	TARGET	cm.	LOG E	D	PAIRS
13	20:1	Tank Top	0.8	0.19	0.90	(13,14), (15,16)
		Shadow	10.0	1.19	1.79	
		White SQ	1.0	0.20	0.94	
14	20:1	Black SQ	8.0	0.93	1.62	
		Grass	6.5 ± 0.5	0.68	1.48	
		White SQ	1.1	0.22	0.98	
15	50:1	White SQ	1.4	0.23	1.00	
		Tank Top	0.8	0.17	0.83	
		Shadow	7.9	0.86	0.80	
16	50:1	Black SQ	7.1	0.75	1.51	(15,16), (13,14)
		White SQ	1.2	0.21	0.96	
		Grass	4.3	0.50	1.34	
47	10:1	Grass	4.3	0.54	1.38	47,46
		Shadow	9.9	1.10	1.73	
		Top Tank	0.0	0.12	0.64	
46	10:1	Top Tank	0.1	0.14	0.74	
		Shadow	10.4	1.16	1.77	
		Grass	5.4	0.64	1.46	
		Side of Tank	1.1	0.22	0.98	
		Top Tank	0.2	0.15	0.77	
45	10:1	Grass	4.4	0.54	1.38	45,44
		Shadow	8.5	0.99	1.65	

TABLE 13: (CON'T) DENSITOMETRY DATA FROM HELIOCOPTER FLIGHT

(Ship Channel, Sept. 8, 1972)

FRAME	RATIO	TARGET	cm.	LOG E	D	PAIRS
45	10:1	Top Tank	1.2	0.24	1.02	
44	10:1	Road(Grass)	4.0	0.50	1.34	
		Shadow	10.3	1.15	1.76	
		Top Tank	0.1	0.12	0.64	
		Side of Tank	5.0	0.58	1.42	
43	10:1	Side of Tank	4.0	0.50	1.34	
		Shadow	9.2	1.50	2.12	
		Top Tank	0.2 (Step 7)	0.15	0.77	
		Grass	---			
49	10:1	Road & Grass	3.4	0.44	1.28	49,48
		White SQ	1.2	0.24	1.02	
		Tank Top	0.7	0.18	0.87	
		Tank Shadow	7.1	0.80	1.54	
48	10:1	Black SQ	5.4	0.64	1.46	
		Ditch Grass	4.7	0.55	1.39	
		Tank Shadow	7.1	0.80	1.54	
		Tank Top	0.8	0.19	0.90	
44	20:1	Grass	5.2	0.56	1.40	
		Shadow	10.6	1.22	1.81	
		Top Tank	0.3	0.12	0.62	
45	20:1	Tank Side	4.1	0.47	1.31	
		Grass	4.9	0.54	1.38	
		Shadow	8.8	0.96	1.64	

TABLE 13:(CON'T) DENSITOMETRY DATA FROM HELIOCOPTER FLIGHT

(Ship Channel, Sept. 8, 1972)

FRAME	RATIO	TARGET	cm.	LOG E	D	PAIRS
45	20:1	Top Tank	0.4	0.13	0.69	
46	20:1	Top Tank	1.0	0.18	0.87	46,47
		Side of Tank	5.6	0.59	1.43	
		Grass	8.0	0.87	1.58	
		Shadow	10.5	1.21	1.81	
47	20:1	Top Tank	0.4	0.13	0.69	
		Shadow	10.0	1.14	1.76	
		Grass	4.8	0.53	1.37	
49	50:1	Road & Grass	3.0	0.35	1.19	(49,48)
		White SQ	0.6	0.15	0.77	
		Tank	0.2	0.10	0.53	
		Tank Shadow	6.5	0.67	1.47	
48	50:1	Black SQ	5.4	0.58	1.42	
		Ditch Grass	4.3	0.49	1.33	
		Tank Shadow	6.6	0.68	1.48	
		Tank Top	0.3	0.12	0.64	
50	20:1	Grass	4.0	0.51	1.35	(46,47 & 50 Same frame)
		Shadow	8.0	0.91	1.61	
		Tank Top	0.2	0.10	0.53	
51	5:1	Tank Top	1.0	0.19	0.83	51, 52
		Shadow	10.9	1.27	1.07	
		Grass	6.5	0.77	1.52	

TABLE 13:(CON'T) DENSITOMETRY DATA FROM HELIOCOPTER FLIGHT

(Ship Channel, Sept. 8, 1972)

FRAME	RATIO	TARGET	cm.	LOG E	D	PAIRS
52	5:1	Tank Top	1.0	0.19	0.83	
		Tank Side	8.0	0.91	1.61	
		Shadow	11.5	1.35	1.93	
		Grass	7.0	0.83	1.56	
53	5:1	Tank Top	0.7	0.15	0.77	53, 54
		Tank Side	4.2	0.53	1.37	
		Shadow	11.1	1.30	1.88	
		Grass	7.0	0.83	1.56	
54	5:1	Tank Top	0.6	0.14	0.74	
		Shadow	12.5	1.49	2.11	
		Tank Side	5.2	0.63	1.46	
		Grass	5 - 8	0.6 - 0.9	1.4 - 1.6	

Table 14: Extinction Coefficients vs Altitude, HATS-175*

Site	Altitude, ft.	q_x	Value
Pasadena	200	q_1	3.3331
"	500	q_2	1.0438
"	500	q_5	2.1364
"	1000	q_3	1.2019
"	1000	q_4	2.9322
"	2000	q_6	1.7205
"	2000	q_7	1.5453
		$\bar{q}_1$	$= 1.9876 \pm 0.8660\sigma$
Baytown	200	q_{15}	1.5940
"	500	q_{10}	2.7065
"	500	q_{13}	2.2795
"	500	q_{14}	0.0127
"	1000	q_8	2.6373
"	1000	q_9	-0.6855
"	1000	q_{11}	1.5567
"	1000	q_{12}	2.1703
		$\bar{q}_2$	$= 1.5339 \pm 1.2419\sigma$

*From these data no significant difference between the $\bar{q}_1$ and $\bar{q}_2$ may be detected at the 90% confidence level.

Table 15: Extinction Coefficients from Nephelometer Data, HATS-175

Site	q_x	Value	Time Interval
Pasadena		1.1465	1300-1400
		1.4336	
		1.3525	
		0.5283	
		1.8383	
		2.4588	
		1.9127	
		1.6410	
		2.8745	
		1.7520	
		1.9159	
		1.1320	
		1.6989	
		$\bar{q} = 1.6680 \pm 0.5953\sigma$	
Baytown		1.0511	
		0.7615	
		0.9056	
		1.1353	
		1.0496	
		0.7592	
		0.9452	
		$\bar{q} = 0.9439 \pm 0.1461\sigma$	

Further examination of the aerial photography made it possible to discard some of the contrast values. When q_1, q_9, q_{14}, q_{15} were neglected the $\bar{q}_1$ for Pasadena was 1.526 and $\bar{q}_2$ for Baytown was 2.1573.

RESULTS, HATS-175

A visual inspection of the aerial photography easily revealed that the heliocopter had not hovered in a manner satisfactorily to keep the zenith angle at a tolerable minimum. Thus the angle of solar light reflected from the targets was not constant from one frame to the next, perhaps accounting for the wide range of extinction coefficients calculated. This hovering instability also may account for the inability to detect a change in q with altitude or change of targets. Indeed, the extinction coefficients were not calculated utilizing data from primary targets as the contrast was not as great as that of the secondary targets. The film/filter channels were also too broad to be very discriminating. Yet a comparison of the ground truth data analyses with those from the remote sensor reveals a remarkably close value for the ship channel, Pasadena site extinction coefficient, 1.668 vs 1.526 for the latter. The Baytown values were not in agreement, 0.9439 compared to 2.153. However, road dust from construction work may have caused the discrepancy. On Figures 17 and 18 it can clearly be seen that a non-uniform mixture of aerosols existed in the atmosphere. These appear as wisps of smoke or contrast changes.

A matter of further interest was revealed by the calculation of the extinction coefficient from the Anderson Air Sampler data. q was 3.1560. This is based on dry weight data and approximates the expected value as reported in the literature. Lower values often occur if a

wet aerosol has formed in the atmosphere. Again, although the relative humidity was less than 70 when the data was collected the morning had been humid with relative humidities greater than 70. Thus the hygroscopic aerosol had not lost its moisture at the time of the overflight and ground-truth activities. The method did reveal the moist aerosol loading of the atmosphere.

The correlation of mass measures with wet aerosol extinction coefficients is known to be fraught with difficulties which cumulate in unpredictability. Thus mass correlations were not completed for this mission. However, a use of figure 15 with the dry weight extinction coefficient shows a mass loading of approximately 70 $\mu g/m^3$ of air. The other on site measure was 67 $\mu g/m^3$ of air which shows good agreement for the ground-truth capabilities.

VIII. Mission #216-175

GROUND-TRUTH ACTIVITIES

A mission was flown, #216-175, on October 3, 1972. Ground truth activities were performed by the principal investigator, Mr. Bill O'Hare, Mr. Jack Peng, Mr. Steve Bryan and contract monitor, Dr. Howard Schneider. Sufficient advance warning of the flight data was given so that both of the air pollution air monitoring systems were activated and high-volume air samples of suspended particulates were collected. The results are shown in Table 16. An air stagnation advisory alert was issued that morning. The data from the Baytown area were reported by the Texas Air Pollution Control Services. Particle size distribution data collected at secondary reflectance targets, storage tanks in Pasadena and Baytown, are presented in Table 17. The high volume air samples of suspended particulates taken at the target sites yielded the following results in Table 18. Road construction was again noted at the Exxon, Baytown target site and undoubtedly accounts for the skewed particle size distribution reported in Table 17 and the high volume air sample at Baytown. Electrostatic precipitation of ambient air aerosols was accomplished but later electron micrographs revealed that the density of particulates per field was too small to permit the establishment of a particle size distribution without a very long, greater than 24 hours, time period.

DATA PROCESSING

The film from Mission 216-175 was reviewed and the appropriate frames were identified for microdensitometry processing. These traces appear in Appendix D. Contact color prints and 2" x 2" slides of the areas were ordered for identification purposes and are shown in Figures 26 and 27. The target areas were observed at 1652071 through 1703587

Table 16: Suspended Particulates, $\mu g/m^3$, Oct. 3, 1972

12-24 O'clock Hi-Vol Samples

	Site No.	Weight
Houston	2	215.2
	3	196.8
	4	94.3
	5	141.1
	7	170.0
	8	121.3
	9	151.2
	10	122.8
	11	110.2
	12	96.5
	13	88.3
	14	151.0
	15	105.5
	16	116.2
	17	170.8
	18	106.7
	19	223.3
	20	96.8
	23	93.6
Deer Park	1	99.2
Pasadena	2	155.9
Baytown	3	79.0

Table 17: Particulate Size Distributions on October 3, 1972

		number of particles per ft^3, Royco #225				
Place	Time	0.3-0.5 μm	0.3-0.7 μm	0.7-1.4 μm	1.4-3.0 μm	3.0-10 μm
Baytown	13:05[1]	42,170	12,587	5,527	2,131	724
		37,759	12,180	7,987	3,156	539
		56,961	16,531	5,466	2,311	829
Pasadena	10:32[2]	66,034	23,287	14,706	7,722	396
		62,171	21,186	12,632	7,579	579
	11:15[3]	68,024	19,484	5,194	2,833	179
		49.740	17,000	6,296	3,456	148
		43,367	14,933	5,993	3,570	186
	12:10[4]	73,130	24,452	7,312	3,977	205
		70,142	26,271	6,605	2,942	154
		92,228	23,453	6,446	2,744	150
		80,021	26,068	7,956	4,187	220
		72,175	18,569	5,913	3,257	202

1. WB/DB = 71/84 or 51% R.H.
2. WB/DB = 64/74 or 58% R.H.
3. WB/DB = 66/76 or 59% R.H.
4. WB/DB = 68/80 or 54% R.H.

Table 18: Suspended Particulates, $\mu g/m^3$, at Targets, 10-3-72

Place	Sampling Time	Weight
Pasadena	1030-1400	79.3
Baytown	1100-1400	380.9

Table 19: MICRODENSITOMETRY DATA, MISSION #216-175, 10-3-72

FRAME	RATIO	TARGET	DENSITY		
22-154	200/1	Tank Top	0.40	D_1	
(Ship Channel)		Tank Shadow	0.90	D_2	
WR 47B		Grass	0.78	D_3	
22-136	200/1	Tank Top	0.35	D_1	
(Baytown)		Tank Shadow	0.95	D_2	
WR 47B		Grass	0.87	D_3	
21-154	200/1	Tank Top	0.11	D_1	
(Ship Channel)		Tank Shadow	0.47-0.52	D_2	
WR 25		Grass	0.33	D_3	
21-136	200/1	Tank Top	0.11	D_1	
(Baytown)		Tank Shadow	0.55	D_2	
WR 25		Grass	0.27	D_3	
			LOG E		DENSITY
23-154	20/1	Tank Top	0.18	D_1	0.87
(Ship Channel)		Tank Shadow	0.65	D_2	1.46
WR 57		Grass	0.81	D_3	1.54
23-136	20/1	Tank Top	0.22	D_1	0.98
(Baytown)		Tank Shadow	0.82	D_2	1.55
WR 57		Grass	0.96	D_3	1.64
04-192		Tank Top	0.43		1.27
(Ship Channel)		Tank Shadow	0.82		1.55
WR 89B		Grass	0.59		1.43
04-210		Tank Top	0.33	D_1	1.15
(Baytown)		Tank Shadow	0.86	D_2	1.58
WR 89B		Grass	0.66	D_3	1.47

FIGURE 26 Ship Channel Site Area (a)

C.2

FIGURE 27 Ship Channel Site Area (b)

Greenwich time. The flight altitude was 5000 ft.

A comparative analysis of the microdensitometry traces with the original frames of film resulted in Table 19 in which contrast values for the secondary reflectance targets are presented. These values were then used to calculate q, the total aerosol size distribution extinction coefficient.

The film/filter channels were much narrower in mission 216-175 than HATS-175 and were similar to those of the first study presented herein as depicted in Table 6. Thus several channel combinations were available from which q could be calculated. Accordingly q was calculated from all possible combinations as shown in Table 20. The calculated values of the extinction coefficients are presented in Table 21.

The extinction coefficient of the total suspended aerosol size distribution was also calculated from the nephelometer data in the regressions analyses. The power law was assumed as the ideal distribution function as previously discussed and the data was regressed on that function. The ground truth data was taken many times during the day but not simultaneously at both sites. However, the distribution appeared not to change substantially from one time to another. The sampling times are in Appendix D and the calculated extinction coefficients are presented in Table 22.

The high volume air sampling data from the City of Houston and State of Texas air sampling networks, as shown in Table 16, was checked for compatibility to computer format and submitted for computer mapping. The resultant isopleth map is presented in Figure 28. The 12 hour average mass appears to be about 145 $\mu g/m^3$ at the Pasadena site while the Baytown site averaged about 80 $\mu g/m^3$. This can be compared to the 79.3 and

Table 20: Extinction Coefficients from Film/Filter Combinations #216-175, 3 October 1972

Mission Film Roll	21-154-25	22-154-47B	23-154-57	04-192-89B
		Ship Channel Site Pasadena		
21-154	---	q_{16}	q_{21}	q_{24}
22-154	---	---	q_{20}	q_{25}
23-154	---	---	---	q_{18}
04-192	---	---	---	---

Mission Film Roll	21-136-25	22-136-47B	23-136-57	04-210-89B
		Baytown Site		
21-136	---	q_{17}	q_{23}	q_{26}
22-136	---	---	q_{22}	q_{27}
23-136	---	---	---	q_{19}
04-210	---	---	---	---

Table 21: Extinction Coefficients q, Mission 216-175, 3 October 1972 Remote Sensor Data

Extinction Coefficient	Site	Value
q_{16}	Pasadena	3.6236
q_{17}	Baytown	3.7780
q_{18}	Pasadena	4.6639
q_{19}	Baytown	3,6207
q_{20}	Pasadena	2.3849
q_{21}	Baytown	4.6892
q_{22}	Baytown	3.2775
q_{23}	Baytown	4.2075
q_{24}	Pasadena	3.7949
q_{25}	Pasadena	3.9651
q_{26}	Baytown	3.0547
q_{27}	Baytown	3.5542

Baytown $\bar{q}_1 = 3.8536$

$s_1 = 0.8462$

Pasadena $\bar{q}_2 = 3.5821$

$s_2 = 0.4006$

There is no significant difference between the total means of each site at the 90% confidence level.

Table 22: Extinction Coefficients, q, Mission 216-175, 3 October 1972 Ground-Truth Data

Pasadena	Baytown
1.9989	1.3889
1.9519	1.4275
1.8178	1.4496
1.9847	
2.1087	
2.1717	
1.9910	
1.9560	
$\bar{q}_1 = 1.9975$	$\bar{q}_2 = 1.4220$
$s_1 = 0.1062$	$s_2 = 0.0307$

380.9 $\mu g/m^3$ that were measured respectively as a 3 hour average during the flight time (Table 18). As previously stated mass prediction based on extinction coefficients have been reported to follow the form $\ln m = kq$ where k is an empirical constant for each area. The relationship between mass and scattering coefficient established nationally and presented in Figure 15 may also be used to predict mass loading. These methods are all summarized in Table 23.

RESULTS: MISSION 216-175

The extinction coefficients determined by data from the film/filter combination broad wavelength channels are much more precise than those determined on Mission-HATS-175. The standard deviation is much smaller in every case. However, the difference between the extinction coefficients determined by ground truth methods versus remote sensor methods is significantly different at each site. It is probable that the remote sensor data yielded the most representative extinction coefficient for the ambient air aerosol loading. The relative humidity at both sites had been low, below 65, for several days and visibility was good. However, local ground conditions influenced the ground truth site measurements unduly. It was not possible to place the high volume air sampler closer than 300 feet from the Baytown gas storage tank while it was within 20 feet of the road where construction work continued. The meteorological conditions were such that a breeze was blowing at low altitudes from Galveston Bay. This undoubtedly accounts for the sea aerosol type extinction coefficient measured at ground level.

The Pasadena site was not far from cooling towers and a steel plant. These sources of small particulates certainly affected visibility although not the relative humidity measurements. The high mass loading

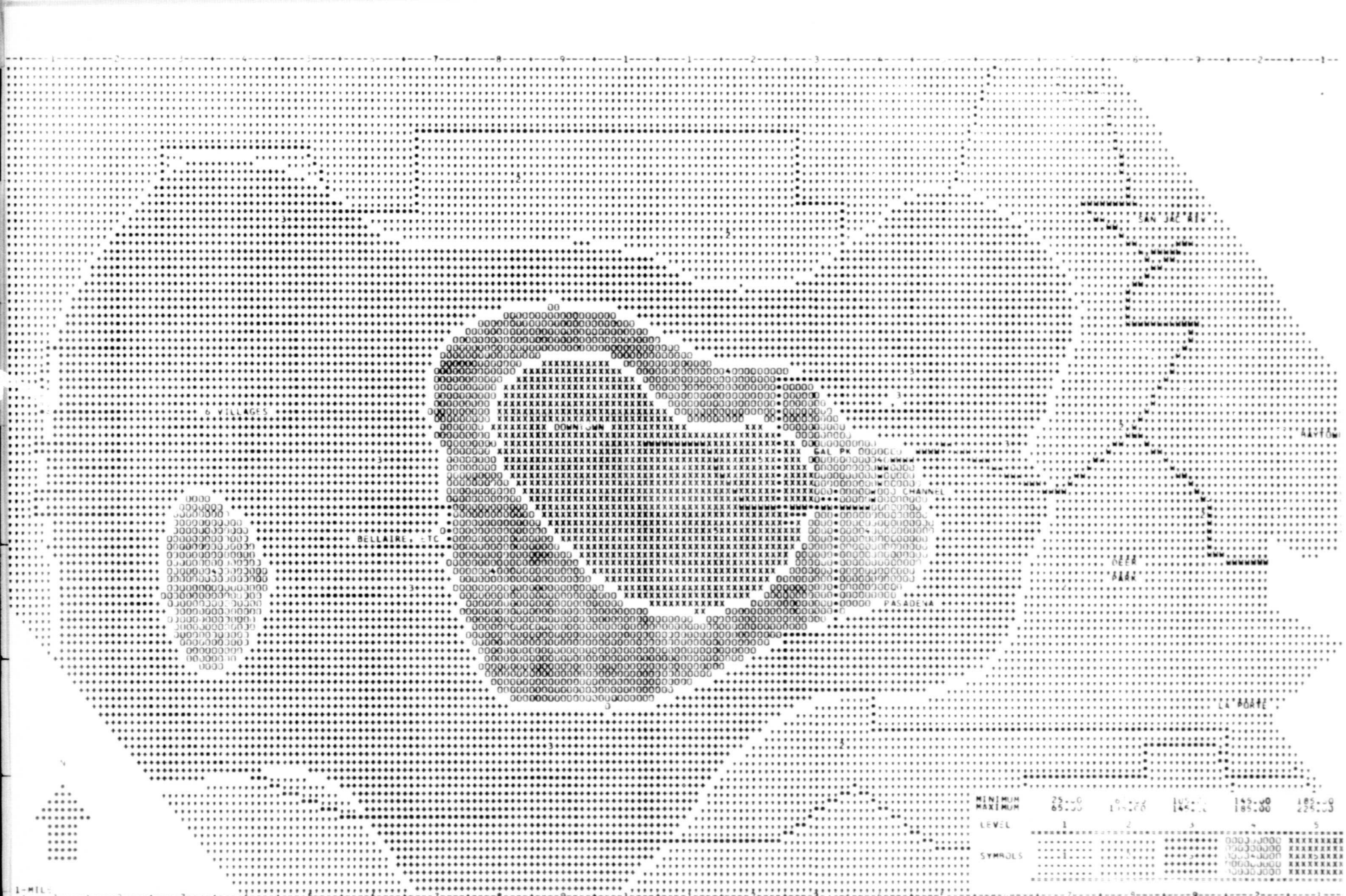
6 VILLAGES
DOWNTOWN
BELLAIRE, ETC
SAN JACINTO
GAL PK
CHANNEL
DEER PARK
PASADENA
LA PORTE
MINIMUM 25.:0 65.:0 105.:0 145.:0 185.:0
MAXIMUM 65.:0 105.:0 145.:0 185.:0 225.:0
LEVEL 1 2 3 4 5
SYMBOLS
1-MILE MAP
1.337 MINUTES FOR MAP
TIME = 1.418
C SUSPENDED PARTICULATES, UG/M3
C 12-24 O'CLOCK SAMPLES, OCTOBER 1, 1972
C 93 UG/M3 ASSUMED BACKGROUND

Figure 28

was successfully predicted from remote sensor measurements when the national average figure was used.

This was the final mission for which all data was analyzed.

Table 23: Mass Prediction from Extinction Coefficients

Mission HATS-175

$k = \ln m/q$ at Pasadena

$k = 4.2268/1.597$ m = 68.5, q from ground-truth

$k = 2.6467$

Mission 216-175

$k = 4.3820/3.5821$ at Pasadena

$k = 1.2233$ m = 80, q from remote sensor data

$m = e^{kq}$

Site	Measured $\mu g/m^3$	Predicted $\mu g/m^3$	k Used	q Used
Baytown	381 (3-hr.)	111.5	1.2233	3.8536(r.s.)
Pasadena	80 (3-hr.)	79.9	1.2233	3.5821(r.s.)
Pasadena	145 (12-hr.)	11.5	1.2233	1.9975(g.t.)
Baytown	80 (12-hr.)	5.69	1.2233	1.4220(g.t.)
Baytown	381 (3-hr.)	13,104	2.6467	3.8536(r.s.)
Pasadena	80 (3-hr.)	26,884	2.6467	3.5821(r.s.)
Pasadena	145 (12-hr.)	197.7	2.6467	1.9975(g.t.)
Baytown	80 (12-hr.)	43.1	2.6467	1.4220(g.t.)

Site	Measured $\mu g/m^3$	Predicted From Figure 15	q Used
Baytown	80 (12-hr.)	160	3.8536(r.s.)
Pasadena	145 (12-hr.)	140	3.5821(r.s.)
Pasadena	145 (12-hr.)	65	1.9975(g.t.)
Baytown	80 (12-hr.)	40	1.4220(g.t.)

XI. MISCELLANEOUS GROUND TRUTH DATA

ERTS, 27 NOVEMBER 72

Further ground-truth activities were carried out in connection with an Earth Resources Technological Satellite pass over Houston between 11:00 to 12:00 noon on November 27, 1972. Again, the City of Houston, ambient air quality network collected 12 hour high-volume air samples of suspended particulates. These data are presented in Table 24.

Only a cursary review of the data indicates the day was not one of heavy pollution although the expected levels are found downtown and along the ship channel industrial area. The number of particulates in each size range was again measured using the Royco #225 Nephelometer. This was done at the Houston Department of Public Health (Site #7). These data are presented in Table 25. The relative humidity was less than 70% when the satellite passed overhead. However, the aerosol load represented that of a wet aerosol since the humidity had only recently dropped.

The high volume air sample data was made compatible with computer format requirements and an isopleth map of the data in Table 24 was generated. This in Figure 29.

The linear regression analyses are included in Appendix E while the extinction coefficients calculated from them are tabulated in Table 26.

MISSION 227-175, 27 APRIL, 1973

A mission was flown, #227-175, on April 27, 1973. Ground-truth activities were performed by the project personnel. It was not possible to utilize either state or city pollution networks as April 28, 1973, was a regularly planned sampling period date and the previous day is always

used to set up the equipment. However, the nephelometer data collected is shown on Table 27. The high-volume air sampler data is included there also.

The secondary reflectance target areas are located at the General American Tank Storage Company in Pasadena, Texas and the Exxon refinery in Baytown, Texas as before. Again the Wang computer was used to determine the extinction coefficient a (1) for each particle size distribution. Jung Power Law was postulated and a linear regression line was fitted to the data. The coefficients of that linear equation describe the resultant particle size distribution. These are presented in attached twenty-one unnumbered figures in Appendix F. The extinction coefficients calculated from those ground truth data are presented in Table 28.

The linear regression analyses of the Anderson High-Volume 5-Stage Sampler is presented in Figure 30. Typically, The extinction coefficient q of 3.2981 is different than that determined by the Royco Air Pollution Monitor (nephelometer) which was about 1.900.

No film data was requested or analyzed for this mission. Since a multichannel analyzer was on board and operational, that data would be best analyzed first. However, a new black secondary reflectance target would have to be designated since the shadow limb of the white tank used in these studies is too narrow to be resolved by present multichannel analyzers. This results in a lessening of the contrast ratio and an unrepresentative value for the shadow.

Table 24- Suspended Particulates, $\mu g/m^3$, Nov. 27, 1972

12 hour Hi-Vol Samples

Site No.	Weight
2	93.6
3	82.0
4	46.7
5	72.4
6	57.3
7	51.5
9	52.5
10	47.0
11	39.3
12	51.3
13	65.7
15	91.9
16	103.6
17	56.4
18	82.6
19	122.9
20	65.8
21	63.0
22	62.6
23	29.2
1DP	72.5
2P	94.3

Table 25- Particle Size Distributions on November 27, 1972

number of particles per ft^3, Royco #225

Place	Time	0.3-0.5 μm	0.3-0.7 μm	0.7-1.4 μm	1.4-3.0 μm	3.0-10 μm
#7	900[1]	10,448	6,094	4,536	3,225	317
		11,321	5,891	4,690	3,278	305
		11,581	6,122	4,592	3,520	294
	1115[2]	10,775	6,345	5,230	3,350	343
		11,086	6,199	5,526	3,427	348
	1320[3]	10,460	5,135	3,568	2,372	217
		8,439	4,736	3,696	2,104	200
	1500[4]	7,881	4,341	3,445	2,616	256
		7,982	4,268	3,314	2,335	232

1. WB/DB = 58/61, 89% R.H.
2. WB/DB = 66/73, 69% R.H.
3. WB/DB = 67/78, 56% R.H.
4. WB/DB = 68/77, 63% R.H.

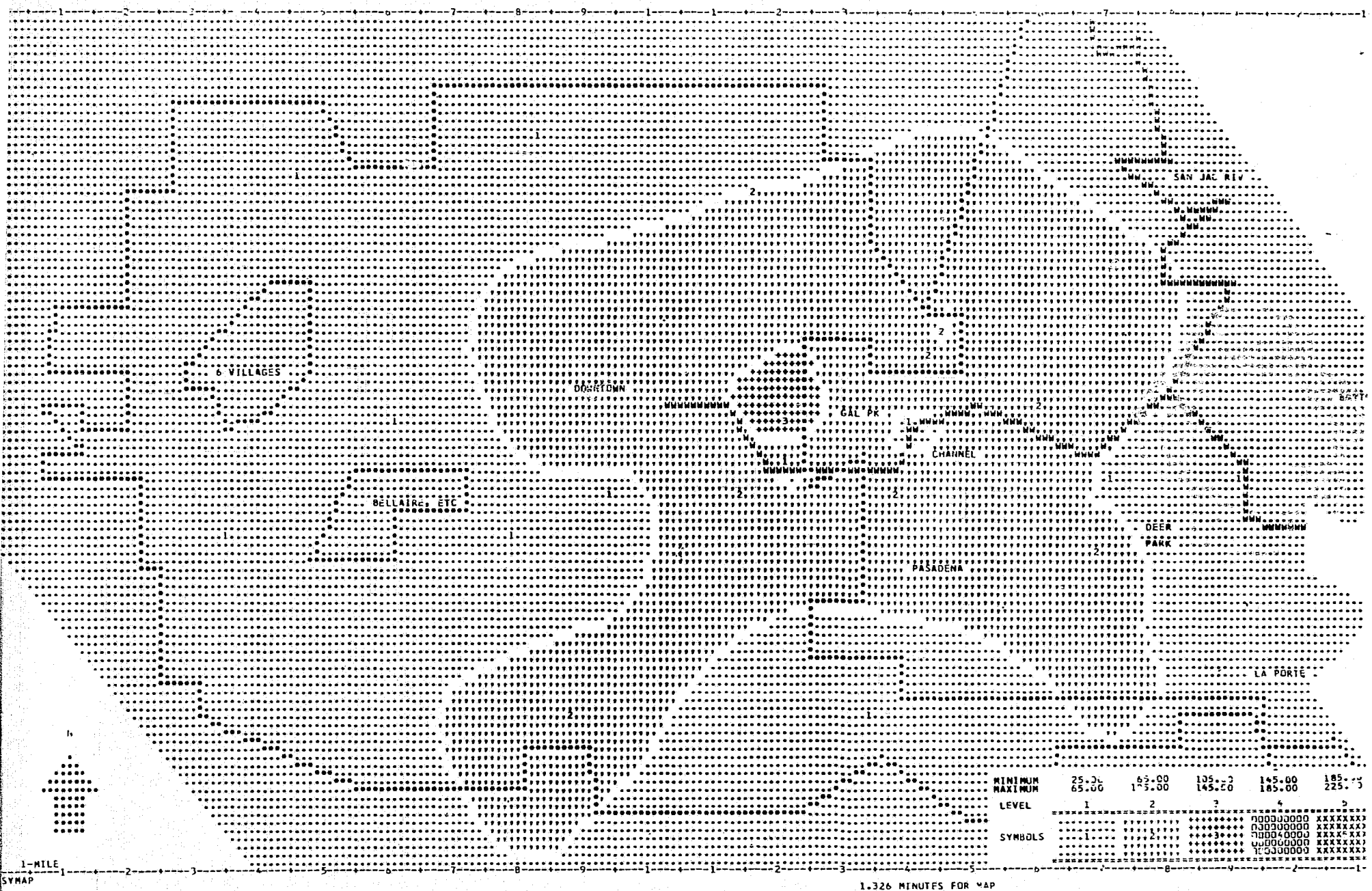

1.326 MINUTES FOR MAP
TIME = 2.837

C SUSPENDED PARTICULATES, UG/M3
C 12-24 O'CLOCK SAMPLES, NOVEMBER 27, 1972
C 35 UG/M3 ASSUMED BACKGROUND

Figure 29

Table 26: Extinction Coefficients from Ground-Truth, 27 November 1972

Site H-7	q	Time
Medical Center	1.1603	900
	1.1865	910
	1.2015	920
	1.1499	1115
	1.1481	1125
	1.2819	1320
	1.2592	1330
	1.1212	1500
	1.1647	1510

TABLE 27: Ground-Truth Data

Site: Pasadena, Houston Ship Channel

Date: April 27, 1973

A. High Volume Sampler: 22 hours 47.72 $\mu g/m^3$
(11 a.m.-9 a.m. next day)

B. Anderson High-Volume Sampler: 7 hours
(10 a.m.-5 p.m.)

Size (μm)	7,7	3.3-7.0	2.0-3.3	1.1-2.0	collection plate
Conc ($\mu g/m^3$)	11.97	11.20	9.42	4.08	35.54

C. Royco Air Pollution Monitor - Nephlelometer Data

Number of particles per cubic foot of air

Sample	Date	Time	Temp. (°F)	Humidity (%)	0.3-0.5 μm	0.5-0.7 μm	0.7-1.4 μm	1.4-3.0 μm	3.0-10.0 μm
1	4-27-73	9:25 a.m.	61/66	75	443,470	180,030	83,600	24,180	620
2		9:50 a.m.	61/67	71	386,080	148,620	63,910	1,890	400
3		10:25 a.m.	61/67	71	422,460	224,190	100,120	50,900	4,380
4		10:55 a.m.	62/68	71	274,780	138,930	44,930	15,370	640
5		11:20 a.m.	63/70	68	687,310	275,090	106,210	57,830	1,260
6		11:30 a.m.	63/71	64	423,870	220,960	66,670	38,780	1,720
7					438,890	239,980	68,430	48,630	1,650
8					467,320	223,760	75,750	57,590	1,550
9					451,490	233,070	72,420	48,970	2,800
10					451,280	244,170	69,240	41,080	1,240
11					396,060	218,210	67,160	39,010	1,240
12		12:05 p.m.	62/71	60	481,180	190,410	54,300	31,920	1,660
13					514,510	209,990	51,010	29,310	780
14					430,130	182,840	41,500	23,800	980
15					320,190	135,210	41,010	32,500	1,130
16[saw airplane flying]					365,770	146,920	37,820	29,510	1,100
17		12:30 p.m.	61/71	56	331,630	137,730	36,010	26,330	1,690
18					335,080	137,850	34,020	26,080	910
19					297,610	133,070	31,220	24,060	950
20					257,680	128,230	29,600	21,900	970
21					307,820	142,600	33,260	21,510	900

Table 28: Extinction Coefficients, q, from Ground-Truth Data, 27 April 1973

Sample No.	Neplelometer Data		
	Site	q	Time
1	Pasadena	1.511	9:25
2	"	2.6178	9:50
3	"	1.5760	10:25
4	"	2.1283	10:55
5	"	1.8778	11:20
6	"	1.8950	11:30
7	"	1.9065	11:30
8	"	1.9171	11:30
9	"	1.7360	11:30
10	"	2.0289	11:30
11	"	1.9844	11:30
12	"	1.9262	12:05
13	"	2.2132	12:05
14	"	2.0873	12:05
15	"	1.8881	12:05
16	"	1.9489	12:05
17	"	1.7840	12:30
18	"	1.9893	12:30
19	"	1.9464	12:30
20	"	1.9072	12:30
21	"	1.9980	12:30
	Anderson Air Sampler Data, 5 Stages		
	Pasadena	3.2981	1000-1700

Figure 30:

LINEAR REGRESSION ANALYSIS (y = a(0) + a(1)x)

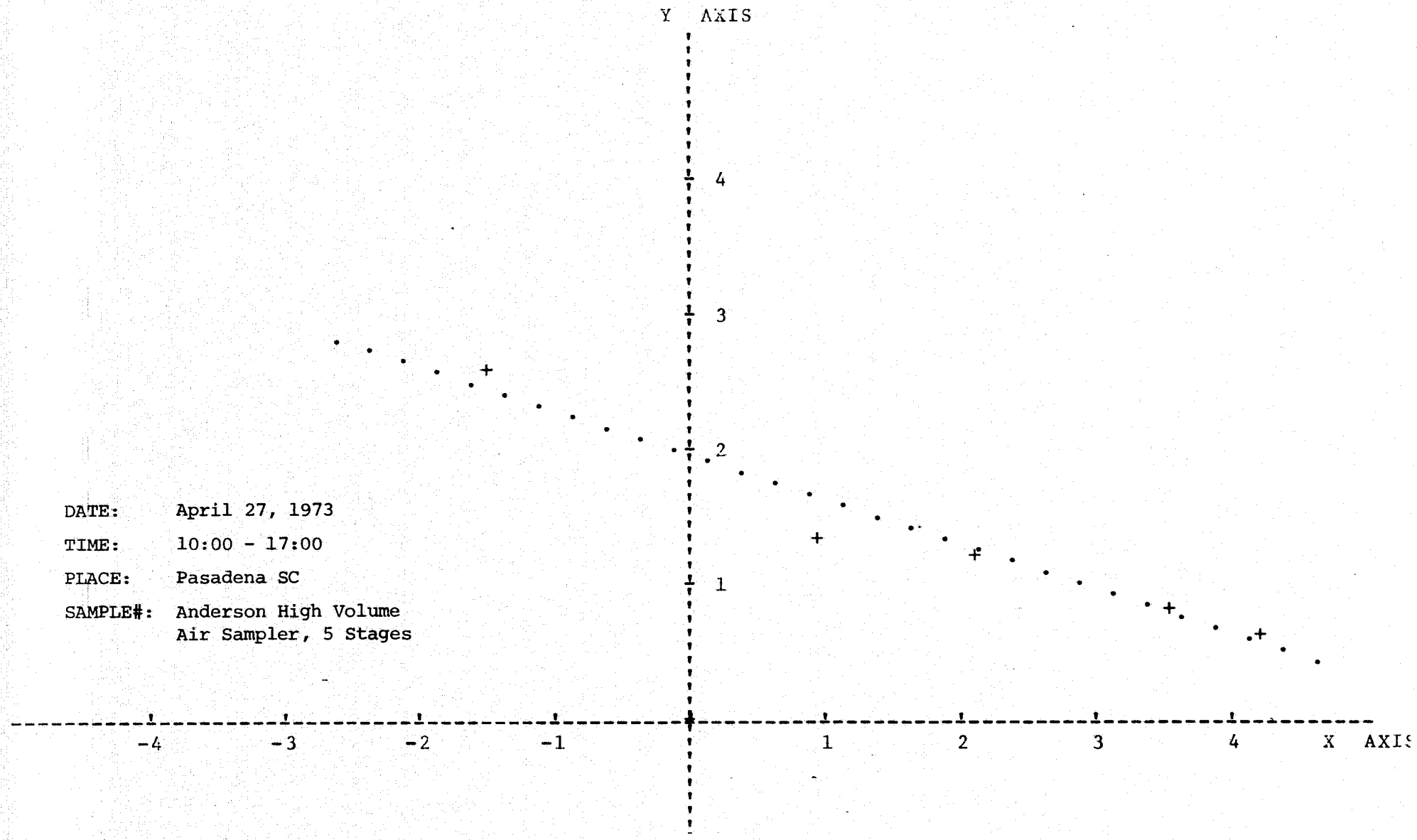

DATE: April 27, 1973

TIME: 10:00 - 17:00

PLACE: Pasadena SC

SAMPLE#: Anderson High Volume
Air Sampler, 5 Stages

3.873669251 = a(0)
-3.298139886 = a(1)
-.976332786 = r
.297283852 = S(x.y)

ONE X AXIS UNIT = .200000000
ONE Y AXIS UNIT = 2.000000000

X. CONCLUSIONS AND RECOMMENDATIONS

The results of this study are not conclusive but do indicate that some of the characteristics of the ambient respirable aerosol concentration can be monitored with remote sensors from high air/space platforms. Most easily measured is the extinction coefficient q, of the aerosol size distribution. This then can be used to predict the mass loading on a time averaged basis. Thus far the prediction of mass loading has not been highly successful but several characteristics have emerged. A 24 hour mass loading of the ambient atmosphere representative of large areas is more likely to be predicted successfully utilizing q than anything representative of purely local ground conditions. The extinction coefficient q can itself be shown to distinguish between aerosols which have sorbed moisture and those that are relatively dry. In fact the extinction coefficient q calculated from remote sensor data is far more closely related to relative humidity than that q calculated from nephelometric ground truth measurements.

Recommendations for future research include the following:

1. ERTS or other satellite frequency band data should be utilized to calculate extinction coefficients for the aerosol size distribution contained under the temperature inversion.

2. These techniques should be utilized with active remote sensors. The Environmental Protection Agency Remote Sensing Laboratory at Las Vegas, Nevada has developed the capability to determine inversion altitudes with lasers mounted in airplanes. A joint program should be explored.

3. Passive or active remote sensors should be used which have well known, narrow, frequency bandwidths. The multi-band spectral analyzer

is an example of one such preferred sensor.

4. New contrast targets should be chosen that can be resolved (defined) with multichannel analyzers or other narrow multi-band frequency sensors. A new black secondary reflectance target would be most useful since it would also eliminate some difficulties in the analyses. The shadow limb of the white tank used in these studies as the black secondary reference standard was thought to be too narrow to be resolved with present multichannel analyzer capability.

5. Gaseous air pollutants which cause degradation of health in humans should be monitored by remote sensors by utilizing the spectral qualities of these pollutants, e.g., organic gases, oxides of nitrogen, carbon monoxide, ozone, and exploiting the concepts and techniques herein developed.

Appendix

A. Typical Flight Log

B. Microdensity Traces

C. HATS-175

   1. Microdensitometry Traces

   2. Linear Regression Analyses of Particle Size Distribution

D. Mission 216-175

   1. Microdensitometry Traces

   2. Linear Regression Analyses of Particle Size Distribution

E. Linear Regression Analyses of Suspended Particulate Distributions November 27, 1972.

F. Linear Regression Analyses of Suspended Particulate Distributions April 27, 1973

APPENDIX A

TYPICAL FLIGHT LOG

NATIONAL AERONAUTICS AND SPACE ADMINISTRATION

LOCAL SUPPORT FLIGHT REQUEST FOR EARTH OBSERVATIONS AIRCRAFT PROGRAM

TO: *(Transmit Original)*
NASA-Manned Spacecraft Center
Earth Observations Aircraft Program Office
ATTN: TC
Houston, Texas 77058

PART I

TEST SITE *(Name and Number)*: Houston Ship Channel, Texas/ 175	APPLICATION DISCIPLINE: Public Health Ecology
AIRCRAFT REQUESTED: [X] NP3A [ ] RB57F [ ] [illegible] [ ] OTHER	FLIGHT DATE REQUESTED: December 1971
TYPE OF MISSION: [X] APPLICATIONS DATA GATHERING [ ] SENSOR DEVELOPMENT	FLIGHT TIME REQUESTED: 20 minutes

NAME OF PRINCIPAL INVESTIGATOR	ORGANIZATION	TELEPHONE
Dr. Richard Severs	UTSPH at Houston	526-5683
Dr. Charles E. Fuller	NASA-MSC	483-3108

INVESTIGATOR'S SIGNATURE: 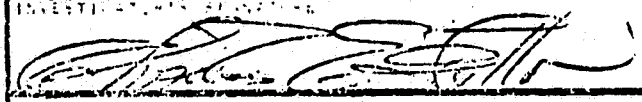

DATE:

PART II (EOAP)

DATE RECEIVED	LOG NUMBER	MISSION MANAGER

APPROVAL SIGNATURE (MANAGER, EOAPO): DATE:

REMARKS:

MSC Form 1038 (Aug 71) PAGE 1 OF 4

PART III

OBJECTIVES

Identify the scientific correlations, and relationships, which may exist between remote sensing information and groundtruth data describing respirable particulates which cause degradation of the air environment and endanger human health. This new program will use remote sensing to assess those facets which exert a marked influence on health and health-related activities.

PART IV

FLIGHT OPERATIONS *(Describe the operational constraints and requirements which must be considered for the flight; e.g. maximum/minimum altitudes, cloudiness, sun angle, tidal cycles, etc. Describe the flight line markers to be employed for the day and/or night flights.)*

1. Altitude 5,000 feet.
2. Less than 20% cloud cover.
3. Flight after 10:00 a.m. and before 2:00 p.m.
4. The turn at 29° 44' latitude; 95° 12' longitude should include banking sharply enough for the sensors to receive information from the downtown Houston skyline.

Note: Please record seriel numbers of lens and filters used.

PART V

GROUND REQUIREMENTS

Ground information will be provided by an environmental health physicist. Sites will be selected along the flight path for groundtruth measurements prior to and during the flight. These data will consist of hi-volume air samples for mass of particulates per volume of air, relative humidity, temperature, and at least one particle size determination.

Spectrometry measurements will be required with support from the Applied Physics Branch of the EOD during over flight.

PART VI - FLIGHT AND INSTRUMENT REQUIREMENTS

IS REQUIRED FLIGHT ALTITUDE
☐ ABOVE THE GROUND ☐ OR ABOVE MEAN SEA LEVEL?

WHAT IS THE MEAN ALTITUDE OF THE TEST SITE ABOVE SEA LEVEL?

AIRCRAFT REQUIRED ☐ WP3A ☐ NC130H ☐ RP57F ☐ OTHER

FLIGHT LINE AND RUN NUMBER	FLIGHT ALTITUDE (1000 FEET)	FLIGHT LINE LENGTH IN NAUTICAL MILES	TIME OF FLIGHT (local)	SENSORS (Identify each sensor required and specify whether mandatory-1 or desired-2.)

Trinity Bay and the Houston ship channel are located in southeastern Texas in Test Site #175. The flight path begins ~~15 nmi East of Morgan's Point and proceeds NE to 29° 47' Latitude, 94° 12' Longitude following the ship channel one direction out to sea.~~ AND CONTINUES IN THE TURNING BASIN. THE FLIGHT PATH ON EACH SIDE OF THE CHANNEL. The flight path is about 20 miles.

TOTAL FLIGHT MILES	

APPENDIX B

MICRODENSITY TRACES

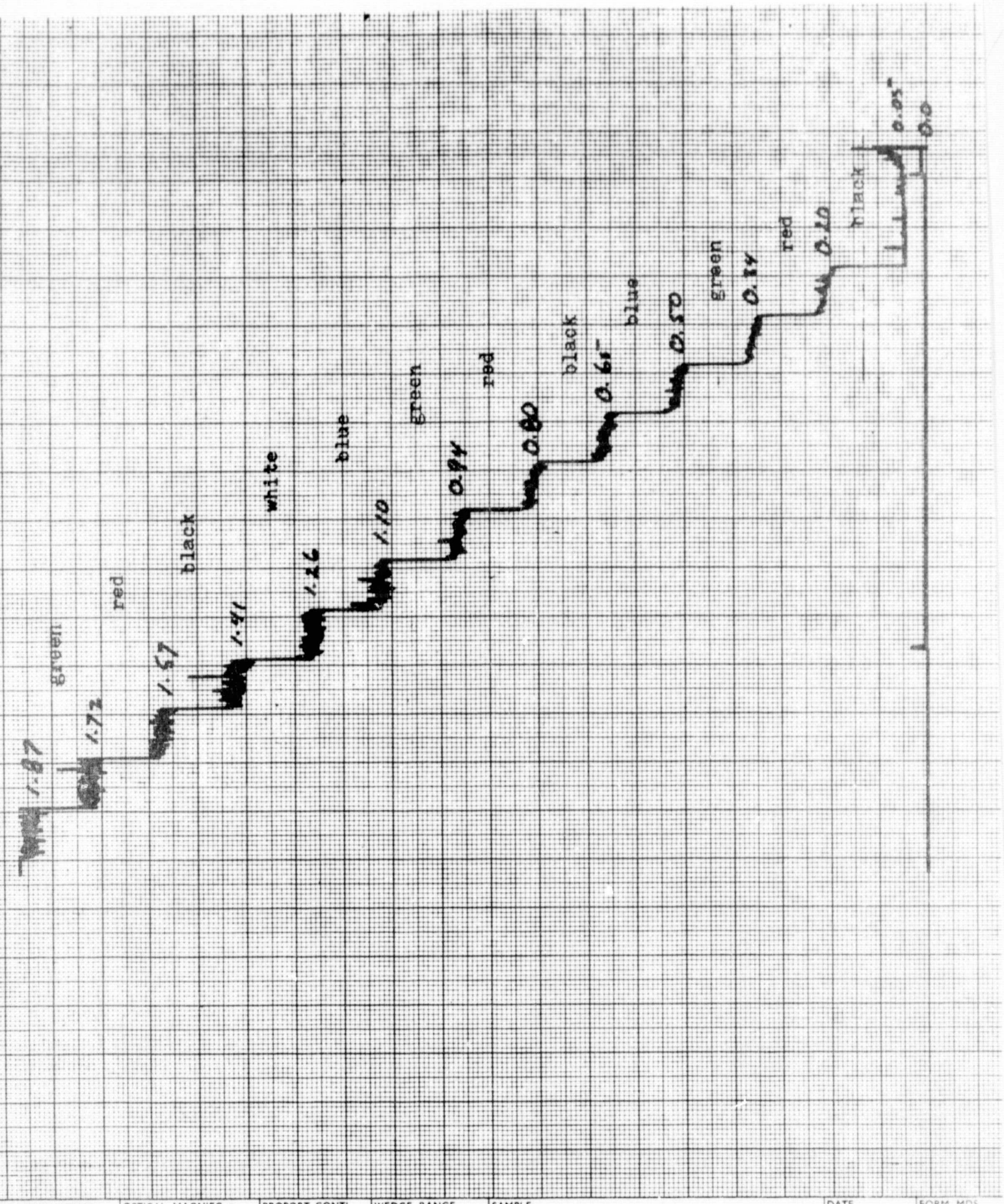

JOYCE LOEBL	OPTICAL MAGNIFC. = OBJECTIVE POWER x 2·2	PROPORT. CONTL.	WEDGE RANGE	SAMPLE: CAL. BRATED WEDGE	DATE	FORM MDS
	SLIT (ACTUAL)	FEEDBACK SETTING	RATIO	REMARKS:	RECORD Nº	

CORDING
CRODENSITOMETER

PART VII - DATA REQUIREMENTS

SENSOR OPERATION (Describe any specific sensor operation requirements; e.g., polarizations for radar and microwave; films, filters, and overlap for cameras; imaging scanner configurations, etc.)

Sensor Operation

Photography

RC-8 Cameras

Camera	Film	Filter	Wavelength
1	Plus X	WR25A	.58 - .72 micron
2	B&W IR	WR89B	.71 - .9 micron

DATA PROCESSING

1. Precision processing on all photography.
2. Provide gamma curves on the photography.
3. Provide flight film for review prior to subsequent film processing.

NOTE: This photography will be used as reference standards to examine particulate material in the atmosphere by microdensitracer.

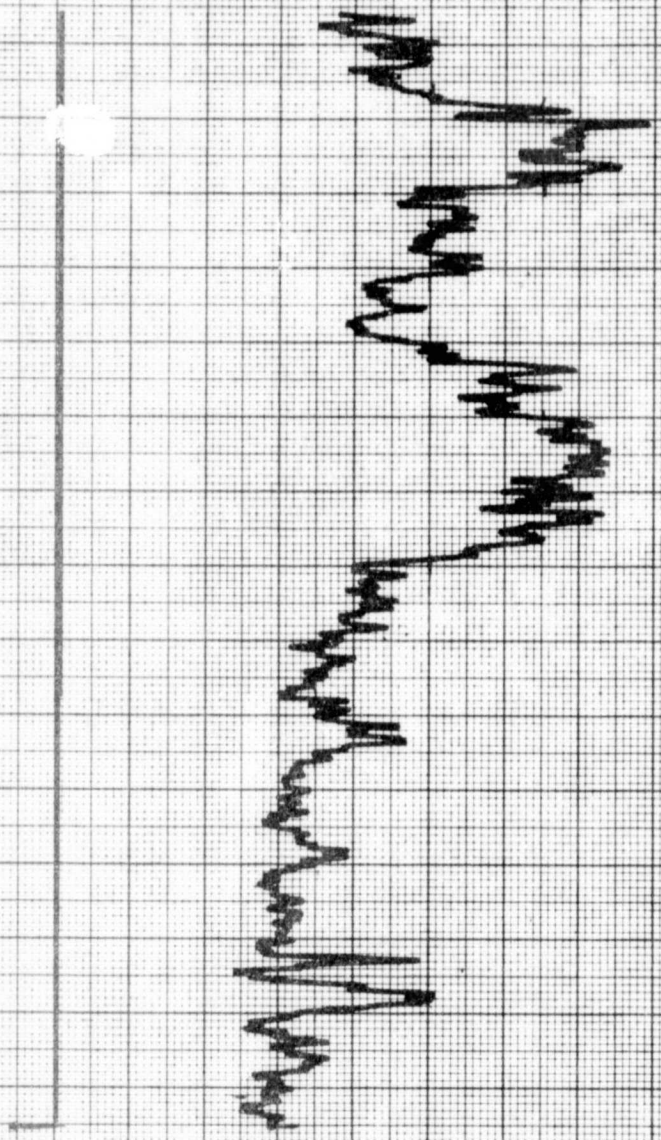

JOYCE LOEBL

OPTICAL MAGNIFC. = OBJECTIVE POWER x 2·2 | PROPORT. CONTL. | WEDGE RANGE | SAMPLE: IR (2) | DATE 11/3 | FORM MDS

SLIT (ACTUAL) | FEEDBACK SETTING | RATIO | REMARKS: SCAN #1 (4750) | RECORD NO.

CORDING

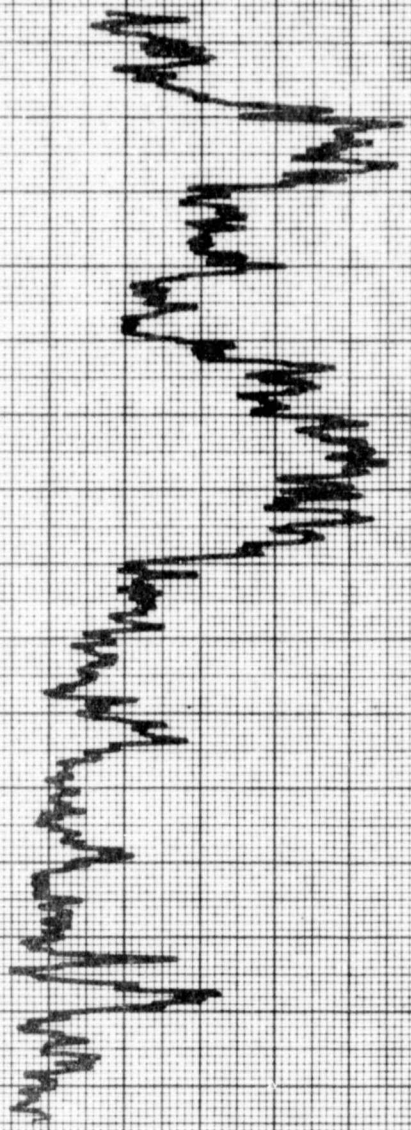

JOYCE LOEBL	OPTICAL MAGNIFC. = OBJECTIVE POWER x 2·2	PROPORT. CONTL.	WEDGE RANGE	SAMPLE: IR (2.)	DATE 11/3
	SLIT (ACTUAL)	FEEDBACK SETTING	RATIO	REMARKS: SCAN # 2 42.746	RECORD Nº

CORDING
CRODENSITOMETER

JOYCE LOEBL & CO. INC. 111. TERRACE HALL AVE. BURLINGTON. MASS.
AFFILIATE OF TECHNICAL OPERATIONS, INCORPORATED

FORM MDS

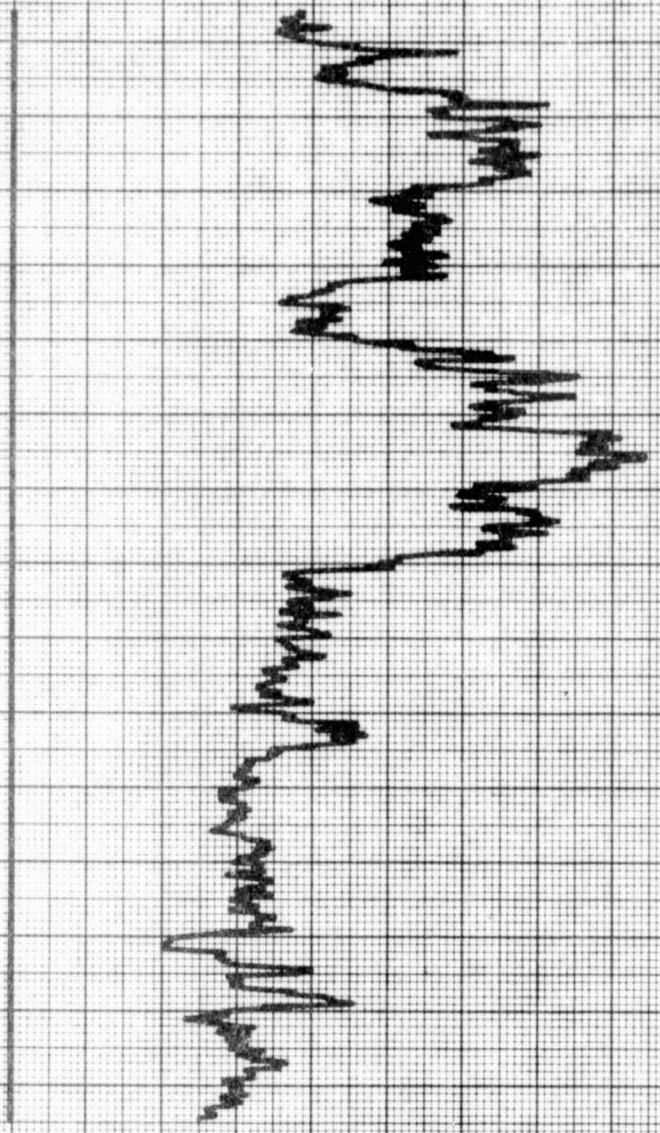

JOYCE LOEBL	OPTICAL MAGNIFC. = OBJECTIVE POWER x 2·2	PROPORT. CONTL.	WEDGE RANGE	SAMPLE: 1R (2)	DATE 11/3	FORM MDS
	SLIT (ACTUAL)	FEEDBACK SETTING	RATIO	REMARKS: SCAN #3 (42742)	RECORD No.	

ORDING
RODENSITOMETER

JOYCE LOEBL & CO. INC. 111 TERRACE HALL AVE. BURLINGTON, MASS.
AFFILIATE OF TECHNICAL OPERATIONS INCORPORATED

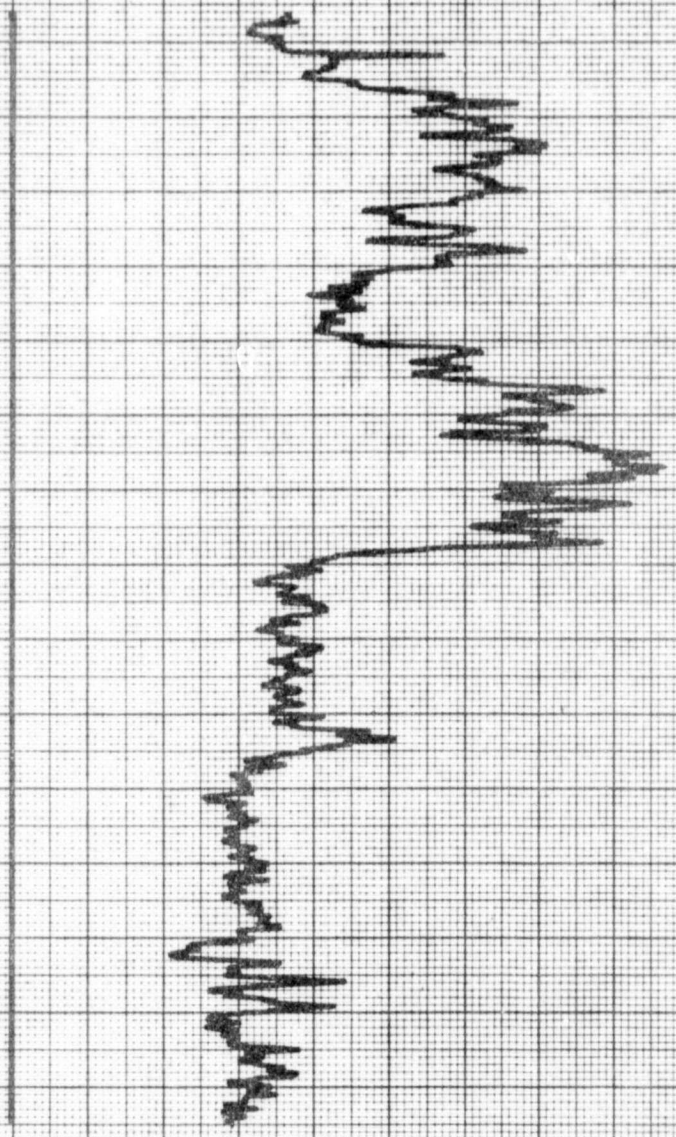

JOYCE LOEBL	OPTICAL MAGNIFC. = OBJECTIVE POWER x 2·2	PROPORT. CONTL.	WEDGE RANGE	SAMPLE: IR (2)	DATE 11/3
	SLIT (ACTUAL)	FEEDBACK SETTING	RATIO	REMARKS: SCAN #4 (42738)	RECORD Nº

CORDING
CRODENSITOMETER

JOYCE LOEBL & CO. INC. 111. TERRACE HALL AVE. BURLINGTON. MASS.
AFFILIATE OF TECHNICAL OPERATIONS, INCORPORATED

FORM MDS

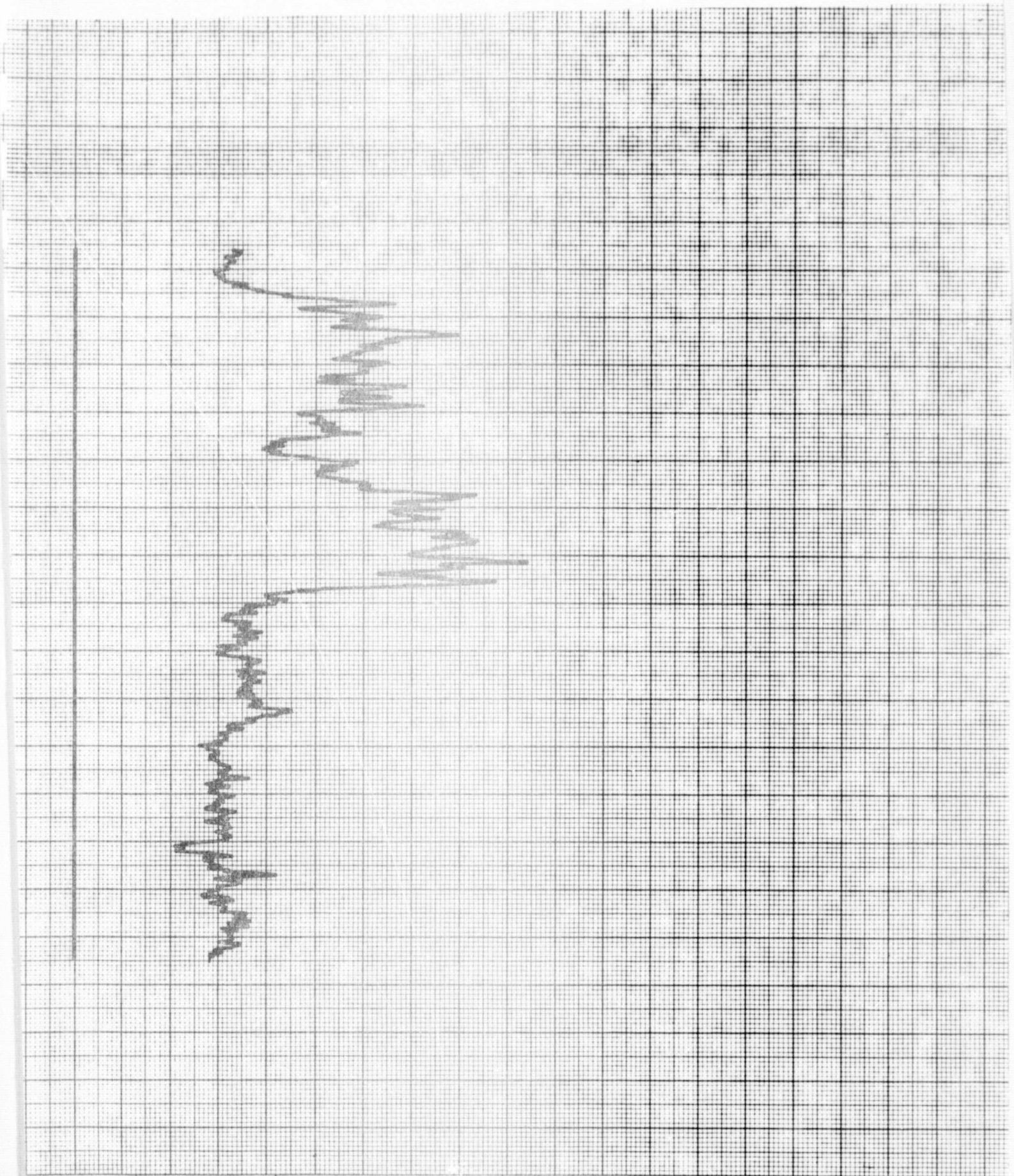

OYCE
OEBL
RDING
)DENSITOMETER

OPTICAL MAGNIFC. = OBJECTIVE POWER x 2·2	PROPORT. CONTL.	WEDGE RANGE	SAMPLE: IR (2)	DATE 11/3	FORM MDS
SLIT (ACTUAL)	FEEDBACK SETTING	RATIO	REMARKS: SCAN #5 (42734)	RECORD No.	

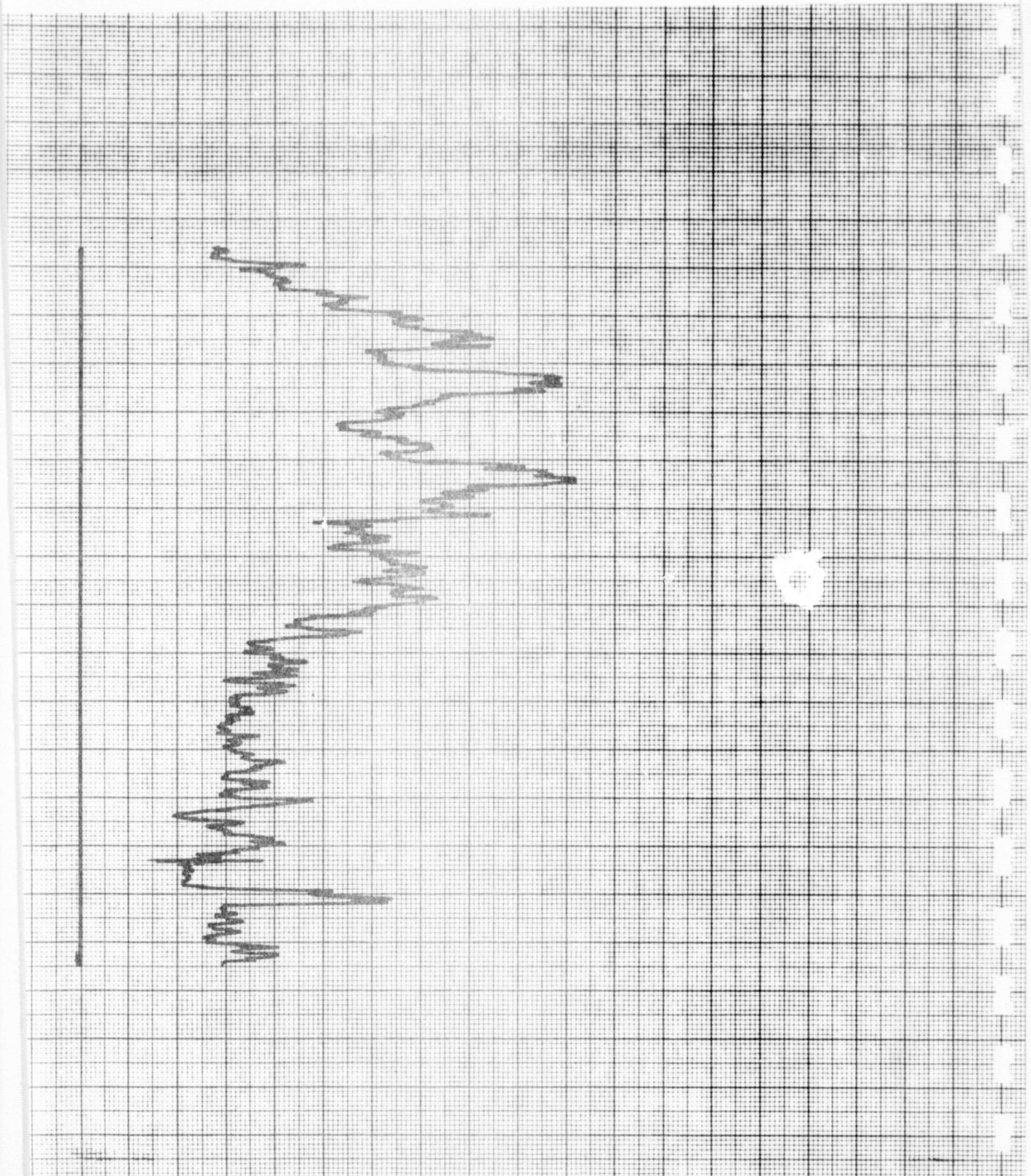

OPTICAL MAGNIFC. = OBJECTIVE POWER x 2·2	PROPORT. CONTL.	WEDGE RANGE	SAMPLE: IR (2)	DATE 11/3	FORM MD
SLIT (ACTUAL)	FEEDBACK SETTING	RATIO	REMARKS: SCAN #6 (42694)	RECORD Nº.	

OYCE
OEBL
RDING
DDENSITOMETER

JOYCE LOEBL & CO. INC. 111. TERRACE HALL AVE. BURLINGTON. MASS.
AFFILIATE OF TECHNICAL OPERATIONS INCORPORATED

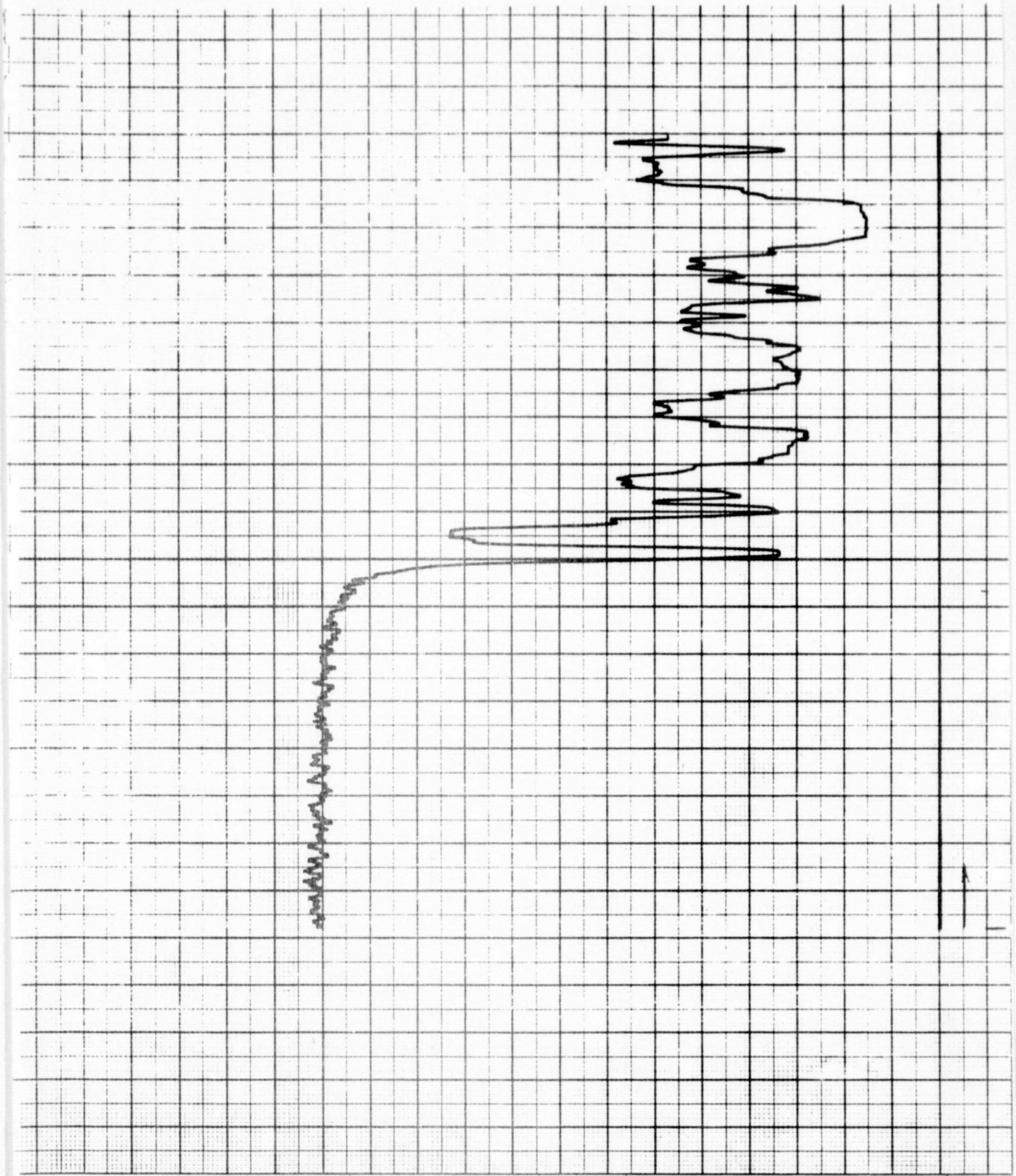

TECH/OPS INSTRUMENTS
NORTHWEST INDUSTRIAL PARK
BURLINGTON, MASS. 01803 (617) 272-2000
A Division of Technical Operations, Inc. (TOI)

JOYCE
LOEBL

OPTICAL MAGNIFIC. = OBJECTIVE POWER x 2.2
PROPORT. CONTL
WEDGE RANGE
SAMPLE FRAME 3-A
DATE 11/10
FORM MDS

SLIT (ACTUAL)
FEEDBACK SETTING
RATIO
REMARKS
RECORD No.

RECORDING

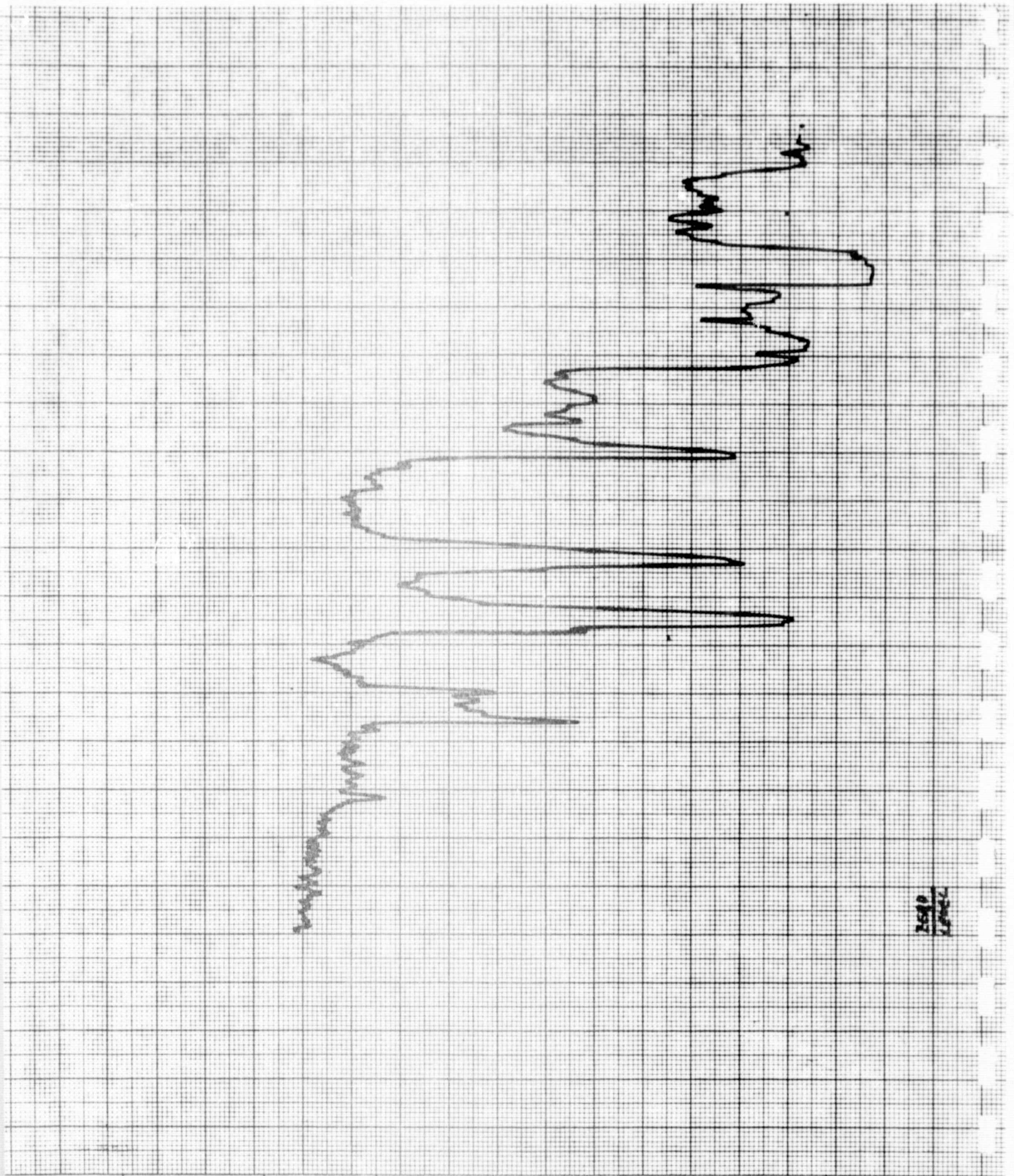

JOYCE LOEBL	OPTICAL MAGNIFC. = OBJECTIVE POWER x 2·2	PROPORT. CONTL.	WEDGE RANGE	SAMPLE: FRAME 3 - 73	DATE 11/10	FORM MDS
	SLIT (ACTUAL)	FEEDBACK SETTING	RATIO	REMARKS:	RECORD Nº.	PDL

ORDING
RODENSITOMETER

JOYCE LOEBL & CO. INC. 111 TERRACE HALL AVE. BURLINGTON. MASS.
AFFILIATE OF TECHNICAL OPERATIONS, INCORPORATED

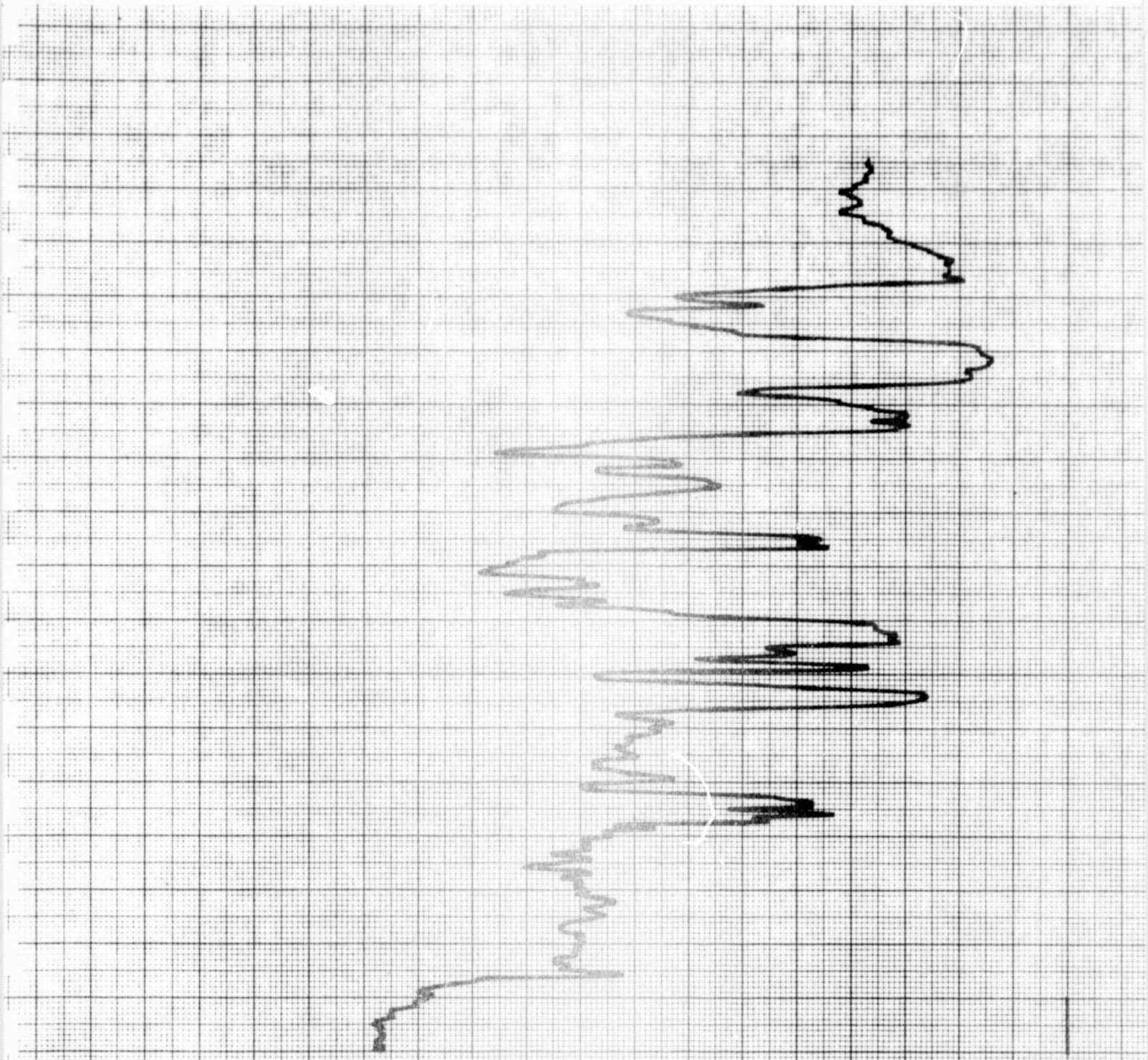

JOYCE LOEBL	OPTICAL MAGNIFC. = OBJECTIVE POWER x 2·2	PROPORT. CONTL.	WEDGE RANGE	SAMPLE: FRAME 3-C	DATE 11/10	FORM MDS
	SLIT (ACTUAL)	FEEDBACK SETTING	RATIO	REMARKS:	RECORD Nº	PDL

CORDING
CRODENSITOMETER

JOYCE LOEBL & CO. INC. 111 TERRACE HALL AVE. BURLINGTON, MASS.
AFFILIATE OF TECHNICAL OPERATIONS, INCORPORATED

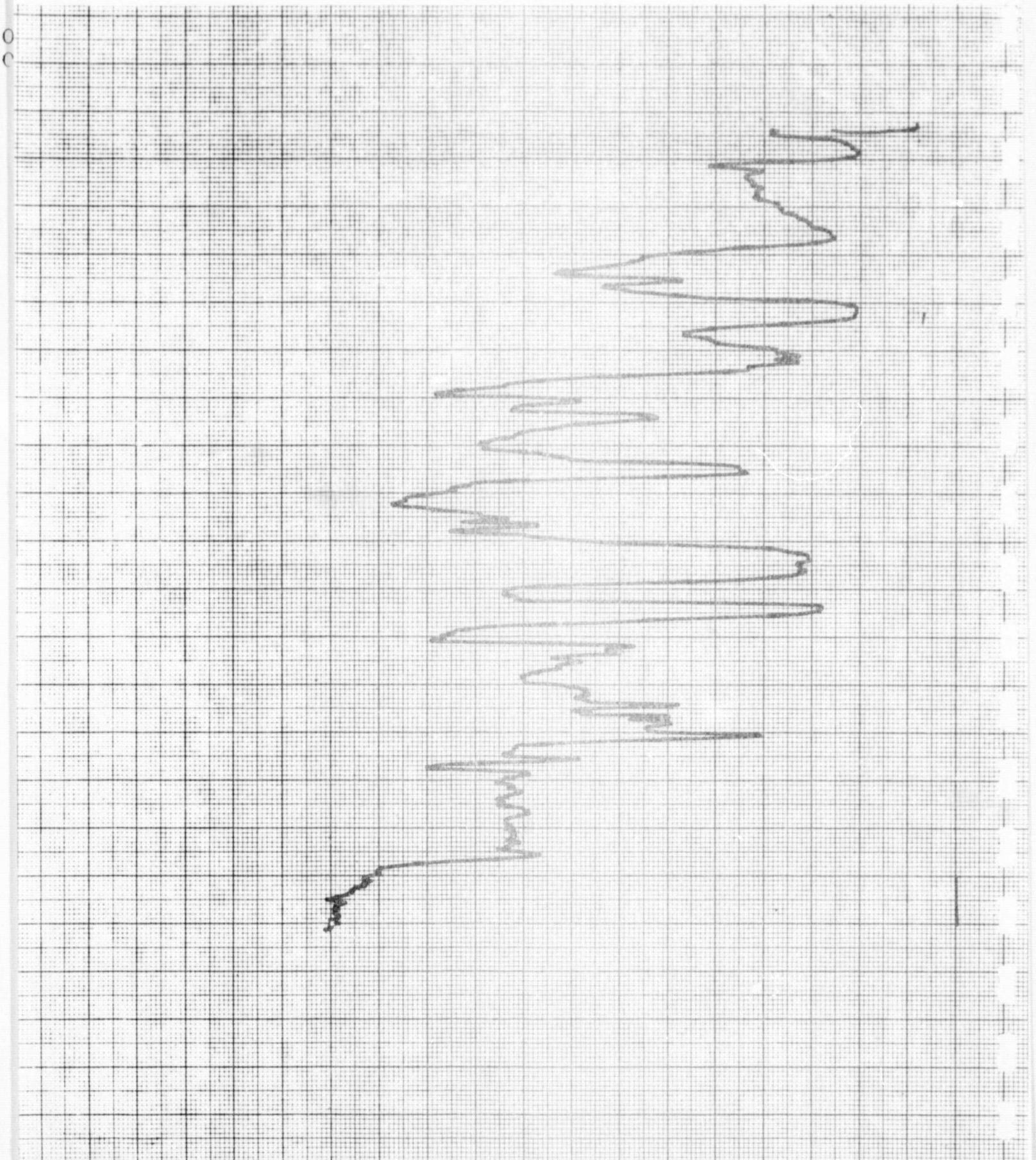

JOYCE LOEBL	OPTICAL MAGNIFC. = OBJECTIVE POWER x 2·2	PROPORT. CONTL.	WEDGE RANGE	SAMPLE: FRAME J-D	DATE 11/10	FORM MD5
	SLIT (ACTUAL)	FEEDBACK SETTING	RATIO	REMARKS:	RECORD Nº.	PDL

ECORDING
IICRODENSITOMETER

JOYCE LOEBL & CO. INC. 111 TERRACE HALL AVE. BURLINGTON, MASS.
AFFILIATE OF TECHNICAL OPERATIONS, INCORPORATED

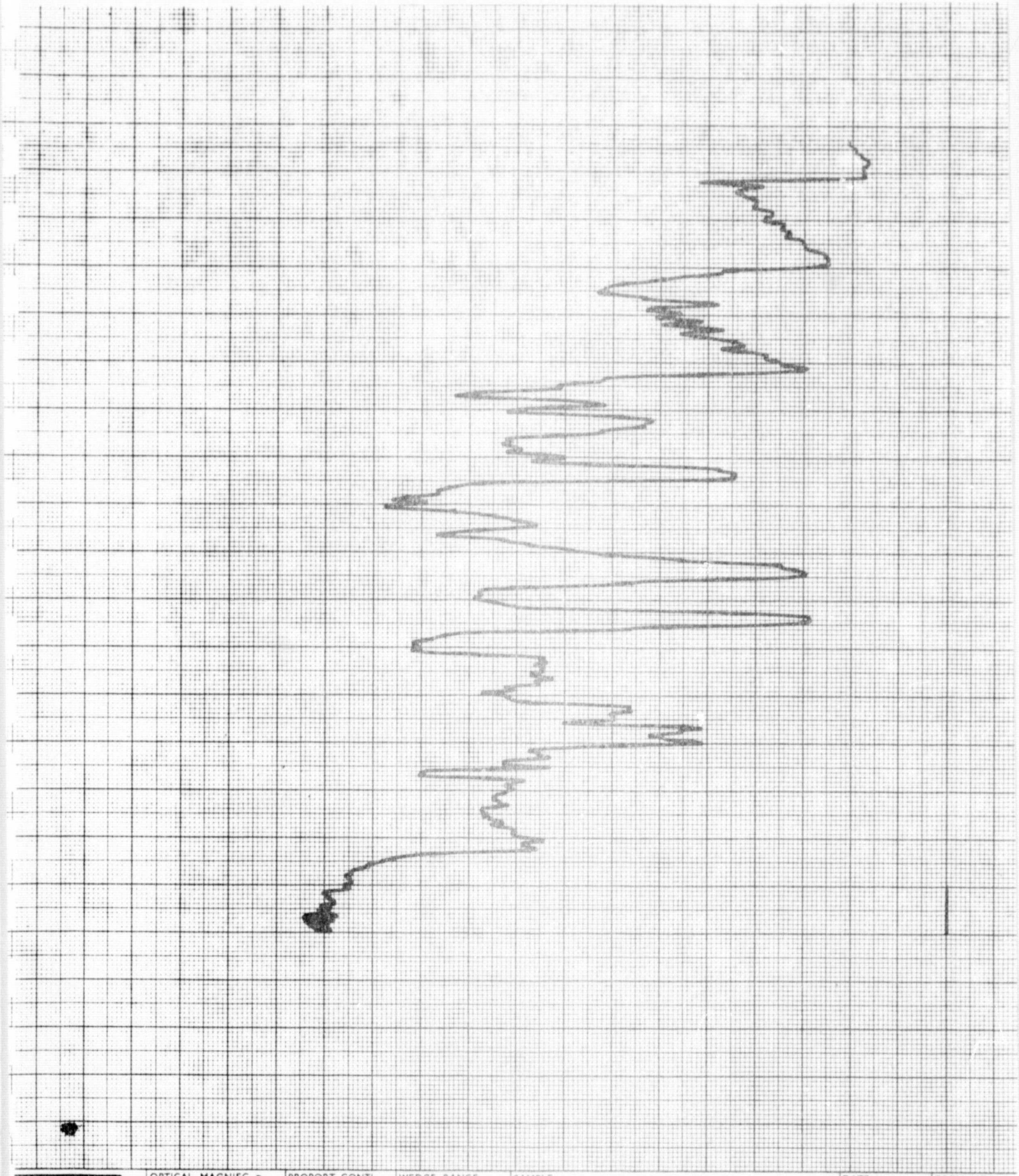

JOYCE LOEBL

ECORDING

OPTICAL MAGNIFC. = OBJECTIVE POWER x 2·2	PROPORT. CONTL.	WEDGE RANGE	SAMPLE: FRAME 3-E	DATE 11/10	FORM MDS
SLIT (ACTUAL)	FEEDBACK SETTING	RATIO	REMARKS:	RECORD Nº.	PDL

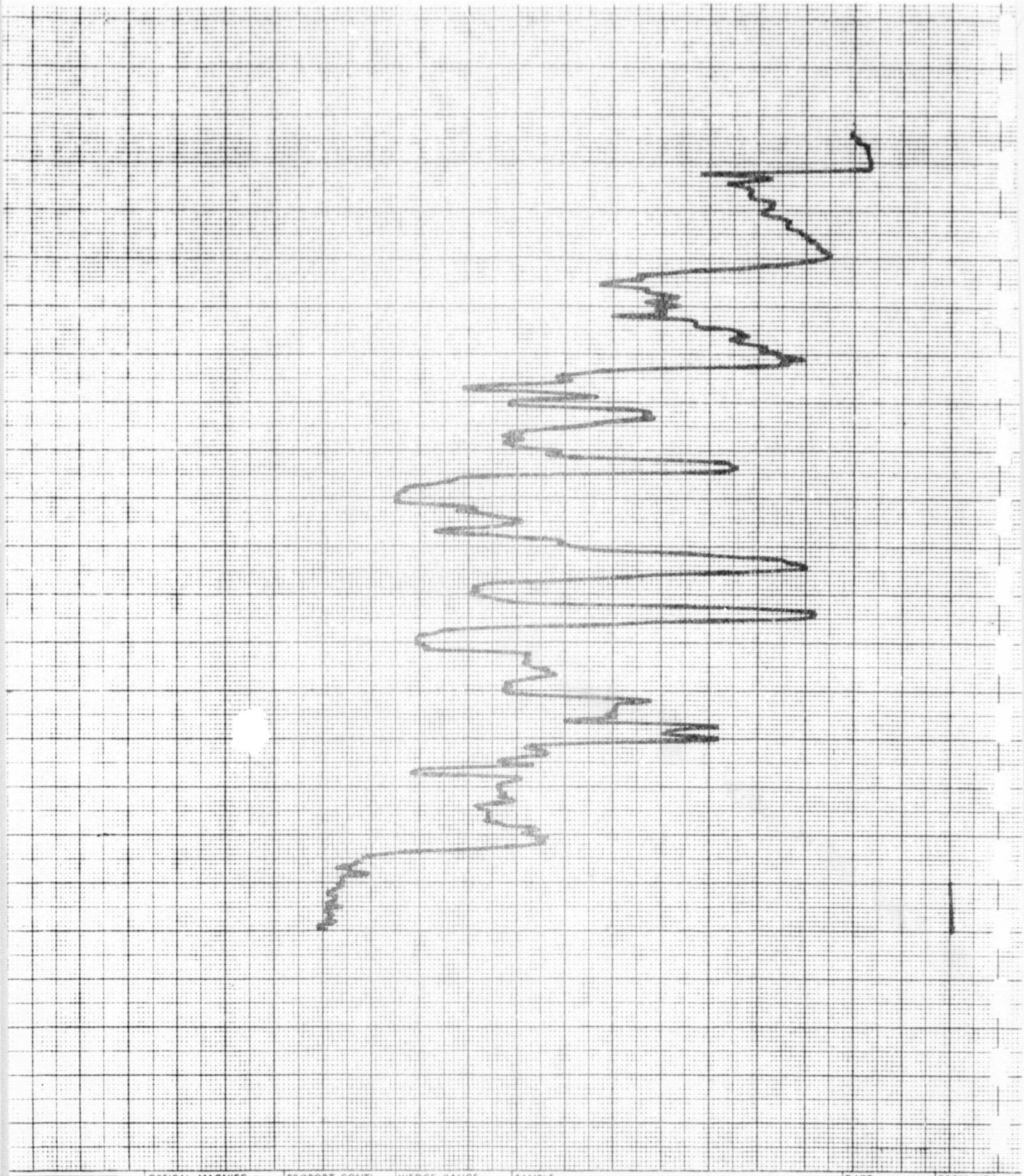

JOYCE LOEBL	OPTICAL MAGNIFC. = OBJECTIVE POWER x 2·2	PROPORT. CONTL.	WEDGE RANGE	SAMPLE: FRAME 3-F	DATE 11/10	FORM MDS
	SLIT (ACTUAL)	FEEDBACK SETTING	RATIO	REMARKS:	RECORD Nº	TDL

ECORDING
1ICRODENSITOMETER

JOYCE LOEBL & CO. INC. 111 TERRACE HALL AVE. BURLINGTON. MASS.
AFFILIATE OF TECHNICAL OPERATIONS, INCORPORATED

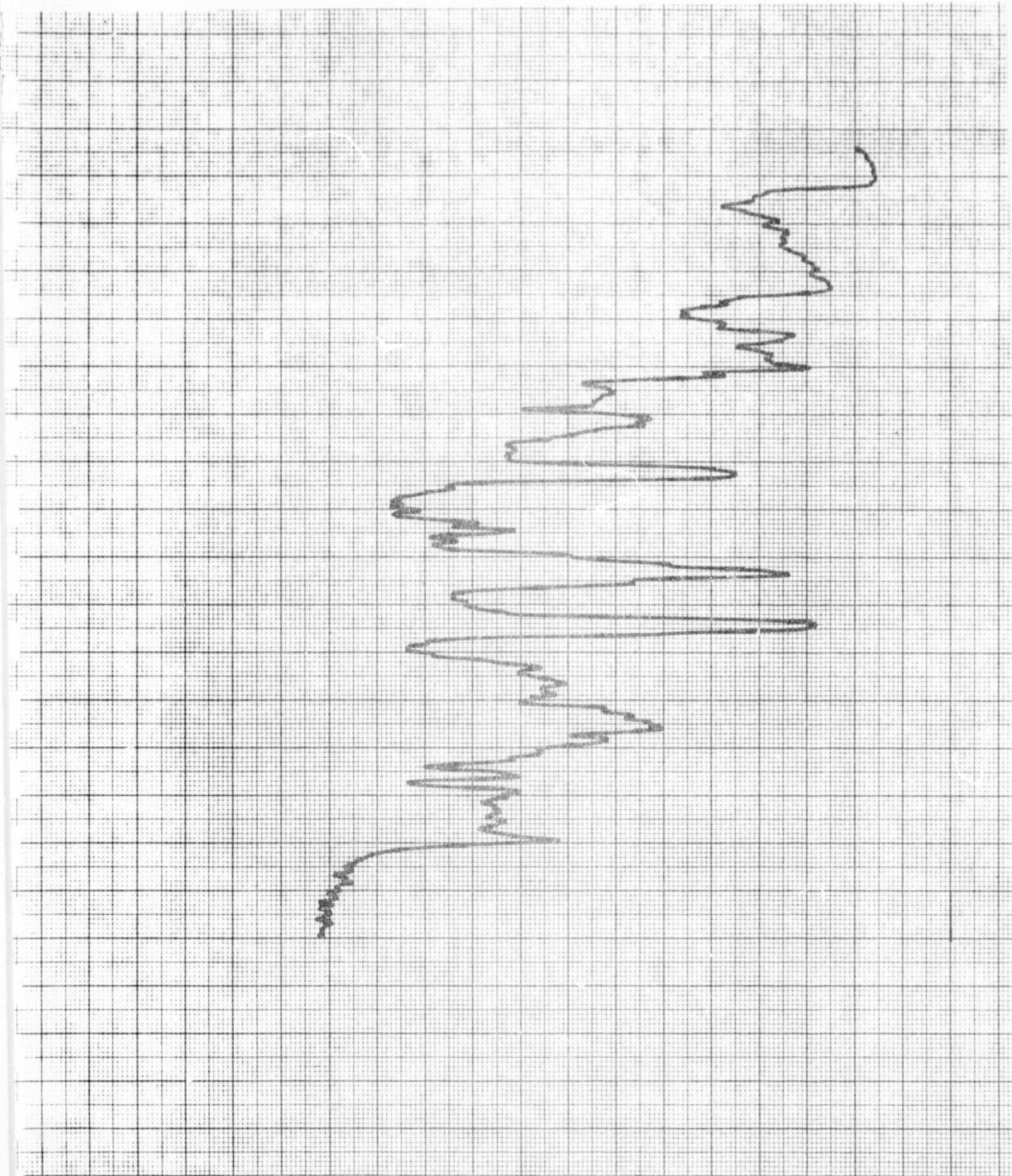

JOYCE LOEBL

CORDING
ICRODENSITOMETER

OPTICAL MAGNIFC. = OBJECTIVE POWER x 2·2	PROPORT. CONTL.	WEDGE RANGE	SAMPLE: FRAME 3 - G	DATE 11/10	FORM MDS
SLIT (ACTUAL)	FEEDBACK SETTING	RATIO	REMARKS:	RECORD Nº.	TDL

JOYCE LOEBL & CO. INC. 111. TERRACE HALL AVE. BURLINGTON. MASS.

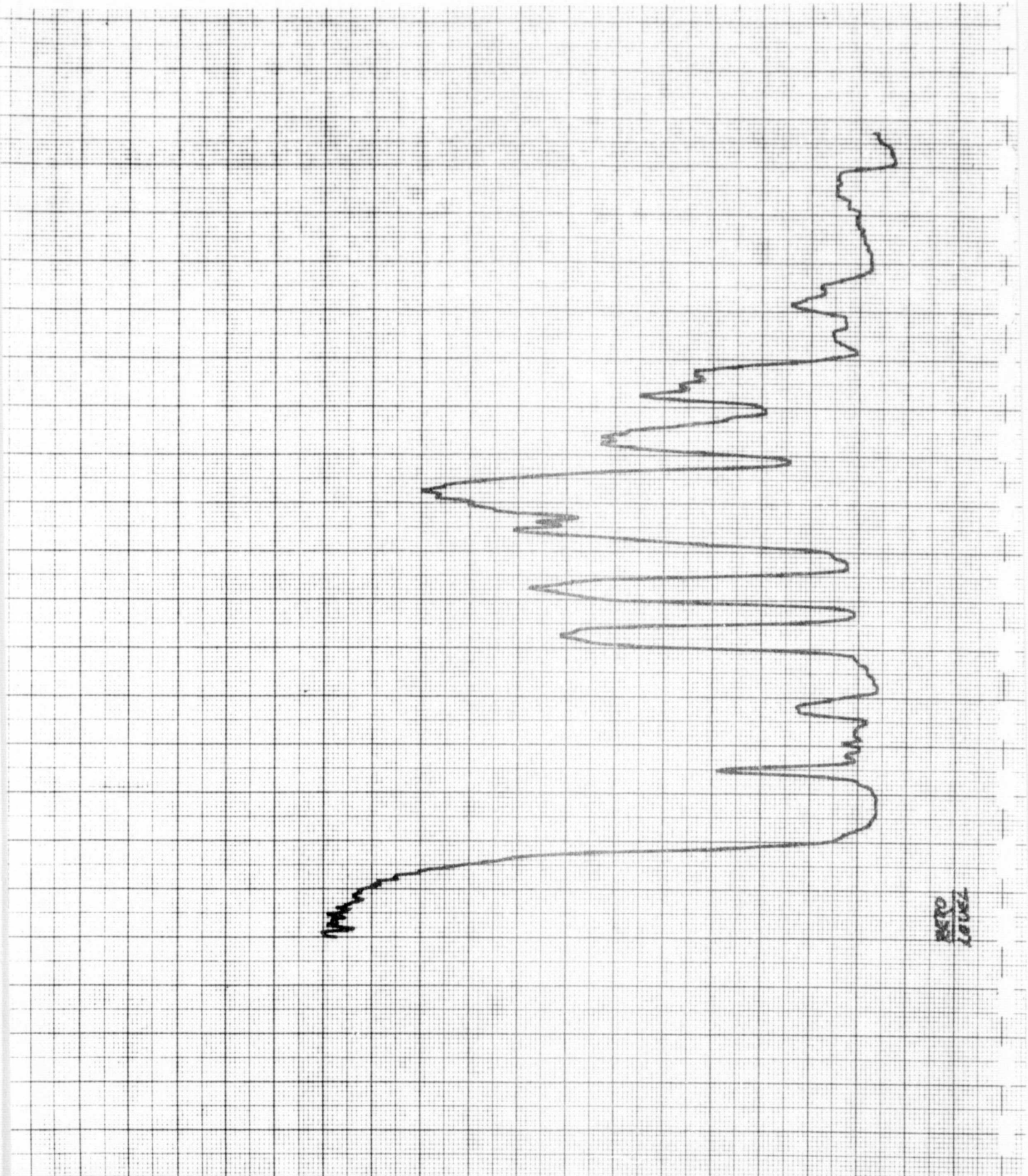

JOYCE LOEBL	OPTICAL MAGNIFC. = OBJECTIVE POWER x 2·2	PROPORT. CONTL.	WEDGE RANGE	SAMPLE: 4	DATE 11/14	FORM MD5
	SLIT (ACTUAL)	FEEDBACK SETTING	RATIO	REMARKS:	RECORD Nº.	A

ECORDING
ICRODENSITOMETER

JOYCE LOEBL & CO. INC. 111. TERRACE HALL AVE. BURLINGTON. MASS.
AFFILIATE OF TECHNICAL OPERATIONS. INCORPORATED

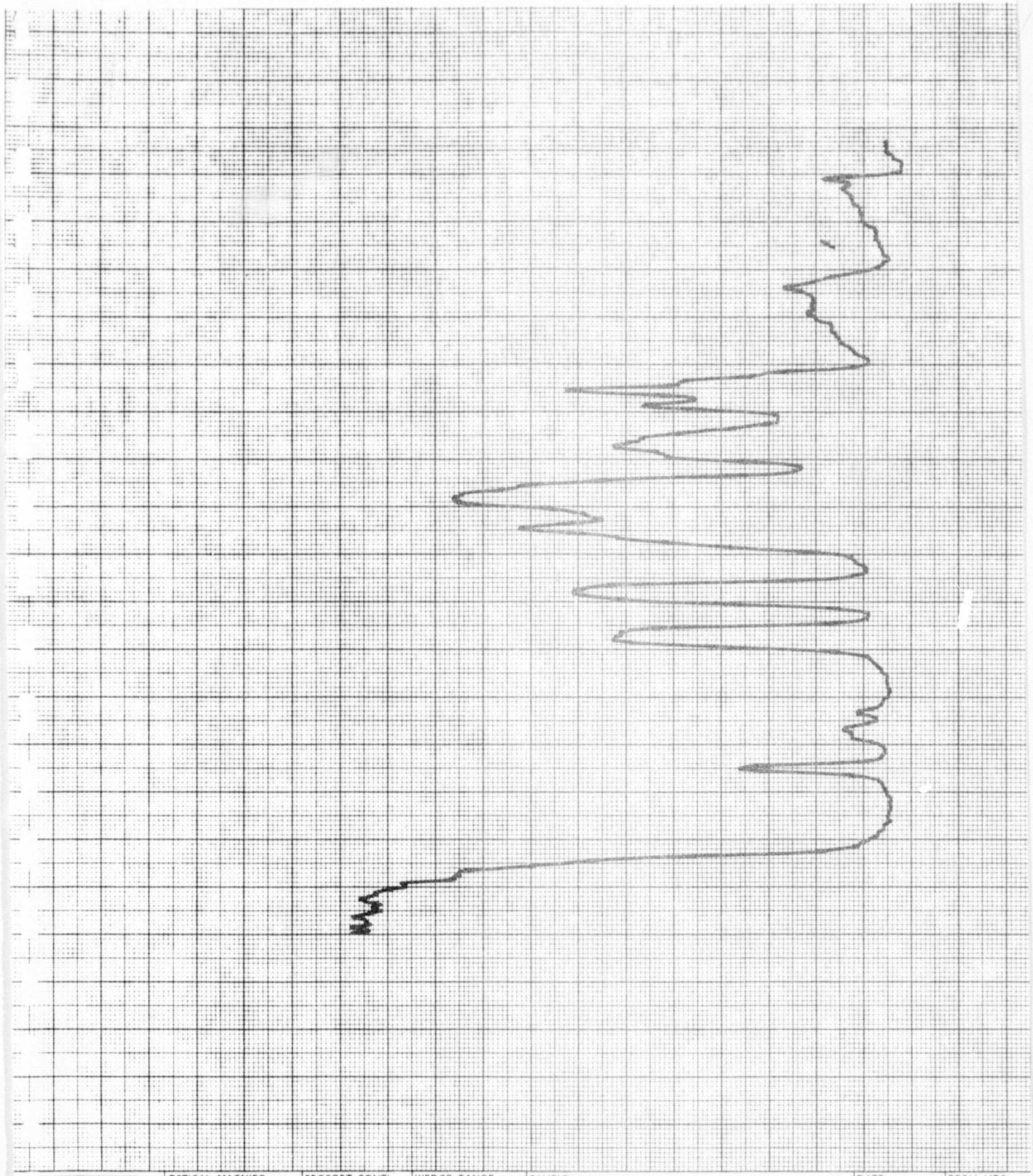

JOYCE LOEBL

CORDING
CRODENSITOMETER

OPTICAL MAGNIFC. = OBJECTIVE POWER x 2·2	PROPORT. CONTL.	WEDGE RANGE	SAMPLE: 4	DATE 11/14	FORM MDS B
SLIT (ACTUAL)	FEEDBACK SETTING	RATIO	REMARKS:	RECORD No.	

JOYCE LOEBL & CO. INC. 111. TERRACE HALL AVE. BURLINGTON. MASS.

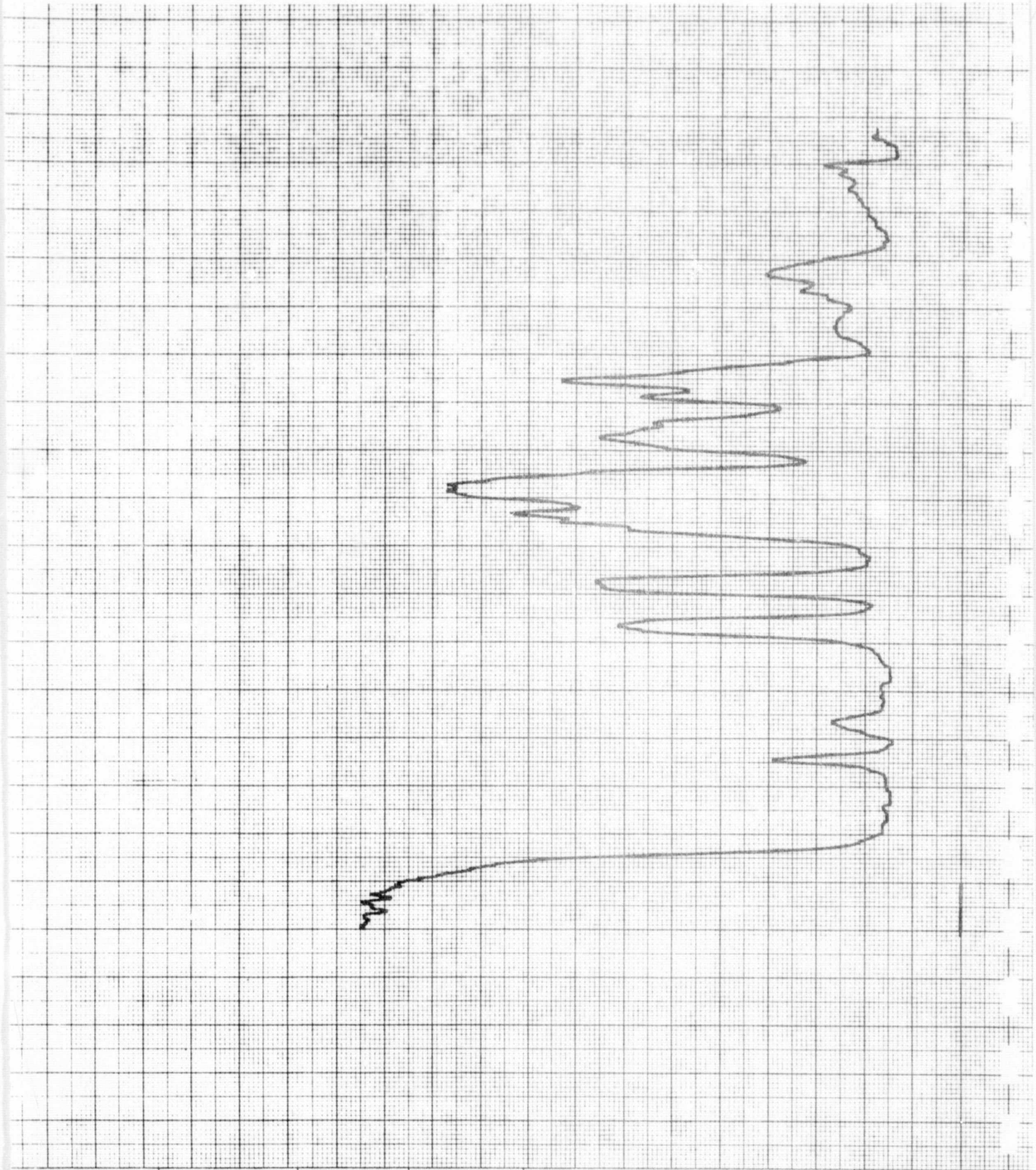

JOYCE LOEBL	OPTICAL MAGNIFC. = OBJECTIVE POWER x 2·2	PROPORT. CONTL.	WEDGE RANGE	SAMPLE: 4	DATE 11/14	FORM MDS
	SLIT (ACTUAL)	FEEDBACK SETTING	RATIO	REMARKS:	RECORD Nº.	C

RECORDING MICRODENSITOMETER

JOYCE LOEBL & CO. INC. 111 TERRACE HALL AVE. BURLINGTON, MASS.
AFFILIATE OF TECHNICAL OPERATIONS, INCORPORATED

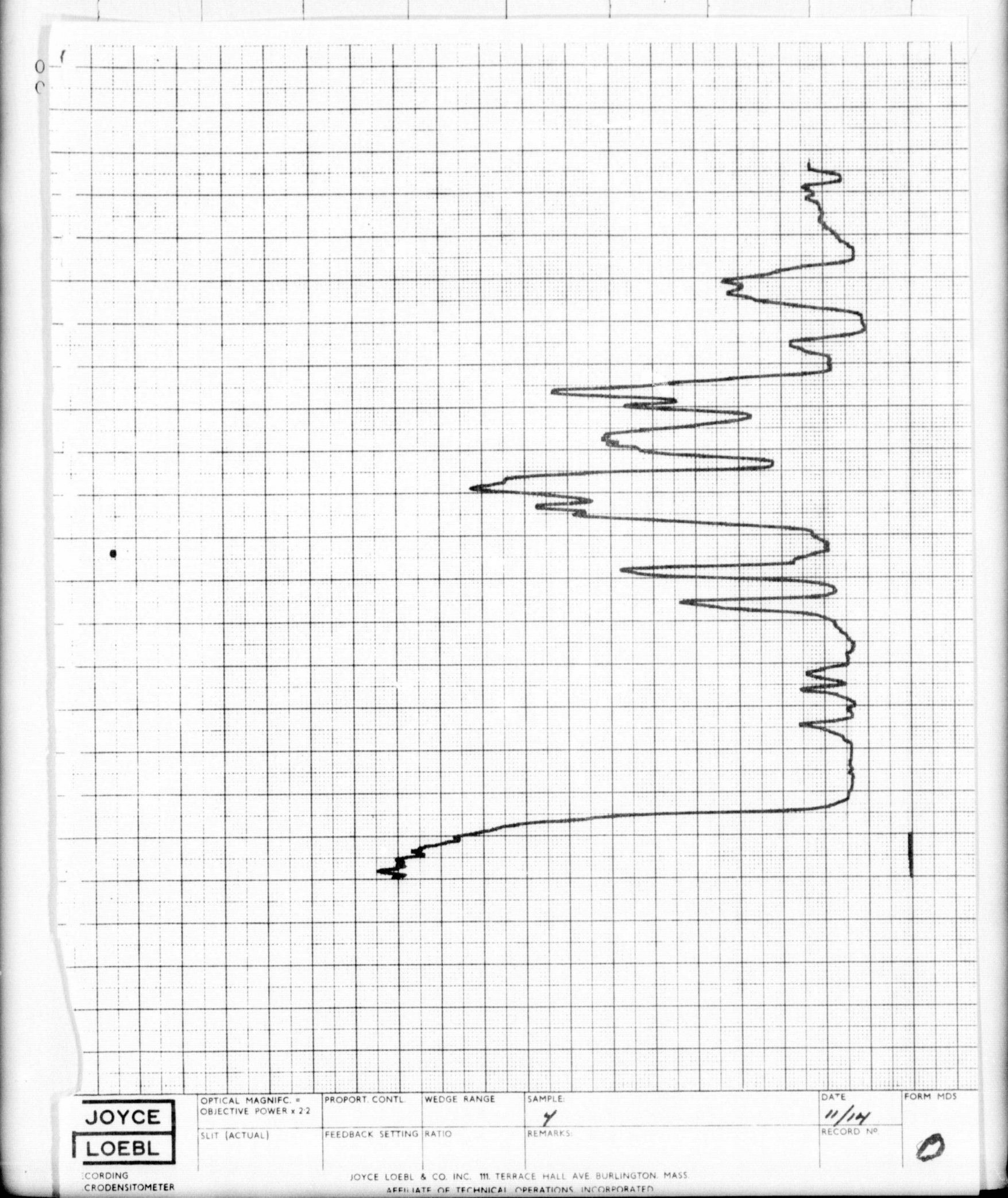

JOYCE LOEBL

OPTICAL MAGNIFC. = OBJECTIVE POWER x 2·2	PROPORT. CONTL.	WEDGE RANGE	SAMPLE: 4	DATE 11/14	FORM MDS
SLIT (ACTUAL)	FEEDBACK SETTING	RATIO	REMARKS:	RECORD Nº	

CORDING
CRODENSITOMETER

JOYCE LOEBL & CO. INC. 111. TERRACE HALL AVE. BURLINGTON. MASS.
AFFILIATE OF TECHNICAL OPERATIONS, INCORPORATED

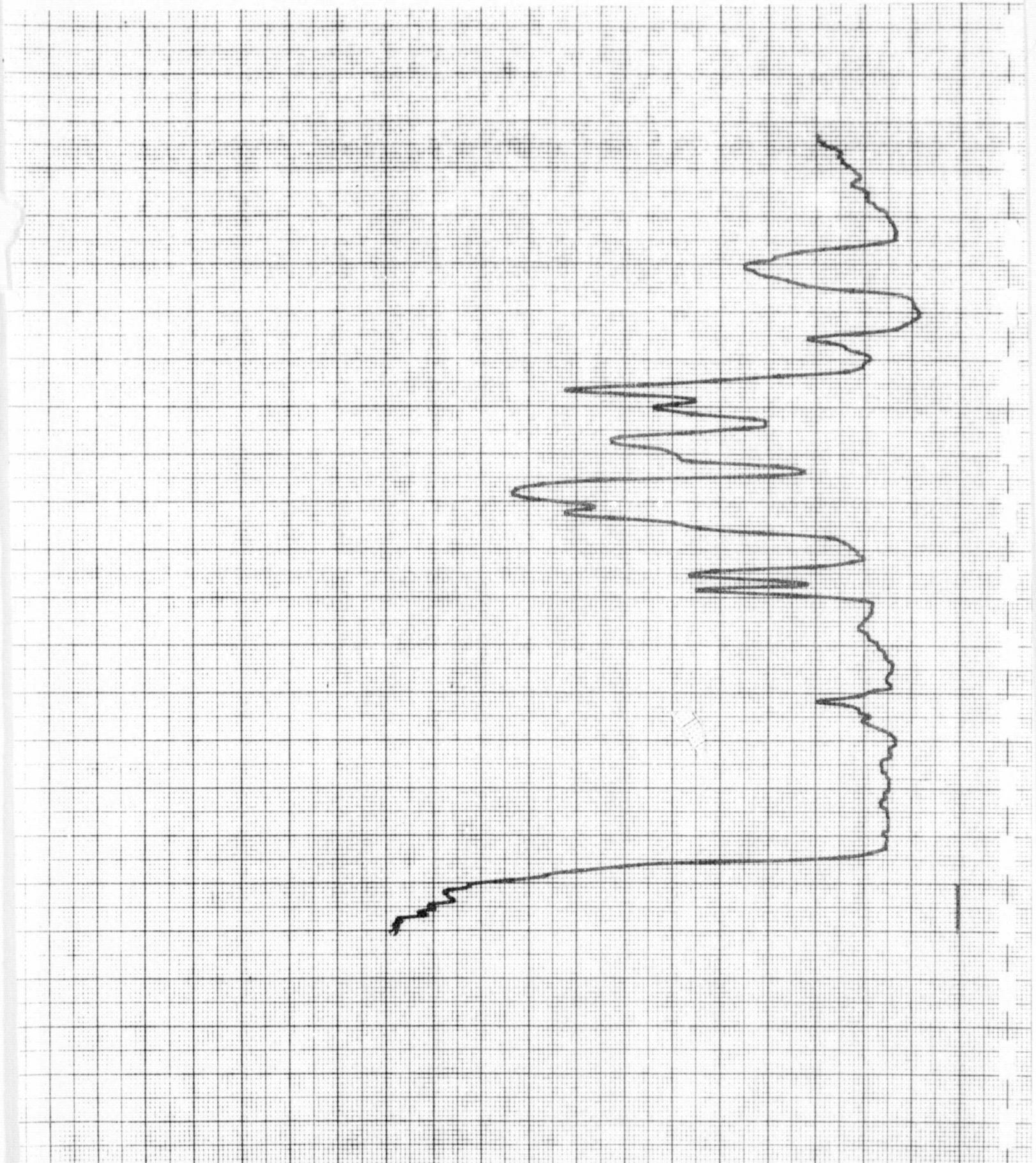

JOYCE LOEBL	OPTICAL MAGNIFC. = OBJECTIVE POWER x 2·2	PROPORT. CONTL.	WEDGE RANGE	SAMPLE: 4	DATE 11/14	FORM MD²
	SLIT (ACTUAL)	FEEDBACK SETTING	RATIO	REMARKS:	RECORD No.	

RECORDING MICRODENSITOMETER

JOYCE LOEBL & CO. INC. 111 TERRACE HALL AVE. BURLINGTON, MASS.
AFFILIATE OF TECHNICAL OPERATIONS, INCORPORATED

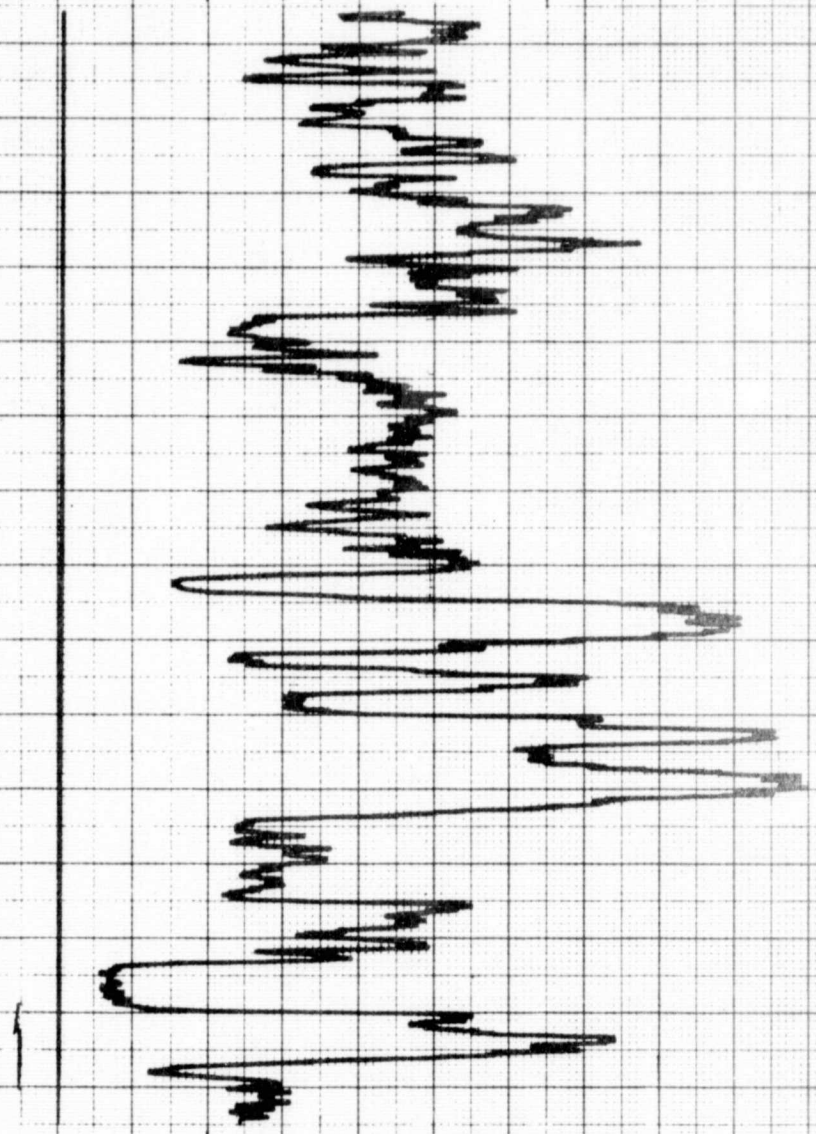

JOYCE LOEBL	OPTICAL MAGNIFC. = OBJECTIVE POWER x 2·2	PROPORT. CONTL.	WEDGE RANGE	SAMPLE:	DATE 11/3	FORM MDS
	SLIT (ACTUAL)	FEEDBACK SETTING	RATIO	REMARKS: SCAN #1 42700	RECORD Nº	

CORDING
CRODENSITOMETER

JOYCE LOEBL & CO. INC. 111. TERRACE HALL AVE. BURLINGTON. MASS.
AFFILIATE OF TECHNICAL OPERATIONS, INCORPORATED

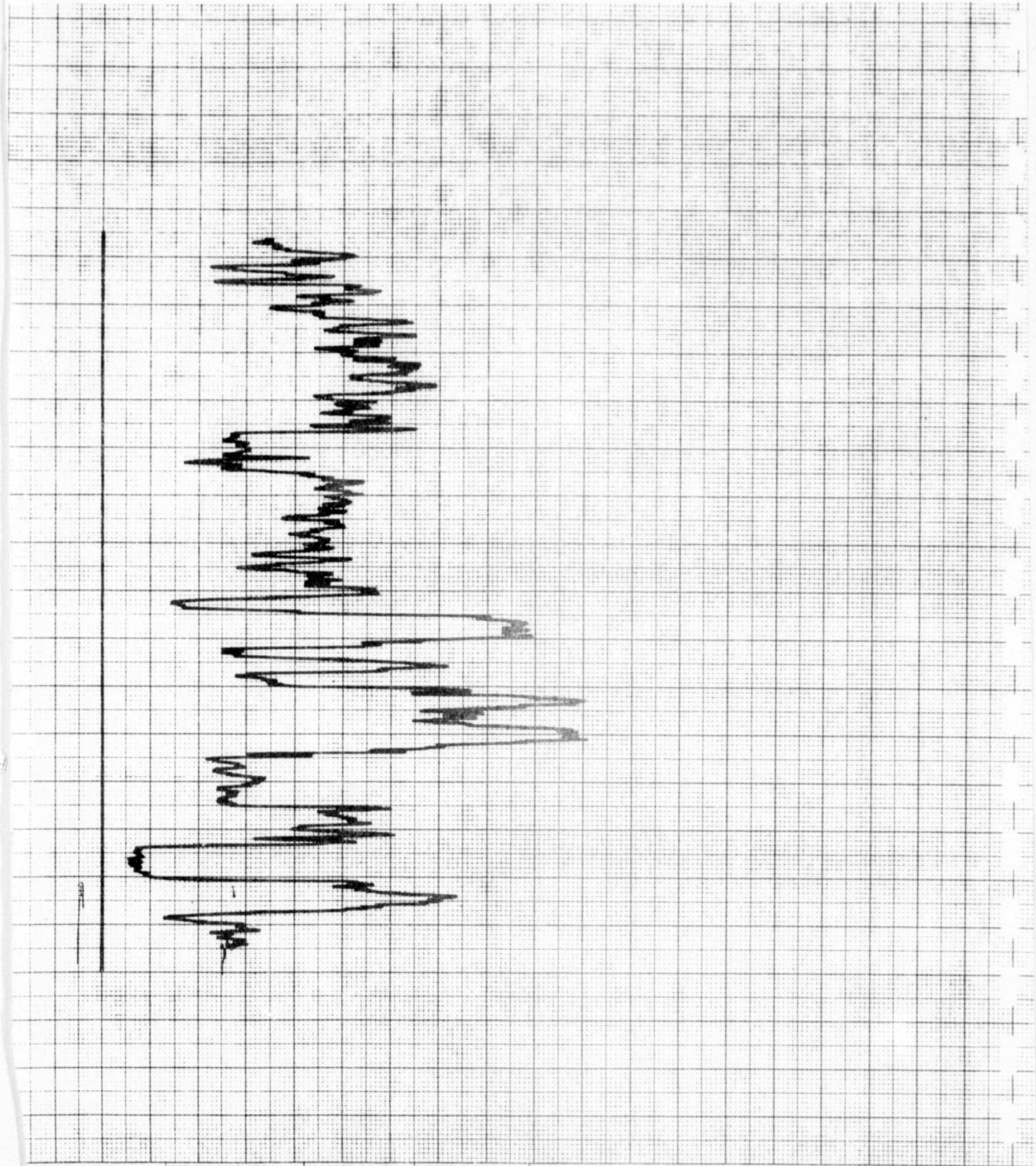

JOYCE LOEBL	OPTICAL MAGNIFC. = OBJECTIVE POWER x 2·2	PROPORT. CONTL.	WEDGE RANGE	SAMPLE:	DATE	FORM M[illegible]
	SLIT (ACTUAL)	FEEDBACK SETTING	RATIO	REMARKS: SCAN #2 42696	RECORD Nº.	

RECORDING MICRODENSITOMETER

JOYCE LOEBL & CO. INC. 111 TERRACE HALL AVE. BURLINGTON, MASS.
AFFILIATE OF TECHNICAL OPERATIONS, INCORPORATED

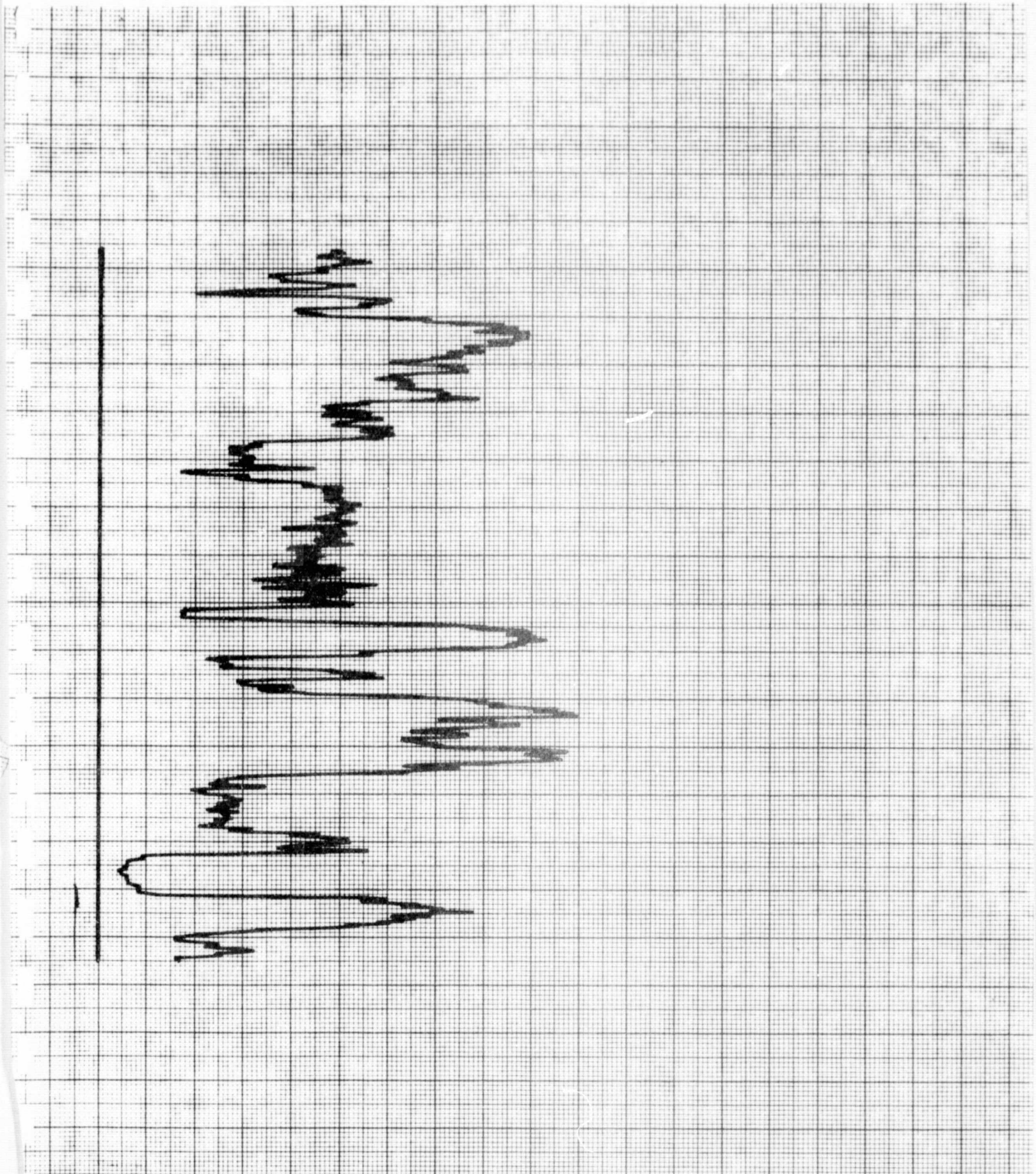

JOYCE LOEBL

OPTICAL MAGNIFC. = OBJECTIVE POWER x 2·2	PROPORT. CONTL.	WEDGE RANGE	SAMPLE: 1	DATE 11/3	FORM MDS
SLIT (ACTUAL)	FEEDBACK SETTING	RATIO	REMARKS: SCAN #3 42692	RECORD Nº.	

DING
DENSITOMETER

JOYCE LOEBL & CO. INC. 111 TERRACE HALL AVE. BURLINGTON, MASS.

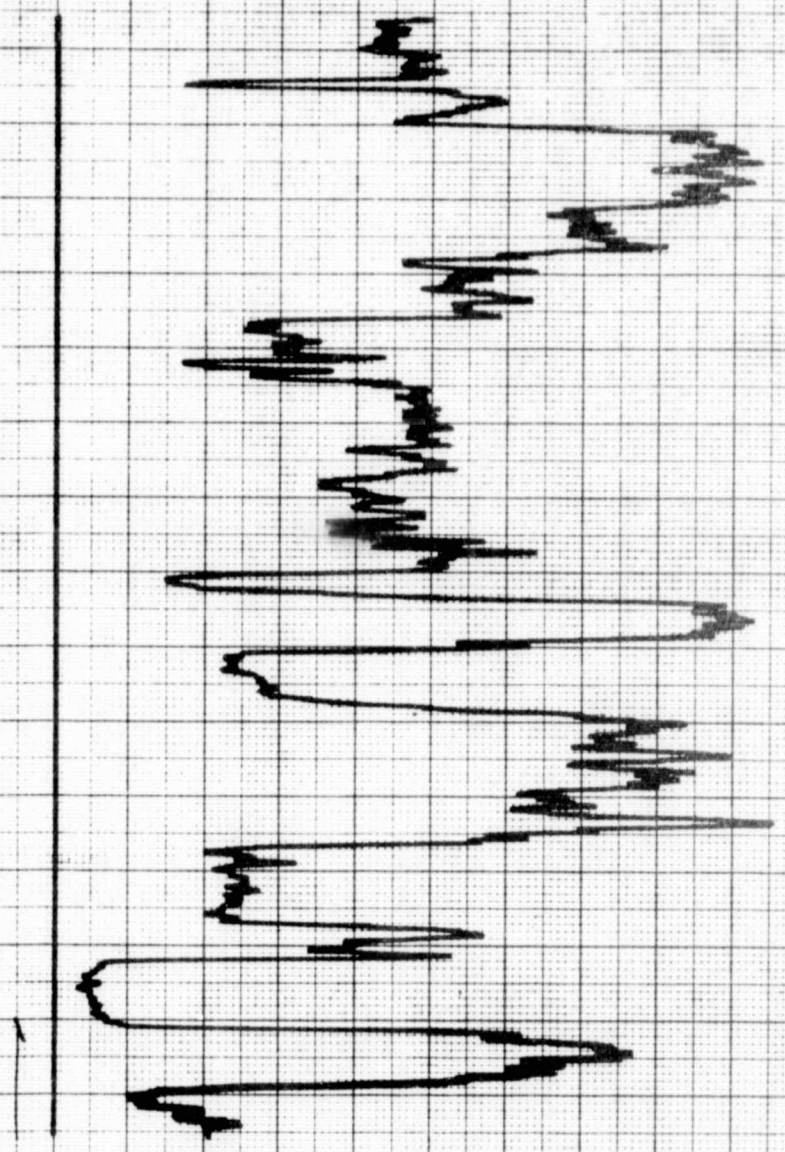

JOYCE LOEBL	OPTICAL MAGNIFC. = OBJECTIVE POWER x 2.2	PROPORT. CONTL.	WEDGE RANGE	SAMPLE:	DATE 11/3	FORM MP*
	SLIT (ACTUAL)	FEEDBACK SETTING	RATIO	REMARKS: SCAN #4 42688	RECORD No.	

RECORDING MICRODENSITOMETER

JOYCE LOEBL & CO. INC. 111 TERRACE HALL AVE. BURLINGTON, MASS.
AFFILIATE OF TECHNICAL OPERATIONS, INCORPORATED

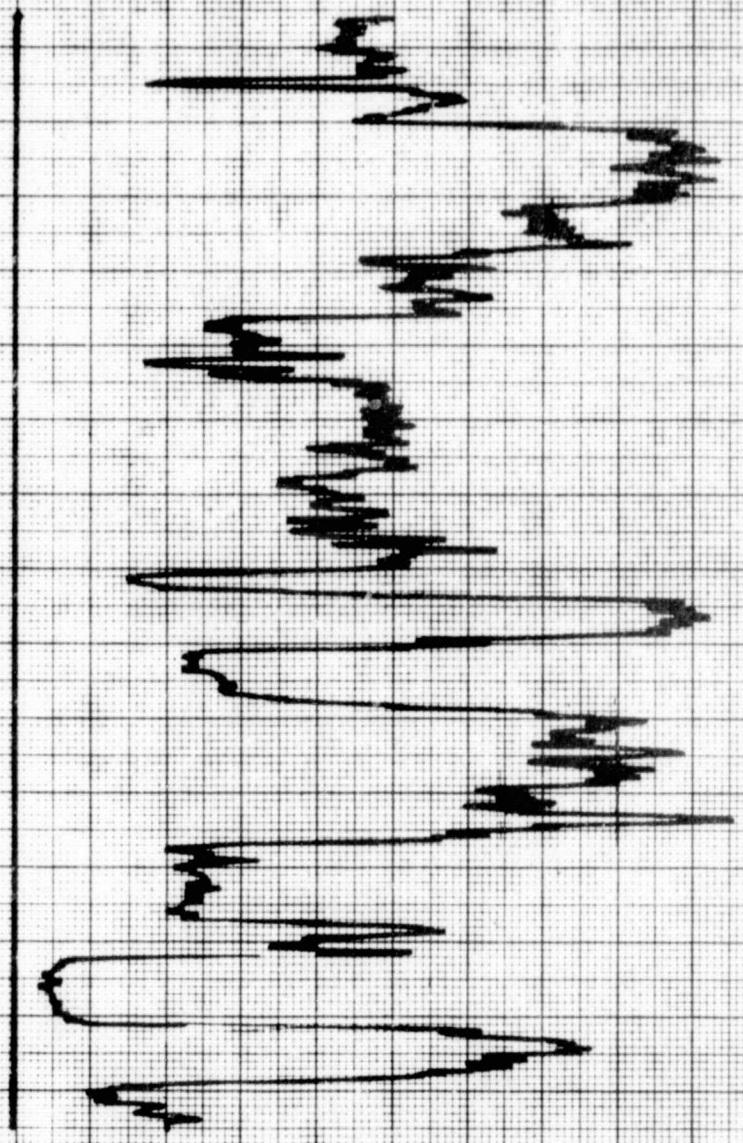

JOYCE LOEBL	OPTICAL MAGNIFC. = OBJECTIVE POWER x 22	PROPORT. CONTL.	WEDGE RANGE	SAMPLE: 1	DATE 11/3	FORM MDS
	SLIT (ACTUAL)	FEEDBACK SETTING	RATIO	REMARKS: SCAN #5 42684	RECORD NO.	

CORDING
CRODENSITOMETER

JOYCE LOEBL & CO. INC. 111 TERRACE HALL AVE. BURLINGTON, MASS.
AFFILIATE OF TECHNICAL OPERATIONS, INCORPORATED

APPENDIX C: HATS-175

1. Microdensitometry traces

2. Linear Regression Analyses of Particle Size Distribution

DATE 12/6/72 CONTROL # ______ TASK Strip Channel PREPARED BY ______

FILM 2420 EMULSION # From 2402 O.N. MFG ______ EXPIRATION DATE ______

2402 EXPOSURE DATA	PROCESSING DATA	DENSITOMETRY	
SENSITOMETER 1-B	PROCESSOR Versamat 11C	INSTRUMENT Macbeth	SPEED ( )
ILLUMINANT 2850 K	CHEMISTRY 641	TYPE TD217 DR	D-MAX 2.7
TIME 1/100 SEC	SPEED ___ TANKS ___ FPM	APERTURE SIZE 2 MM	GAMMA
FILTER 5500	TEMP °F ___ TIME ___	FILTER V+S	BASE + FOG

CHEMICAL ANALYSIS

___ SP GR

___ pH

___ TA

___ TRP

___ KB_r

21	
20	
19	
18	
17	
16	
15	
14	
13	
12	
11	
10	
9	
8	
7	
6	
5	
4	
3	
2	
1	

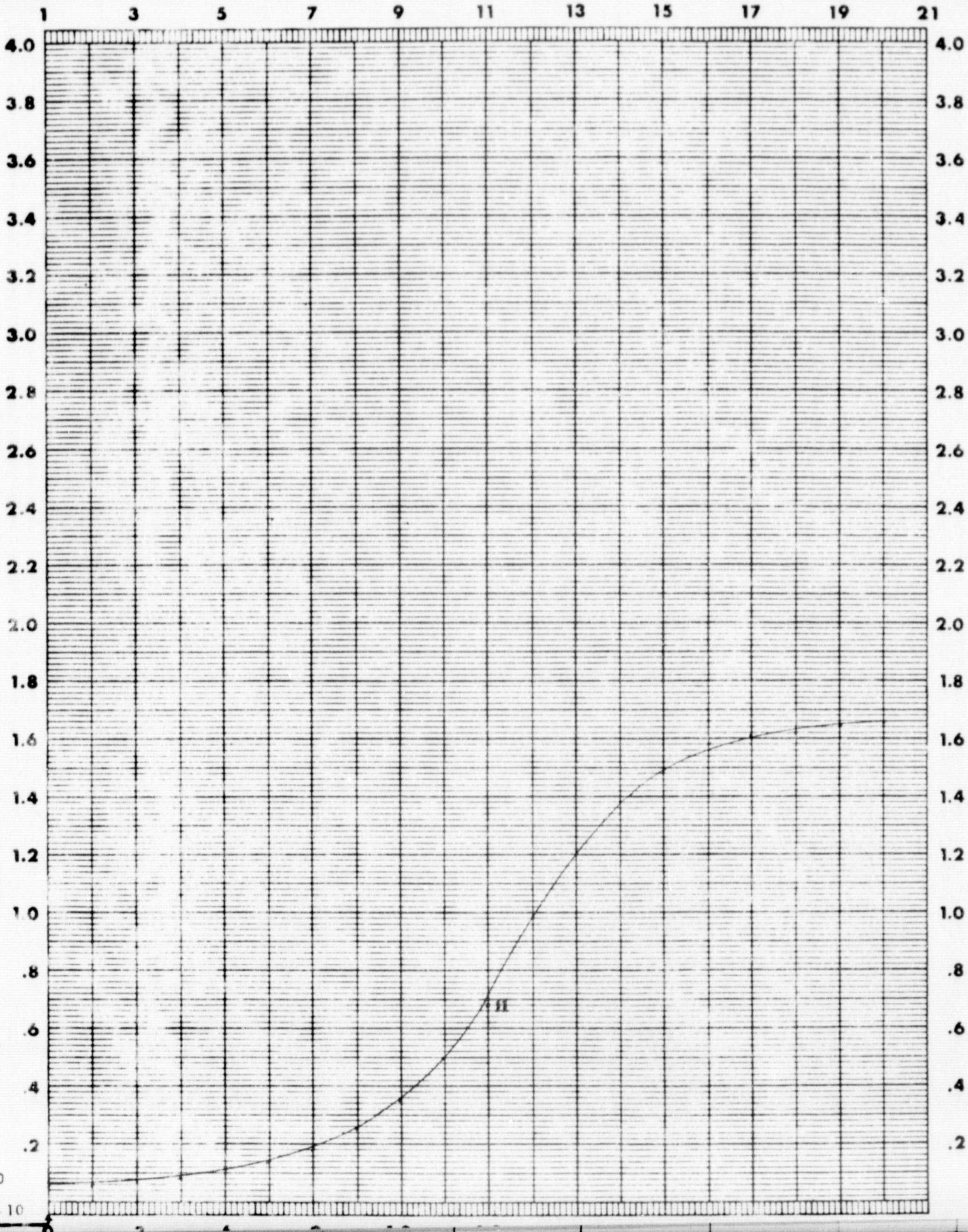

Technicolor

ABSOLUTE LOG E AT R.L.E. 0

6.87 -10

TABLE 1 Calibration Step-Wedge Densitometry Data

9-1-72

Ship Channel Roll 1
2402 NF 1/100sec 2850 5500
Abs Log E 6.87-10

0.68	step 11
0.99	
1.21	
1.38	
1.49	
1.58	
1.61	
1.62	
1.64	
1.65	
0.50	
0.35	
0.25	
0.18	
0.14	
0.10	
0.08	
0.07	
0.06	
0.05	

JOYCE
LOEBL

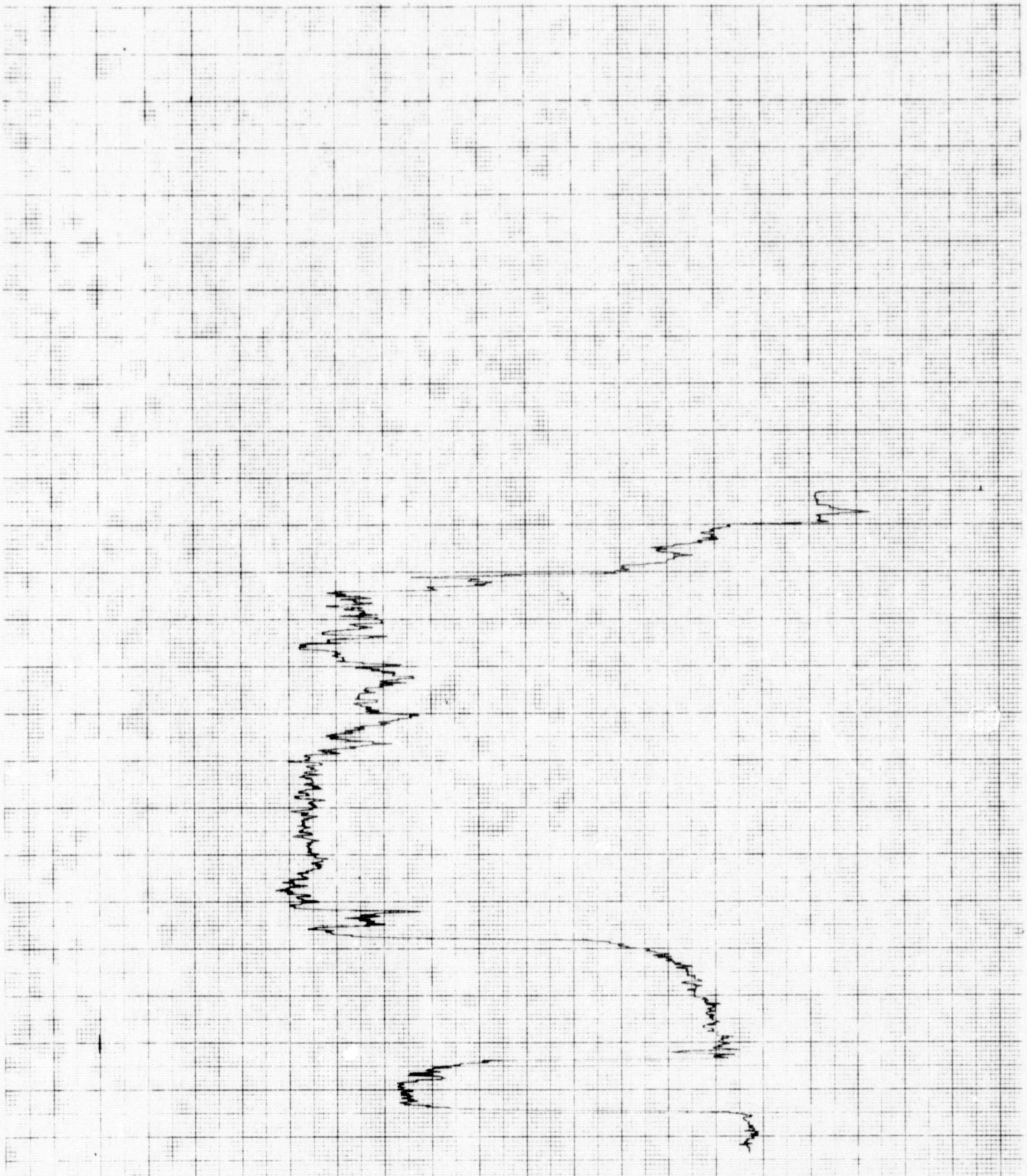

OPTICAL MAGNIFC. = OBJECTIVE POWER x 0·2	PROPORT. CONTL.	WEDGE RANGE	SAMPLE:	DATE	FORM MDS
SLIT (ACTUAL)	FEEDBACK SETTING	RATIO	REMARKS	RECORD No.	

JOYCE LOEBL

RECORDING MICRODENSITOMETER

JOYCE LOEBL & CO. INC. 111 TERRACE HALL AVE. BURLINGTON, MASS.
AFFILIATE OF TECHNICAL OPERATIONS, INCORPORATED

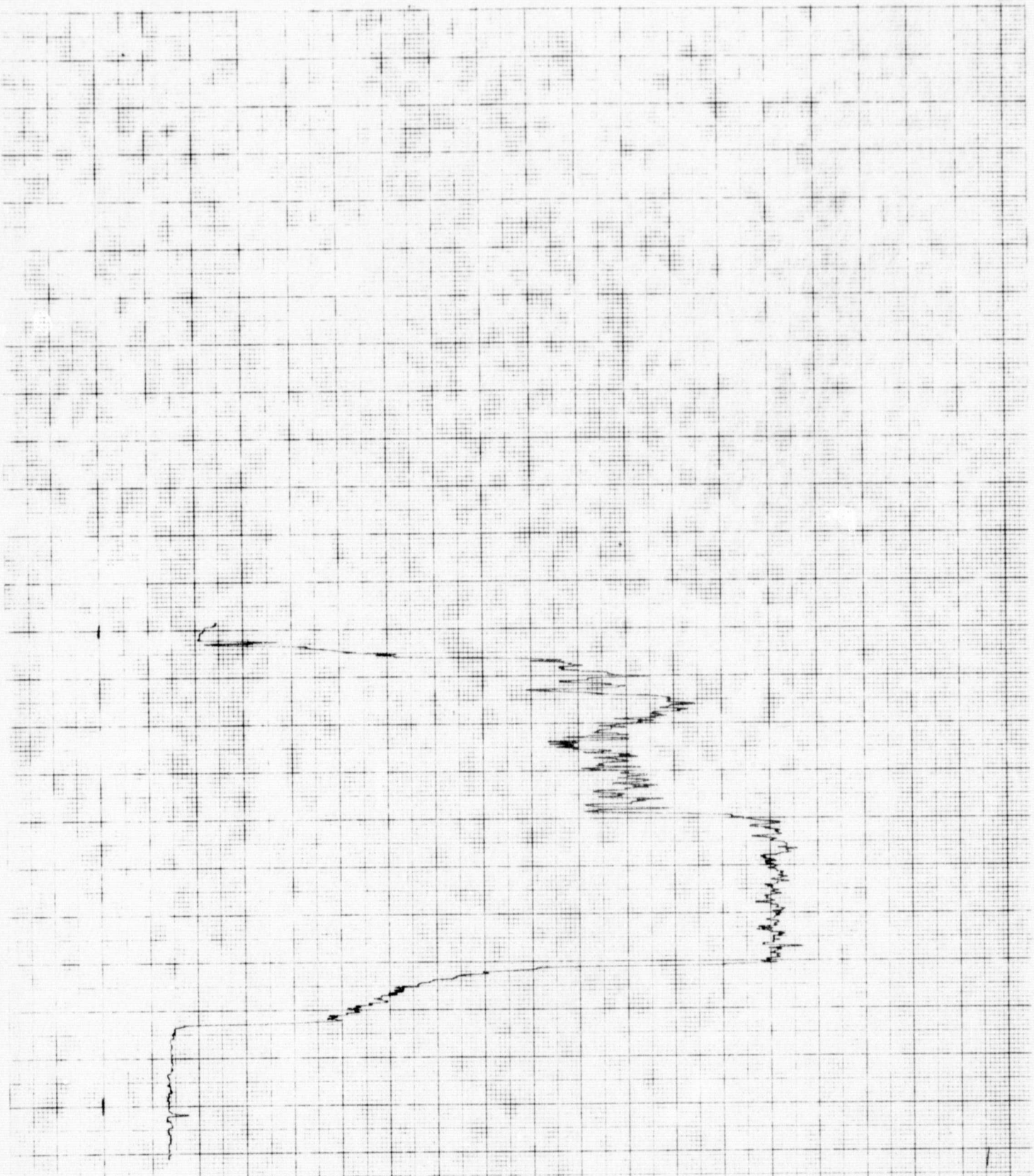

JOYCE LOEBL

RECORDING MICRODENSITOMETER

OPTICAL MAGNIFIC. = OBJECTIVE POWER x 22

PROPORT. CONTL.

WEDGE RANGE

SAMPLE:

DATE

FORM MDS

SLIT (ACTUAL)

FEEDBACK SETTING

RATIO

REMARKS

RECORD NO.

JOYCE LOEBL & CO., INC., 111 TERRACE HALL AVE. BURLINGTON, MASS.
AFFILIATE OF TECHNICAL OPERATIONS, INCORPORATED

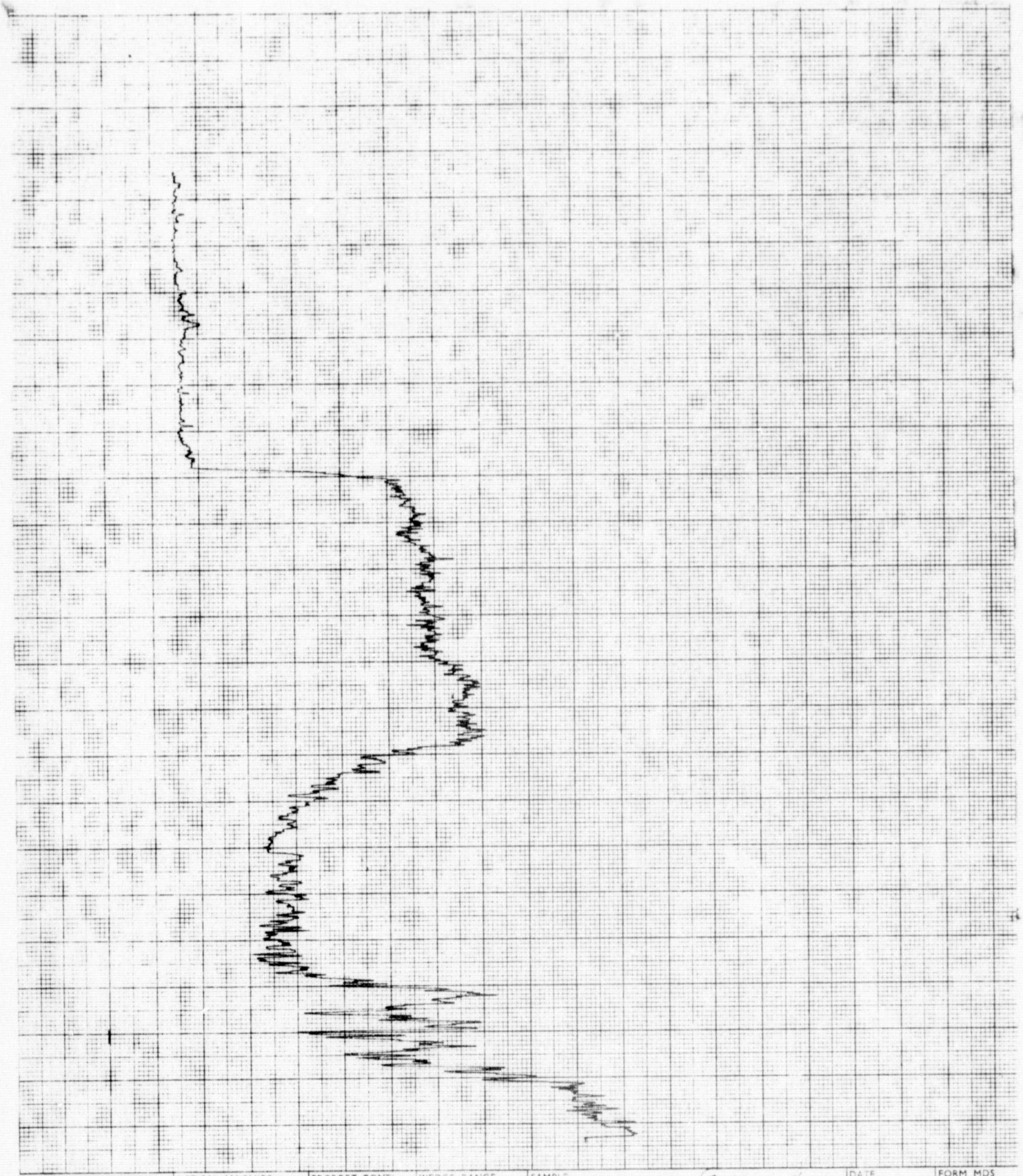

JOYCE LOEBL	OPTICAL MAGNIFC. = OBJECTIVE POWER x 22	PROPORT. CONTL.	WEDGE RANGE 6 : 7	SAMPLE: Fr 8. 930 (corner ... turn - #4)	DATE
	SLIT (ACTUAL) 20µ	FEEDBACK SETTING	RATIO 5 : 1	REMARKS:	RECORD No.

FORM MDS

RECORDING MICRODENSITOMETER

JOYCE LOEBL & CO. INC. 111 TERRACE HALL AVE. BURLINGTON, MASS.
AFFILIATE OF TECHNICAL OPERATIONS, INCORPORATED

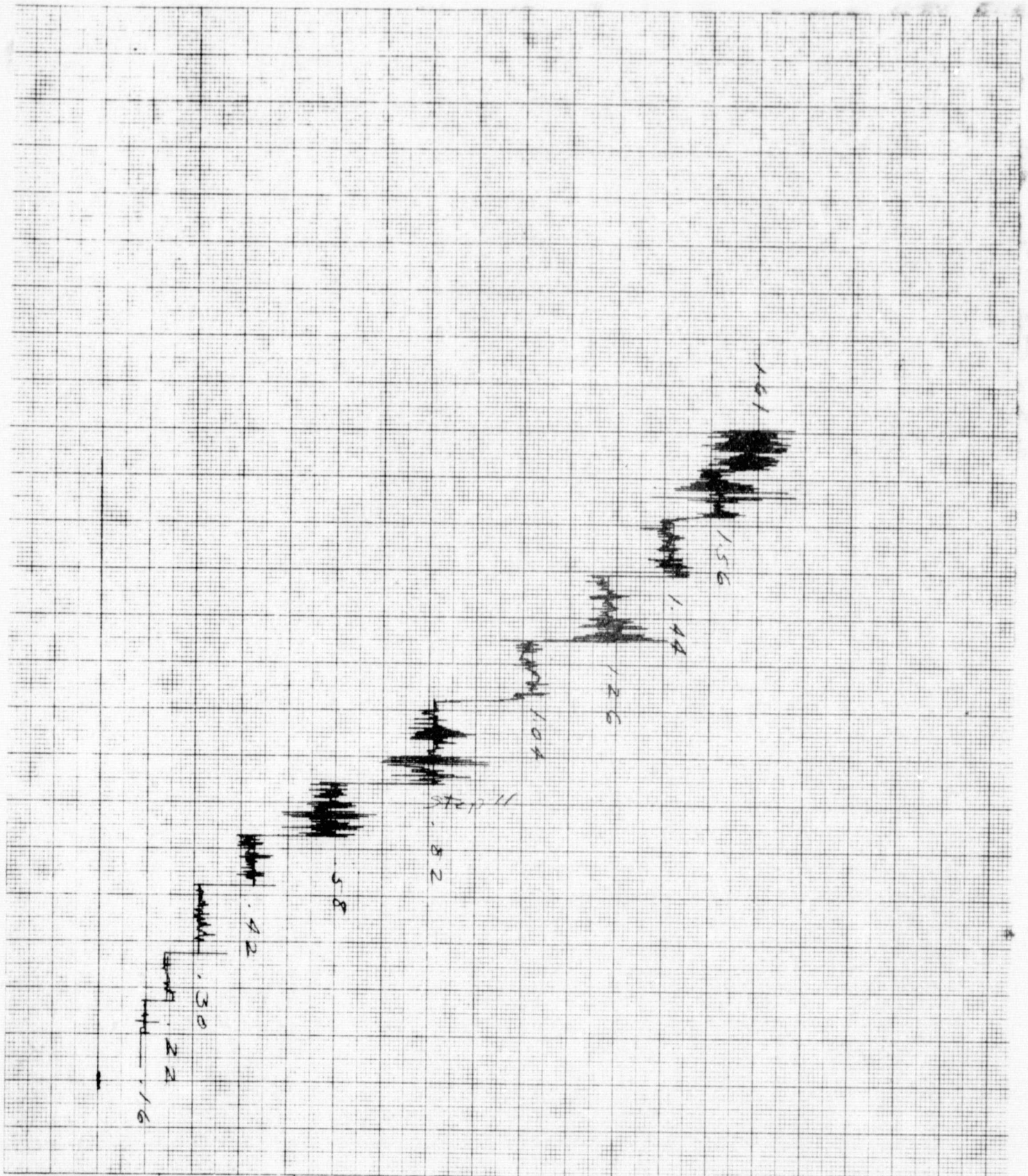

JOYCE LOEBL	OPTICAL MAGNIFC. = OBJECTIVE POWER x 22	PROPORT. CONTL.	WEDGE RANGE 0 - 2.7	SAMPLE: 82931-30	DATE	FORM MDS
	SLIT (ACTUAL) 40 μ	FEEDBACK SETTING	RATIO 10:1	REMARKS: #5, 6, 7, 8	RECORD Nº.	

RECORDING MICRODENSITOMETER

JOYCE LOEBL & CO. INC. 111 TERRACE HALL AVE. BURLINGTON, MASS.
AFFILIATE OF TECHNICAL OPERATIONS, INCORPORATED

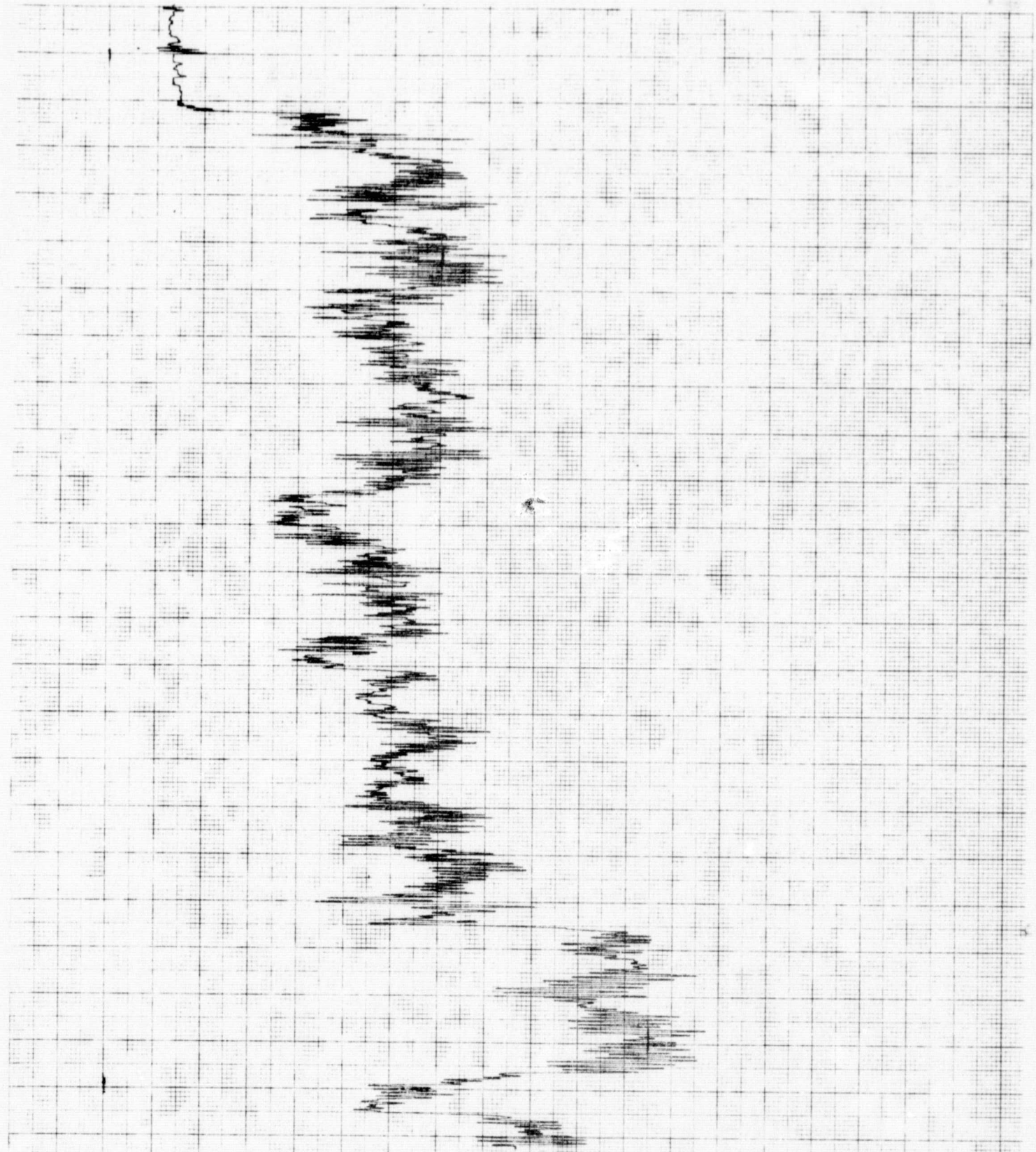

JOYCE LOEBL

RECORDING MICRODENSITOMETER

OPTICAL MAGNIFC. × OBJECTIVE POWER x 2.2 | PROPORT. CONTL | WEDGE RANGE | SAMPLE: Fx 3 [illegible] | DATE 1/2/72 | FORM MDS

SLIT (ACTUAL) .09 | FEEDBACK SETTING RATIO | REMARKS | RECORD NO.

JOYCE LOEBL & CO. INC. 111 TERRACE HALL AVE. BURLINGTON, MASS.
AFFILIATE OF TECHNICAL OPERATIONS, INCORPORATED

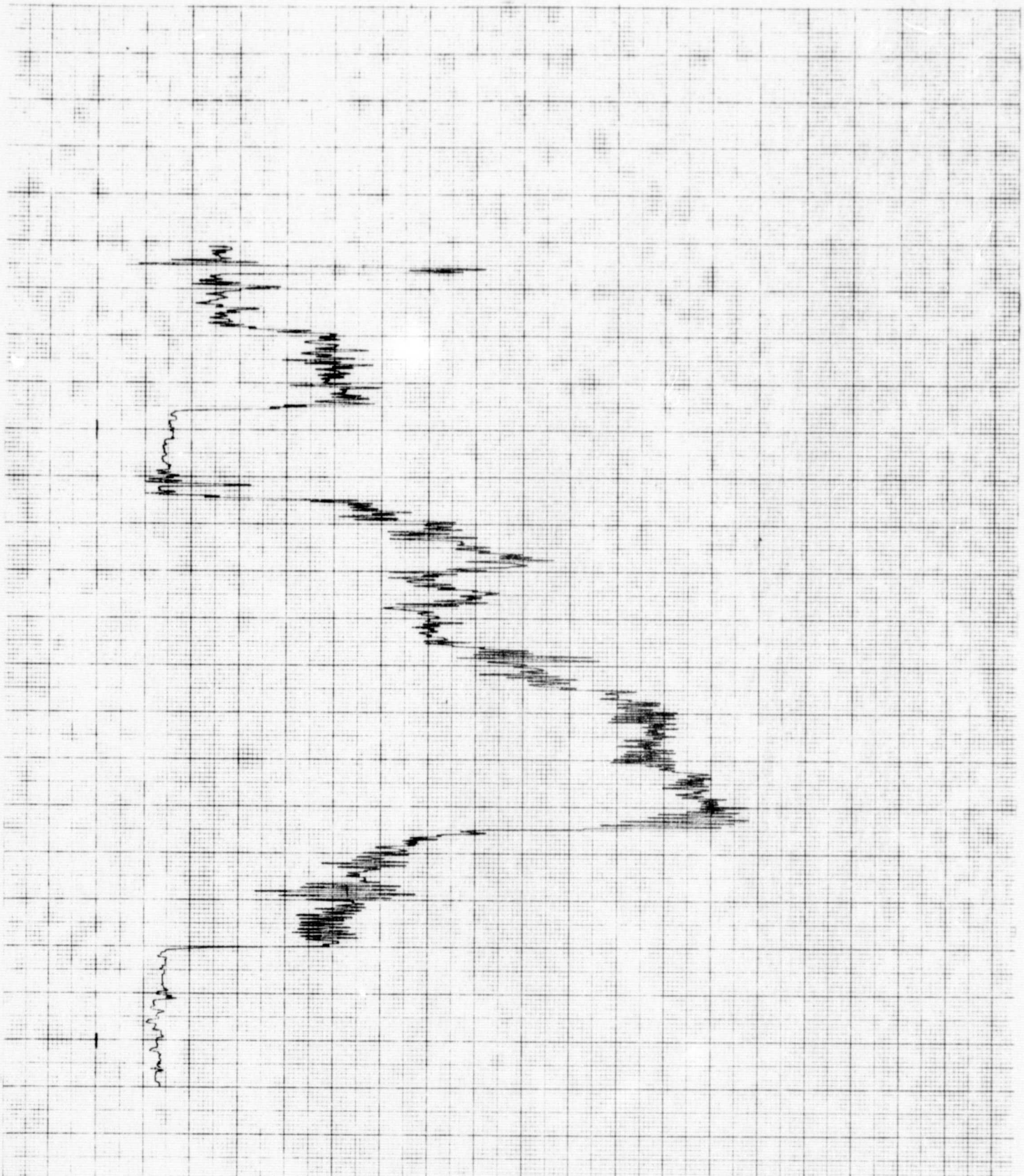

JOYCE LOEBL

RECORDING MICRODENSITOMETER

OPTICAL MAGN/FC. = OBJECTIVE POWER x 2·2	PROPORT. CONTL.	WEDGE RANGE	SAMPLE:	DATE	FORM MD5
SLIT (ACTUAL)	FEEDBACK SETTING	RATIO	REMARKS:	RECORD Nº.	

JOYCE LOEBL & CO. INC. 115 TERRACE HALL AVE. BURLINGTON, MASS.
AFFILIATE OF TECHNICAL OPERATIONS, INCORPORATED

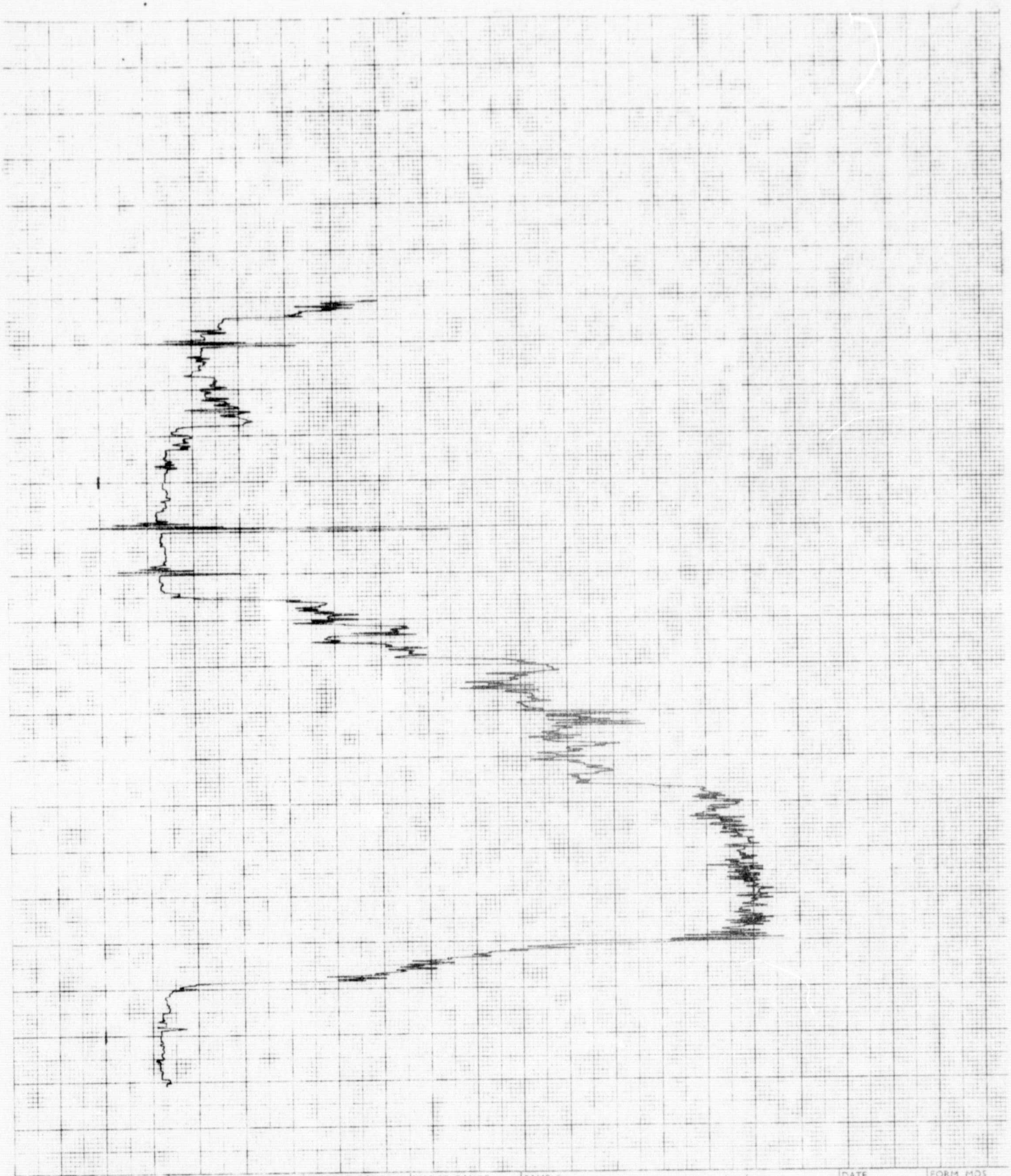

OPTICAL MAGNIFIC. × OBJECTIVE POWER × 2.2	PROPORT CONTL	WEDGE RANGE 0.2	SAMPLE	DATE	FORM MDS
SLIT (ACTUAL)	FEEDBACK SETTING	RATIO 10	REMARKS	RECORD №	

JOYCE LOEBL

RECORDING MICRODENSITOMETER

JOYCE LOEBL & CO. INC. 111 TERRACE HALL AVE. BURLINGTON, MASS.
AFFILIATE OF TECHNICAL OPERATIONS, INCORPORATED

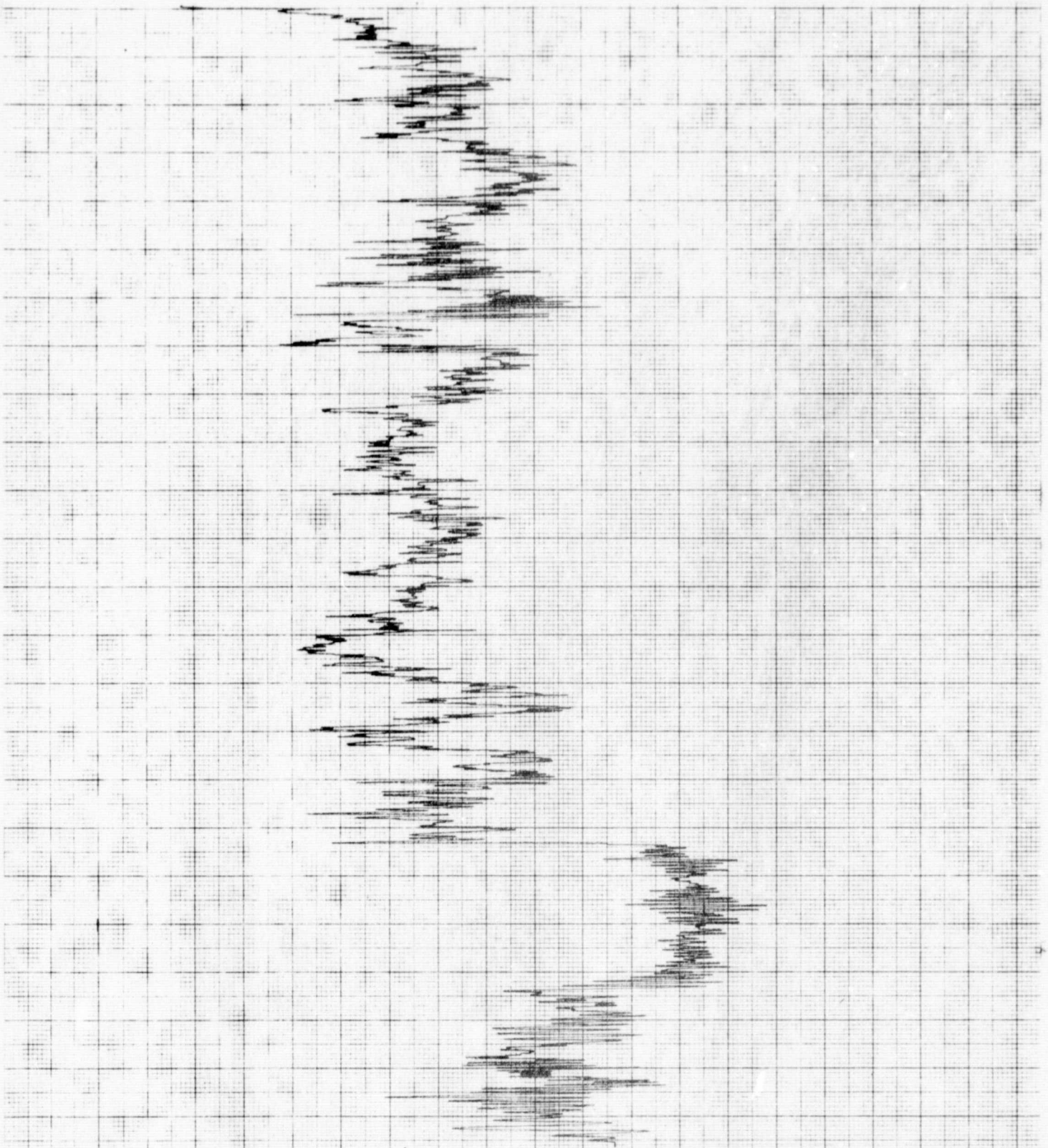

JOYCE LOEBL

RECORDING MICRODENSITOMETER

OPTICAL MAGNIFICATION / OBJECTIVE POWER x 2.2	PROPORT. CONTL.	WEDGE RANGE	SAMPLE:	DATE	FORM MDS
SLIT (ACTUAL)	FEEDBACK SETTING	RATIO	REMARKS:	RECORD Nº	

JOYCE LOEBL & CO. INC. 111 TERRACE HALL AVE. BURLINGTON, MASS.
AFFILIATE OF TECHNICAL OPERATIONS, INCORPORATED

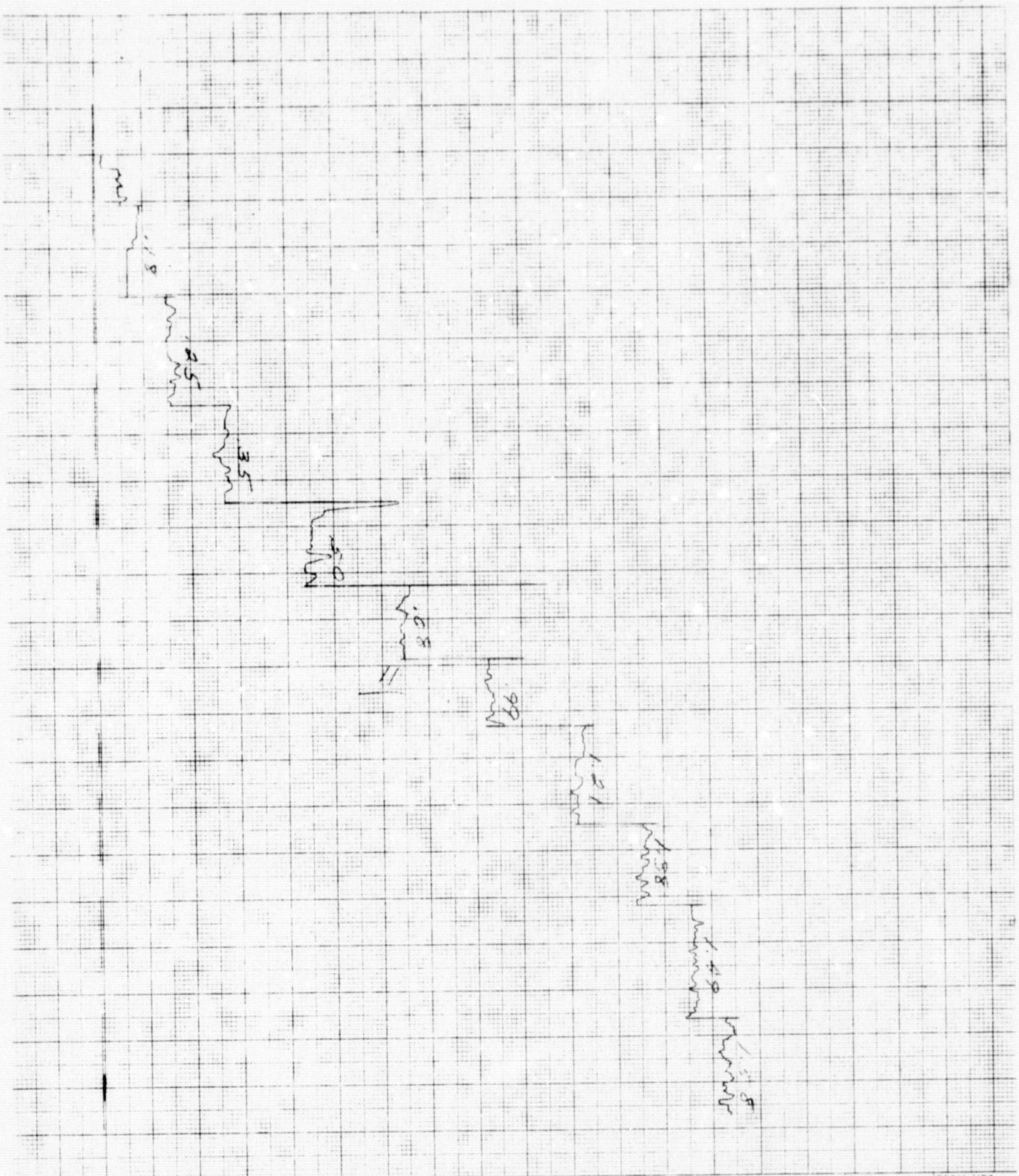

JOYCE LOEBL	OPTICAL MAGNIFC. = OBJECTIVE POWER x 22	PROPORT. CONTL.	WEDGE RANGE	SAMPLE	DATE
	SLIT (ACTUAL)	FEEDBACK SETTING	RATIO	REMARKS:	RECORD Nº

FORM MDS

RECORDING MICRODENSITOMETER

JOYCE LOEBL & CO. INC. 111 TERRACE HALL AVE. BURLINGTON, MASS.
AFFILIATE OF TECHNICAL OPERATIONS, INCORPORATED

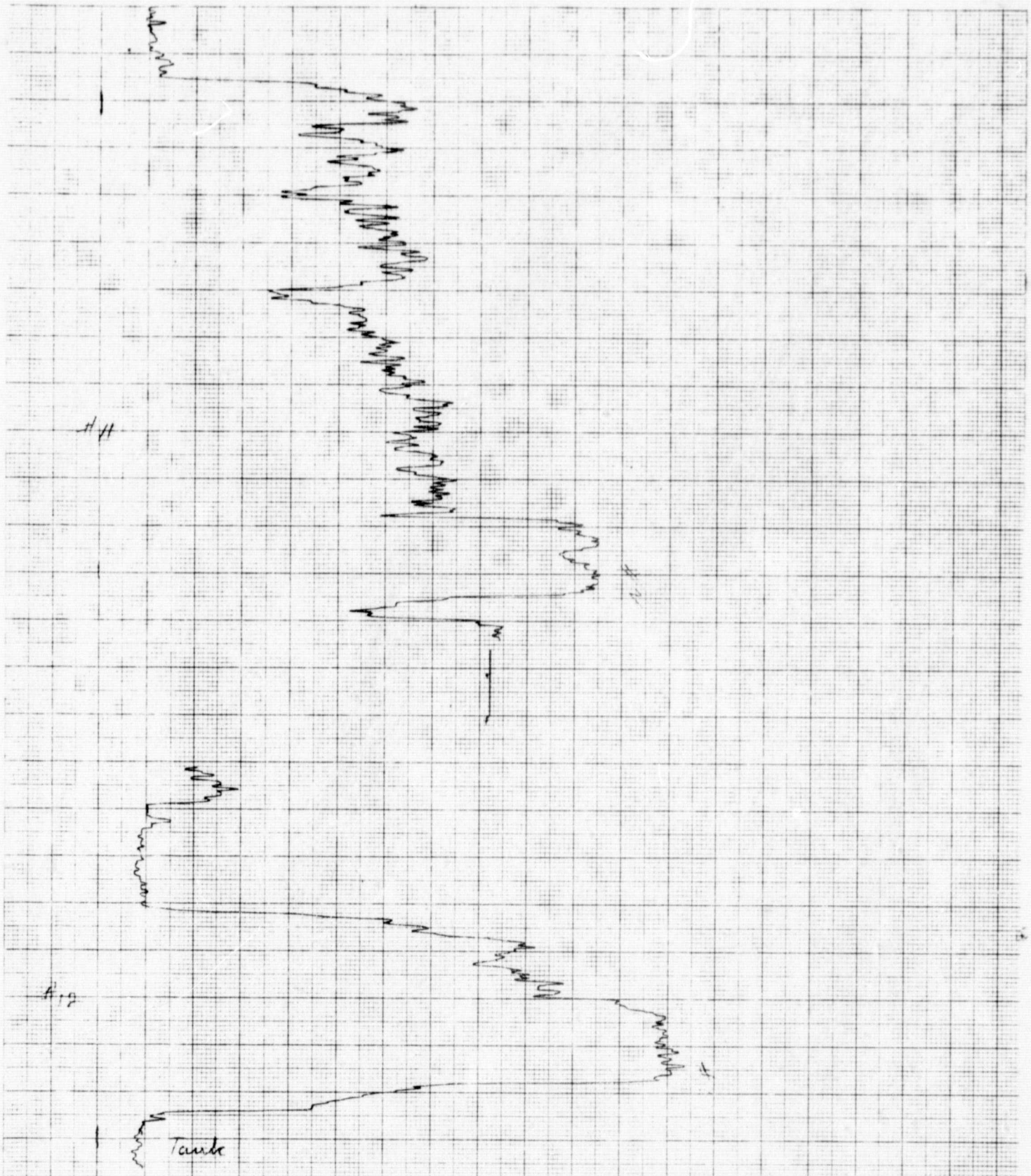

JOYCE LOEBL

RECORDING MICRODENSITOMETER

OPTICAL MAGNIFC. = OBJECTIVE POWER x 2·2	PROPORT. CONTL.	WEDGE RANGE	SAMPLE: # 11, 12	DATE
SLIT (ACTUAL) 6	FEEDBACK SETTING	RATIO	REMARKS:	RECORD Nº

FORM MDS

JOYCE LOEBL & CO. INC. 111 TERRACE HALL AVE. BURLINGTON, MASS.
AFFILIATE OF TECHNICAL OPERATIONS, INCORPORATED

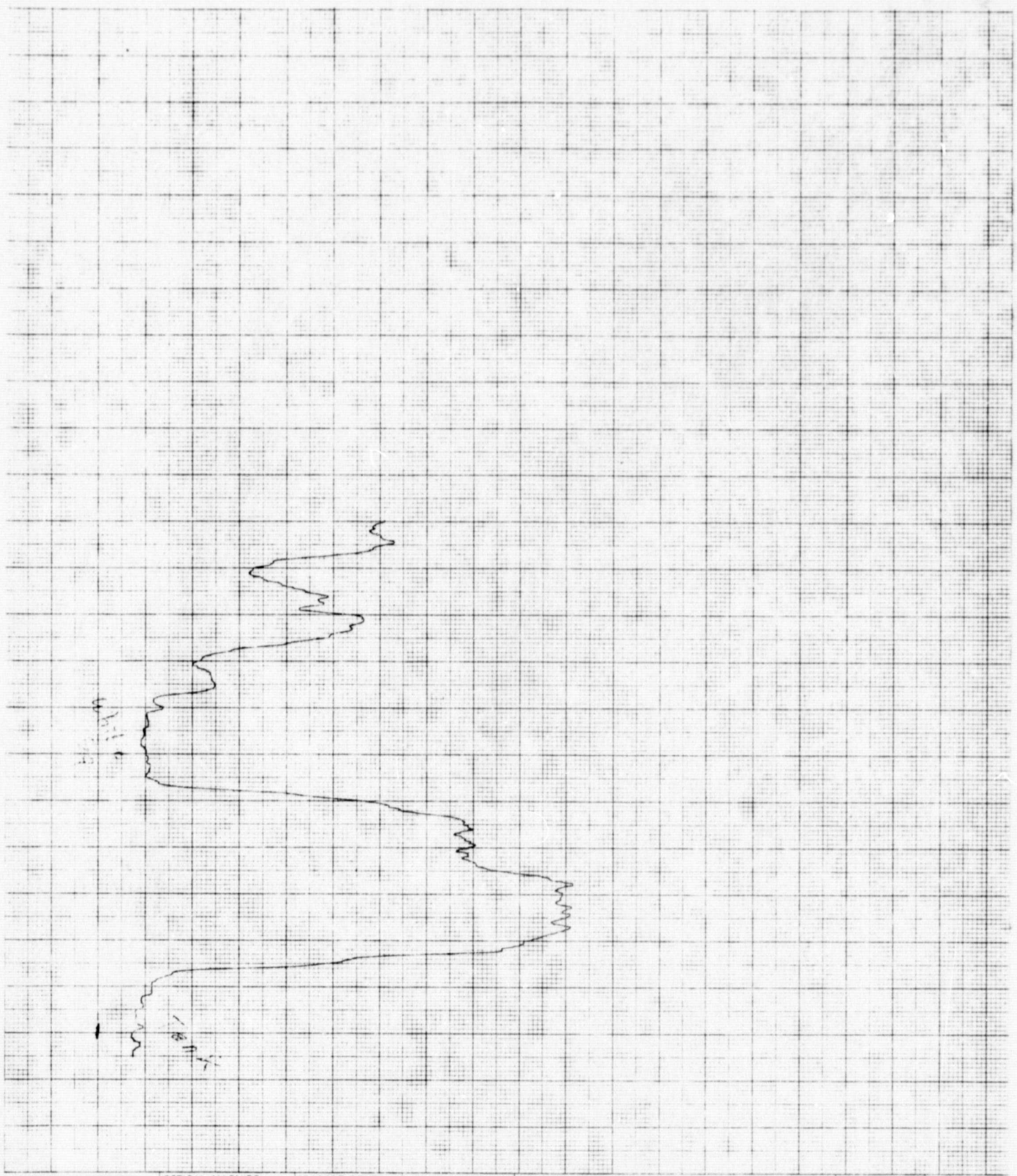

JOYCE LOEBL	OPTICAL MAGNIFC. = OBJECTIVE POWER x 2·2	PROPORT. CONTL.	WEDGE RANGE	SAMPLE:	DATE	FORM MDS
	SLIT (ACTUAL)	FEEDBACK SETTING	RATIO	REMARKS:	RECORD Nº.	

RECORDING MICRODENSITOMETER

JOYCE LOEBL & CO. INC. 111 TERRACE HALL AVE. BURLINGTON, MASS.
AFFILIATE OF TECHNICAL OPERATIONS, INCORPORATED

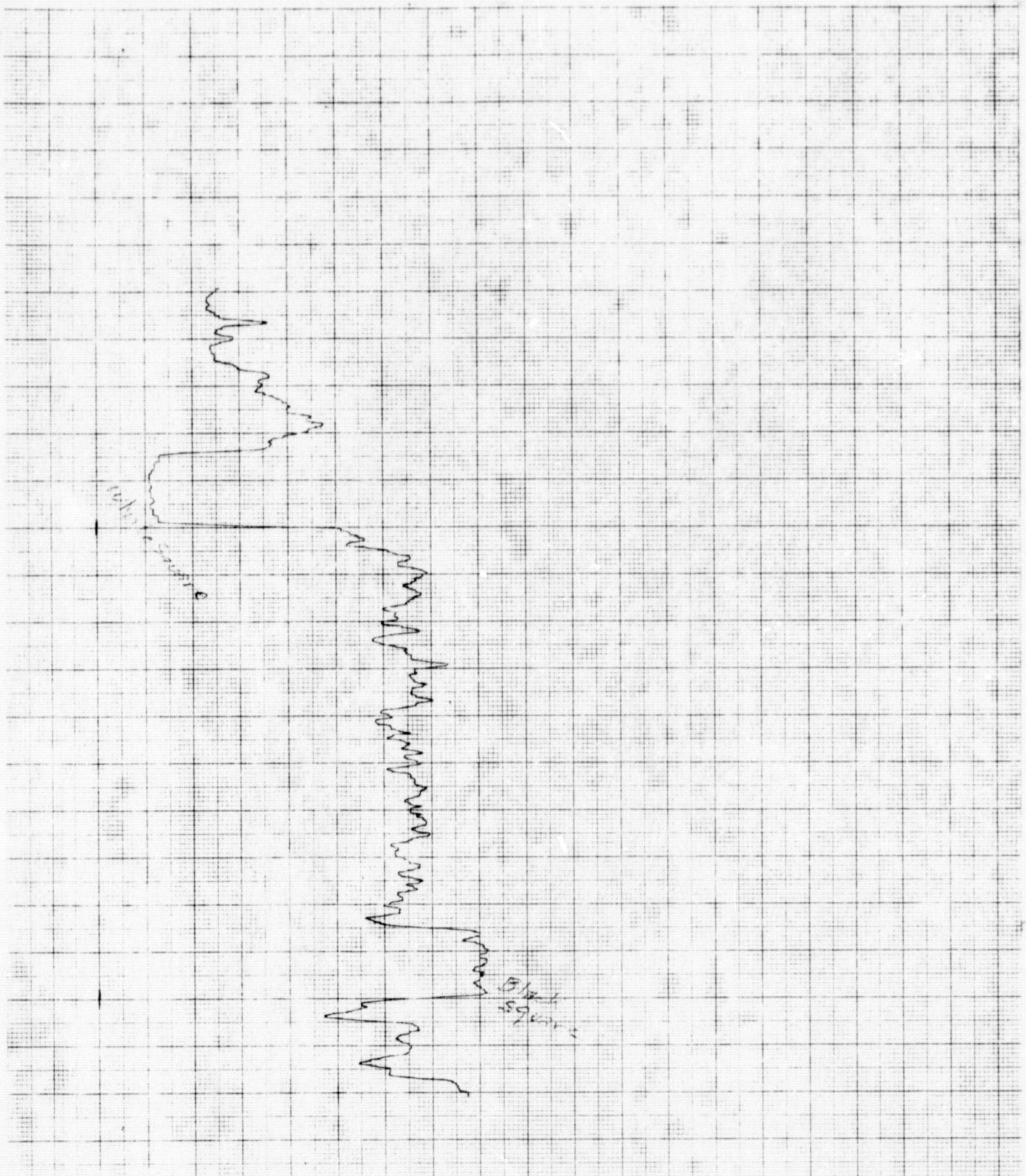

JOYCE LOEBL	OPTICAL MAGNIFIC. = OBJECTIVE POWER x 2	PROPORT. CONTL	WEDGE RANGE	SAMPLE:	DATE
	SLIT (ACTUAL)	FEEDBACK SETTING	RATIO	REMARKS:	RECORD N°

FORM MDS

RECORDING MICRODENSITOMETER

JOYCE LOEBL & CO. INC. 111. TERRACE HALL AVE. BURLINGTON, MASS.
AFFILIATE OF TECHNICAL OPERATIONS, INCORPORATED

JOYCE LOEBL

OPTICAL MAGNIFIC. = OBJECTIVE POWER x 22

PROPORT. CONTL.

WEDGE RANGE

SAMPLE:

DATE

FORM MDS

SLIT (ACTUAL)

FEEDBACK SETTING RATIO

REMARKS:

RECORD N°

RECORD N°
MICRODENSITOMETER

JOYCE LOEBL & CO. INC. 111 TERRACE HALL AVE. BURLINGTON, MASS.
AFFILIATE OF TECHNICAL OPERATIONS, INCORPORATED

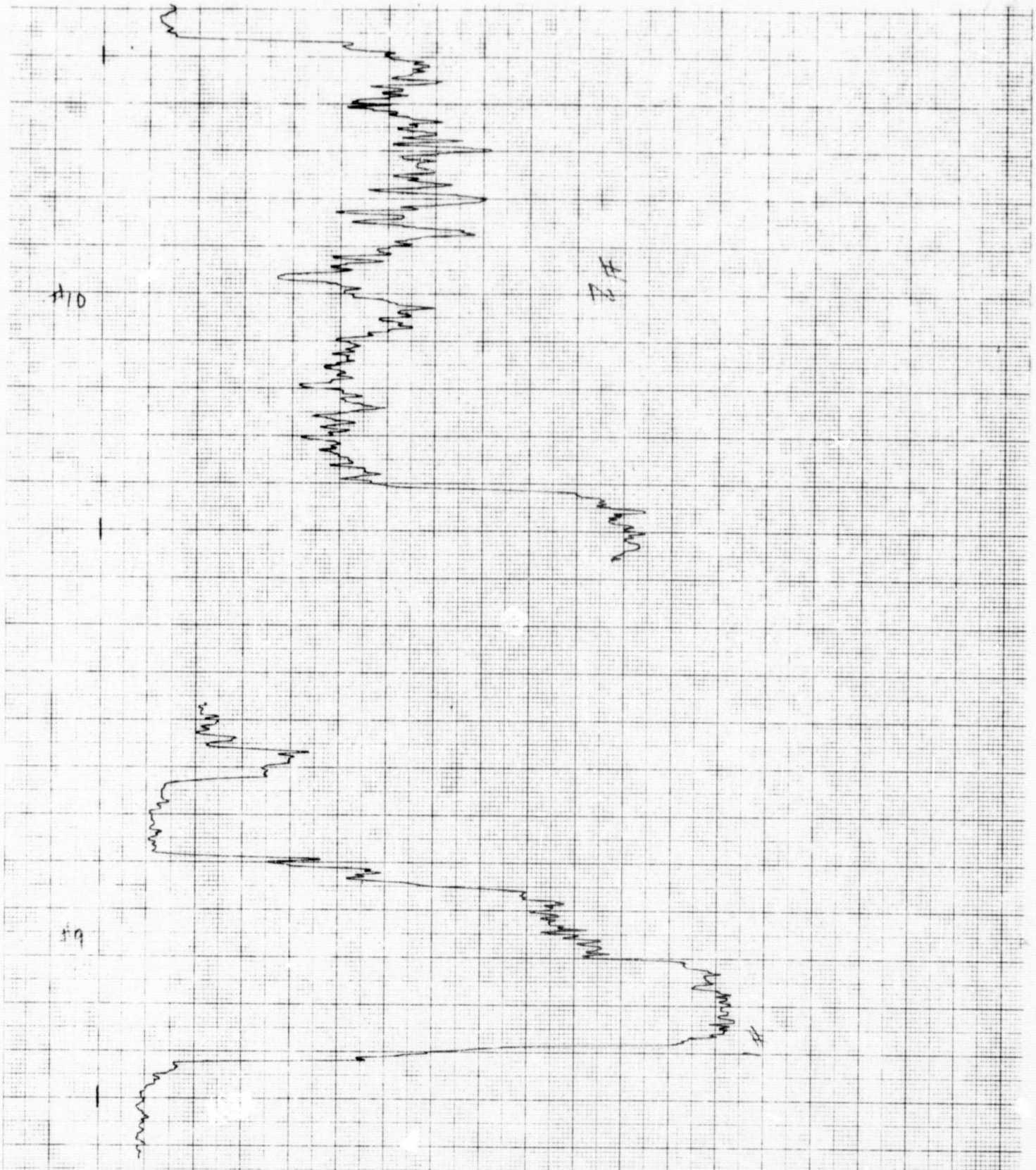

JOYCE LOEBL

RECORDING MICRODENSITOMETER

OPTICAL MAGNIFC. = OBJECTIVE POWER x 2.5	PROPORT. CONTL.	WEDGE RANGE 0 - 7	SAMPLE: FR 8294 - 2 #10.9	DATE 1/61
SLIT (ACTUAL) 6µ	FEEDBACK SETTING RATIO 2:1		REMARKS #1 [illegible] #2 [illegible]	RECORD Nº.

FORM MDS

JOYCE LOEBL & CO. INC. 111 TERRACE HALL AVE. BURLINGTON, MASS.
AFFILIATE OF TECHNICAL OPERATIONS, INCORPORATED

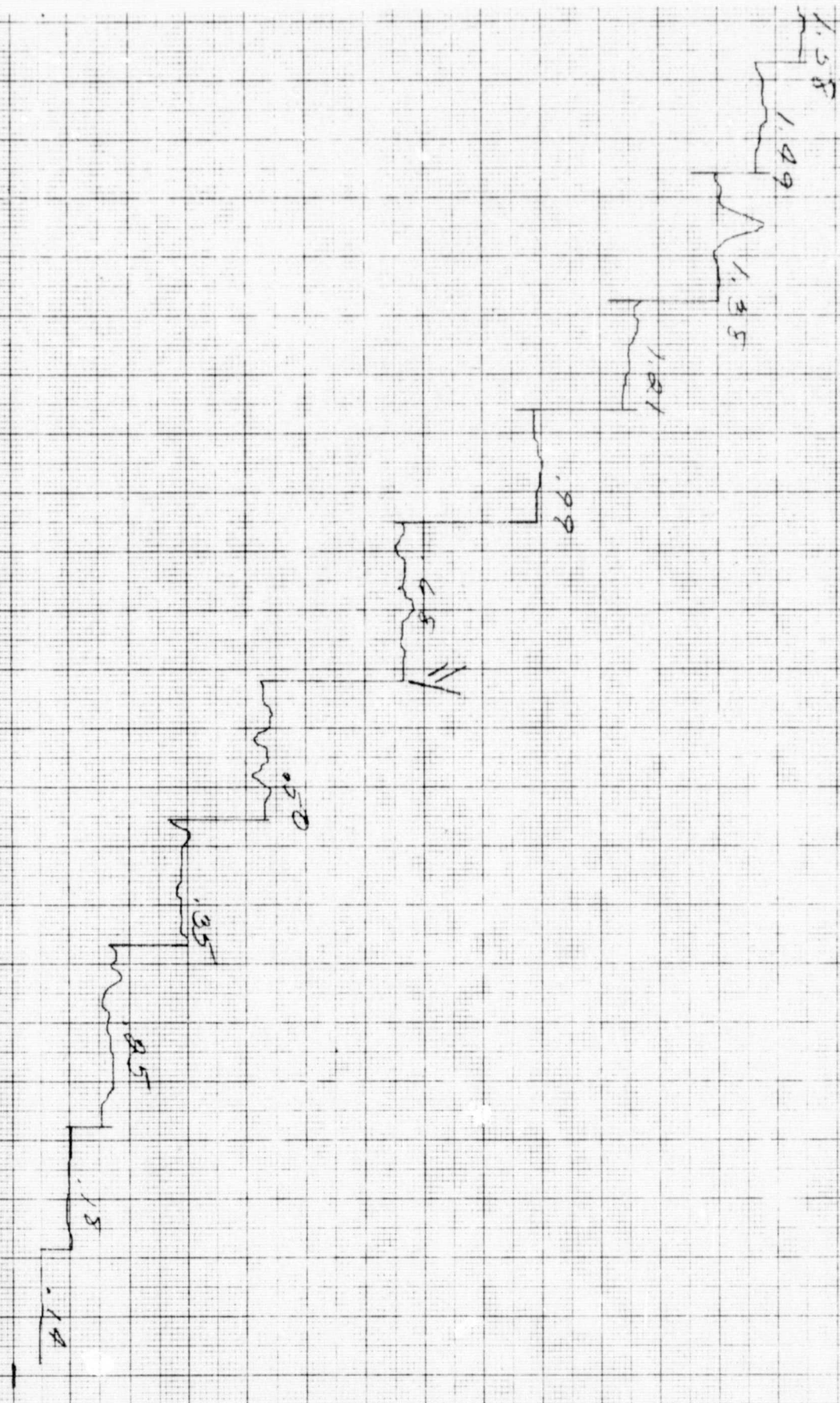

JOYCE LOEBL

ECORDING
ICRODENSITOMETER

OPTICAL MAGNIFC. = OBJECTIVE POWER x 2·2	PROPORT. CONTL.	WEDGE RANGE	SAMPLE:	DATE	FORM MDS
SLIT (ACTUAL)	FEEDBACK SETTING	RATIO 5	REMARKS:	RECORD NO.	

JOYCE LOEBL & CO. INC. 111. TERRACE HALL AVE. BURLINGTON. MASS.
AFFILIATE OF TECHNICAL OPERATIONS, INCORPORATED

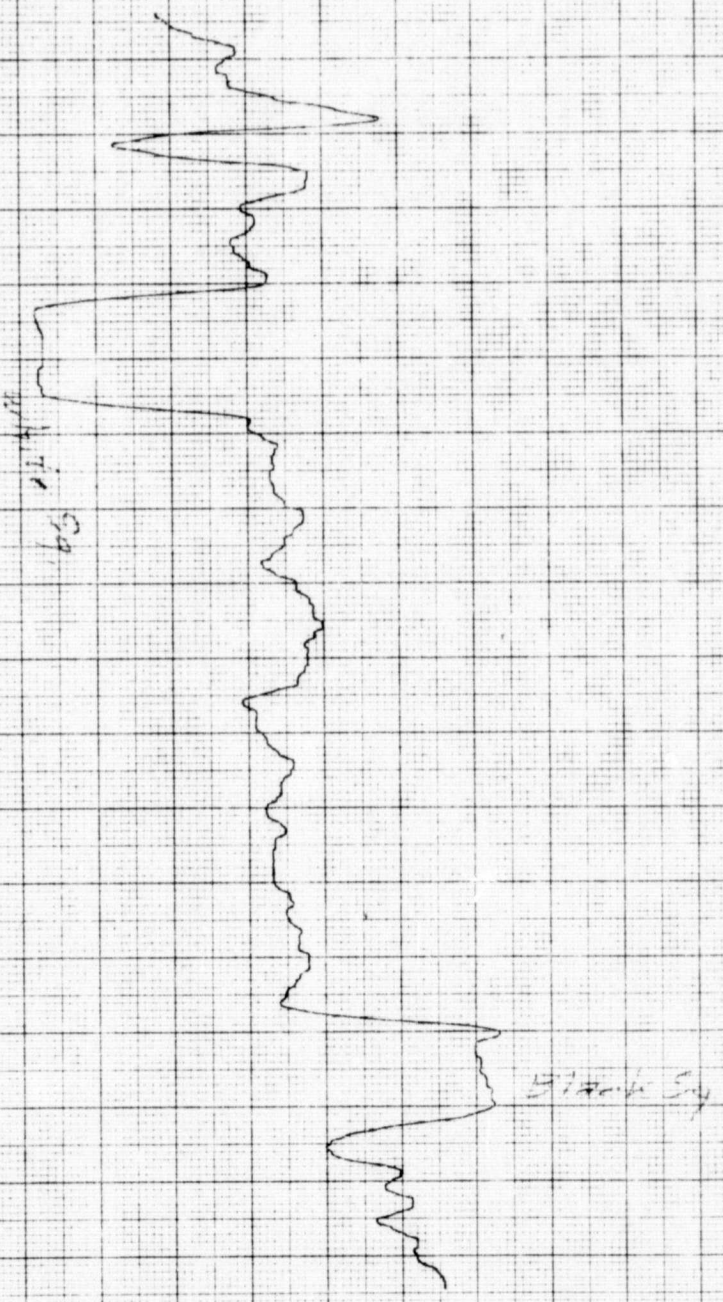

JOYCE LOEBL	OPTICAL MAGNIFC. = OBJECTIVE POWER x 2·2	PROPORT. CONTL.	WEDGE RANGE	SAMPLE:	DATE / FORM MDS
	SLIT (ACTUAL)	FEEDBACK SETTING	RATIO	REMARKS:	RECORD Nº

ECORDING
ICRODENSITOMETER

JOYCE LOEBL & CO. INC. 111 TERRACE HALL AVE BURLINGTON, MASS.
AFFILIATE OF TECHNICAL OPERATIONS, INCORPORATED

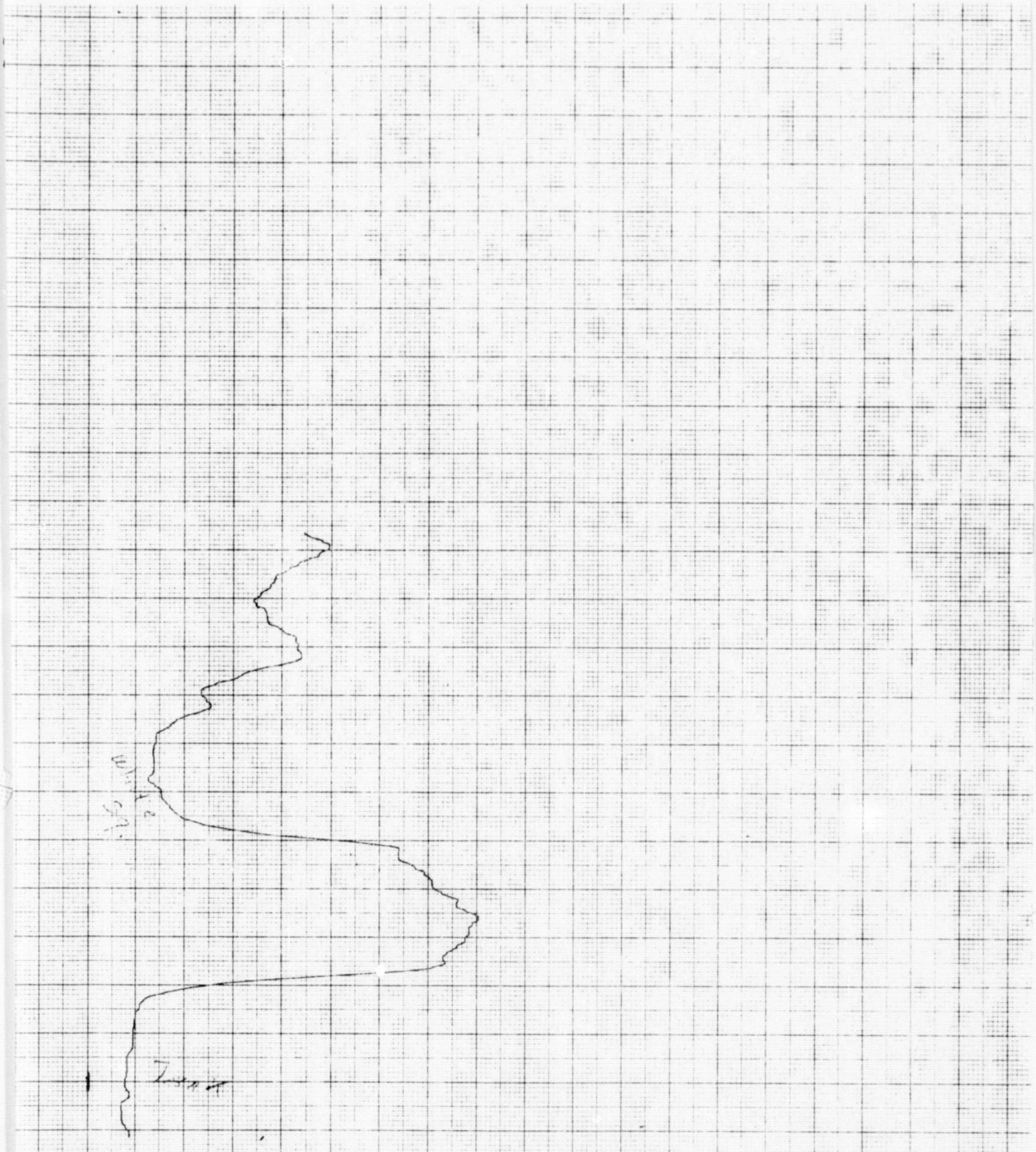

JOYCE LOEBL

ECORDING
ICRODENSITOMETER

OPTICAL MAGNIFC. = OBJECTIVE POWER x 2·2	PROPORT. CONTL.	WEDGE RANGE	SAMPLE: H/15	DATE	FORM MDS
SLIT (ACTUAL)	FEEDBACK SETTING	RATIO	REMARKS:	RECORD Nº	

JOYCE LOEBL & CO. INC. 111 TERRACE HALL AVE. BURLINGTON, MASS.
AFFILIATE OF TECHNICAL OPERATIONS, INCORPORATED

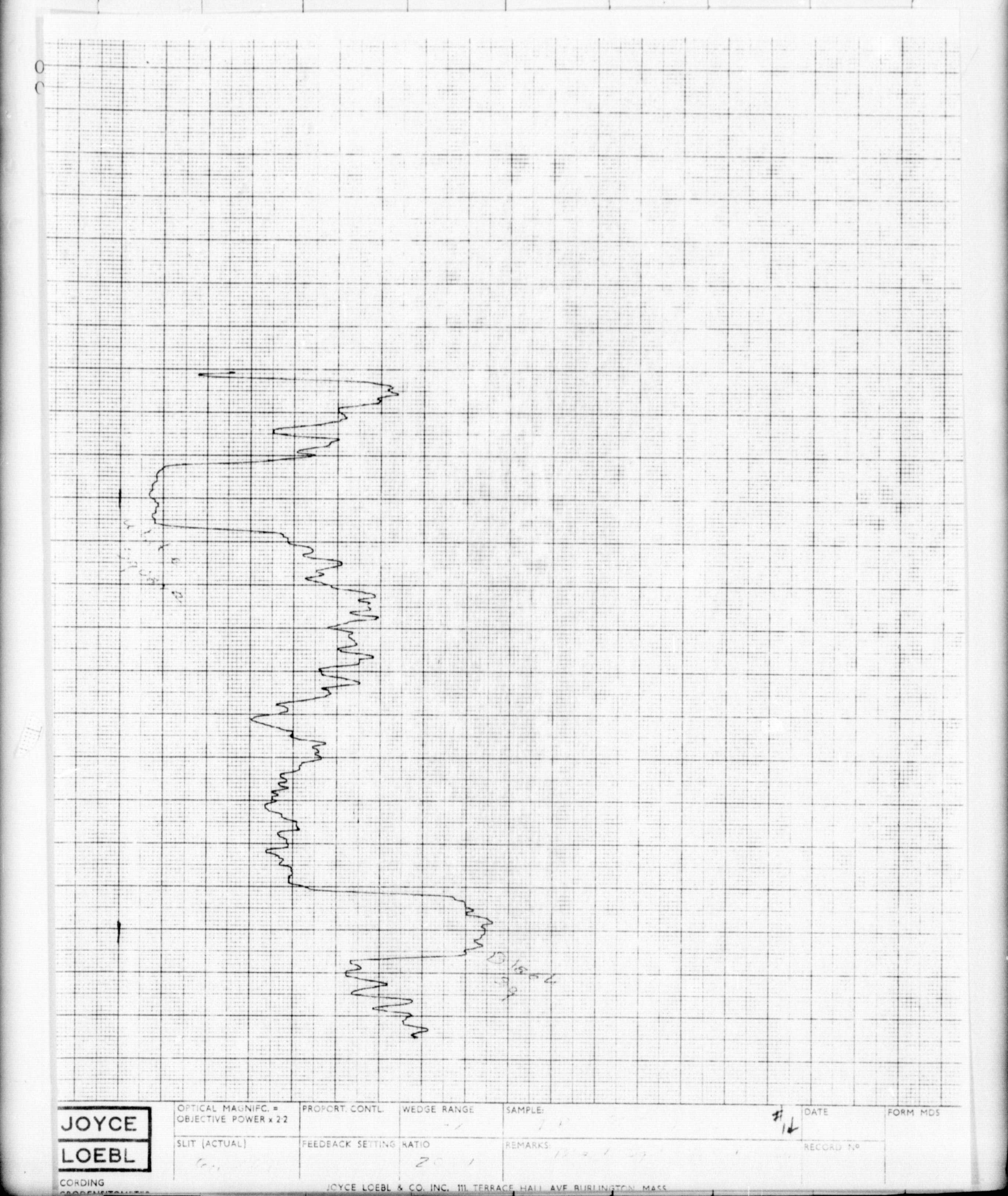

JOYCE LOEBL

CORDING

OPTICAL MAGNIFC. = OBJECTIVE POWER x 2·2	PROPORT. CONTL.	WEDGE RANGE	SAMPLE:	DATE	FORM MDS
SLIT (ACTUAL)	FEEDBACK SETTING	RATIO	REMARKS:	RECORD No.	

JOYCE LOEBL & CO. INC. 111 TERRACE HALL AVE. BURLINGTON, MASS.

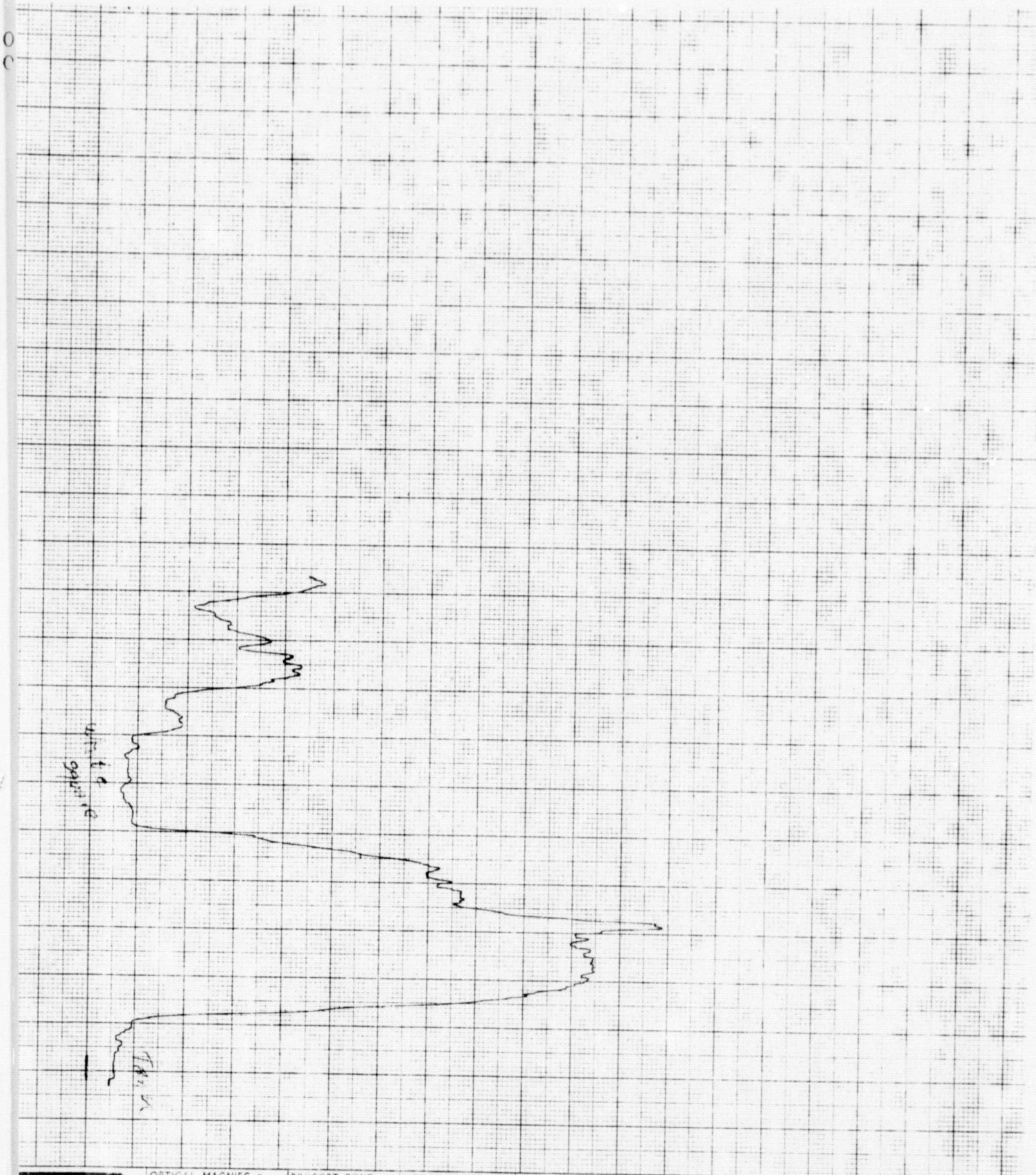

JOYCE LOEBL

CORDING
CRODENSITOMETER

OPTICAL MAGNIFC. = OBJECTIVE POWER x 2.2	PROPORT. CONTL.	WEDGE RANGE	SAMPLE:	DATE	FORM MDS
SLIT (ACTUAL)	FEEDBACK SETTING	RATIO	REMARKS:	RECORD NO.	

JOYCE LOEBL & CO. INC. 111 TERRACE HALL AVE. BURLINGTON, MASS.
AFFILIATE OF TECHNICAL OPERATIONS, INCORPORATED

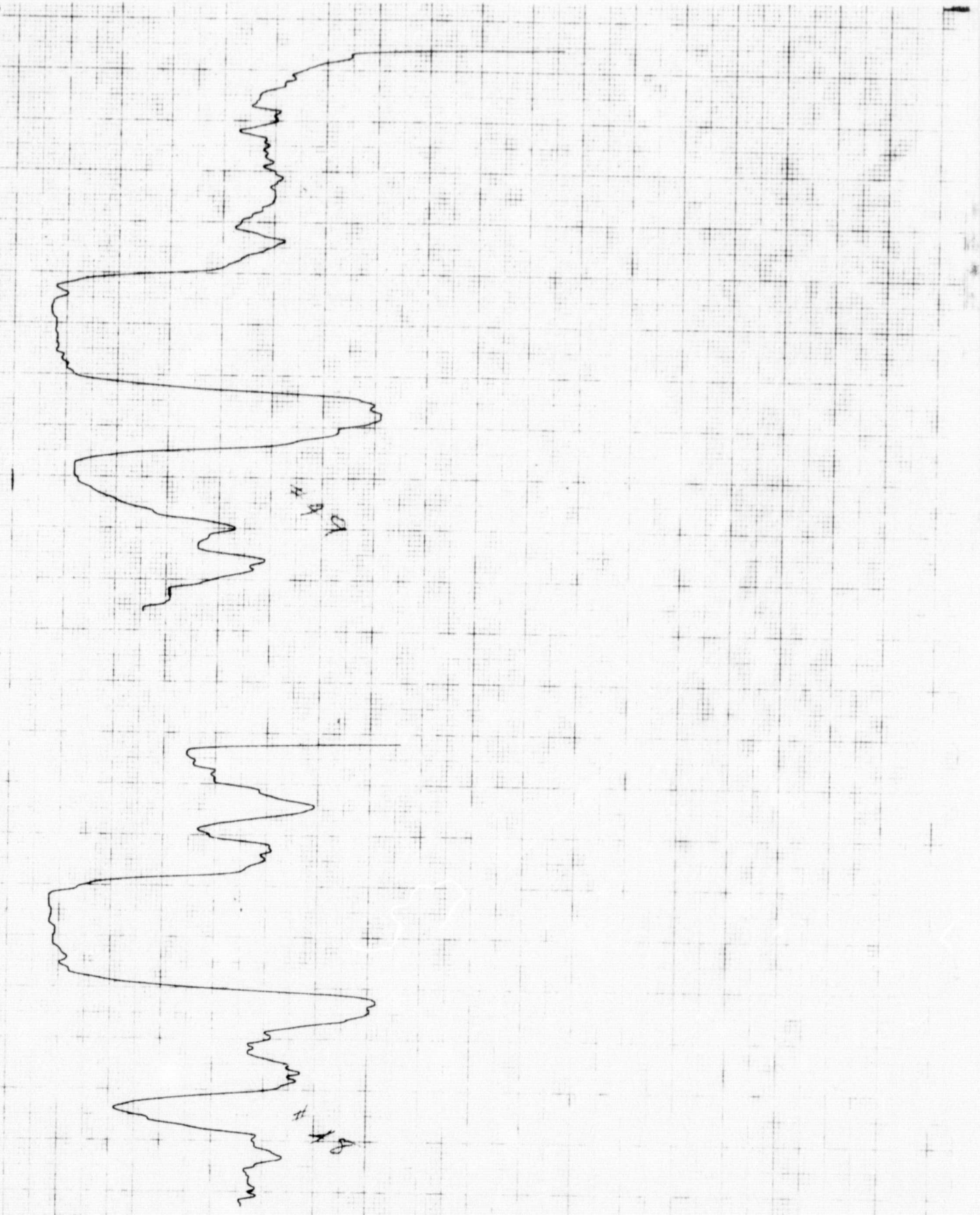

DYCL
DEBL
DING
DENSITOMETER

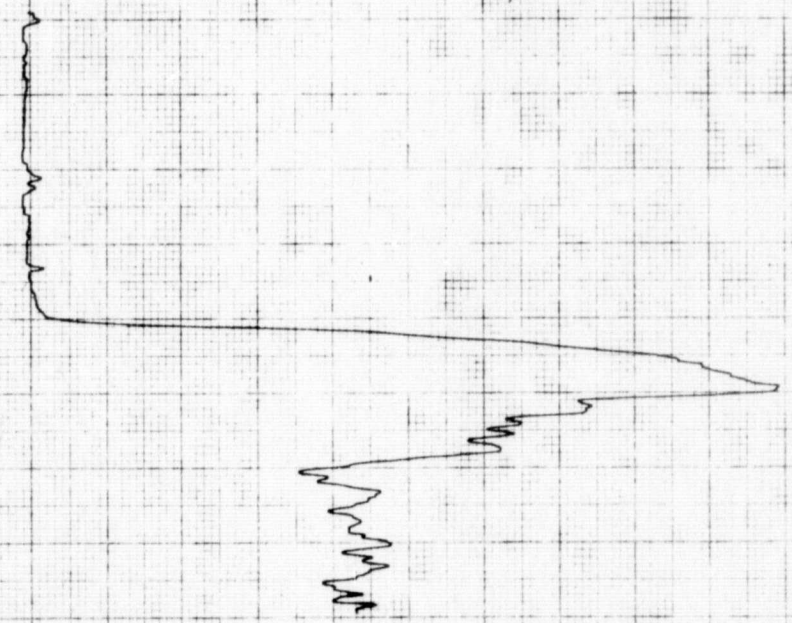

JOYCE LOEBL

RECORDING MICRODENSITOMETER

OPTICAL MAGNIFC. = OBJECTIVE POWER x 22

SLIT (ACTUAL) 60 x 60μ

REPORT CONTL

WEDGE RANGE

FEEDBACK SETTING

RATIO 10:1

SAMPLE: Tank + Jee to top #47

REMARKS: Er 8292 1/2

DATE

FORM NO.

RECORD NO.

JOYCE LOEBL & CO., INC. 111 TERRACE HALL AVE. BURLINGTON, MASS.
AFFILIATE OF TECHNICAL OPERATIONS, INCORPORATED

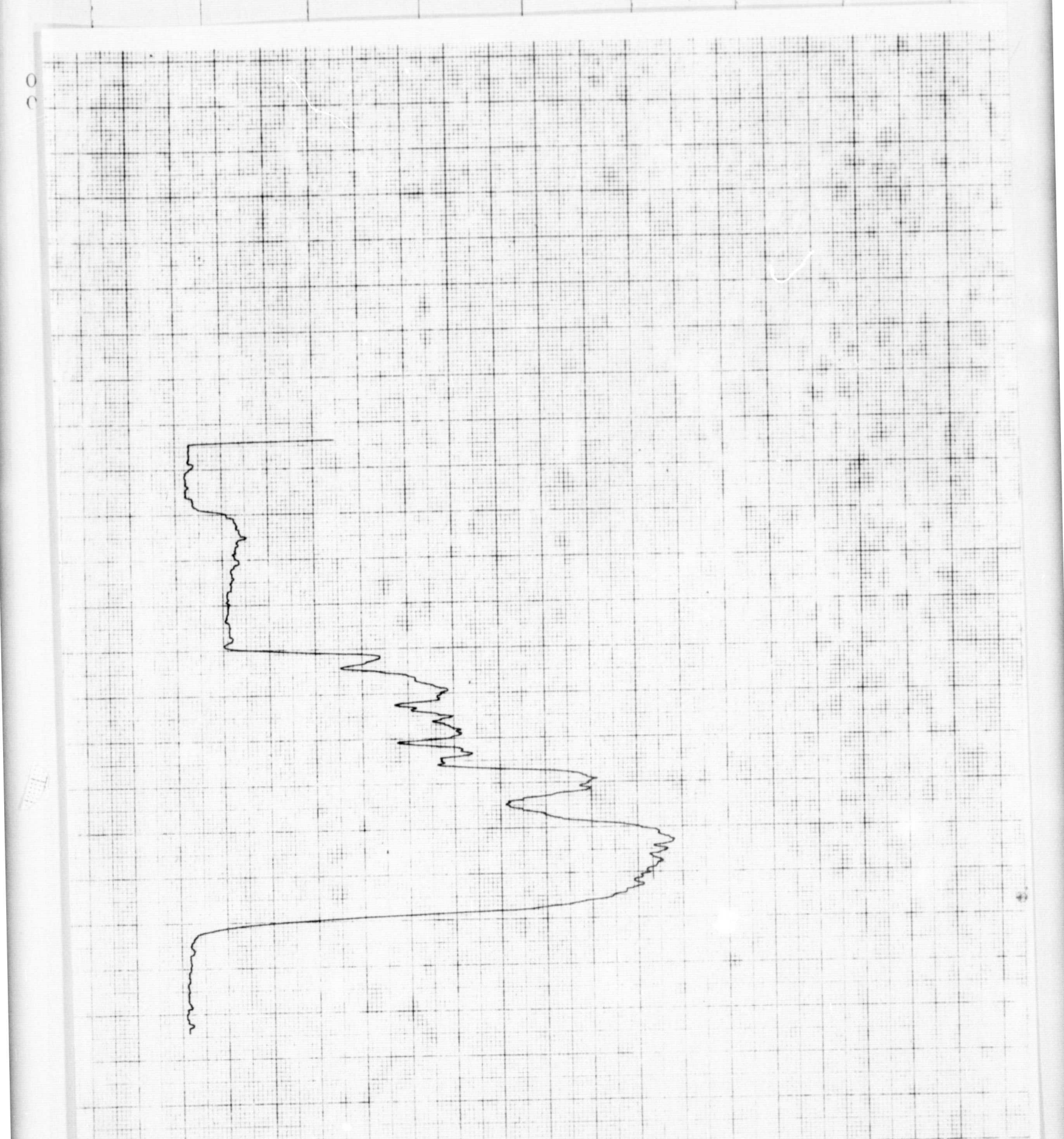

OPTICAL MAGNIFICATION
OBJECTIVE POWER x 22

SLIT (ACTUAL)
0.9μ x 6.2μ

REPORT CONTROL

WEDGE RANGE
0-2.7

SAMPLE:
FR 52921 #6

DATE

FORM MD

RECORD NO.

BEAM SPLITTING RATIO
10:1

REMARKS:
Tank Top First Polarity to Tank Top

JOYCE LOEBL

CORDING
CRODENSITOMETER

JOYCE LOEBL & CO. INC. 111, TERRACE HALL AVE. BURLINGTON, MASS.
AFFILIATE OF TECHNICAL OPERATIONS, INCORPORATED

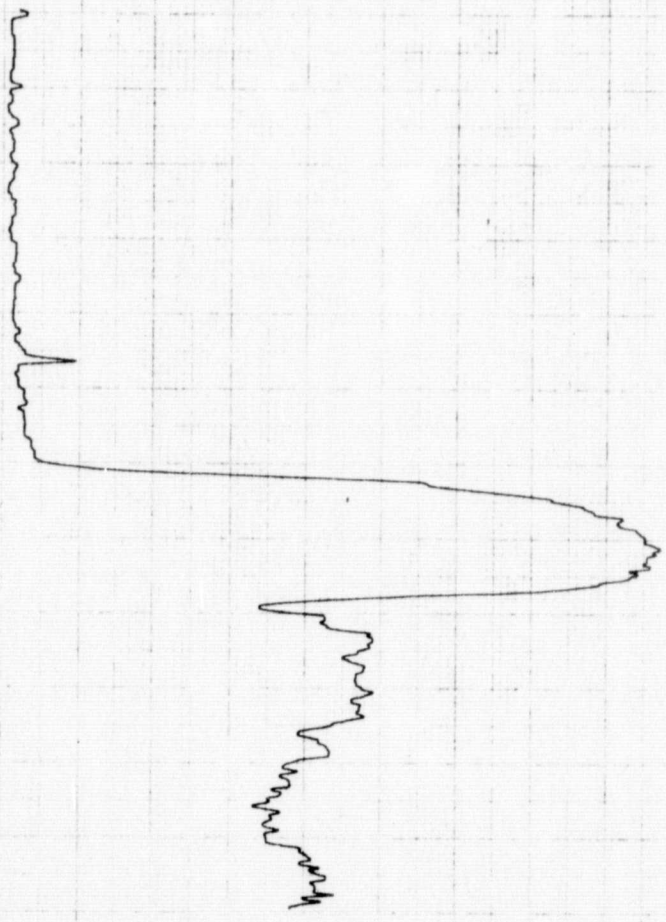

JOYCE
LOEBL
CORDING
RODENSITOMETER

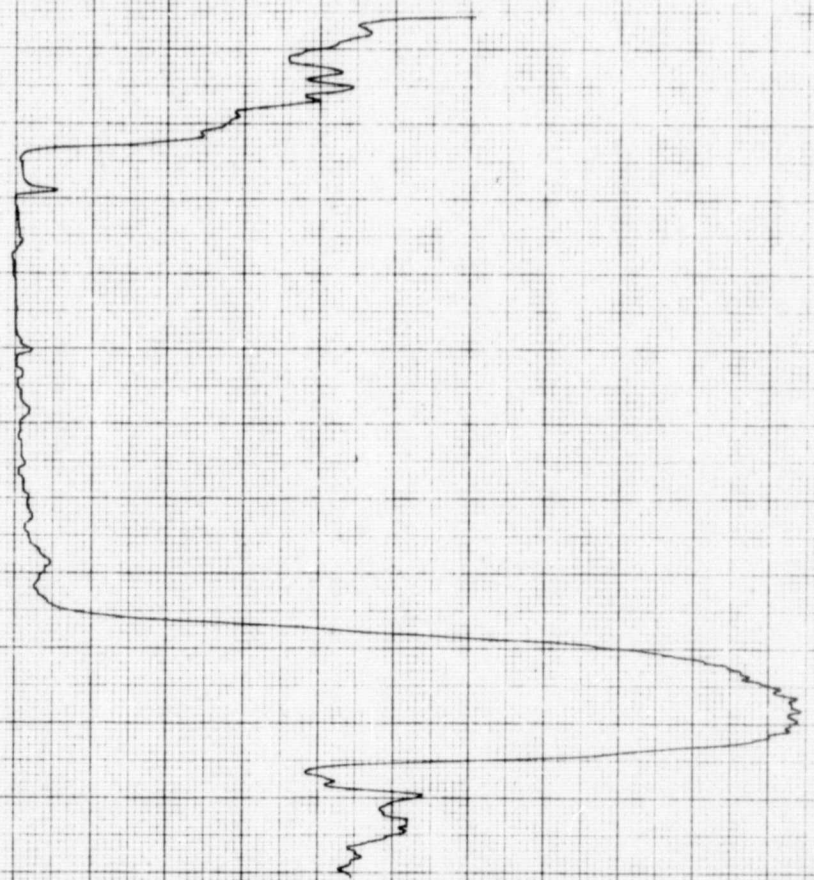

OPTICAL MAGNIFC. = OBJECTIVE POWER x 2.2	PROPORT. CONTL.	WEDGE RANGE	SAMPLE:	DATE	FORM MD5
SLIT (ACTUAL)	FEEDBACK SETTING	RATIO	REMARKS:	RECORD Nº	

OYCE
OEBL
DING
DENSITOMETER

JOYCE LOEBL & CO. INC. 111. TERRACE HALL AVE. BURLINGTON, MASS.
AFFILIATE OF TECHNICAL OPERATIONS, INCORPORATED

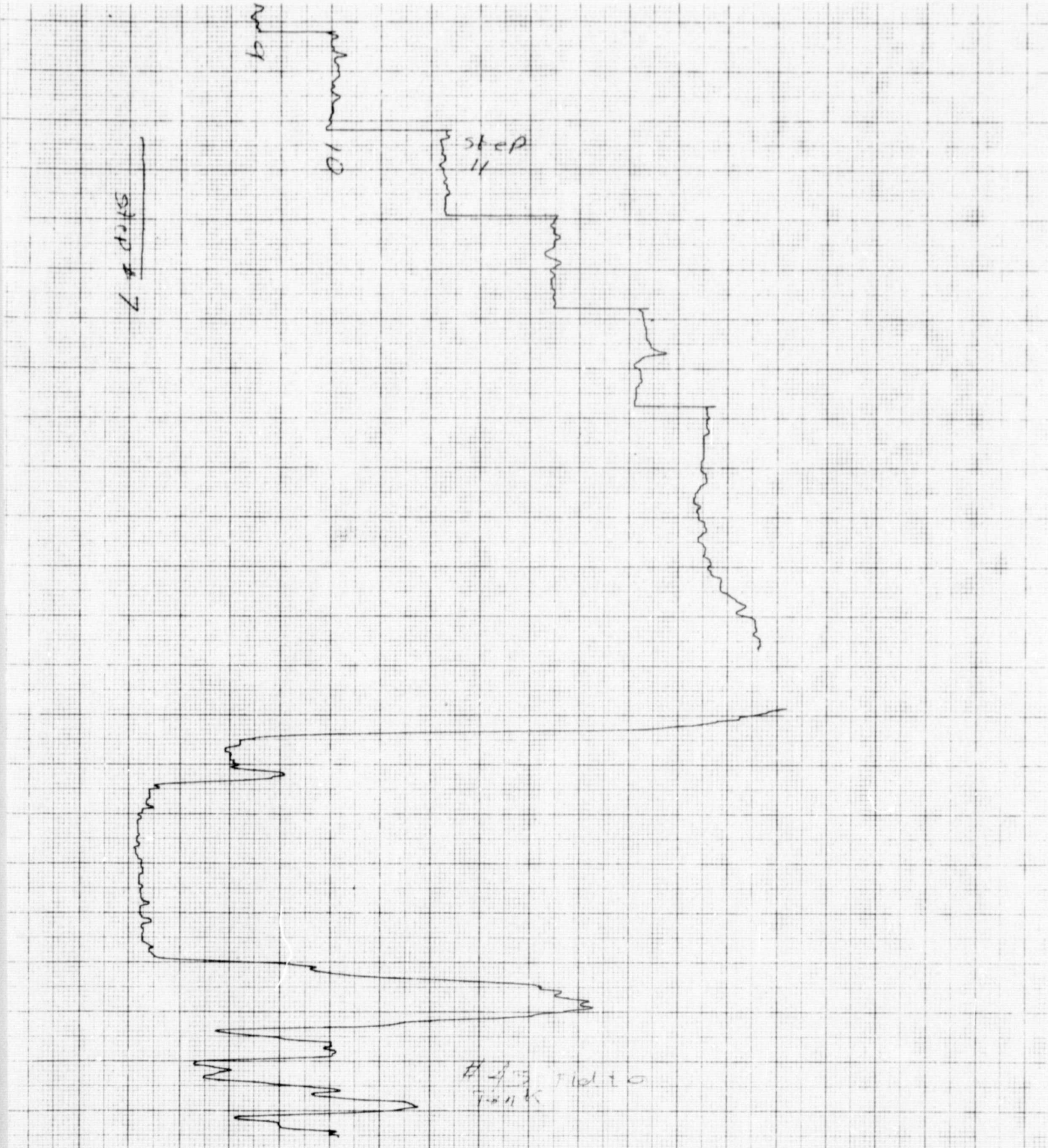

JOYCE LOEBL	OPTICAL MAGNIFC. = OBJECTIVE POWER x 2·2	PROPOR... NTL.	WEDGE RANGE	SAMPLE:	DATE / FORM MDS
	SLIT (ACTUAL)	FEEDBACK SETTING	RATIO 1:1	REMARKS:	RECORD Nº

ECORDING
ICRODENSITOMETER

JOYCE LOEBL & CO. INC. 111. TERRACE HALL AVE. BURLINGTON. MASS.
AFFILIATE OF TECHNICAL OPERATIONS, INCORPORATED

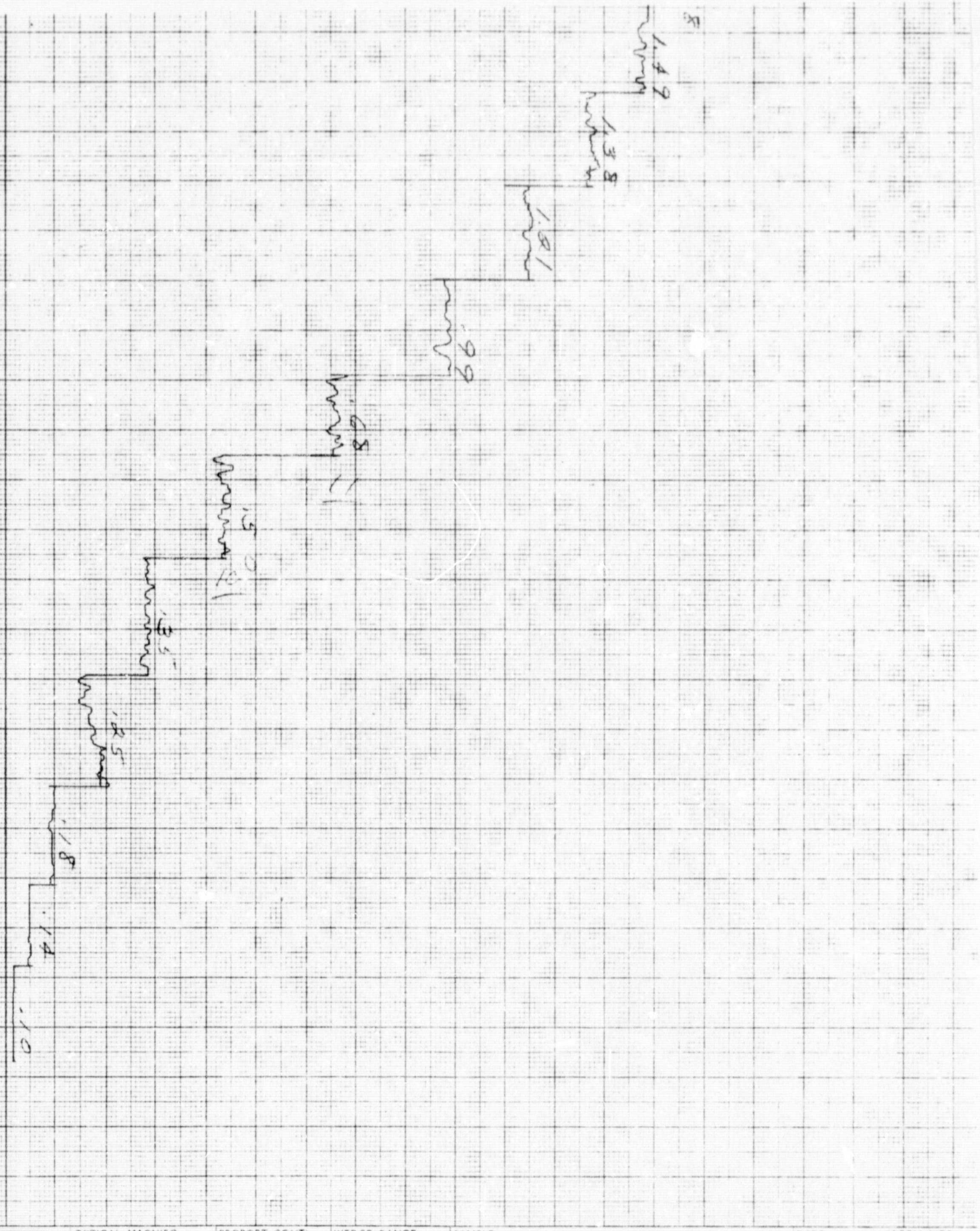

JOYCE LOEBL	OPTICAL MAGNIFC. = OBJECTIVE POWER x 2·2	PROPORT. CONTL.	WEDGE RANGE	SAMPLE: #44 - 49	DATE
	SLIT (ACTUAL)	FEEDBACK SETTING	RATIO	REMARKS:	RECORD N°

FORM MDS

SCANNING MICRODENSITOMETER

JOYCE LOEBL & CO. INC. 111 TERRACE HALL AVE. BURLINGTON, MASS.
AFFILIATE OF TECHNICAL OPERATIONS, INCORPORATED

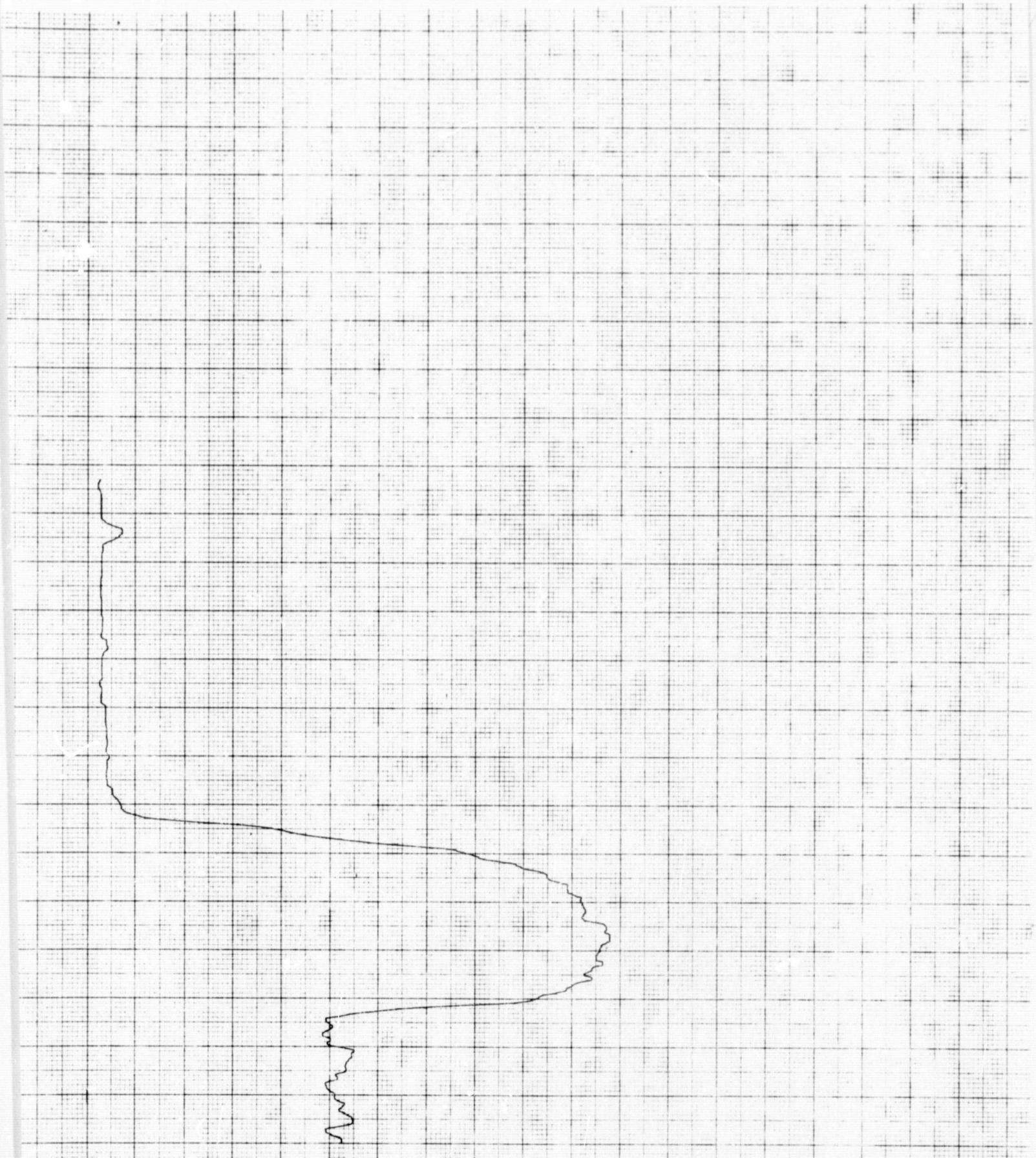

JOYCE LOEBL	OPTICAL MAGNIFC. = OBJECTIVE POWER x 2.2	PROPORT. CONTL.	WEDGE RANGE	SAMPLE	DATE
	SLIT (ACTUAL)	FEEDBACK SETTING	RATIO	REMARKS	RECORD NO.

CORDING
CRODENSITOMETER

JOYCE LOEBL & CO. INC. 111. TERRACE HALL AVE. BURLINGTON. MASS
AFFILIATE OF TECHNICAL OPERATIONS, INCORPORATED

FORM MD5

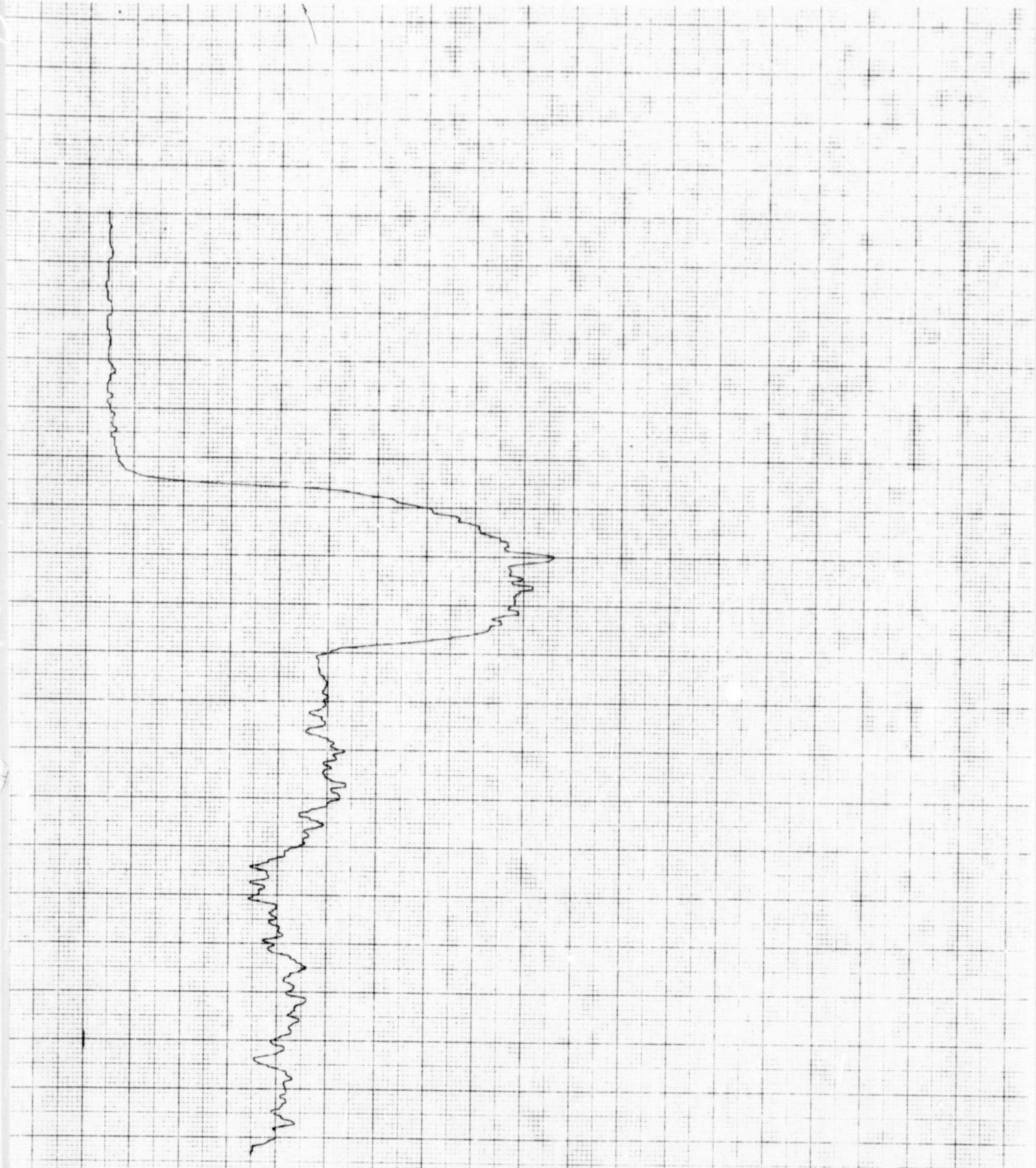

JOYCE LOEBL

ECORDING
IGRODENSITOMETER

OPTICAL MAGNIFC. = OBJECTIVE POWER x 2·2	PROPORT. CONTL.	WEDGE RANGE	SAMPLE:	ATE	FORM MD5
SLIT (ACTUAL)	FEEDBACK SETTING PATIO		REMARKS:	RECORD Nº	

JOYCE LOEBL & CO. INC. 111 TERRACE HALL AVE. BURLINGTON, MASS.
AFFILIATE OF TECHNICAL OPERATIONS, INCORPORATED

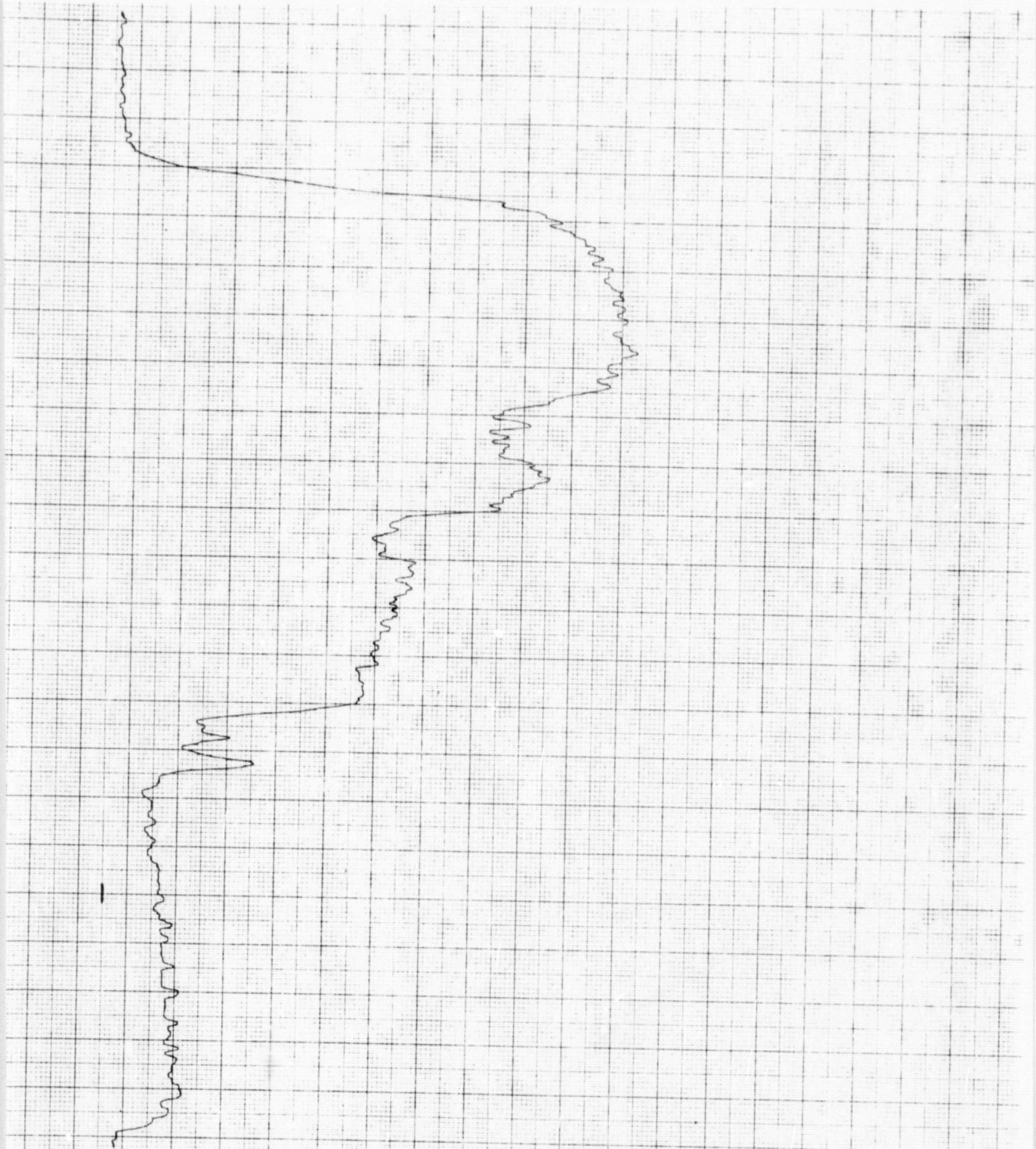

JOYCE LOEBL

CORDING
CRODENSITOMETER

OPTICAL MAGNIFC = OBJECTIVE POWER x 2.2	PROPORT. CONTL.	WEDGE RANGE	SAMPLE:	DATE	FORM MDS
SLIT (ACTUAL)	FEEDBACK SETTING	RATIO	REMARKS	RECORD No.	

JOYCE LOEBL & CO. INC. 111 TERRACE HALL AVE. BURLINGTON, MASS.
AFFILIATE OF TECHNICAL OPERATIONS, INCORPORATED

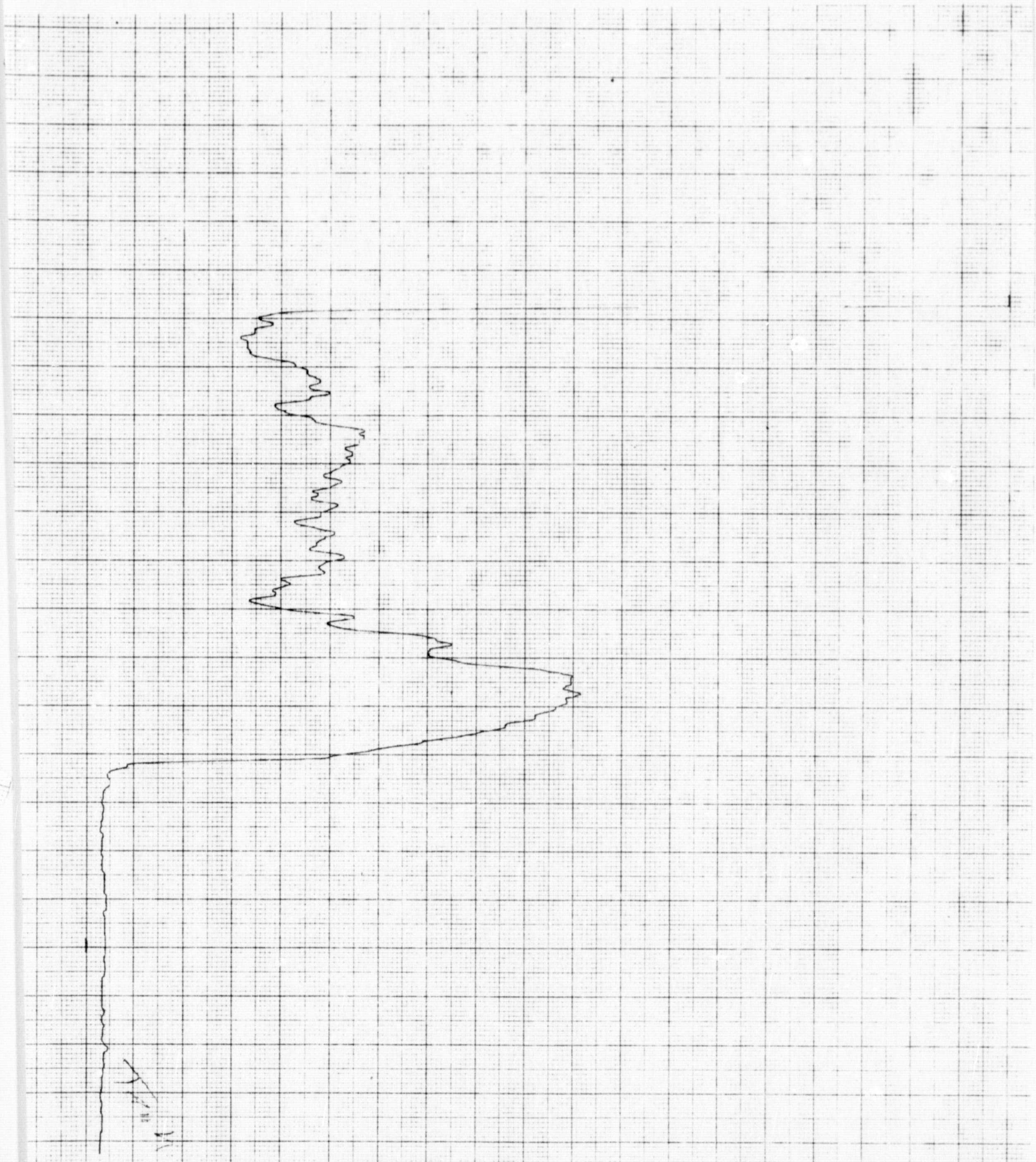

JOYCE LOEBL	OPTICAL MAGNIFC. = OBJECTIVE POWER x 2·2	PROPORT. CONTL.	WEDGE RANGE	SAMPLE:	DATE / FORM MD1
	SLIT (ACTUAL)	FEEDBACK SETTING	RATIO	REMARKS:	RECORD NO.

ORDING
ODENSITOMETER

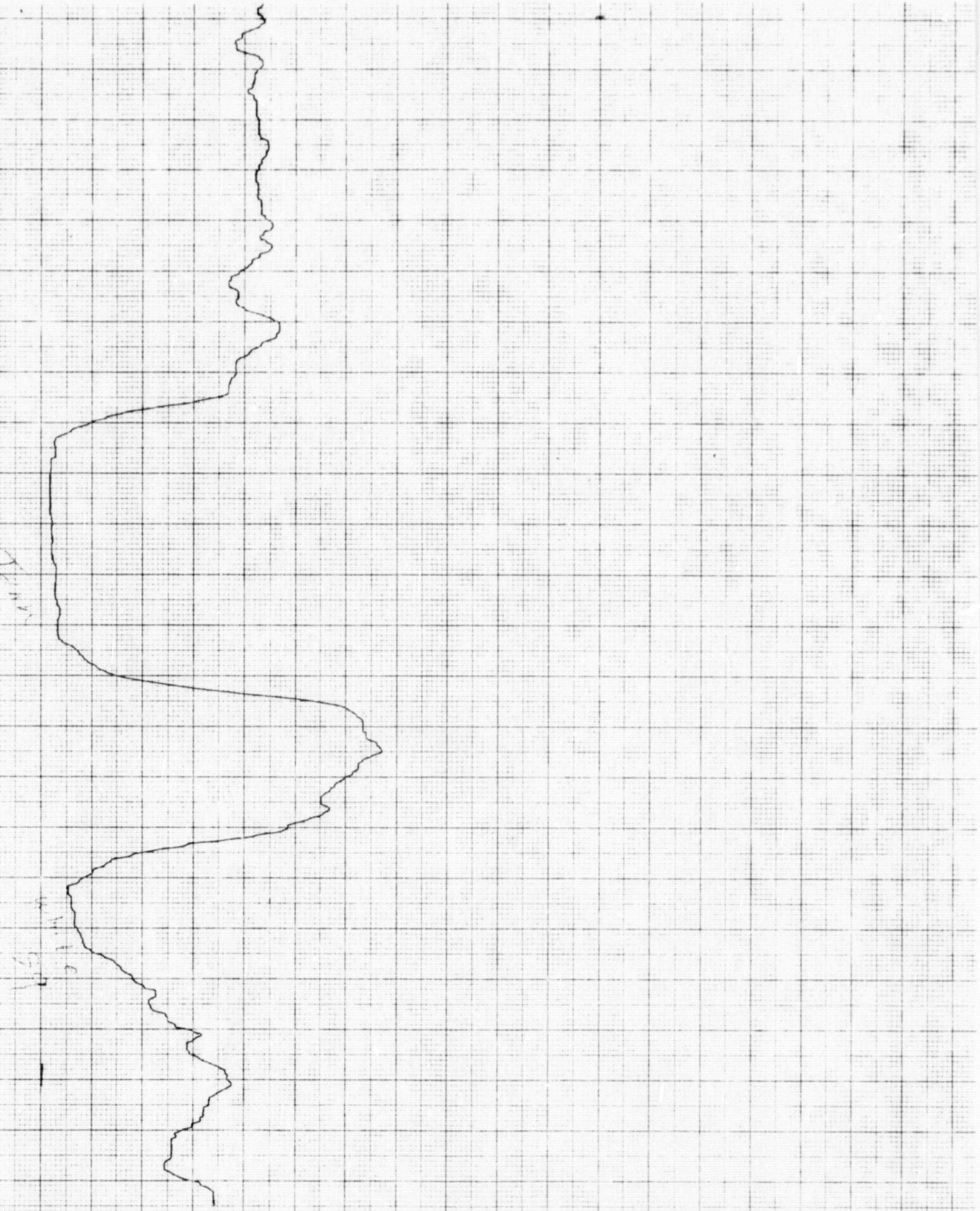

JOYCE LOEBL	OPTICAL MAGNIFC. = OBJECTIVE POWER x 2.2	PROPORT. CONTL.	WEDGE RANGE 0 – 2 /	SAMPLE: T, Y – 9 – G	DATE	FORM MDS
	SLIT (ACTUAL)	FEEDBACK SETTING RATIO		REMARKS:	RECORD Nº

RECORDING MICRODENSITOMETER

JOYCE LOEBL & CO. INC. 111 TERRACE HALL AVE. BURLINGTON, MASS.
AFFILIATE OF TECHNICAL OPERATIONS, INCORPORATED

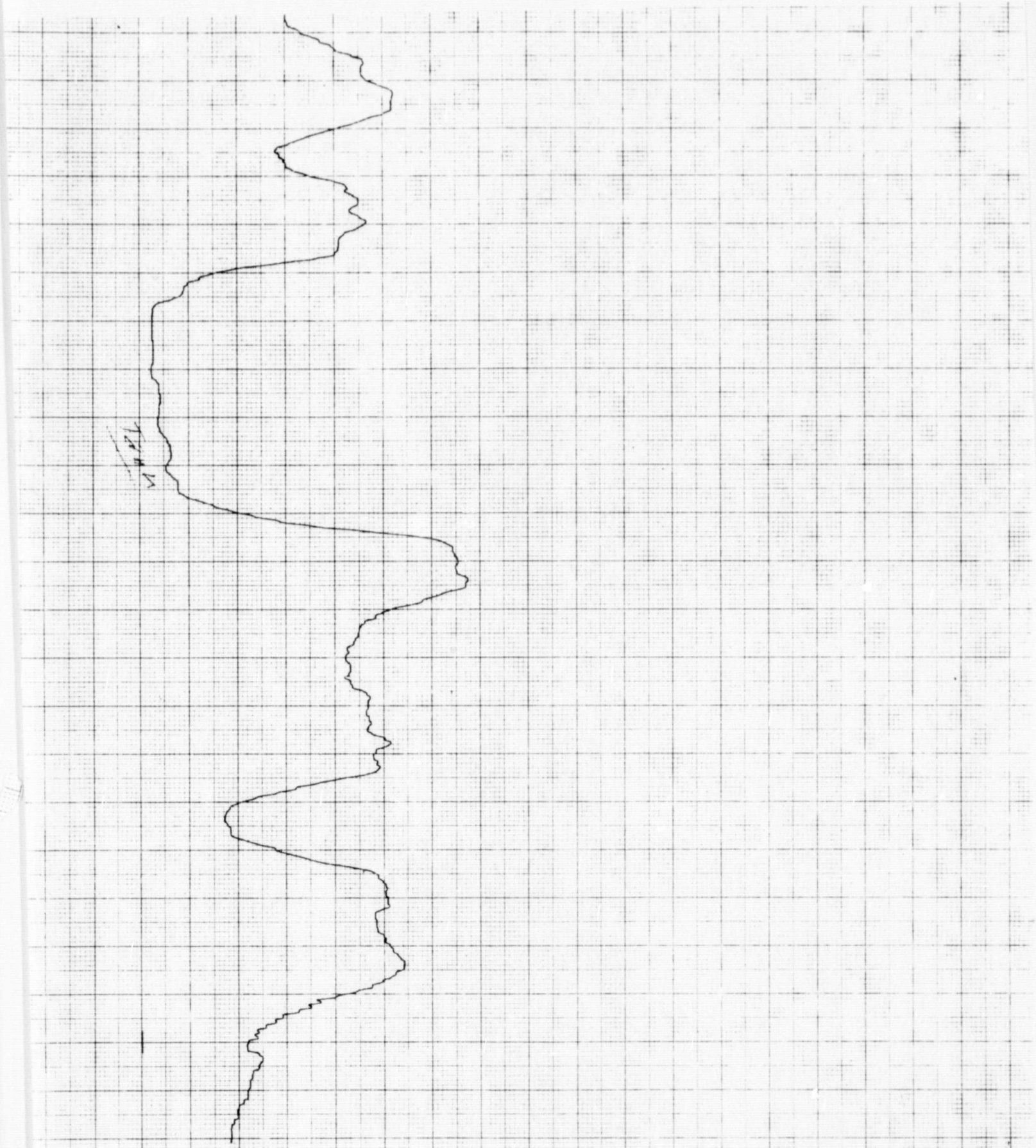

JOYCE LOEBL	OPTICAL MAGNIFC. = OBJECTIVE POWER x 2.2	PROPORT. CONTL	WEDGE RANGE	SAMPLE	DATE
	SLIT (ACTUAL)	FEEDBACK SETTING	RATIO	REMARKS	RECORD #

ORDING
RODENSITOMETER

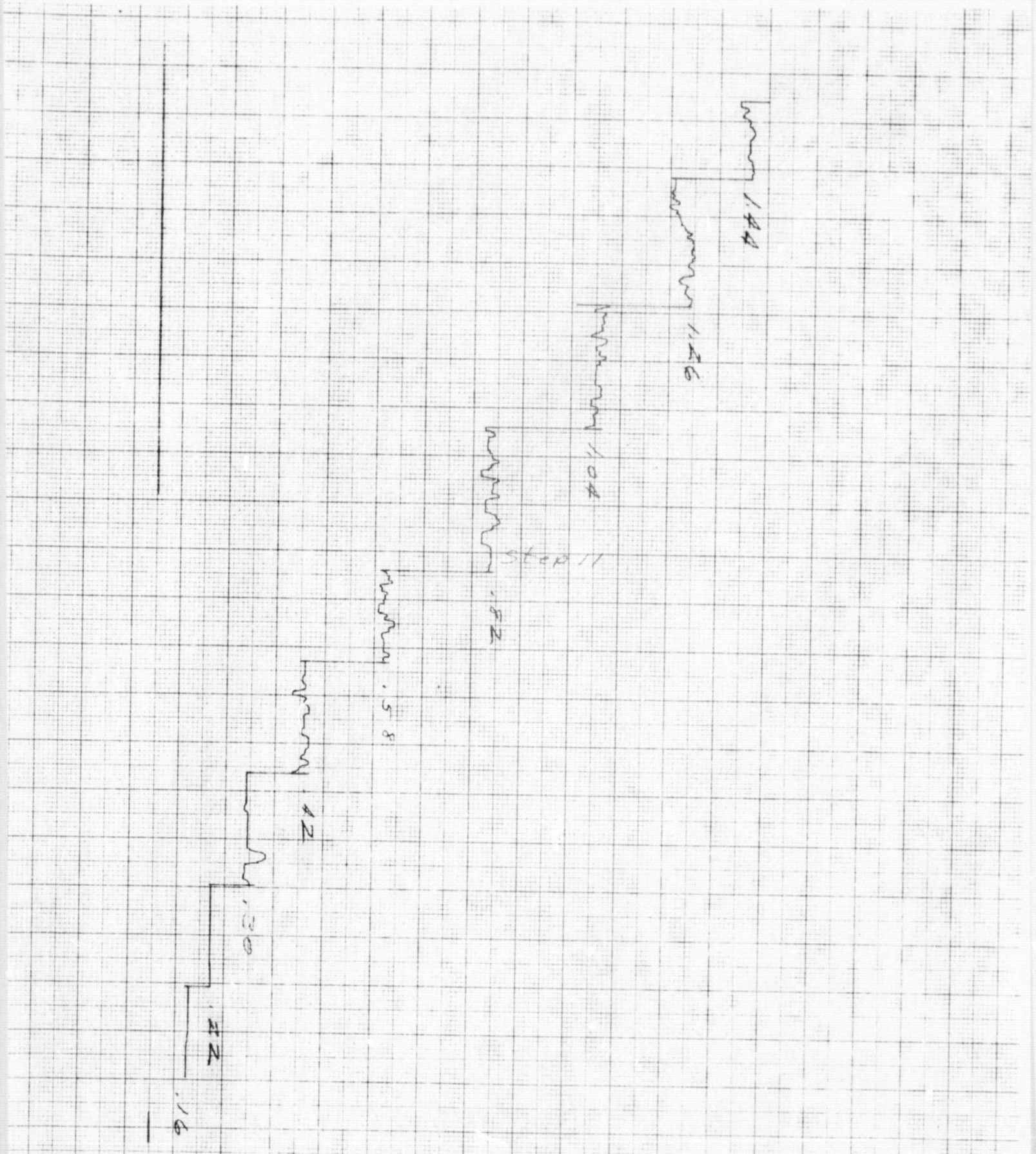

JOYCE LOEBL

CORDING
CRODENSITOMETER

OPTICAL MAGNIFC. = OBJECTIVE POWER x 2·2	PROPORT CONTL.	WEDGE RANGE	SAMPLE: #50 - 5d	DATE	FORM MDS
SLIT (ACTUAL)	FEEDBACK SETTING RATIO		REMARKS:	RECORD No.	

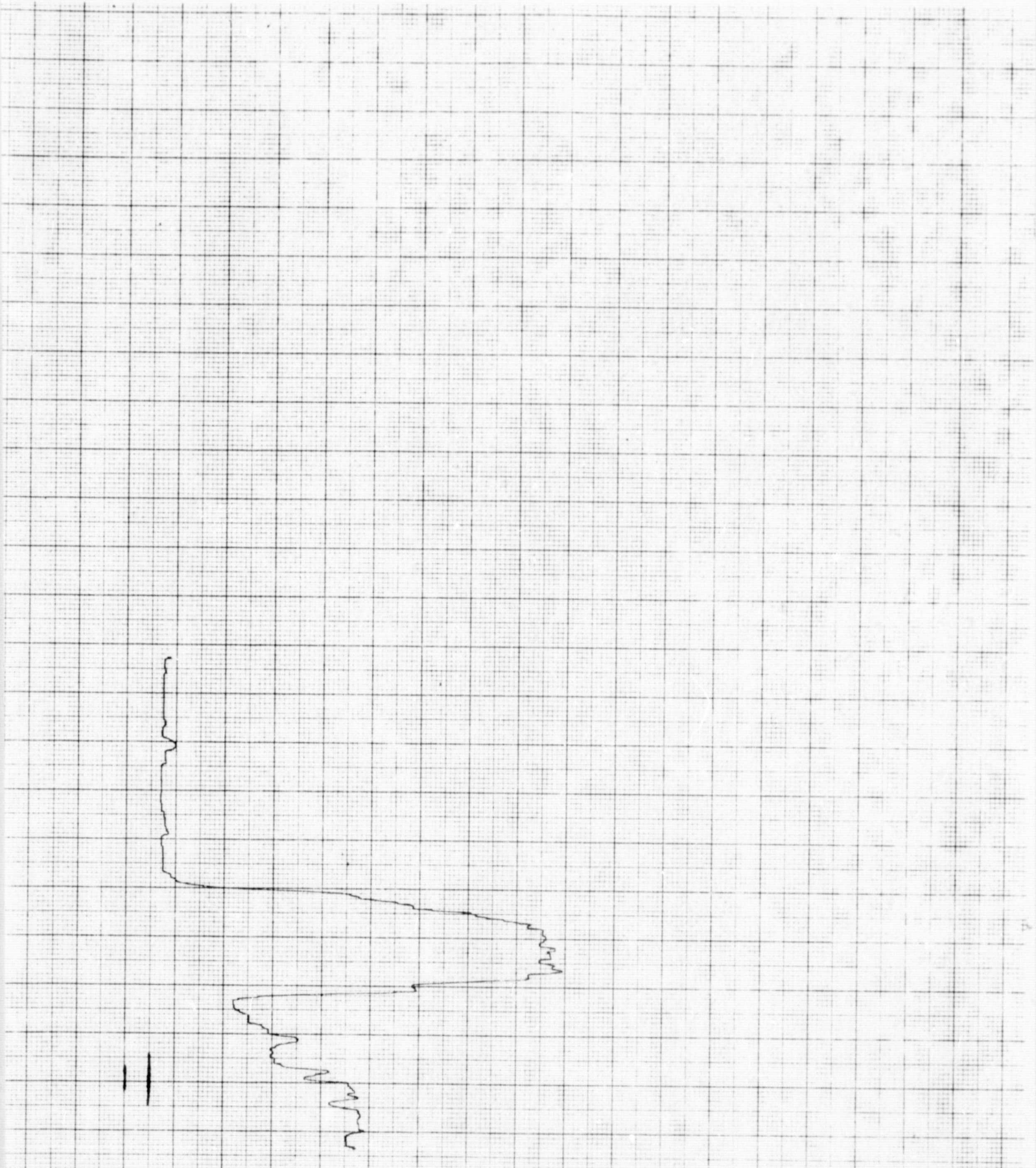

JOYCE LOEBL	OPTICAL MAGNIFC. = OBJECTIVE POWER x 2.2	PROPORT. CONTL.	WEDGE RANGE 0 - 2.7	SAMPLE: [illegible] #50	DATE	FORM MDS
	SLIT (ACTUAL)	FEEDBACK SETTING	RATIO	REMARKS	RECORD N°	

CORDING
CRODENSITOMETER

JOYCE LOEBL & CO. INC. 111 TERRACE HALL AVE. BURLINGTON, MASS.
AFFILIATE OF TECHNICAL OPERATIONS, INCORPORATED

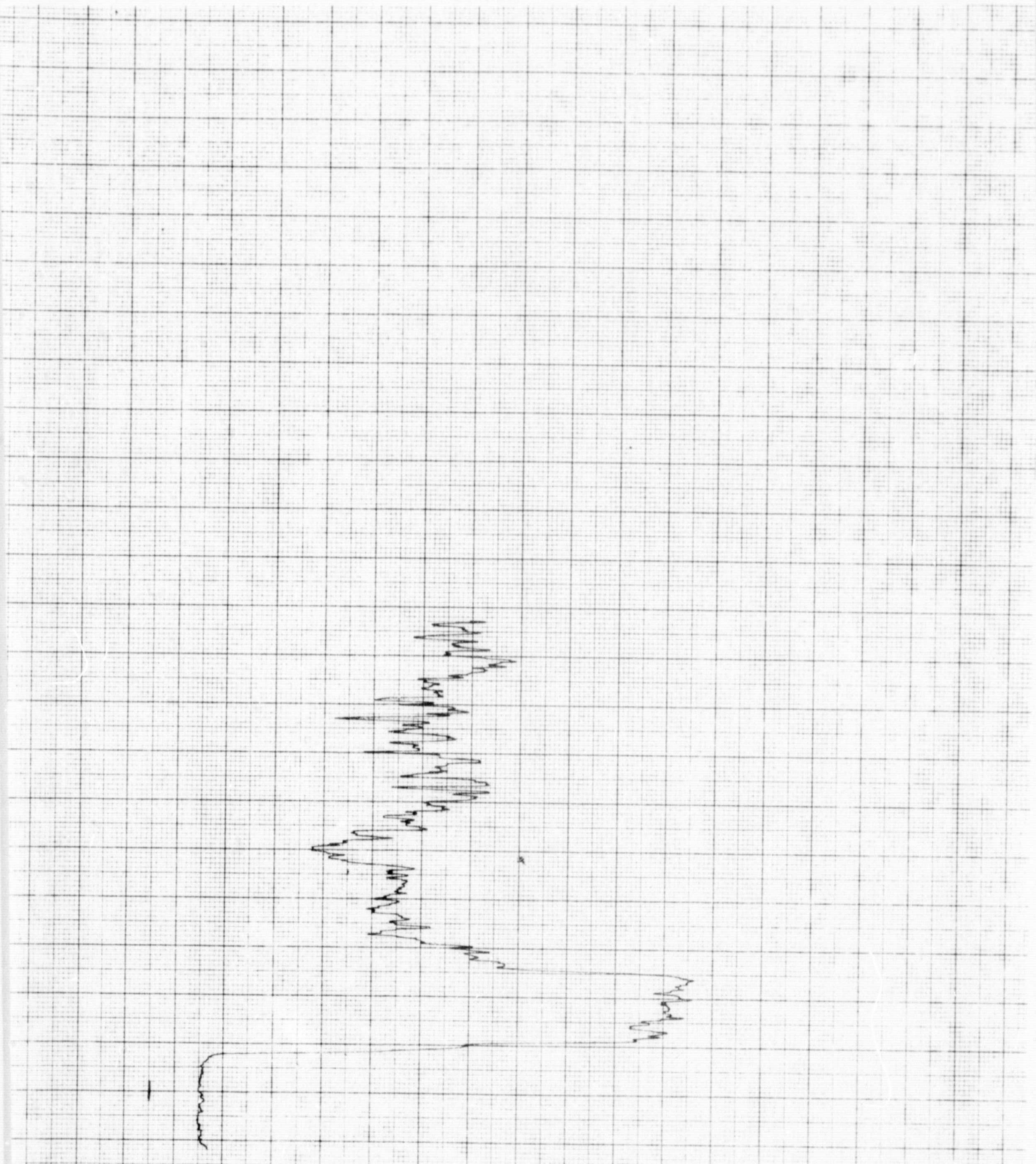

JOYCE LOEBL

RDING
RODENSITOMETER

OPTICAL MAGNIFC. = OBJECTIVE POWER x 2·2	PROPORT. CONTL.	WEDGE RANGE	SAMPLE:	DATE	FORM MDS
SLIT (ACTUAL)	FEEDBACK SETTING	RATIO	REMARKS	RECORD No.	

JOYCE LOEBL & CO. INC. 111 TERRACE HALL AVE. BURLINGTON, MASS.
AFFILIATE OF TECHNICAL OPERATIONS, INCORPORATED

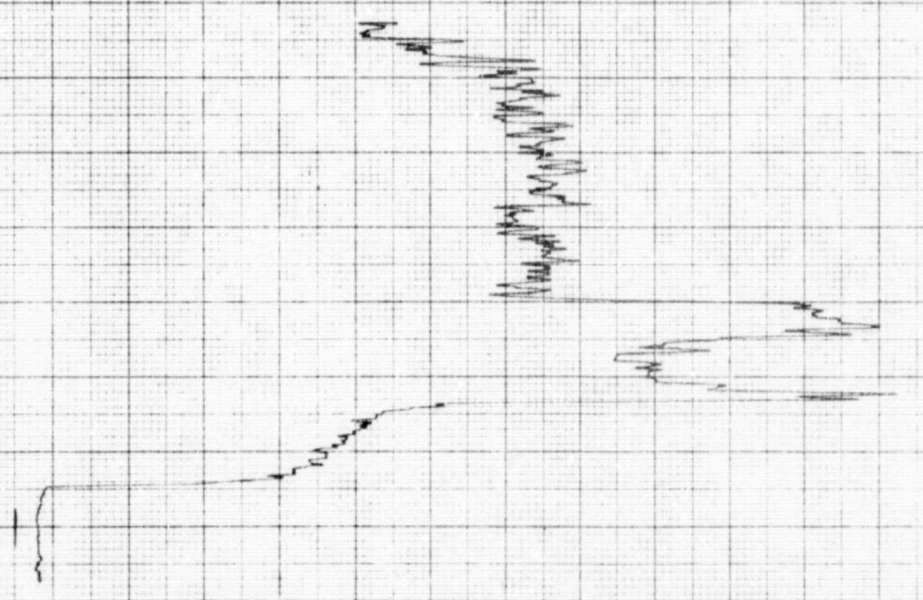

JOYCE LOEBL	OPTICAL MAGNIFC. = OBJECTIVE POWER x 22	PROPORT CONTL	WEDGE RANGE	SAMPLE	DATE	FORM MDS
	SLIT (ACTUAL)	FEEDBACK SETTING	RATIO	REMARKS	RECORD NO.	

CORDING
CRODENSITOMETER

JOYCE LOEBL & CO. INC. 111 TERRACE HALL AVE. BURLINGTON, MASS.
AFFILIATE OF TECHNICAL OPERATIONS, INCORPORATED

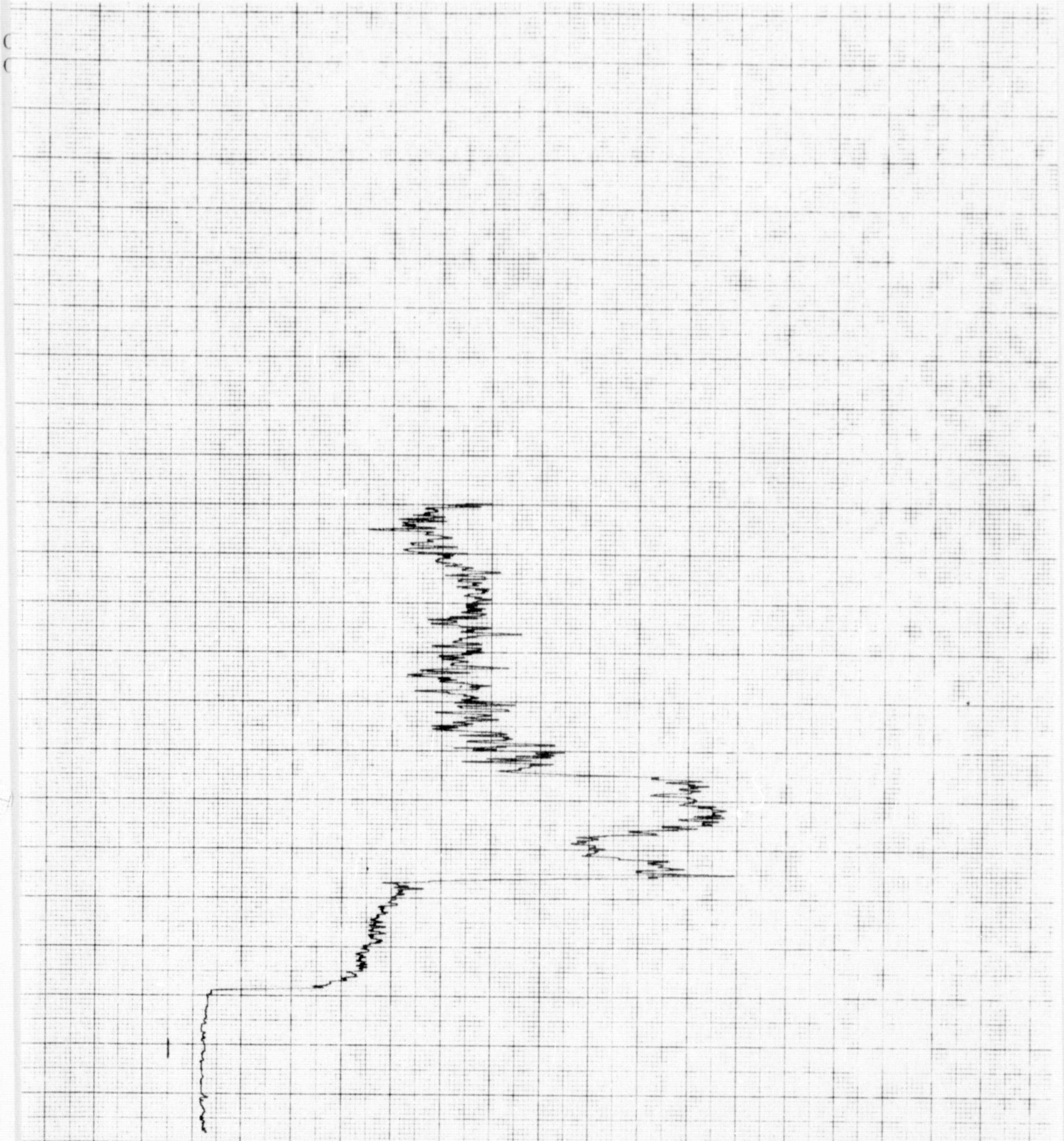

JOYCE LOEBL

ECORDING
ICRODENSITOMETER

OPTICAL MAGNIFC. = OBJECTIVE POWER x 2·2	PROPORT. CONTL.	WEDGE RANGE 2	SAMPLE. E-1 < 29 < 3 1153	DATE	FORM 1105
SLIT (ACTUAL)	FEEDBACK SETTING	RATIO 5	REMARKS	RECORD No.	

JOYCE LOEBL & CO. INC. 111 TERRACE HALL AVE. BURLINGTON, MASS.
AFFILIATE OF TECHNICAL OPERATIONS, INCORPORATED

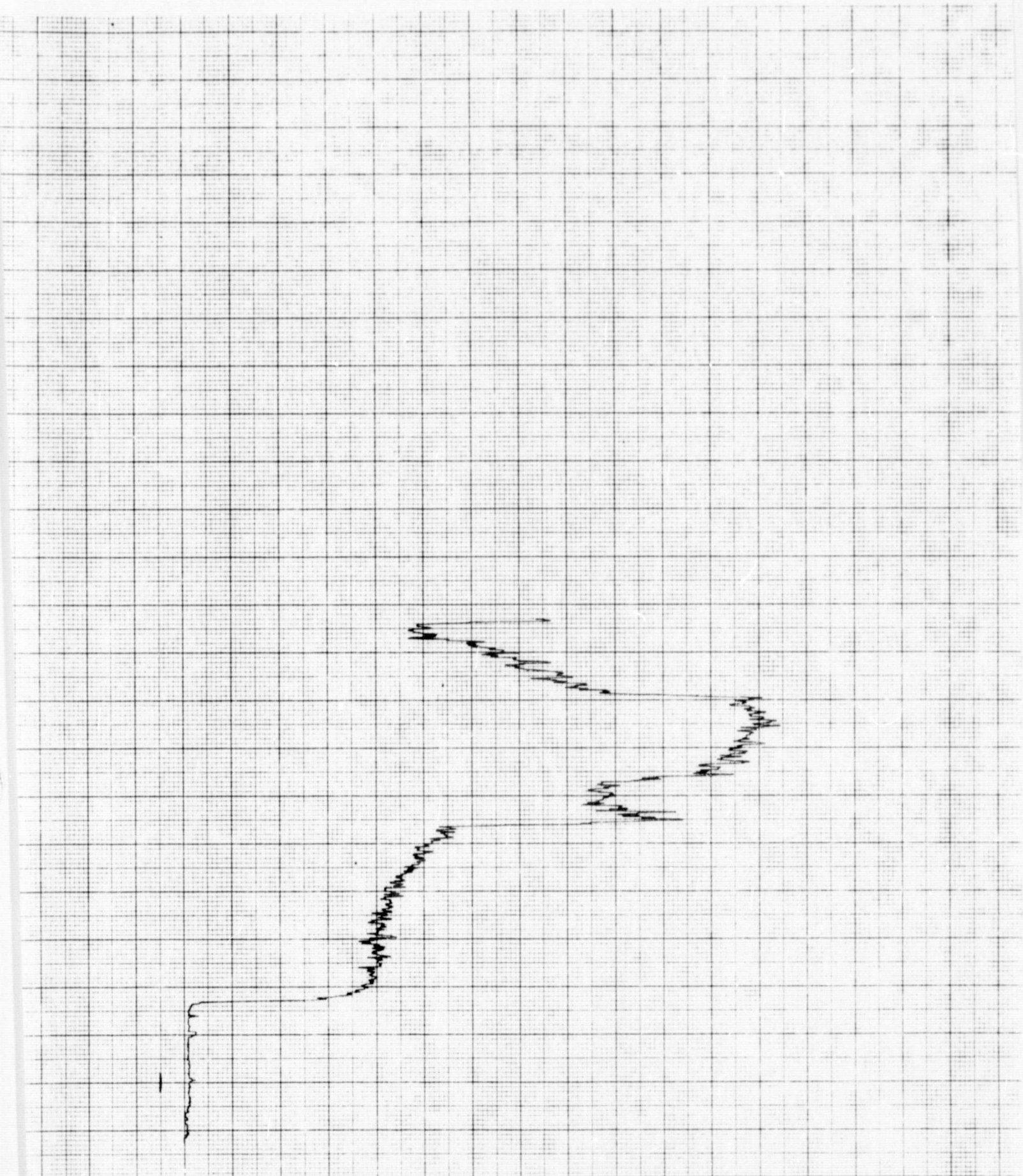

JOYCE LOEBL	OPTICAL MAGNIFC. = OBJECTIVE POWER x 2·2	PROPORT. CONTL.	WEDGE RANGE 0 to 2·7	SAMPLE: Fr 52 92-1	DATE
	SLIT (ACTUAL) 1-3/4	FEEDBACK SETTING	RATIO 5:1	REMARKS:	RECORD No.

FORM MDS

LORDING
RODENSITOMETER

JOYCE LOEBL & CO. INC. 111. TERRACE HALL AVE. BURLINGTON. MASS.
AFFILIATE OF TECHNICAL OPERATIONS, INCORPORATED

FIGURE . Particle Size Distribution

LINEAR REGRESSION ANALYSIS (y = a(0) + a(1)x)

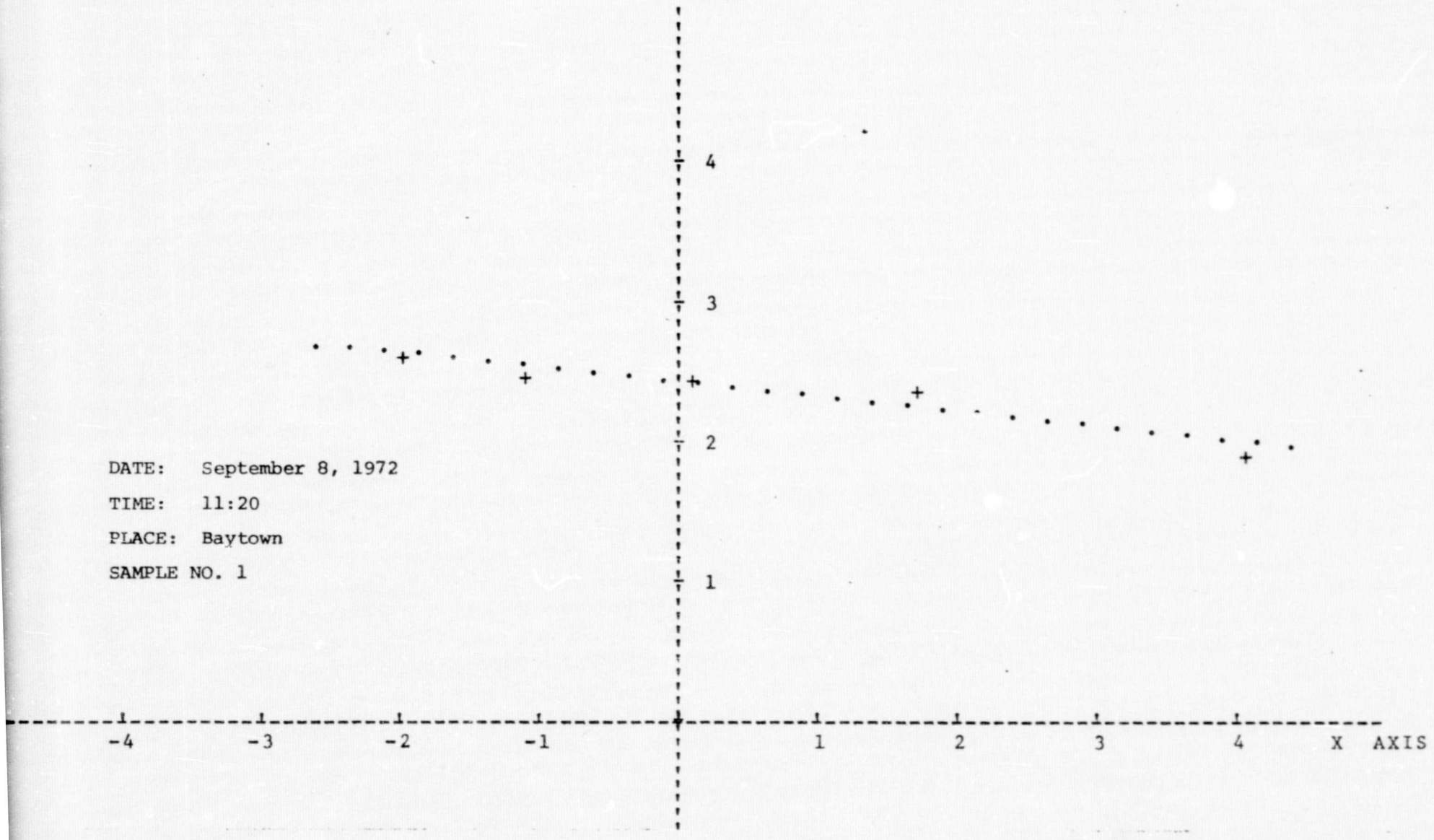

DATE: September 8, 1972

TIME: 11:20

PLACE: Baytown

SAMPLE NO. 1

4.809723165 = a(0)
-1.051125503 = a(1)
-.947794719 = r
.152036020 = S(x.y)

ONE X AXIS UNIT = .200000000
ONE Y AXIS UNIT = 2.000000000

FIGURE . Particle Size Distribution

LINEAR REGRESSION ANALYSIS (y = a(0) + a(1)x)

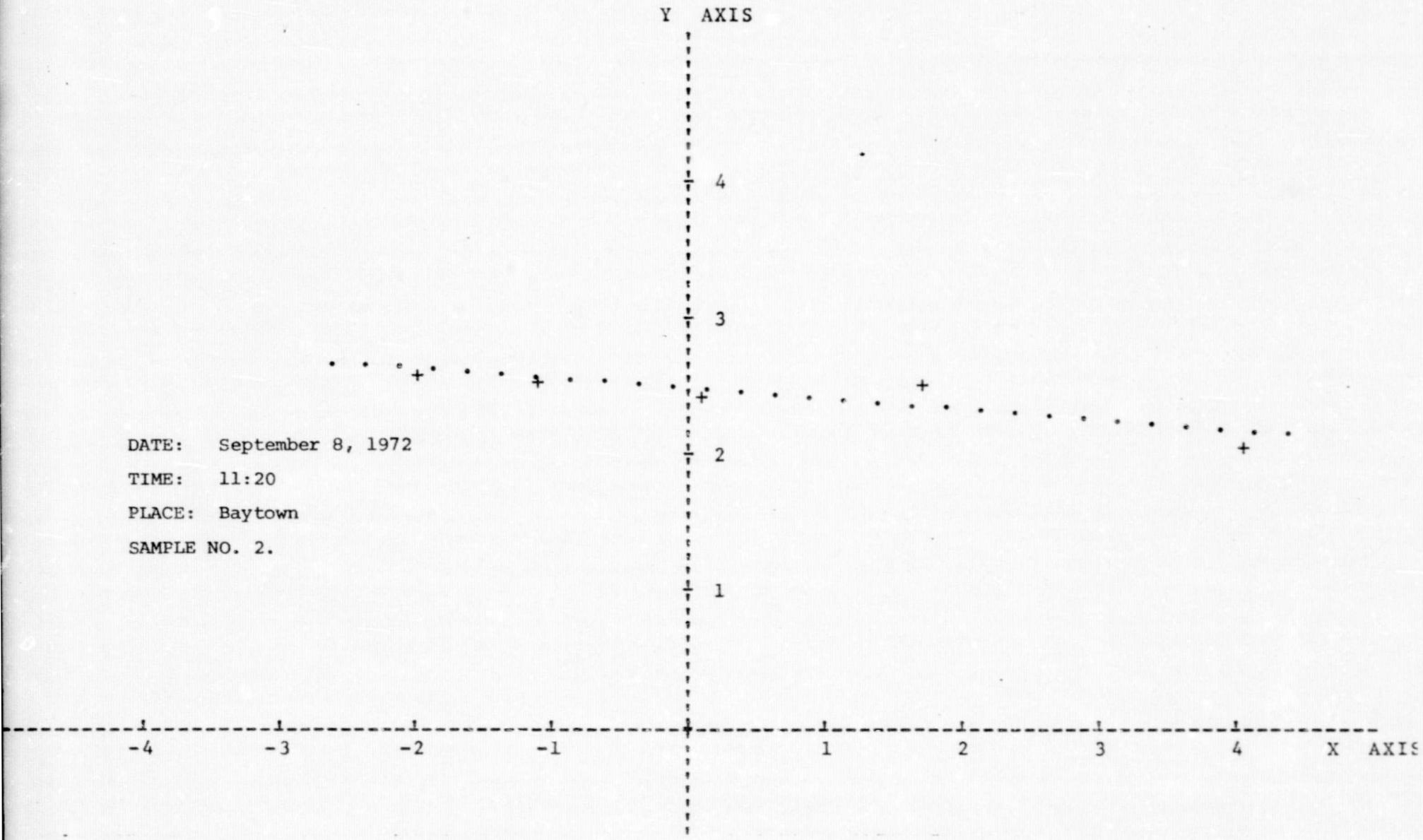

DATE: September 8, 1972

TIME: 11:20

PLACE: Baytown

SAMPLE NO. 2.

4.908275837 = a(0)
-.761513549 = a(1)
-.868306138 = r
.187020384 = S(x.y)

ONE X AXIS UNIT = .200000000
ONE Y AXIS UNIT = 2.000000000

FIGURE . Particle Size Distribution

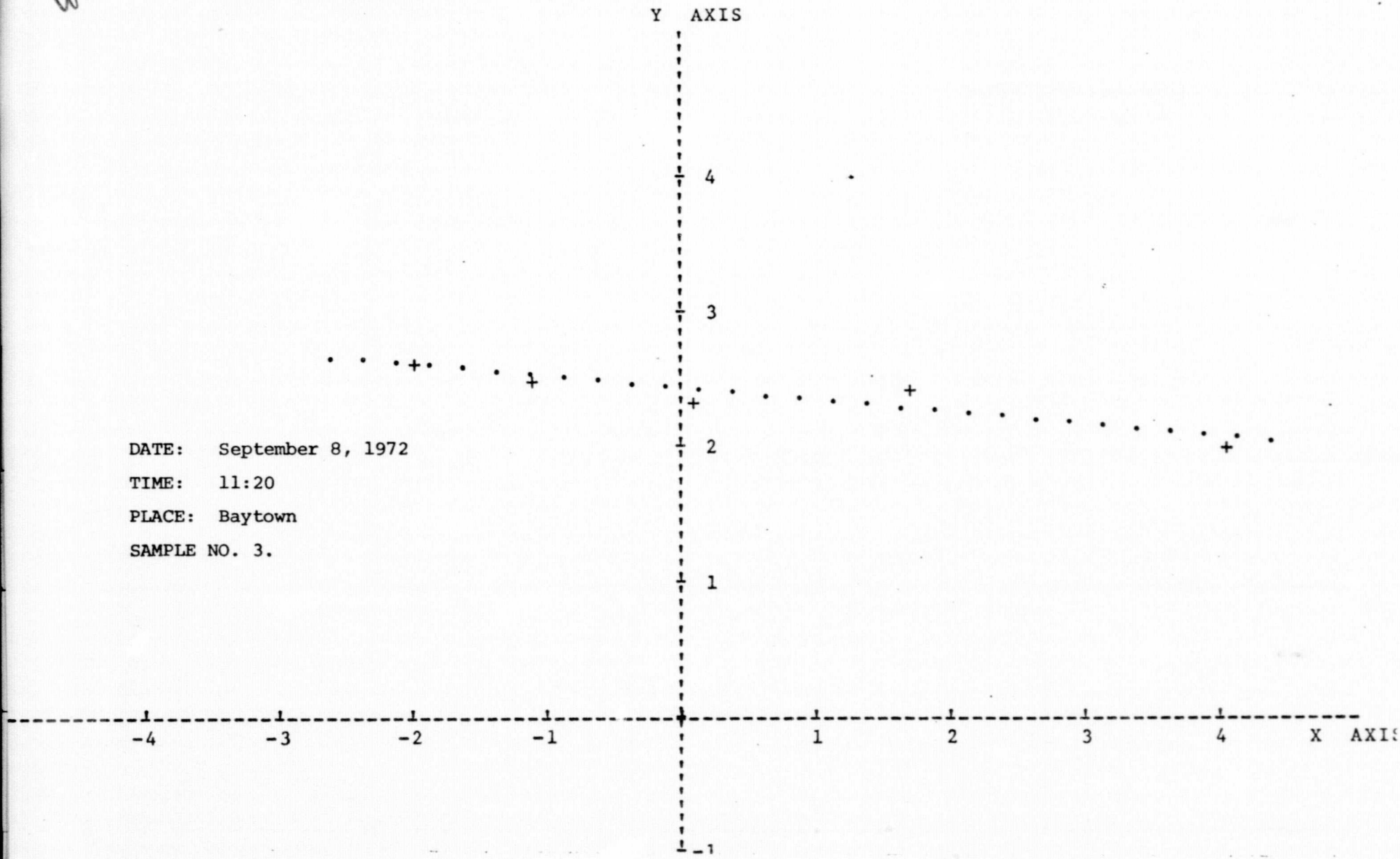

4.812204822 = a(0)
-.905624354 = a(1)
-.914674622 = r
.172046348 = S(x.y)

ONE X AXIS UNIT = .200000000
ONE Y AXIS UNIT = 2.000000000

FIGURE . Particle Size Distribution

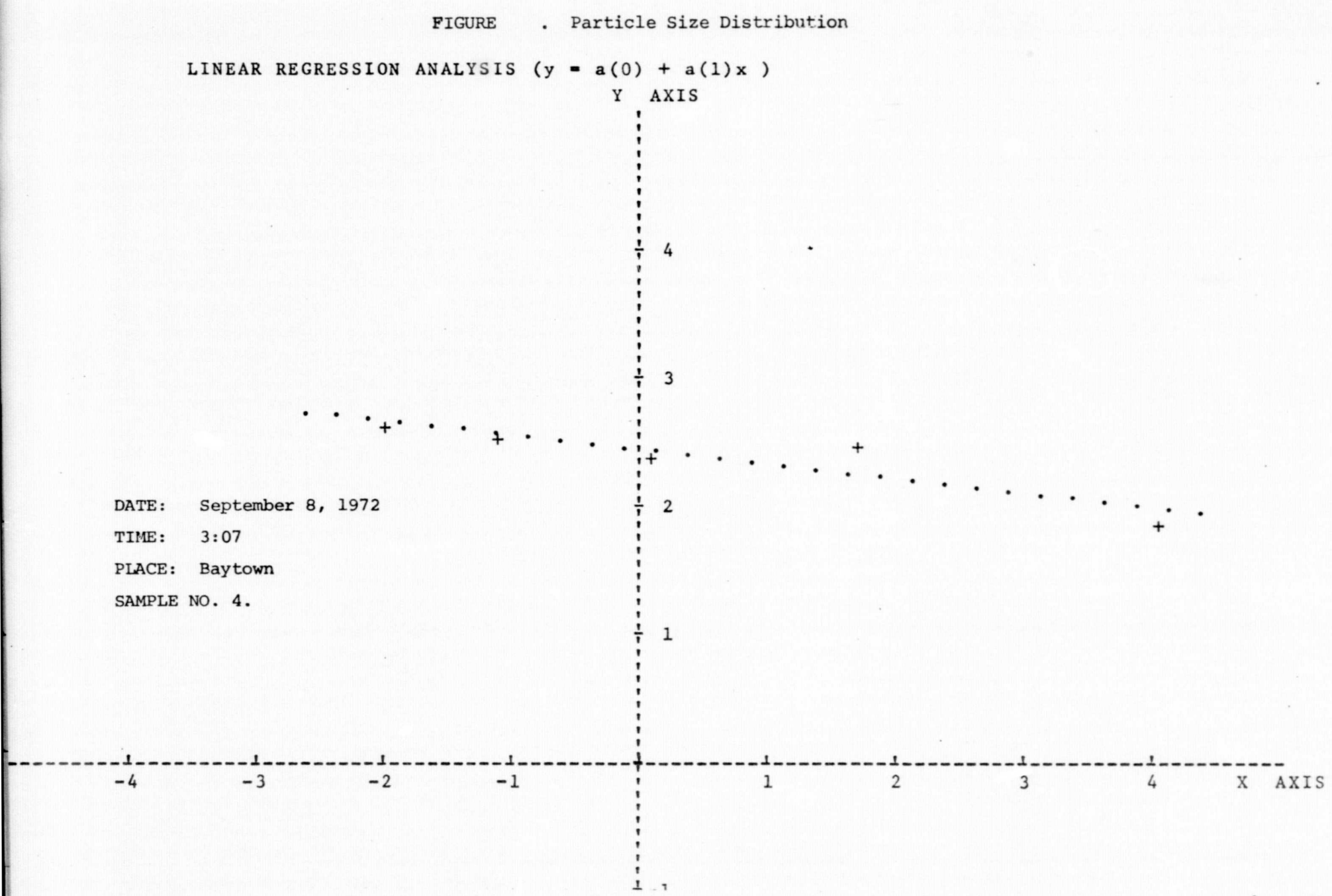

FIGURE . Particle Size Distribution

LINEAR REGRESSION ANALYSIS (y = a(0) + a(1)x)

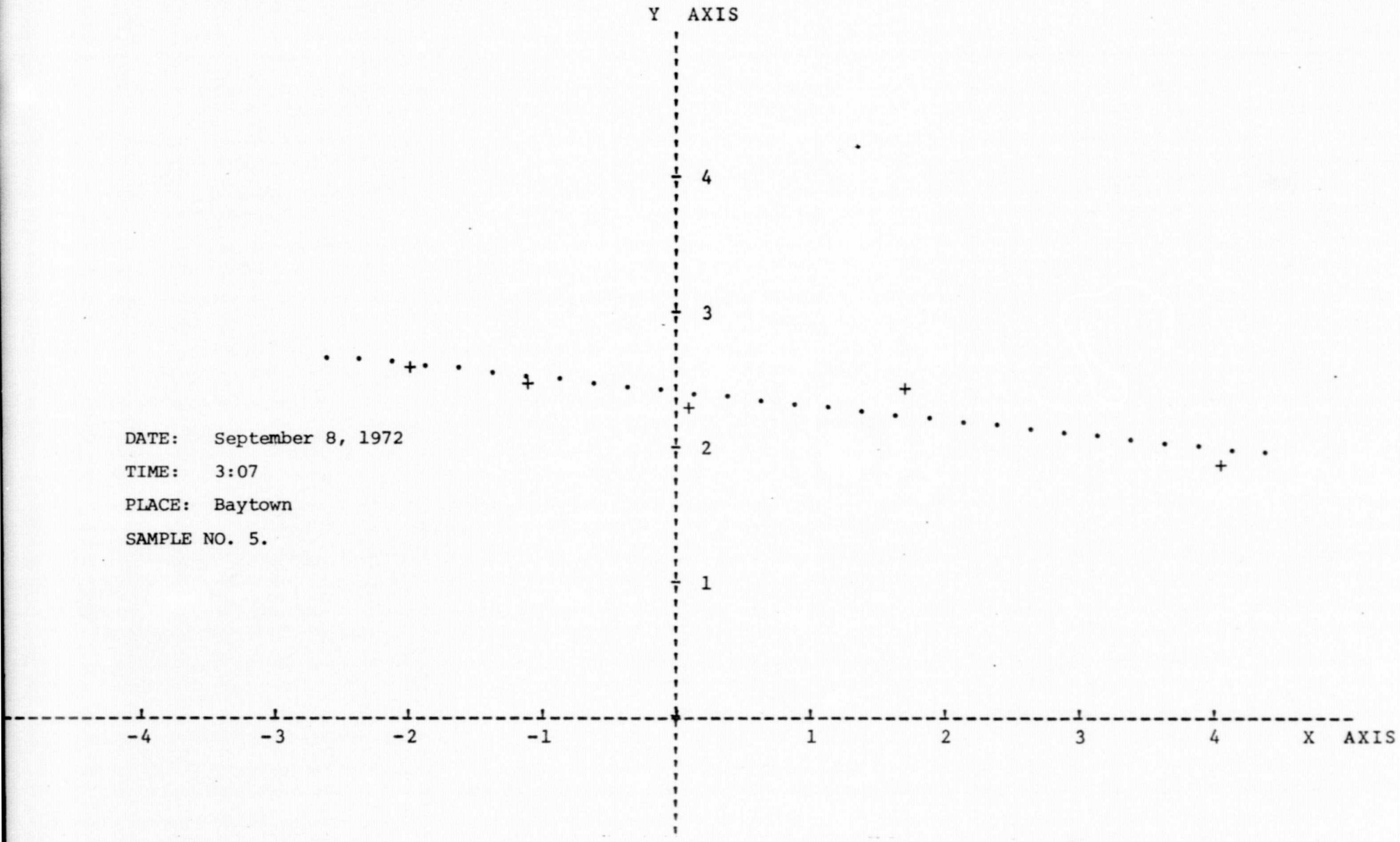

DATE: September 8, 1972

TIME: 3:07

PLACE: Baytown

SAMPLE NO. 5.

4.783236693 = a(0)
-1.049671893 = a(1)
-.887249815 = r
.234616403 = S(x.y)

ONE X AXIS UNIT = .200000000
ONE Y AXIS UNIT = 2.000000000

FIGURE . Particle Size Distribution

LINEAR REGRESSION ANALYSIS (y = a(0) + a(1)x)

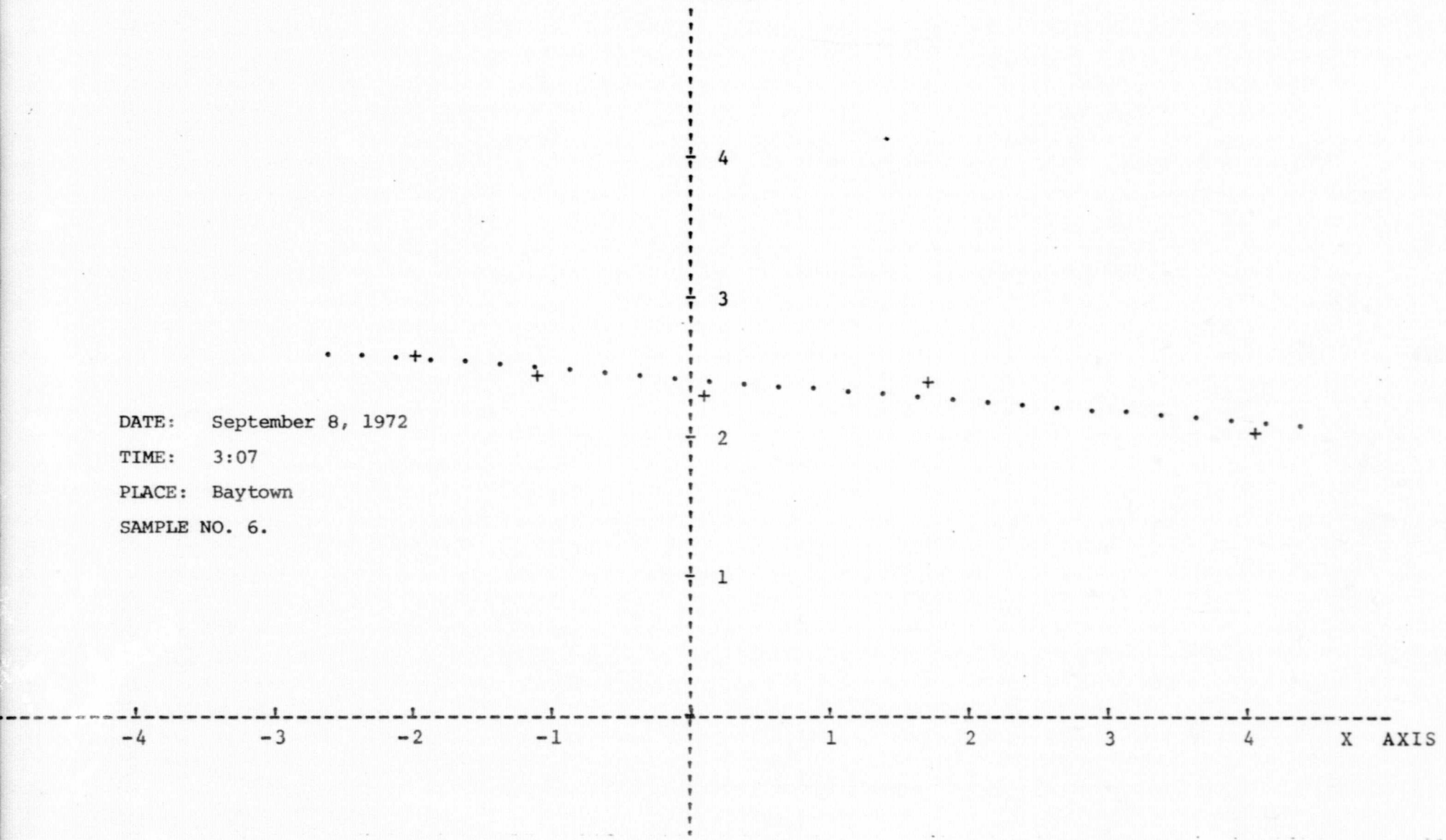

DATE: September 8, 1972

TIME: 3:07

PLACE: Baytown

SAMPLE NO. 6.

4.796293549 = a(0)
-.759176882 = a(1)
-.895244850 = r
.162442211 = S(x.y)

ONE X AXIS UNIT = .200000000
ONE Y AXIS UNIT = 2.000000000

FIGURE . Particle Size Distribution

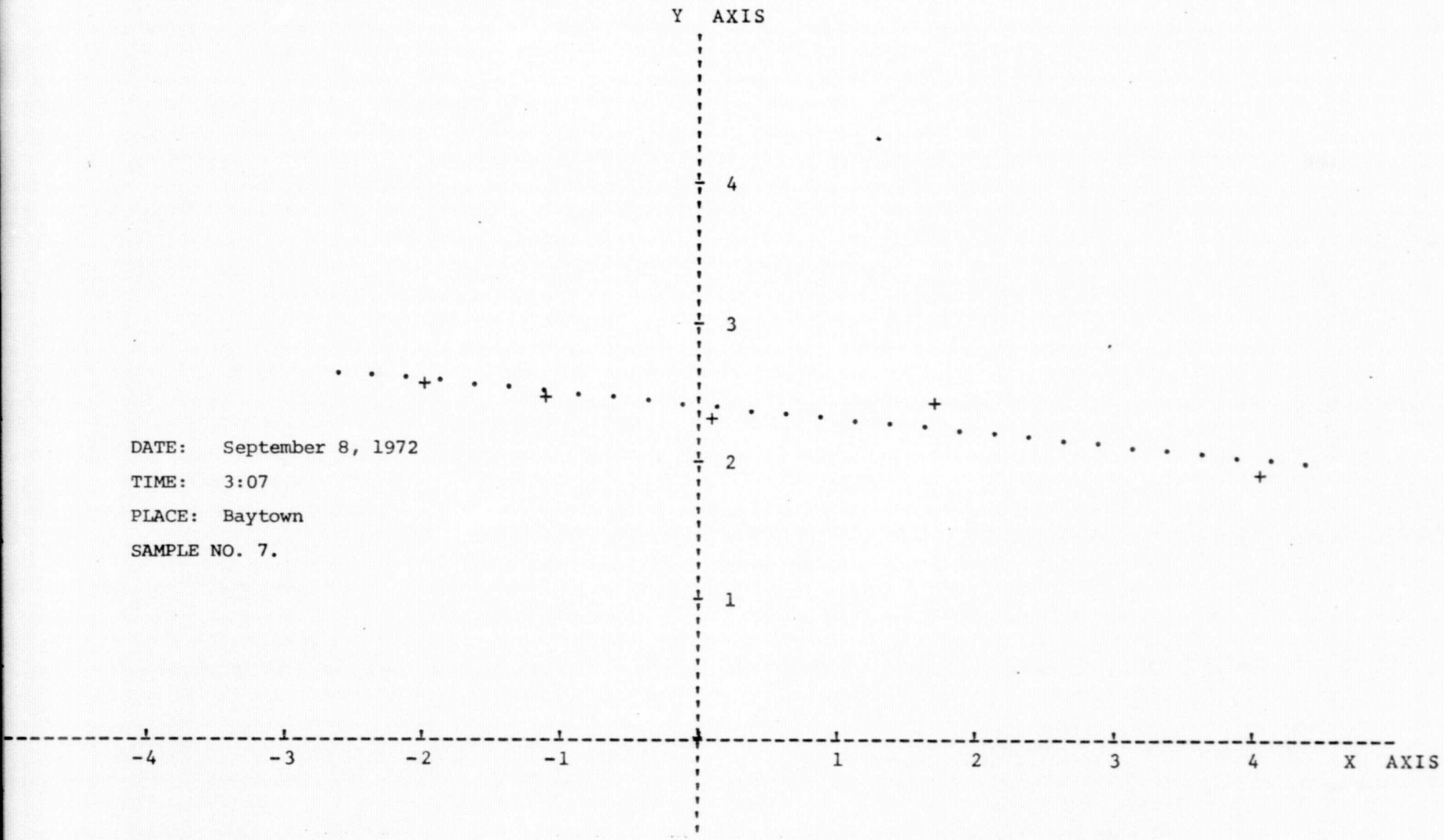

FIGURE . Particle Size Distribution

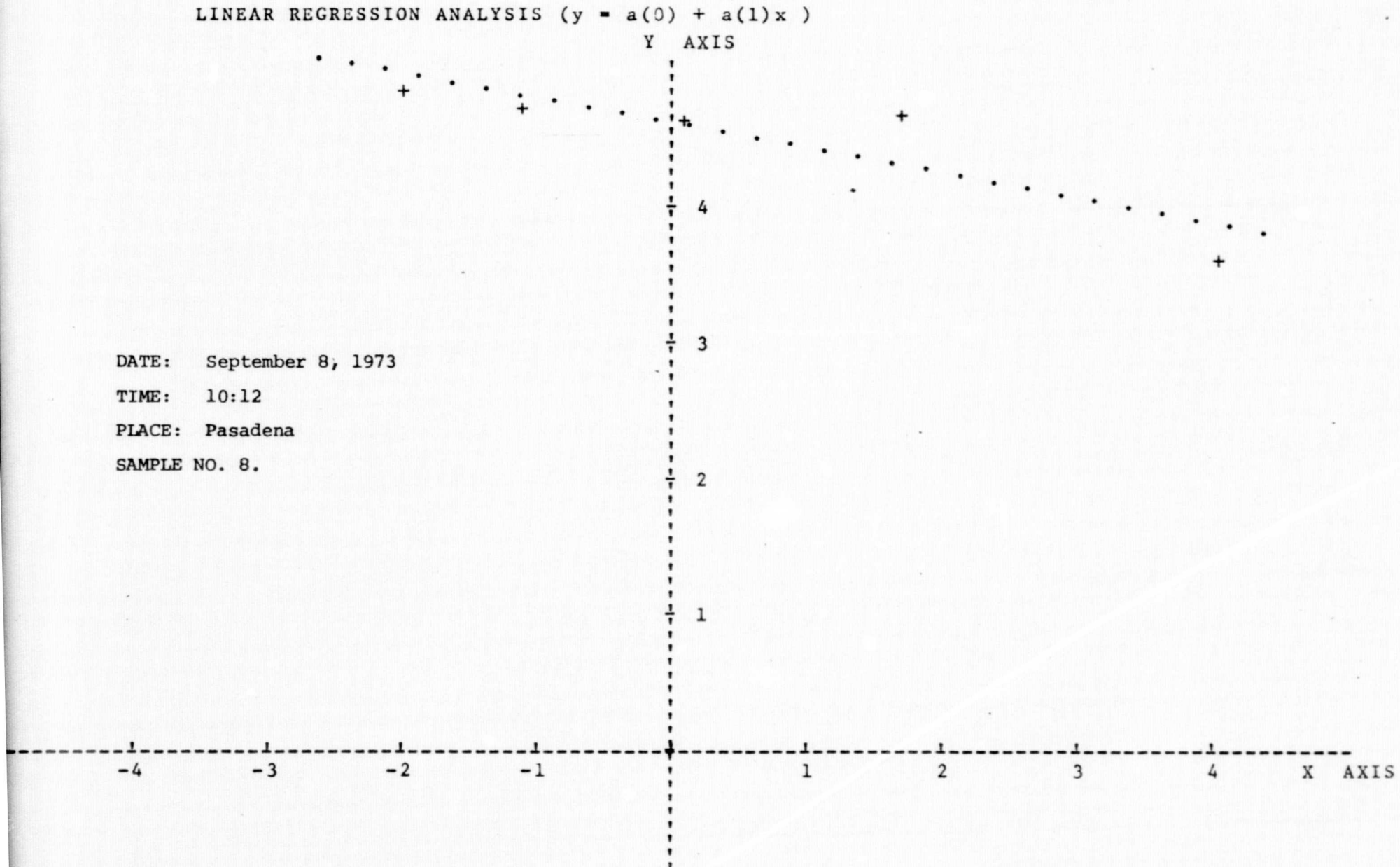

FIGURE . Particle Size Distribution

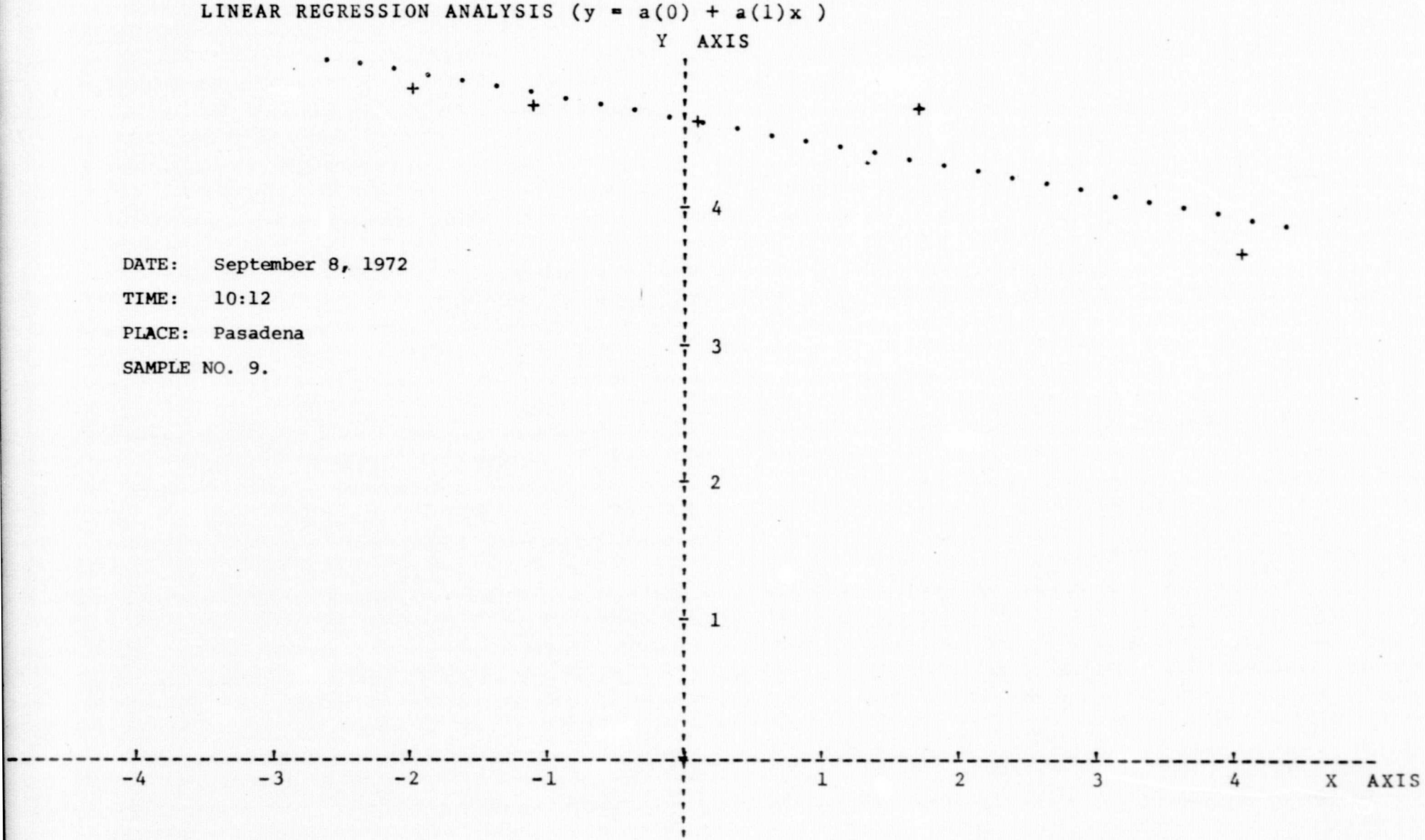

FIGURE . Particle Size Distribution

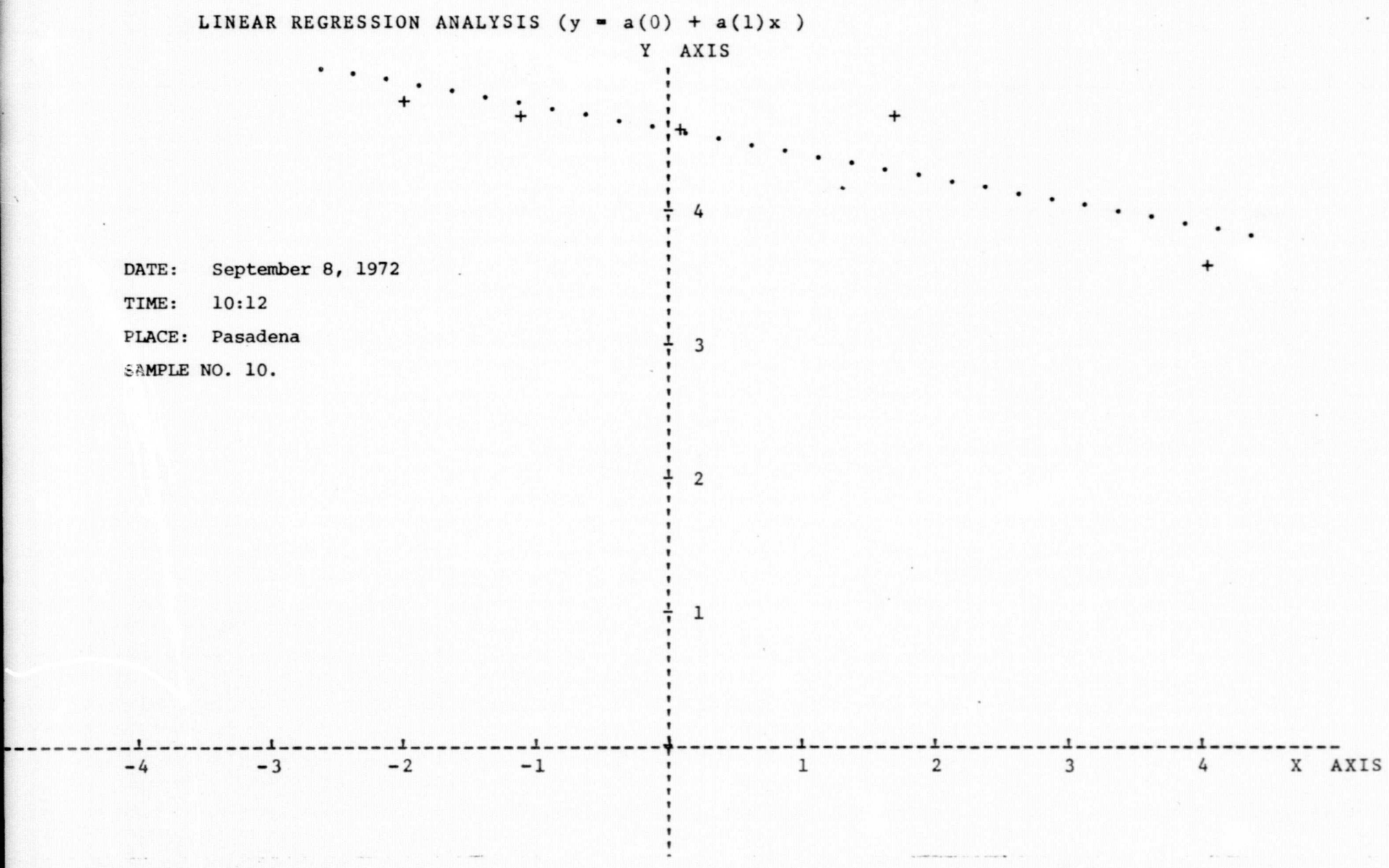

FIGURE . Particle Size Distribution

LINEAR REGRESSION ANALYSIS (y = a(0) + a(1)x)

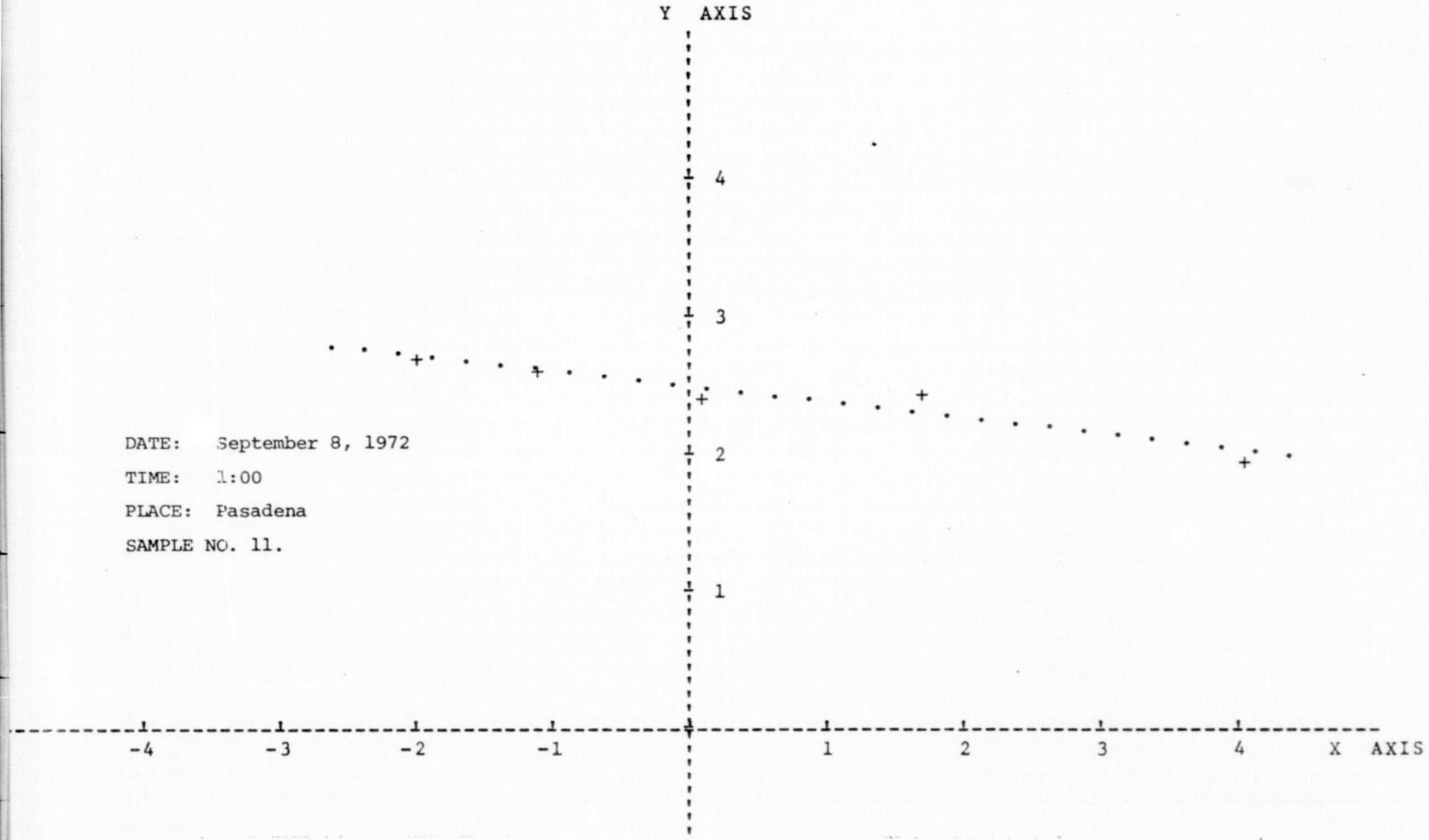

DATE: September 8, 1972

TIME: 1:00

PLACE: Pasadena

SAMPLE NO. 11.

4.944874941 = a(0)
-1.146522879 = a(1)
-.952052383 = r
.158390278 = S(x.y)

ONE X AXIS UNIT = .200000000
ONE Y AXIS UNIT = 2.000000000

FIGURE . Particle Size Distribution

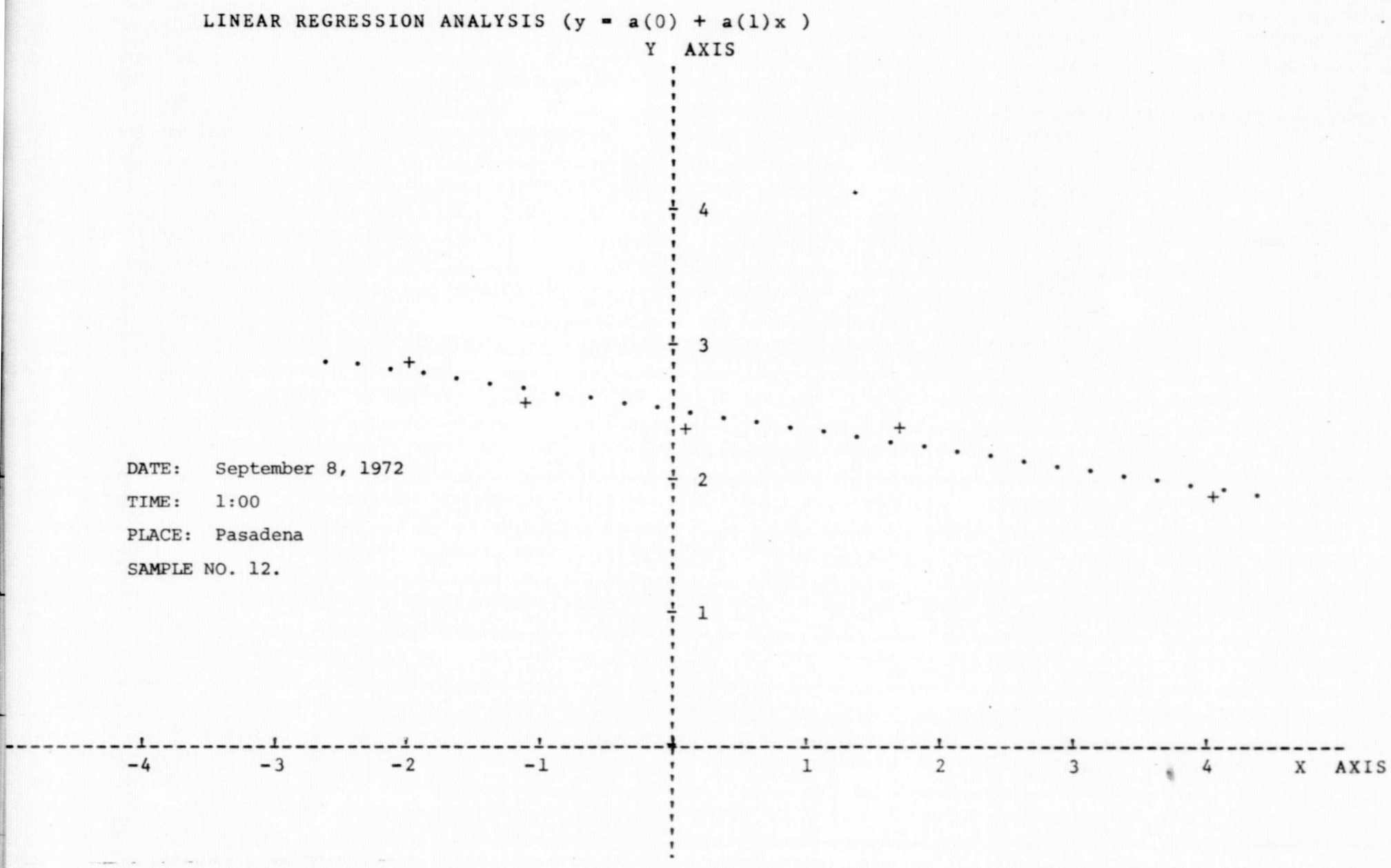

FIGURE . Particle Size Distribution

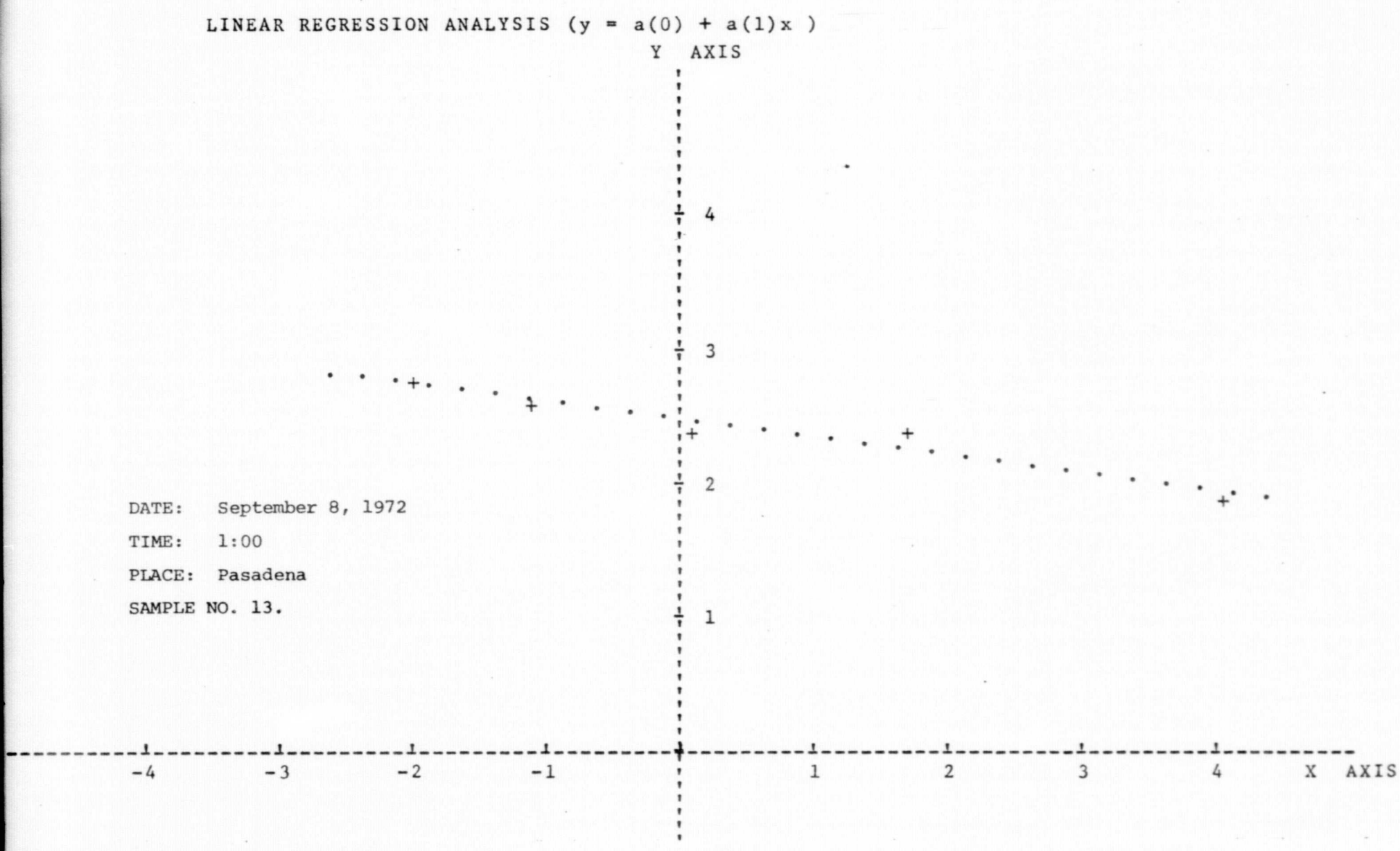

FIGURE . Particle Size Distribution

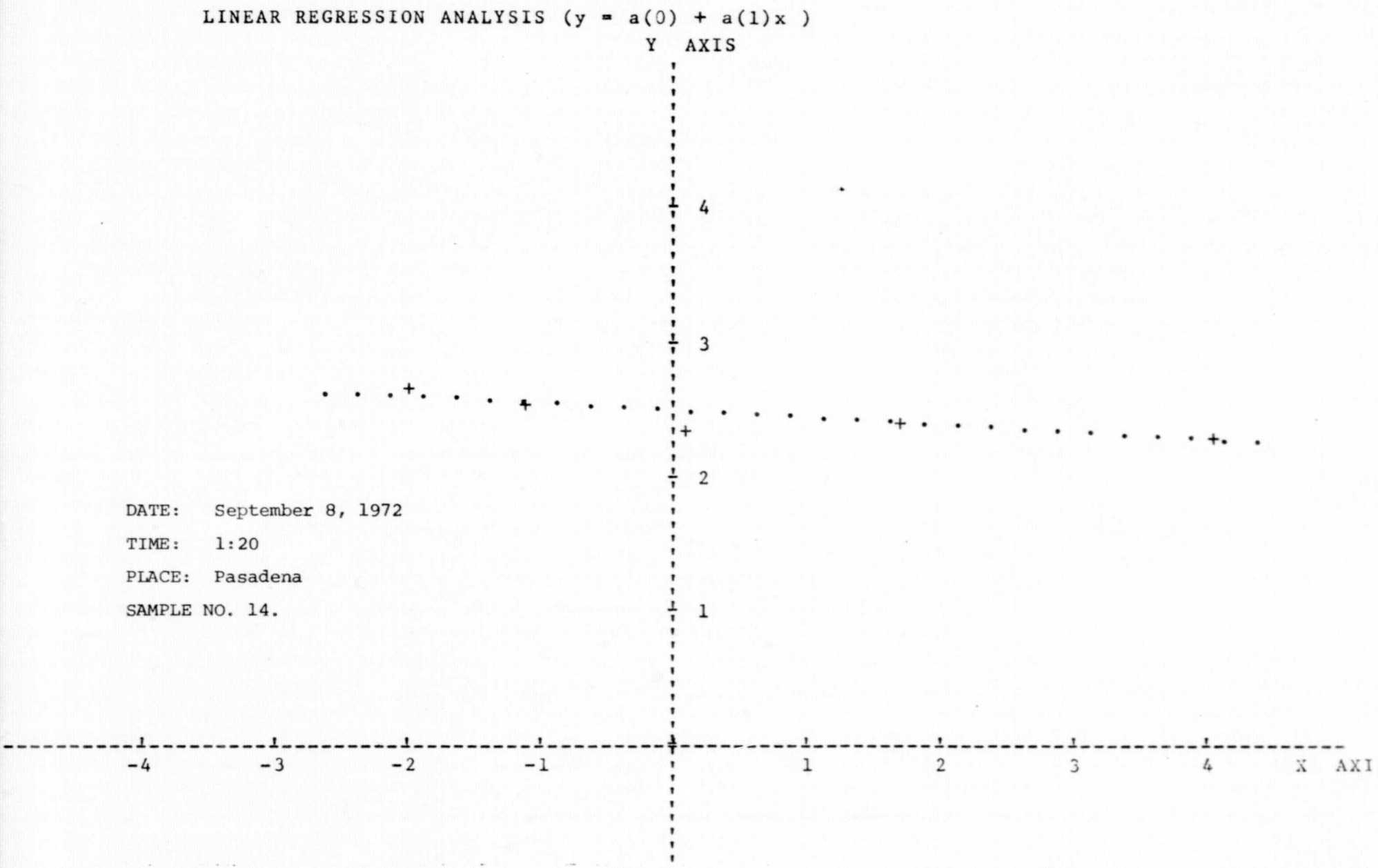

FIGURE . Particle Size Distribution

LINEAR REGRESSION ANALYSIS (y = a(0) + a(1)x)

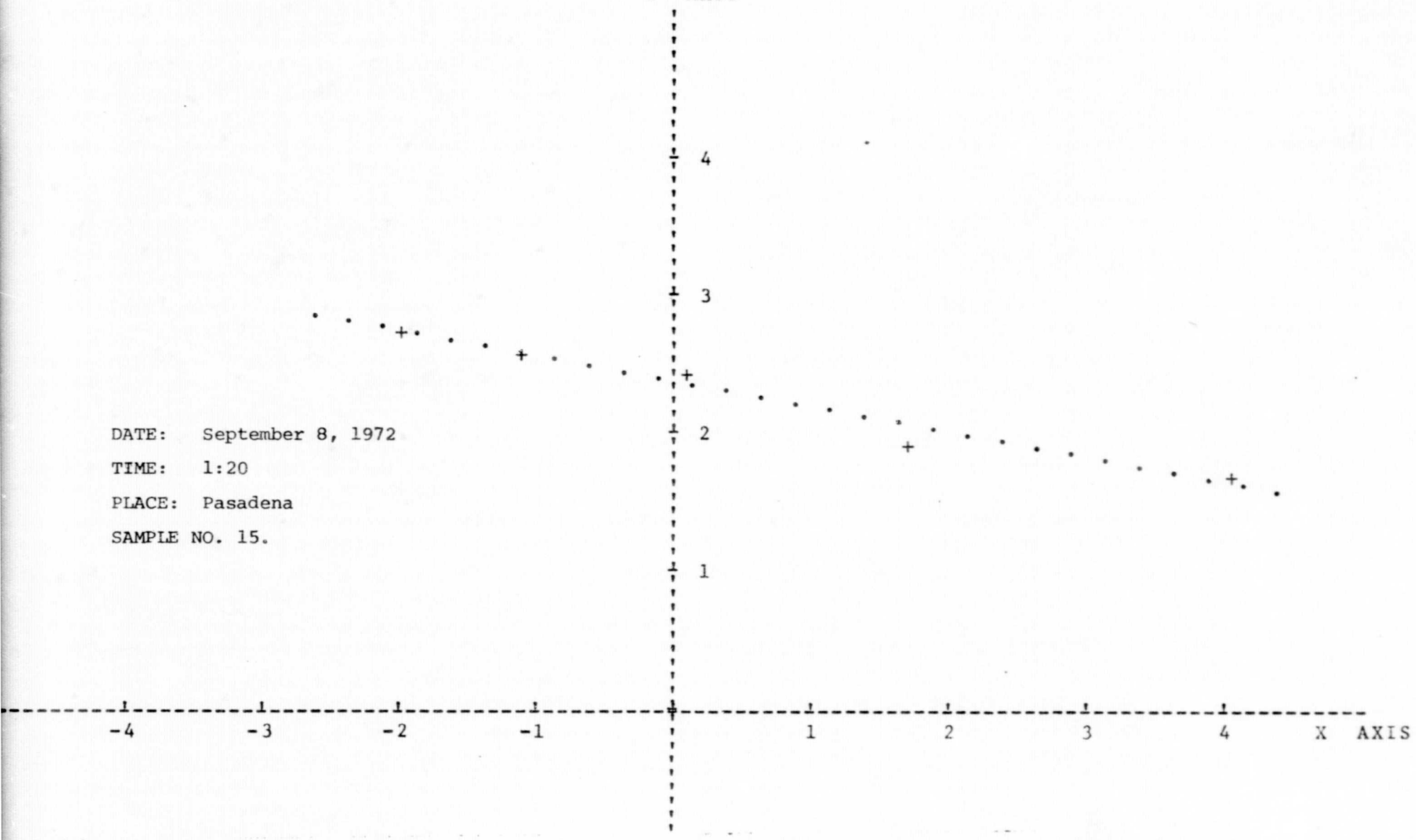

DATE: September 8, 1972

TIME: 1:20

PLACE: Pasadena

SAMPLE NO. 15.

4.723910603 = a(0)
-1.838319269 = a(1)
-.981602760 = r
.153725954 = S(x,y)

ONE X AXIS UNIT = .200000000
ONE Y AXIS UNIT = 2.000000000

FIGURE . Particle Size Distribution

LINEAR REGRESSION ANALYSIS (y = a(0) + a(1)x)

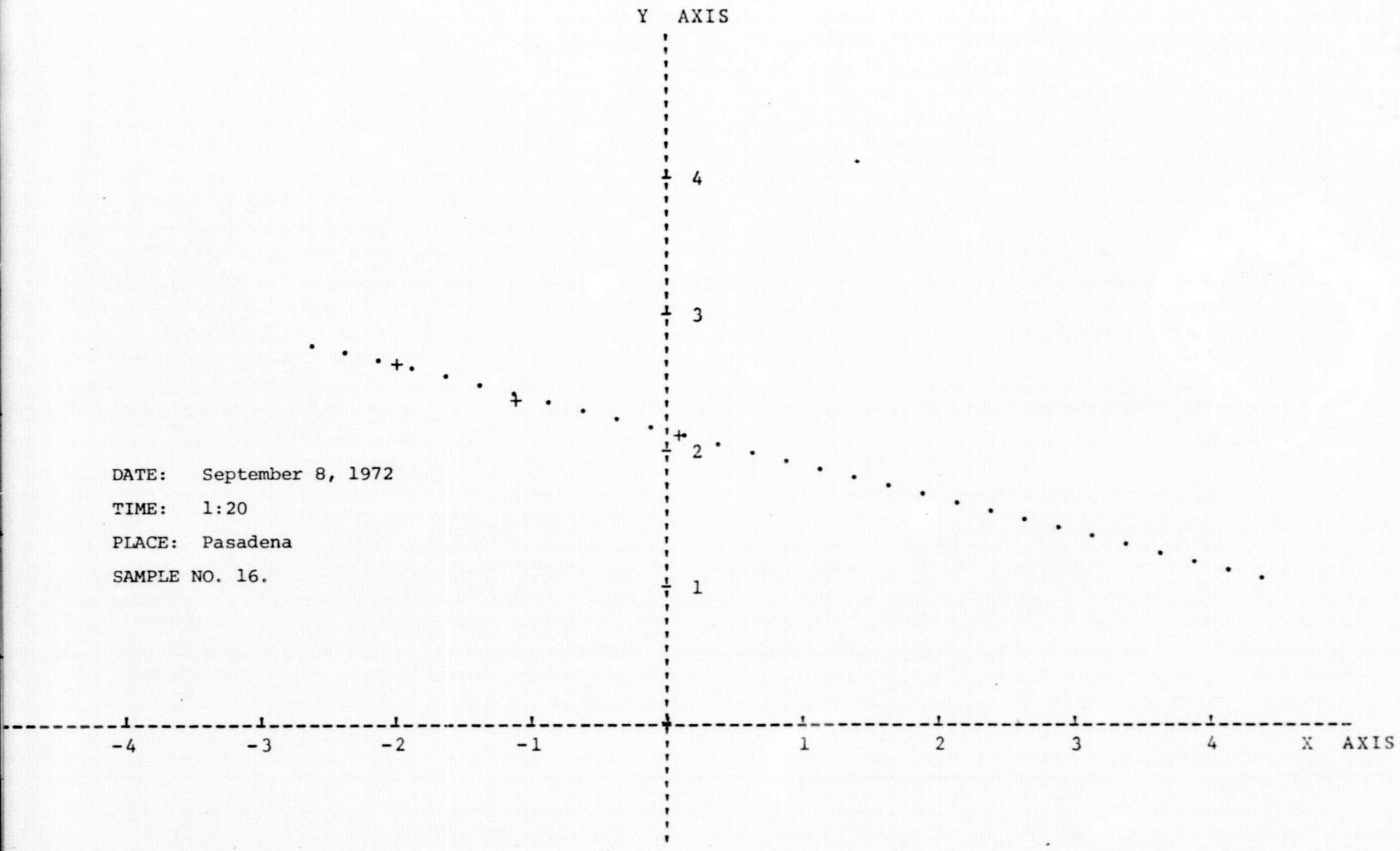

DATE: September 8, 1972

TIME: 1:20

PLACE: Pasadena

SAMPLE NO. 16.

4.247453806 = a(0)
-2.458872357 = a(1)
-.993373767 = r
.048883500 = S(x.y)

ONE X AXIS UNIT = .200000000
ONE Y AXIS UNIT = 2.000000000

FIGURE . Particle Size Distribution

LINEAR REGRESSION ANALYSIS (y = a(0) + a(1)x)

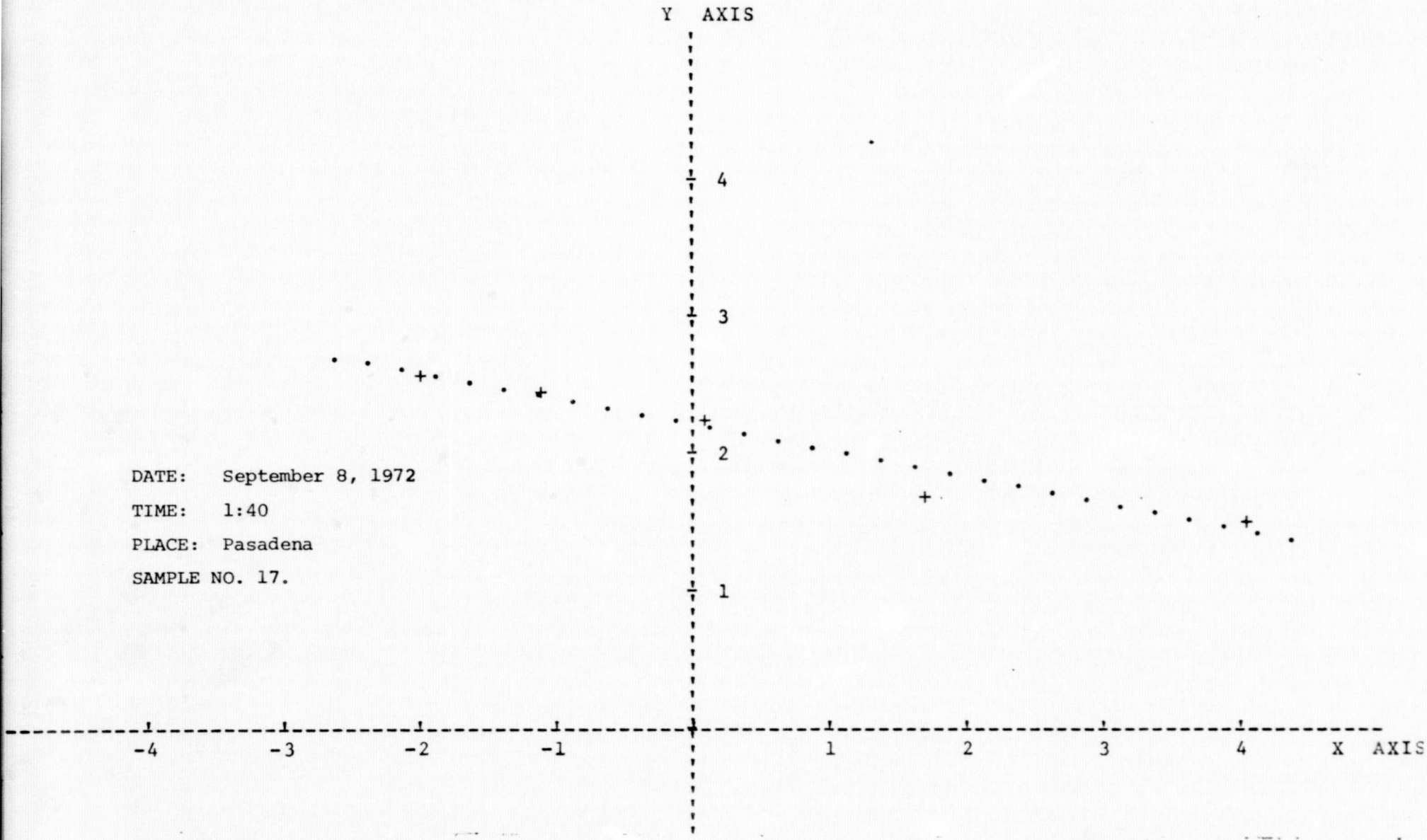

DATE: September 8, 1972

TIME: 1:40

PLACE: Pasadena

SAMPLE NO. 17.

4.376948067 = a(0)
-1.912760057 = a(1)
-.972128938 = r
.198316307 = S(x.y)

ONE X AXIS UNIT = .200000000
ONE Y AXIS UNIT = 2.000000000

FIGURE . Particle Size Distribution

LINEAR REGRESSION ANALYSIS (y = a(0) + a(1)x)

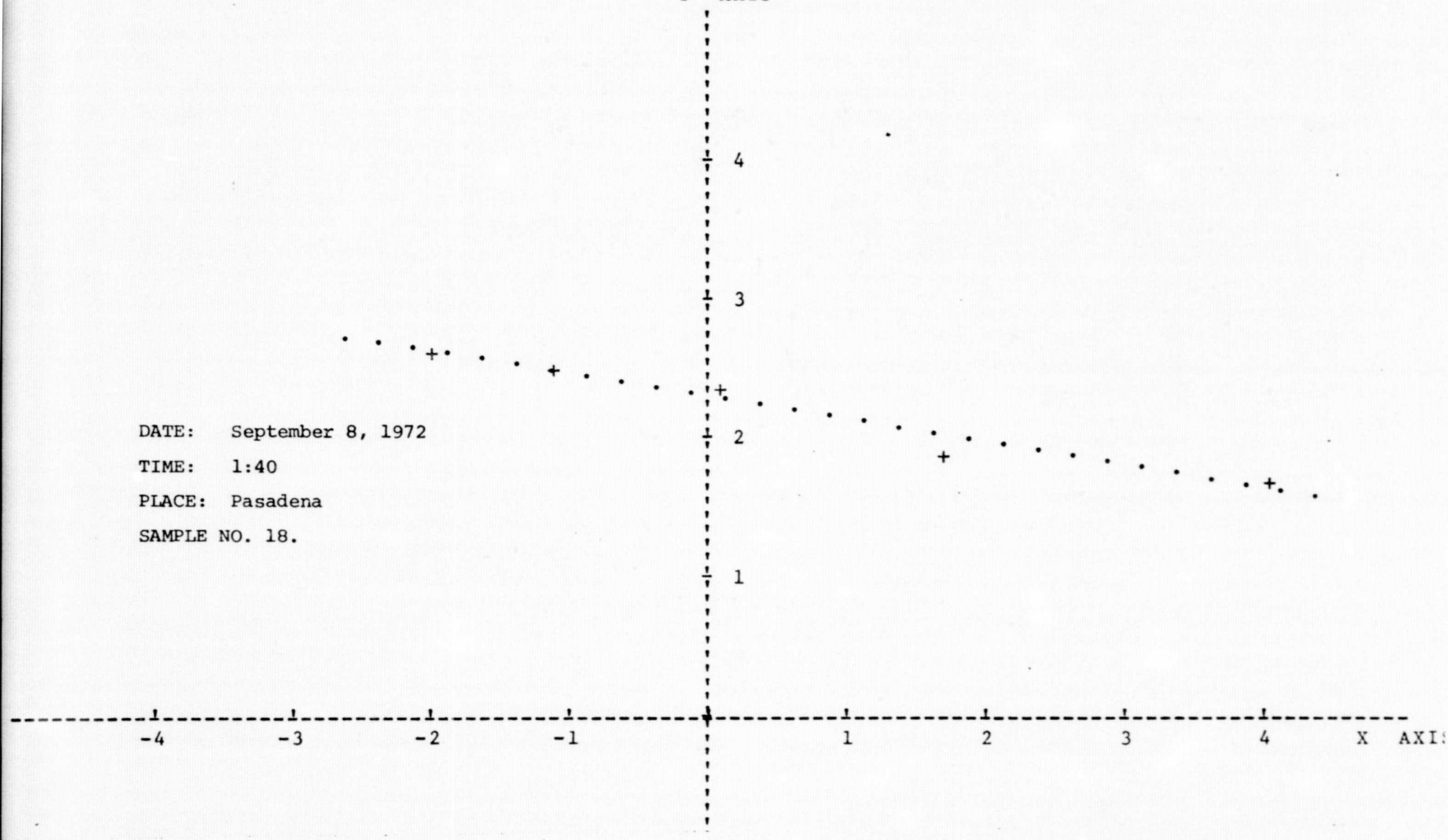

DATE: September 8, 1972

TIME: 1:40

PLACE: Pasadena

SAMPLE NO. 18.

4.552996849 = a(0)
-1.641035670 = a(1)
-.978647549 = r
.148175769 = S(x.y)

ONE X AXIS UNIT = .200000000
ONE Y AXIS UNIT = 2.000000000

FIGURE . Particle Size Distribution

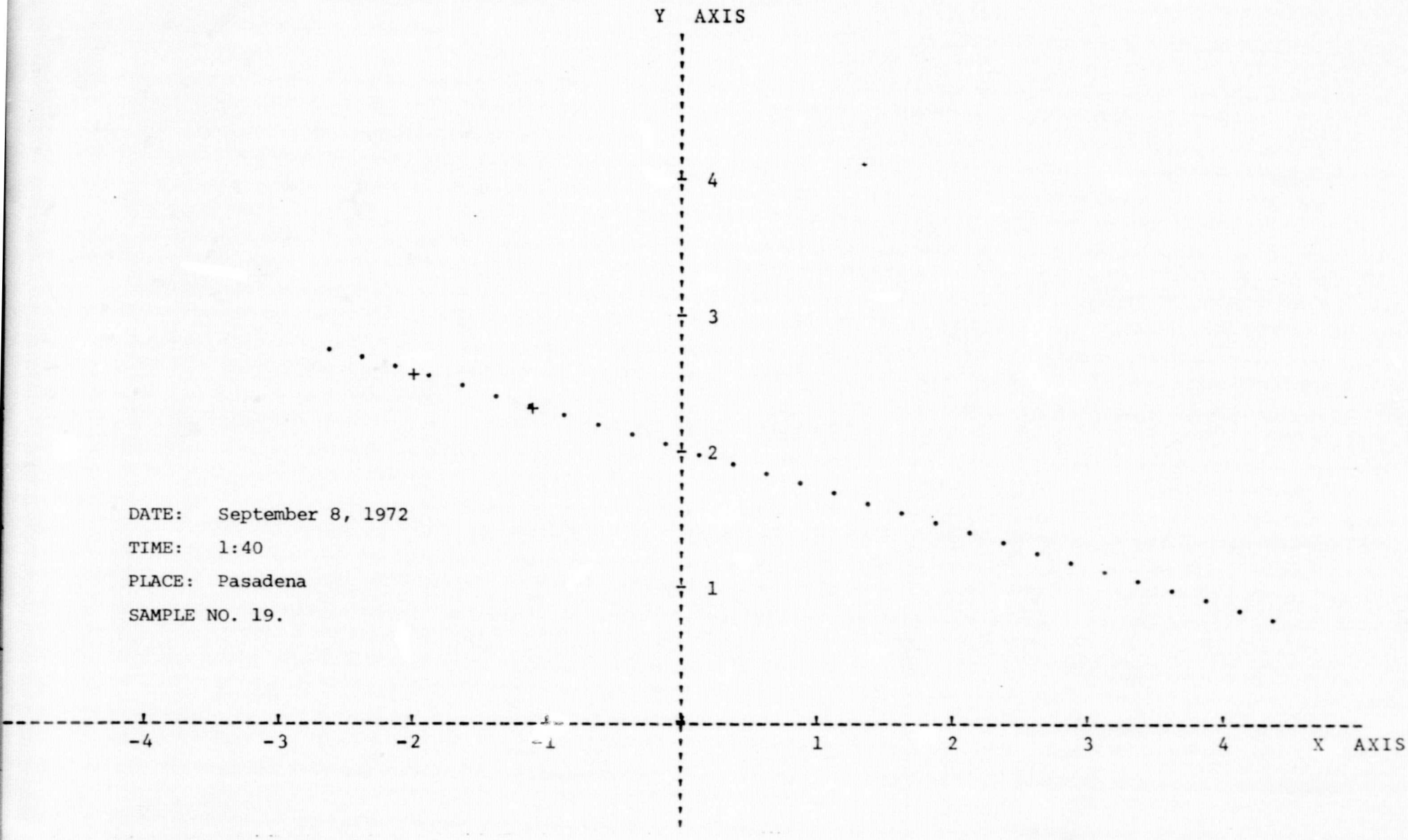

FIGURE . Particle Size Distribution

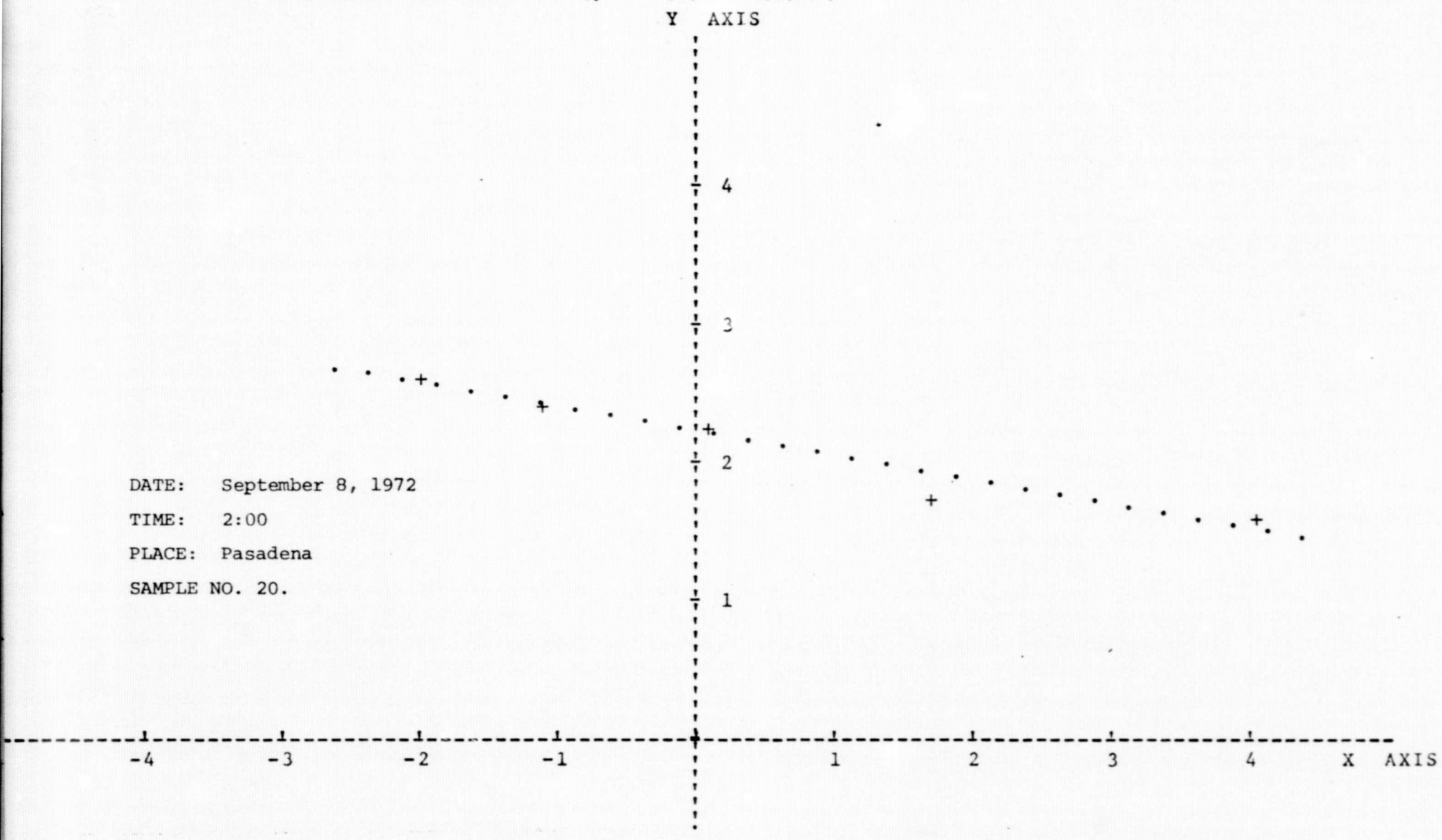

FIGURE . Particle Size Distribution

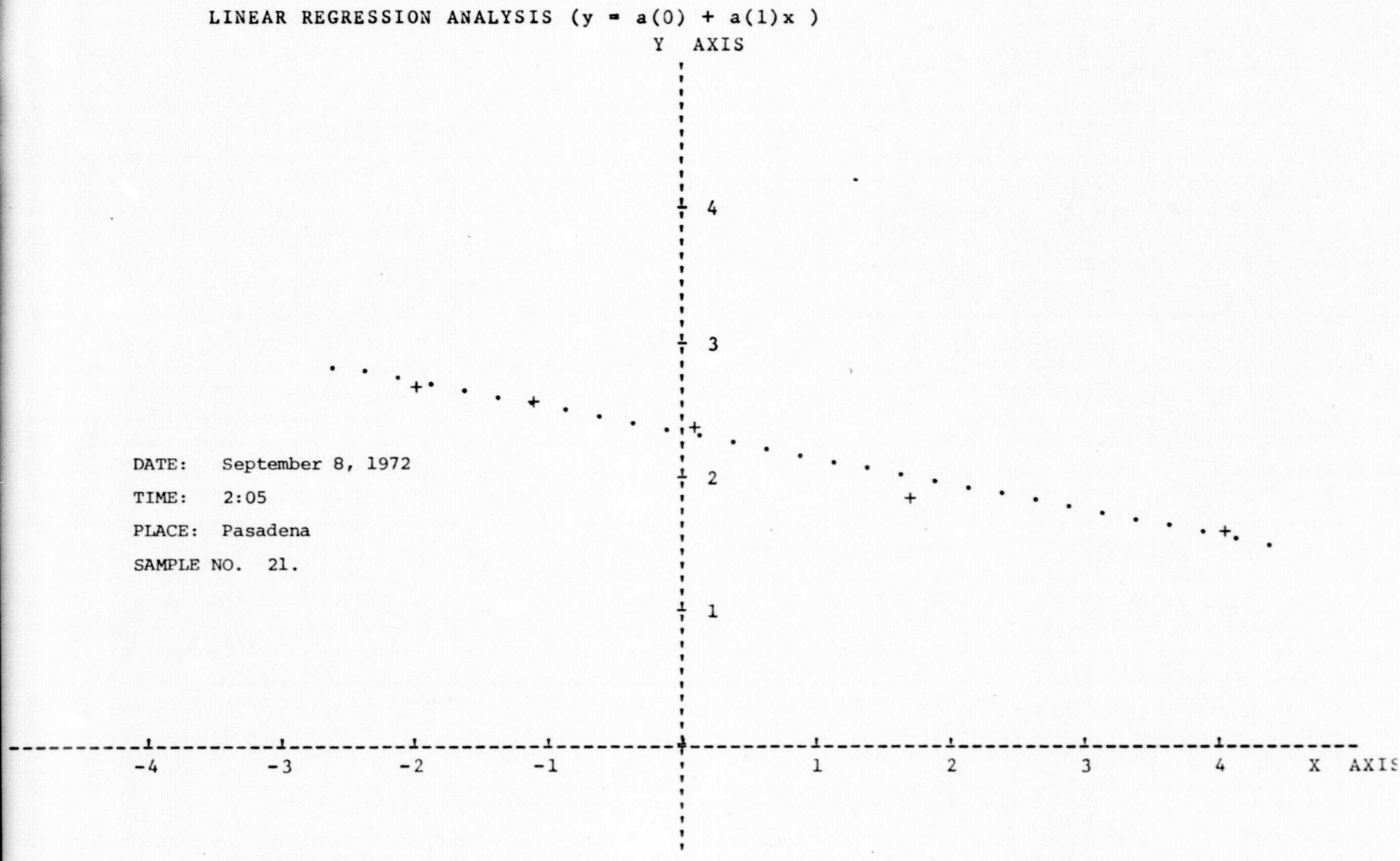

FIGURE . Particle Size Distribution

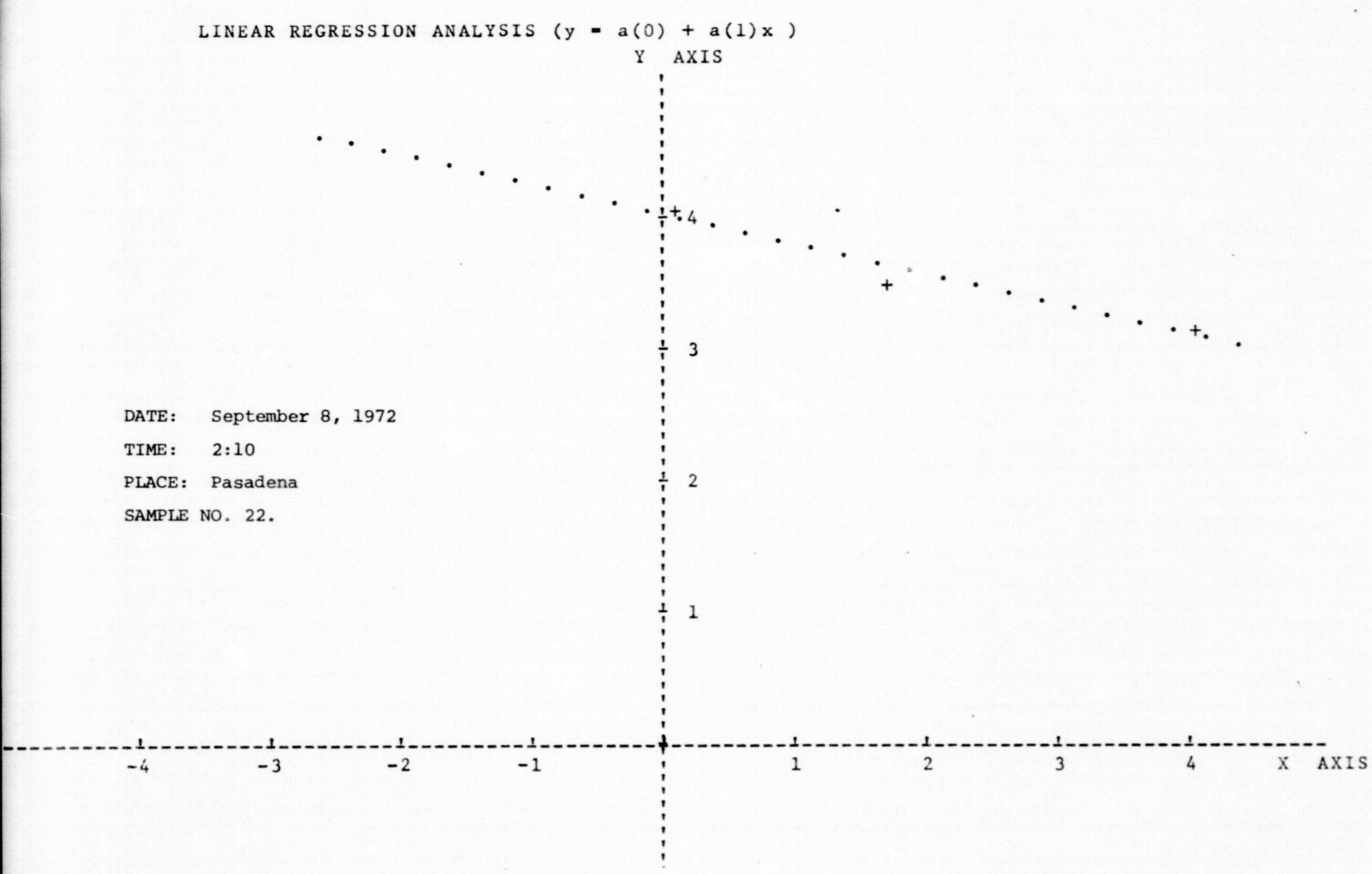

FIGURE . Particle Size Distribution

LINEAR REGRESSION ANALYSIS (y = a(0) + a(1)x)

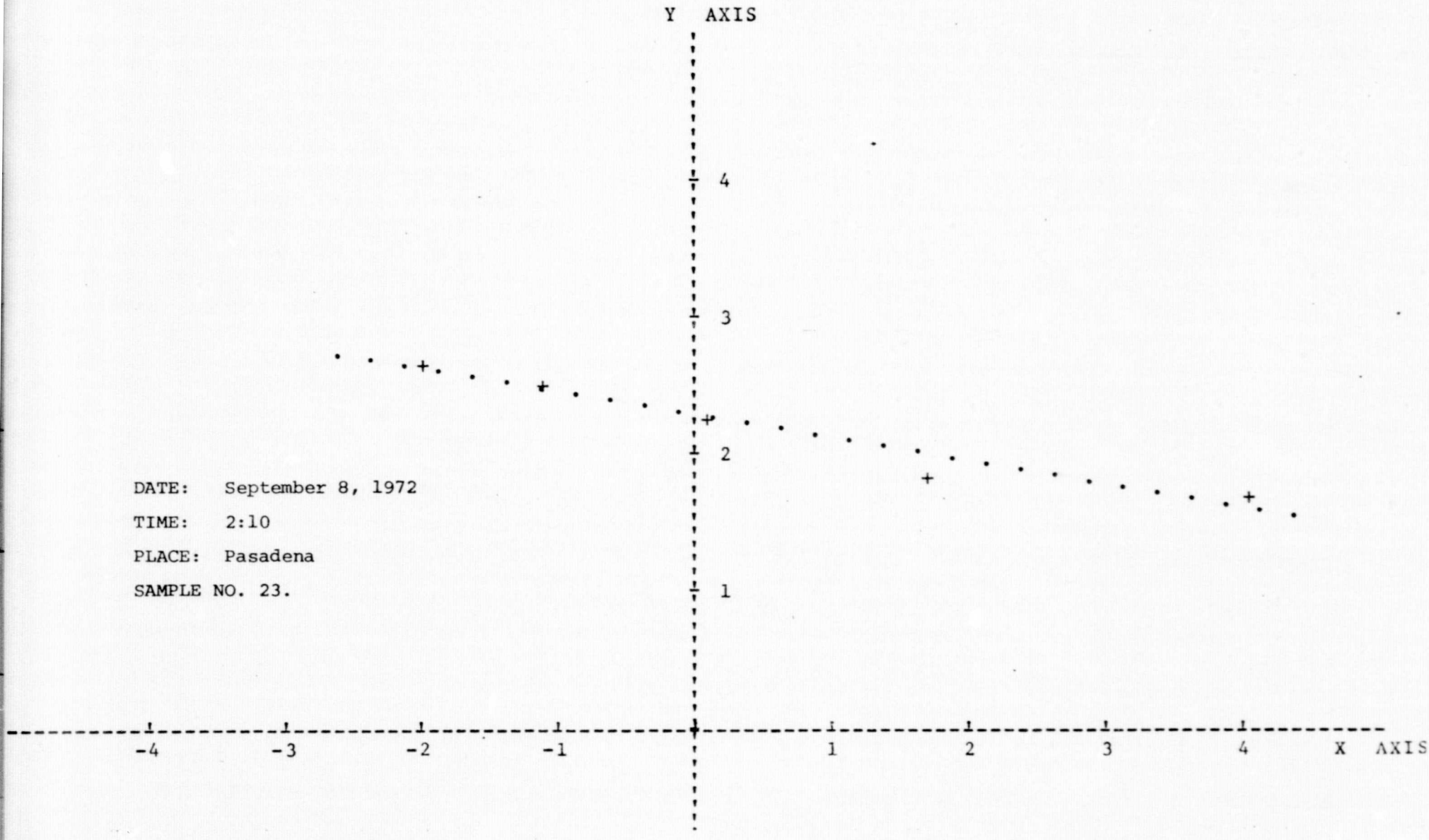

DATE: September 8, 1972

TIME: 2:10

PLACE: Pasadena

SAMPLE NO. 23.

4.536399509 = a(0)
-1.698970752 = a(1)
-.970817069 = r
.180431976 = S(x.y)

ONE X AXIS UNIT = .200000000
ONE Y AXIS UNIT = 2.000000000

FIGURE . Particle Size Distribution

LINEAR REGRESSION ANALYSIS (y = a(0) + a(1)x)

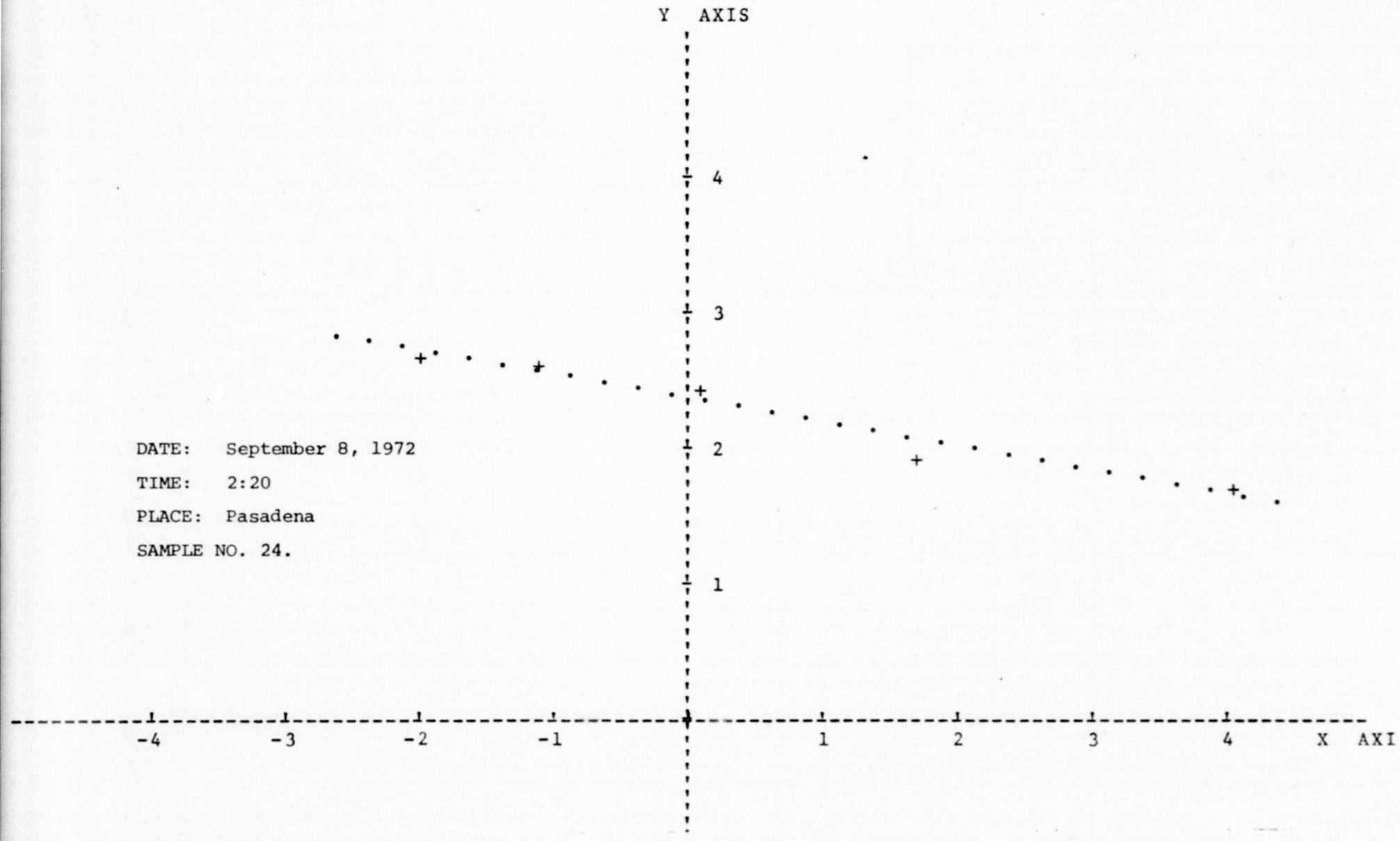

DATE: September 8, 1972

TIME: 2:20

PLACE: Pasadena

SAMPLE NO. 24.

4.717540561 = a(0)
-1.765716112 = a(1)
-.977176021 = r
.165022748 = S(x.y)

ONE X AXIS UNIT = .200000000
ONE Y AXIS UNIT = 2.000000000

FIGURE . Particle Size Distribution

LINEAR REGRESSION ANALYSIS (y = a(0) + a(1)x)

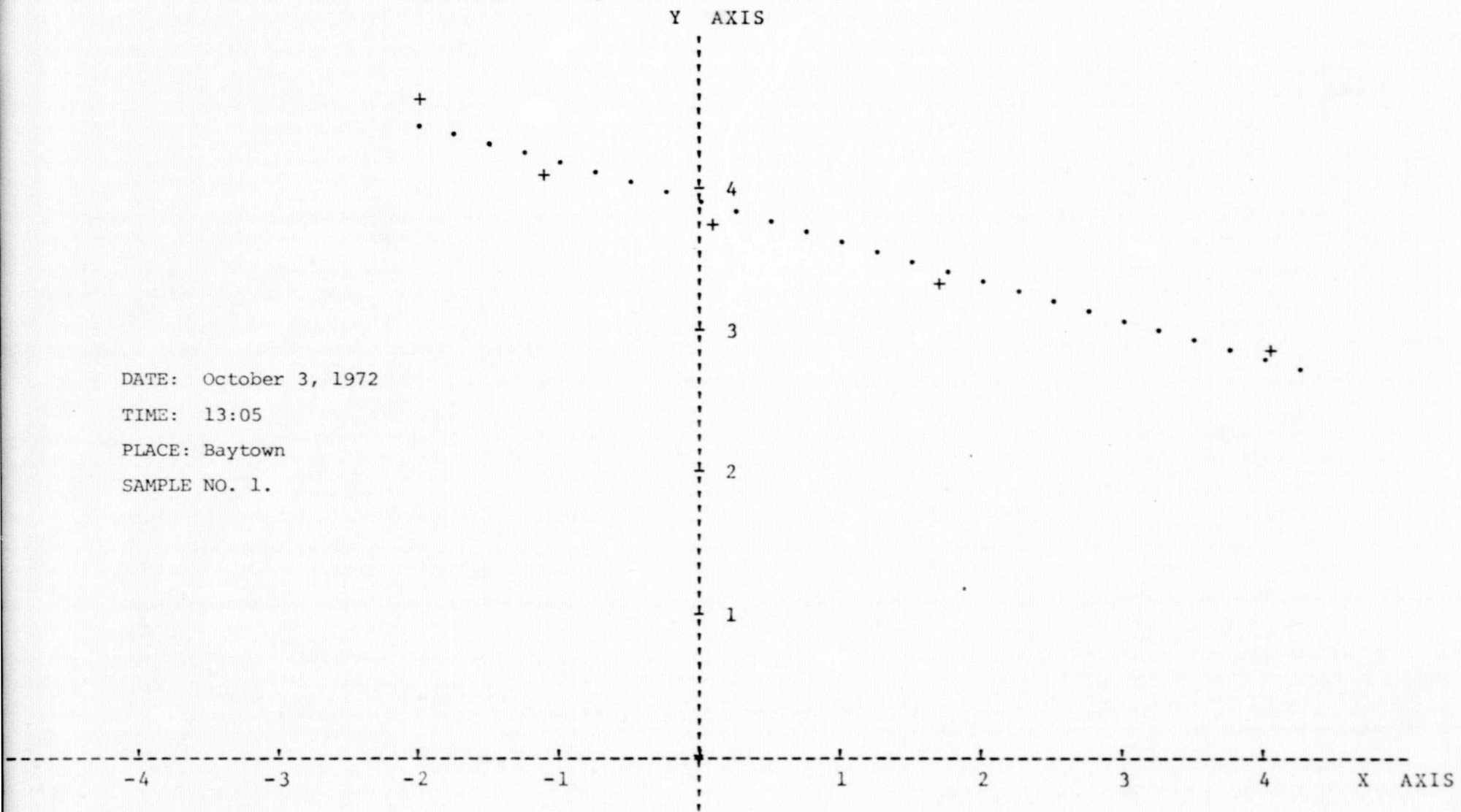

DATE: October 3, 1972

TIME: 13:05

PLACE: Baytown

SAMPLE NO. 1.

3.885797783 = a(0)
-1.388900303 = a(1)
-.979905992 = r
.121540107 = S(x.y)

ONE X AXIS UNIT = .200000000
ONE Y AXIS UNIT = 1.000000000

FIGURE . Particle Size Distribution

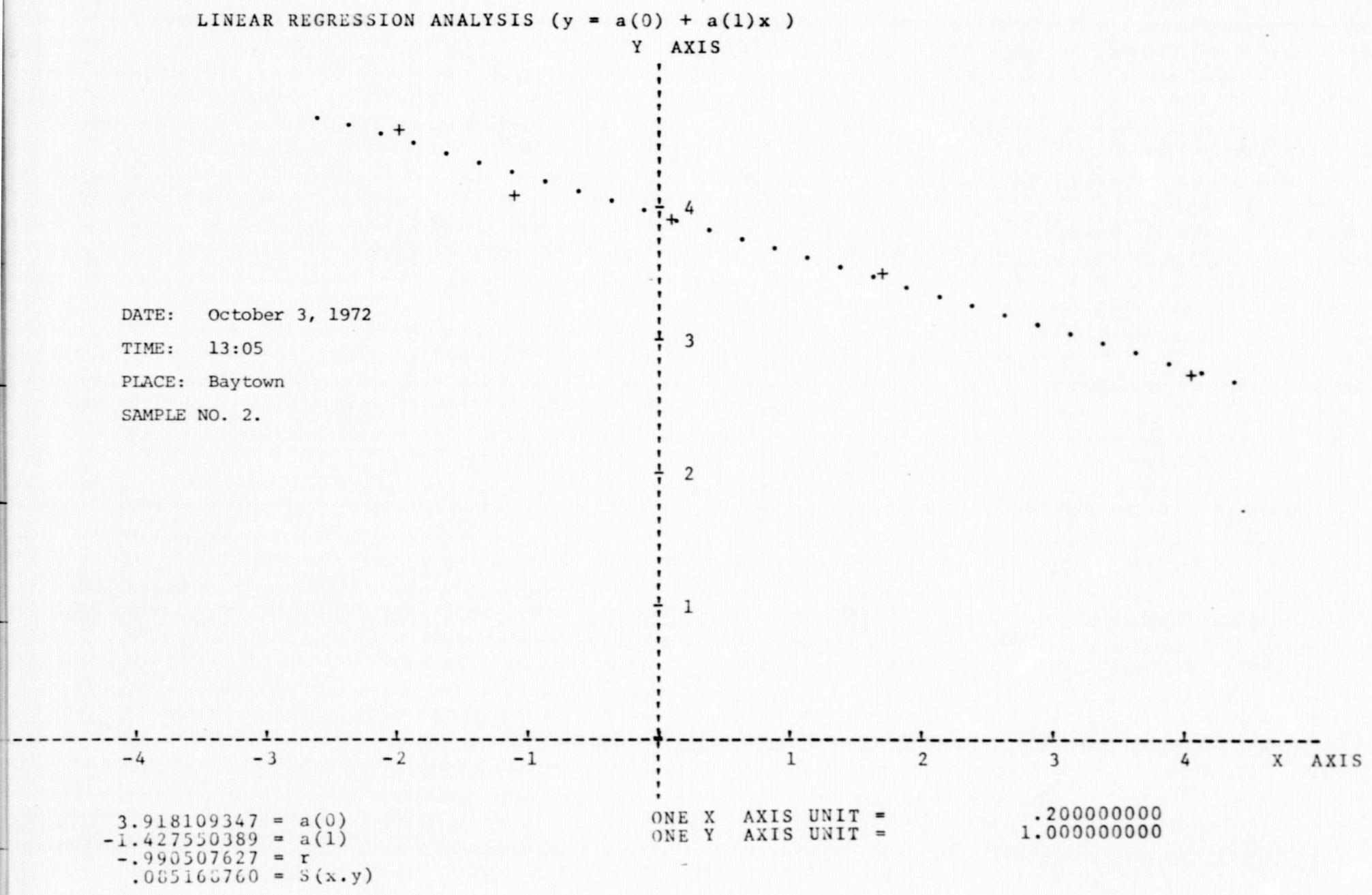

FIGURE . Particle Size Distribution

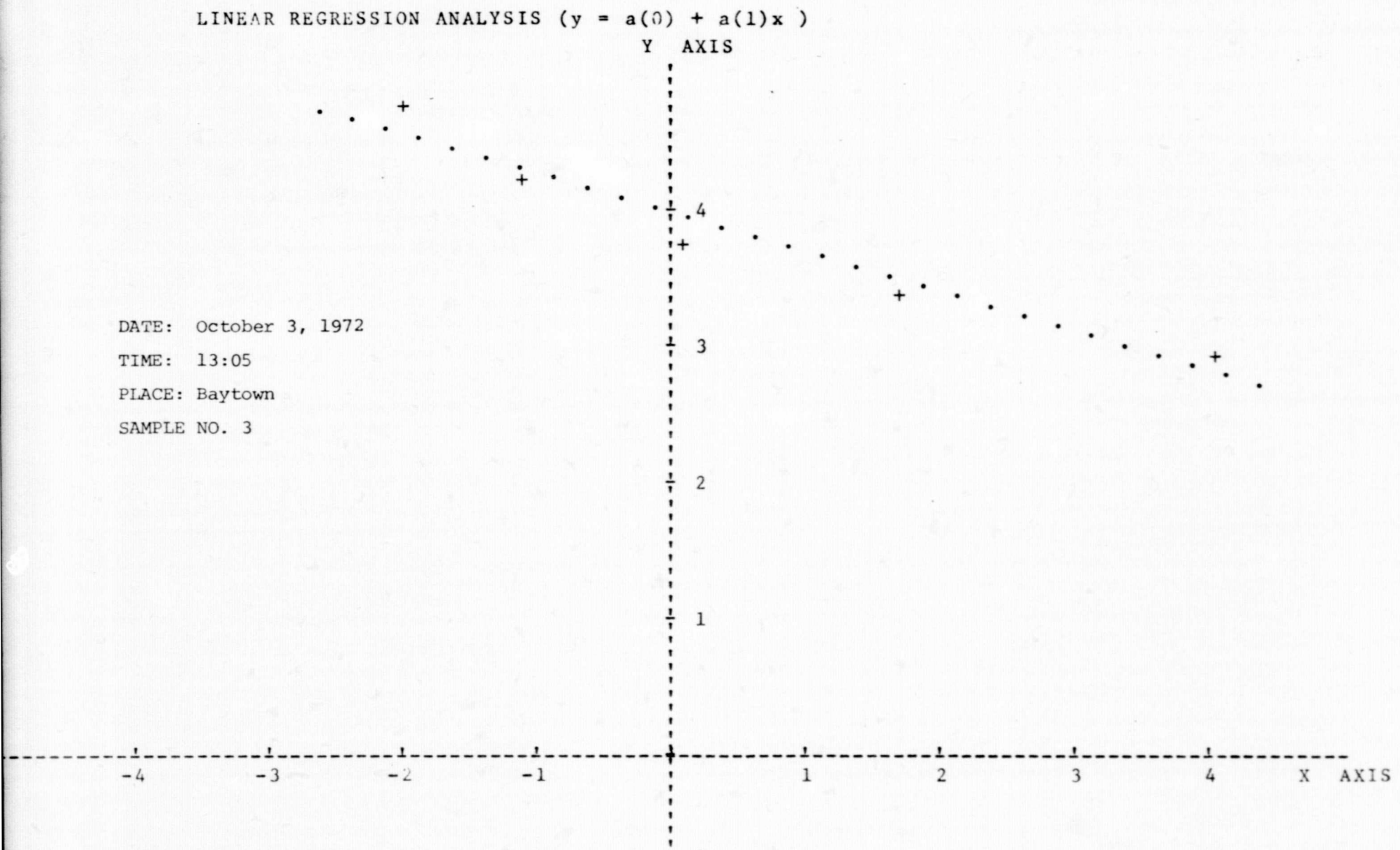

FIGURE . Particle Size Distribution

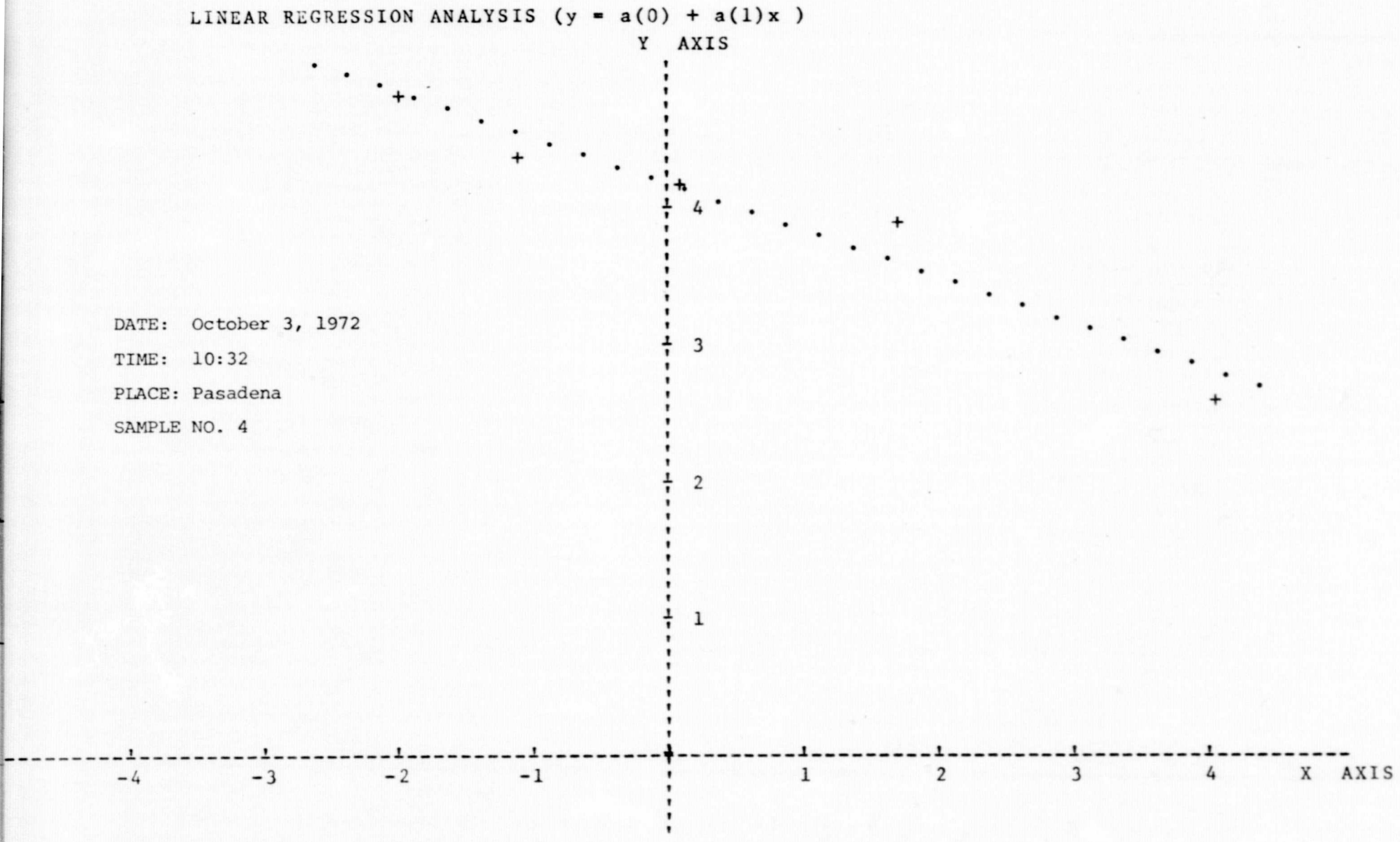

FIGURE . Particle Size Distribution

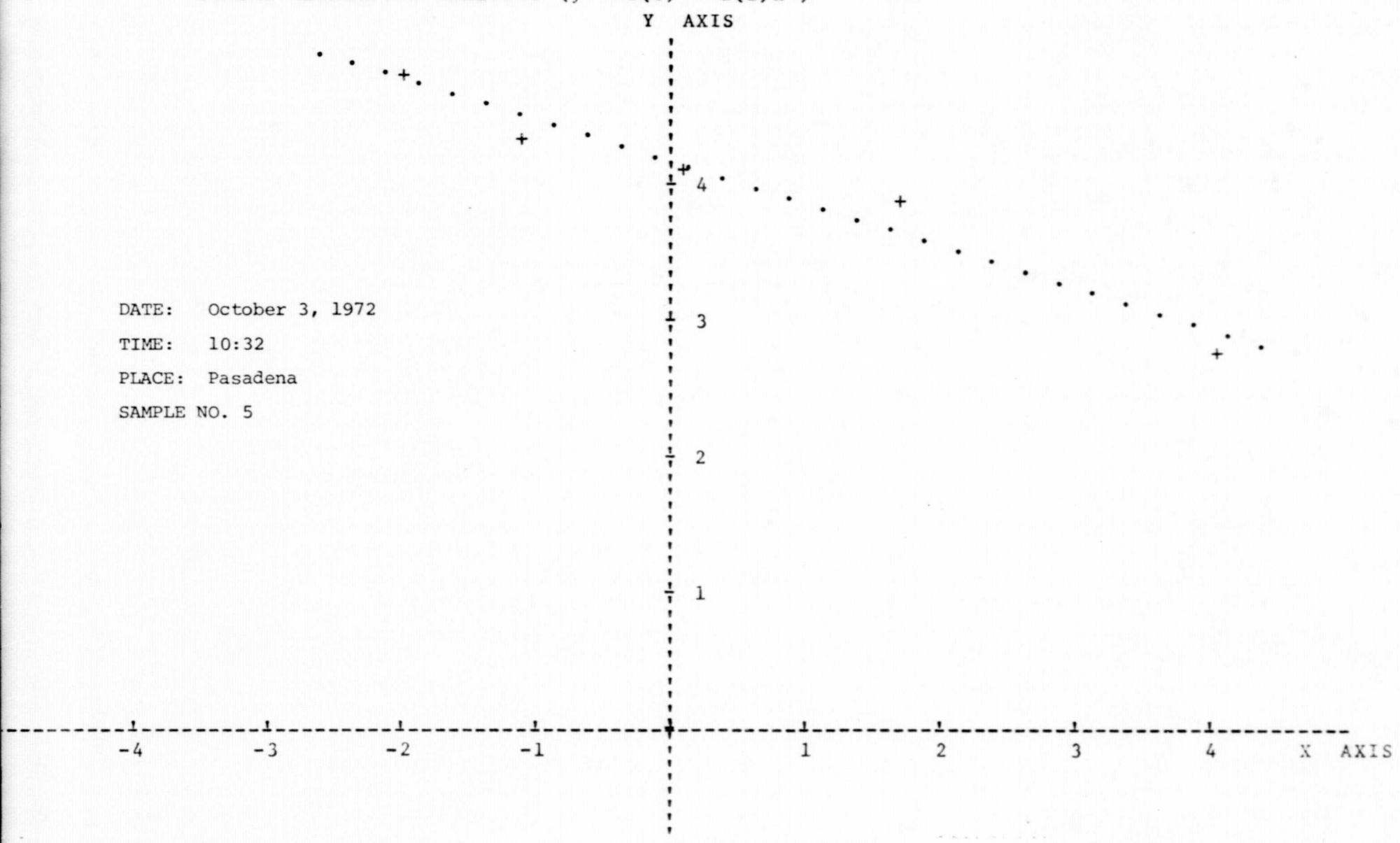

FIGURE . Particle Size Distribution

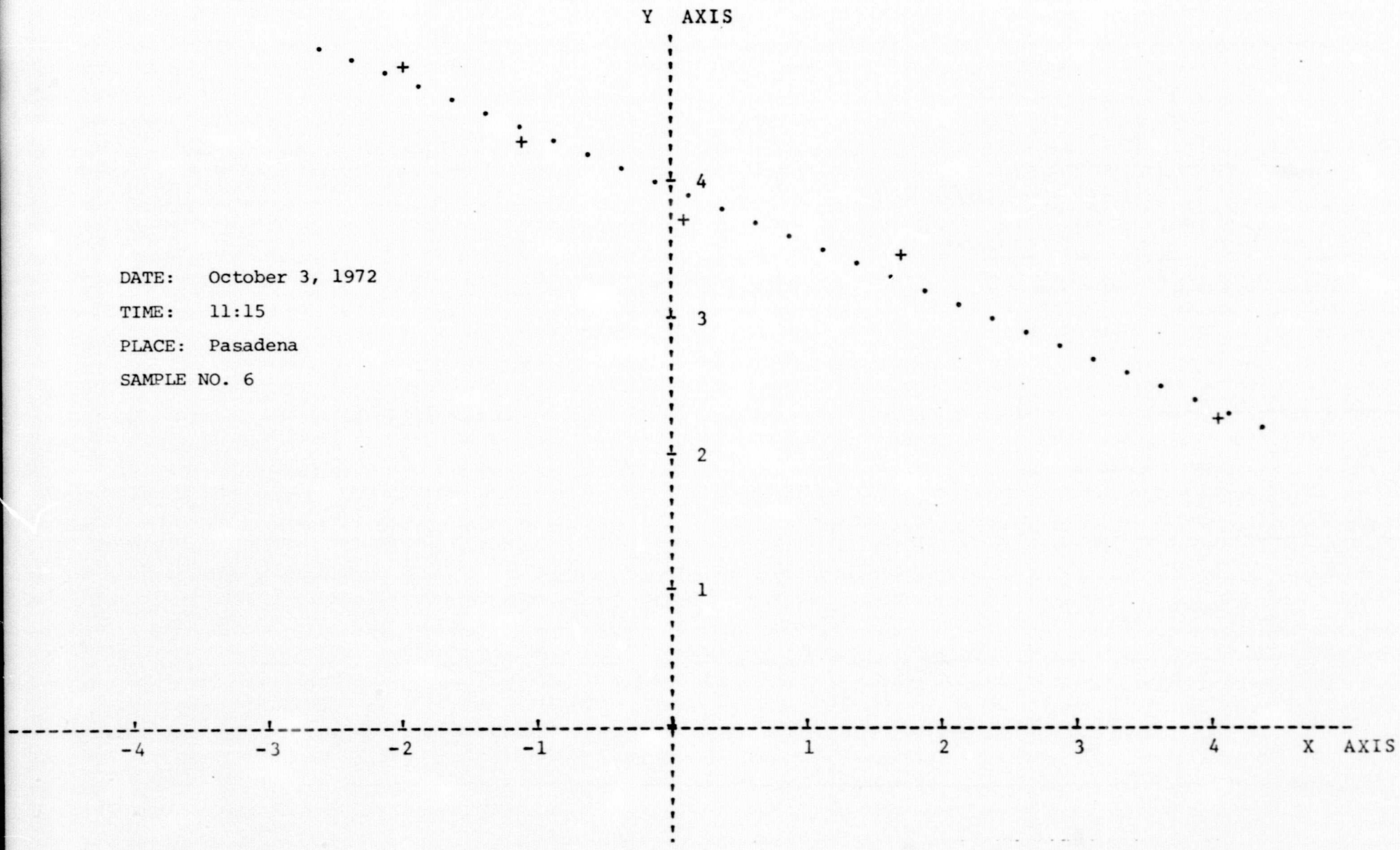

FIGURE . Particle Size Distribution

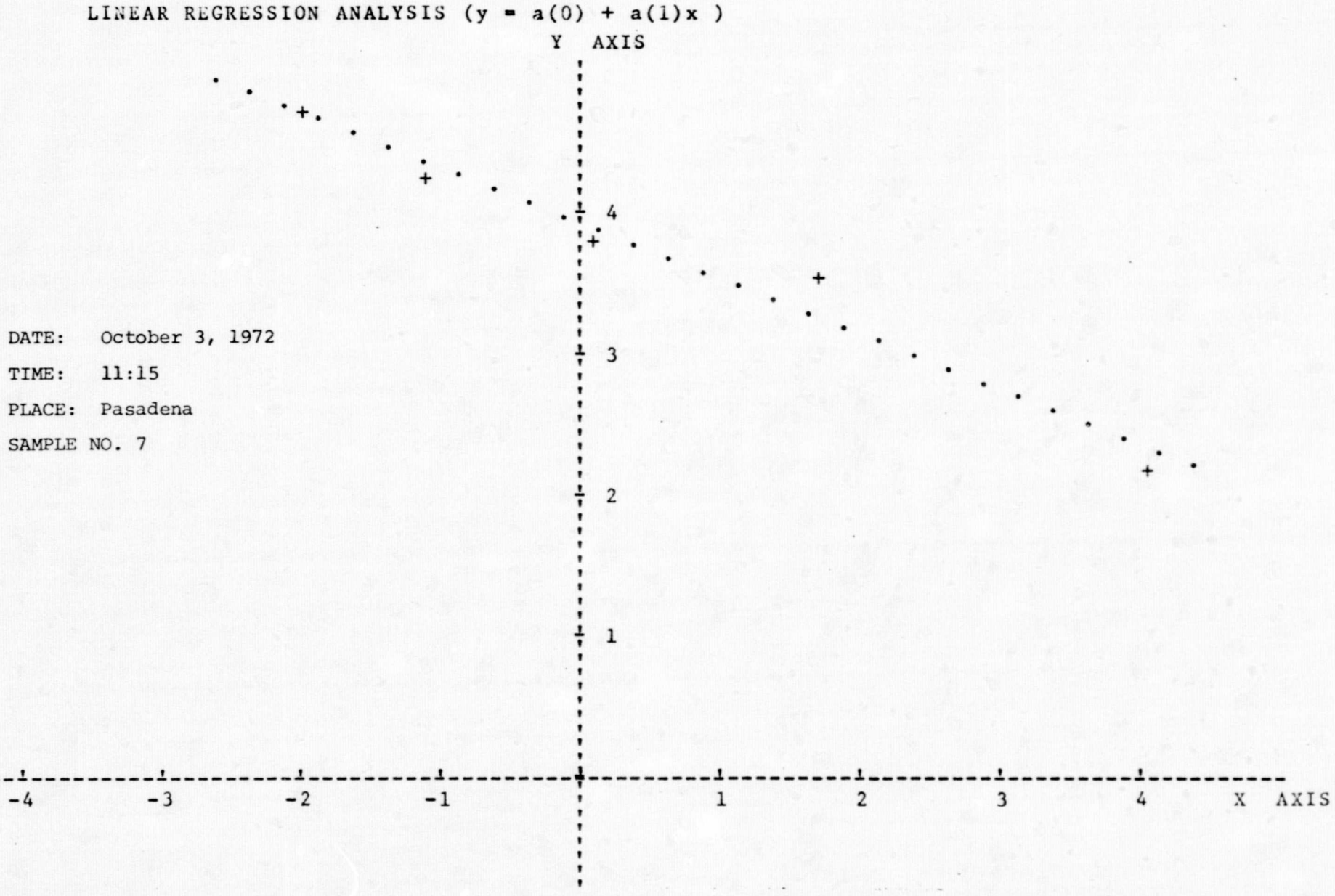

FIGURE . Particle Size Distribution

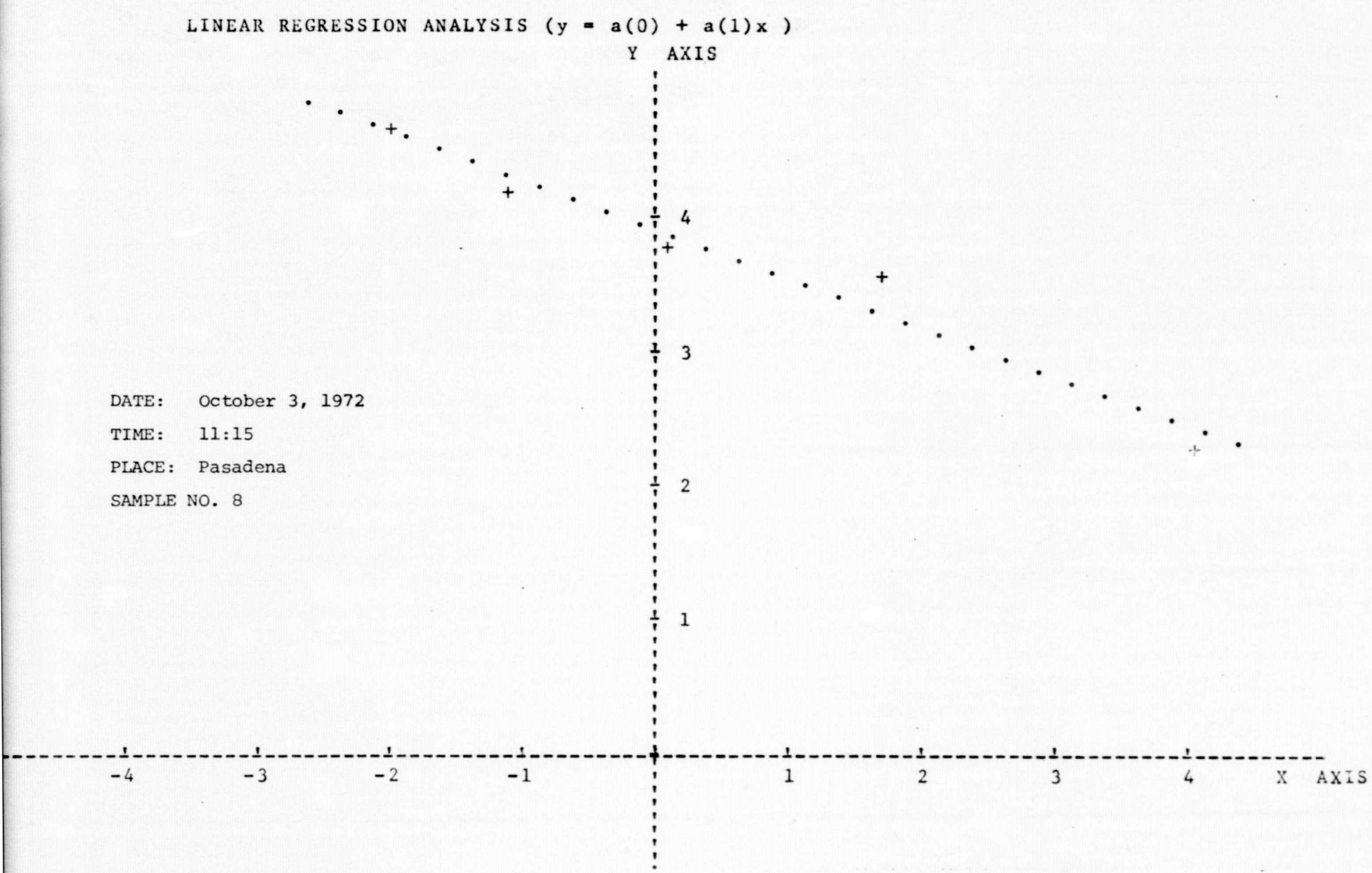

FIGURE . Particle Size Distribution

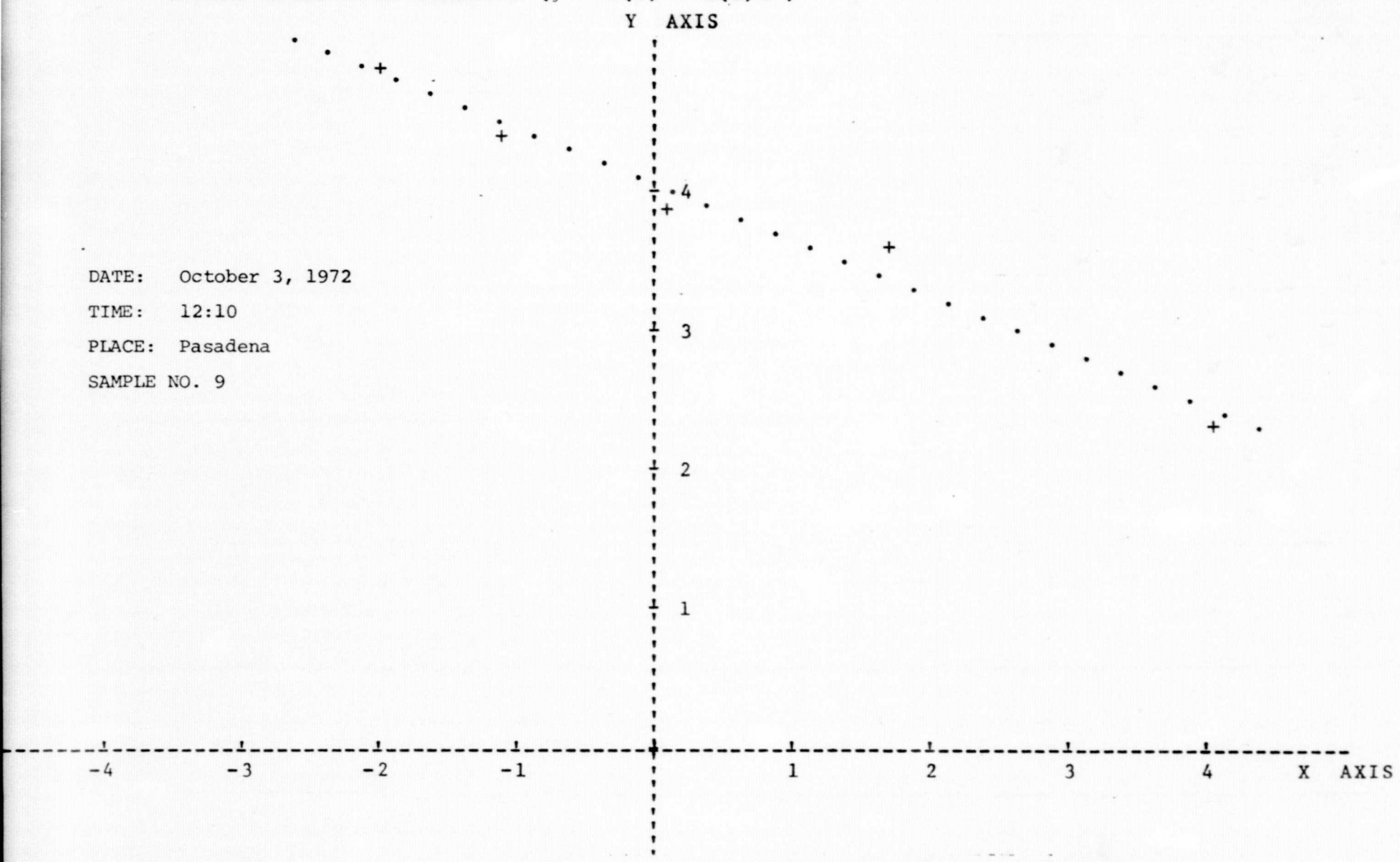

FIGURE . Particle Size Distribution

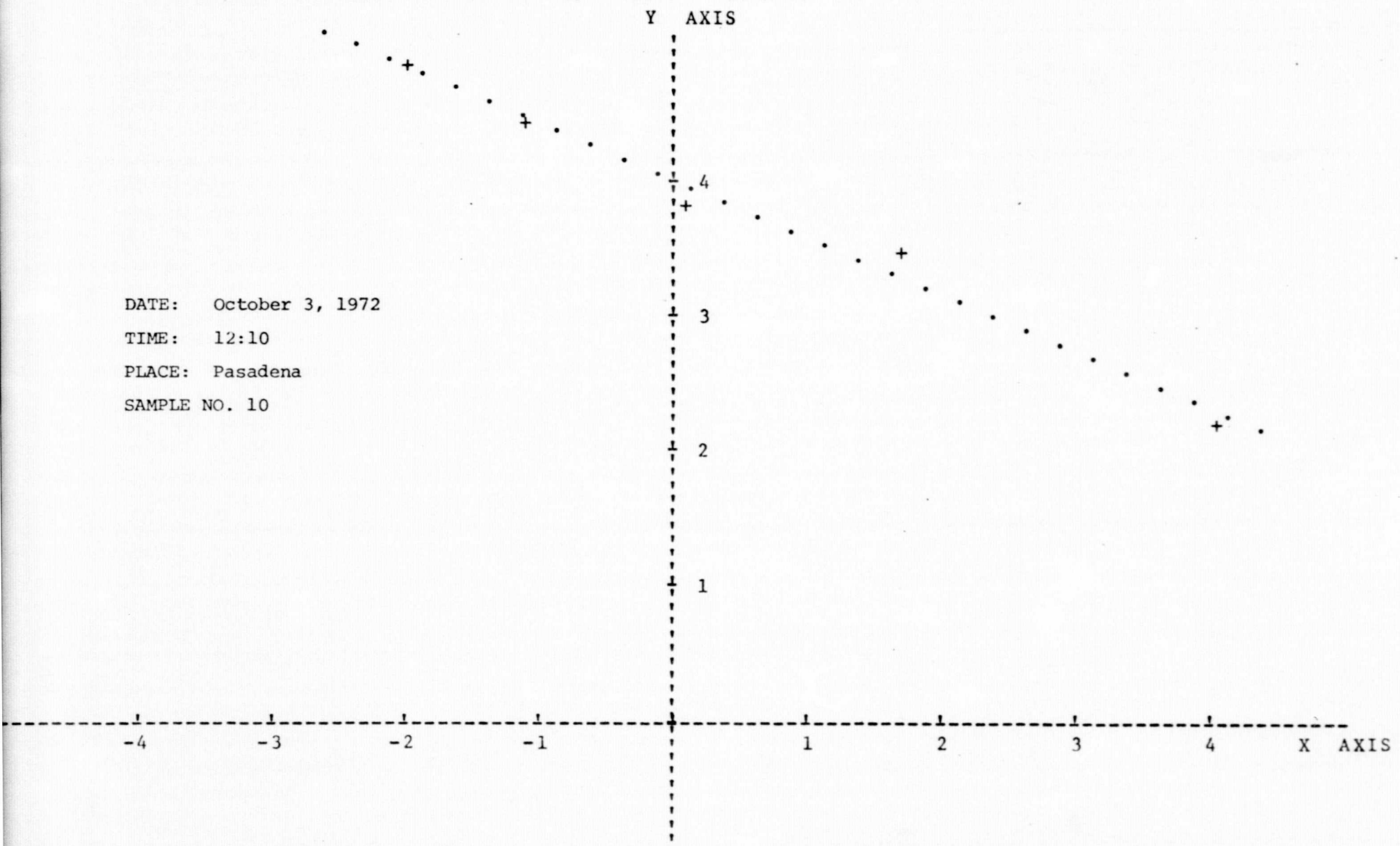

FIGURE . Particle Size Distribution

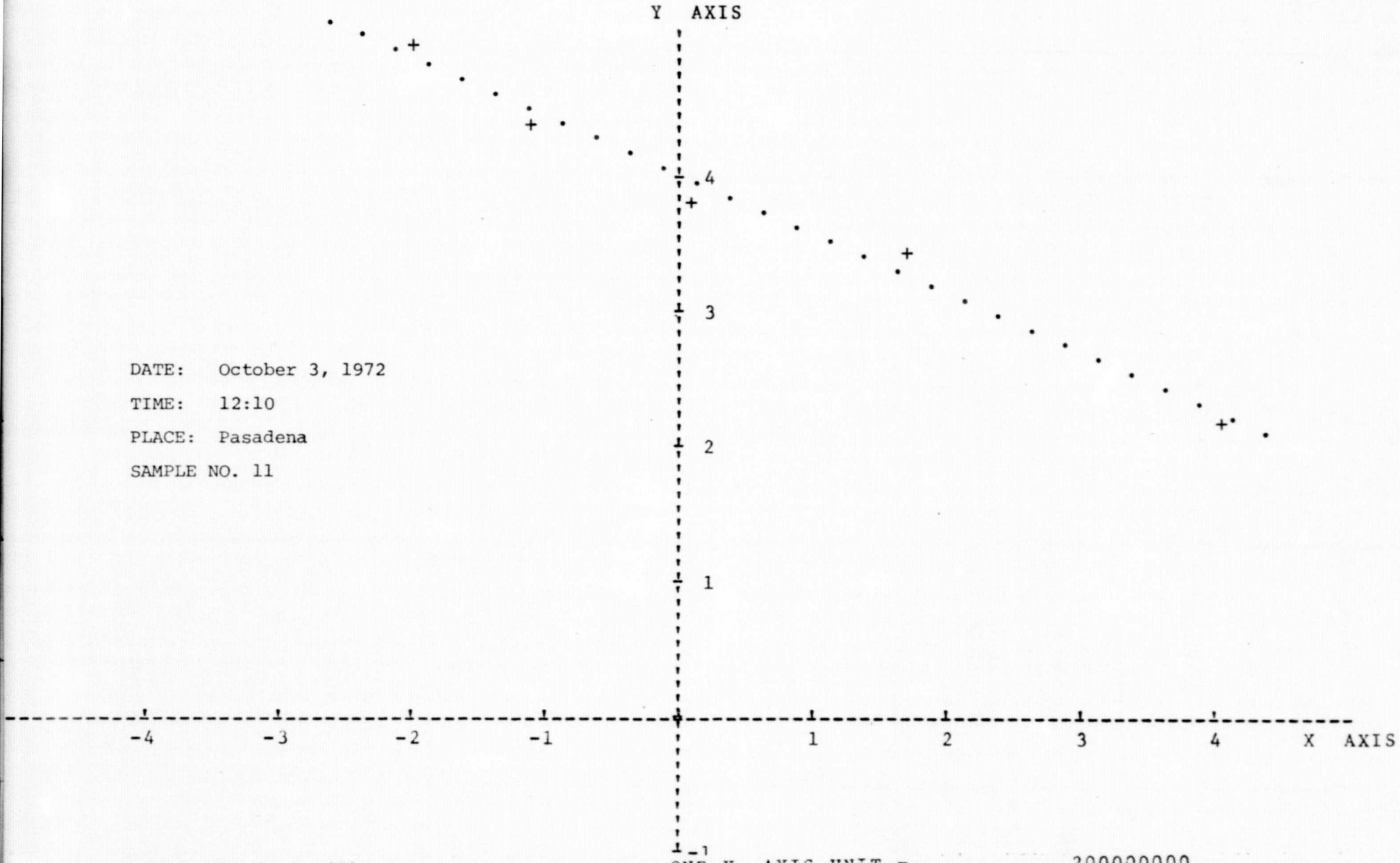

FIGURE . Particle Size Distribution

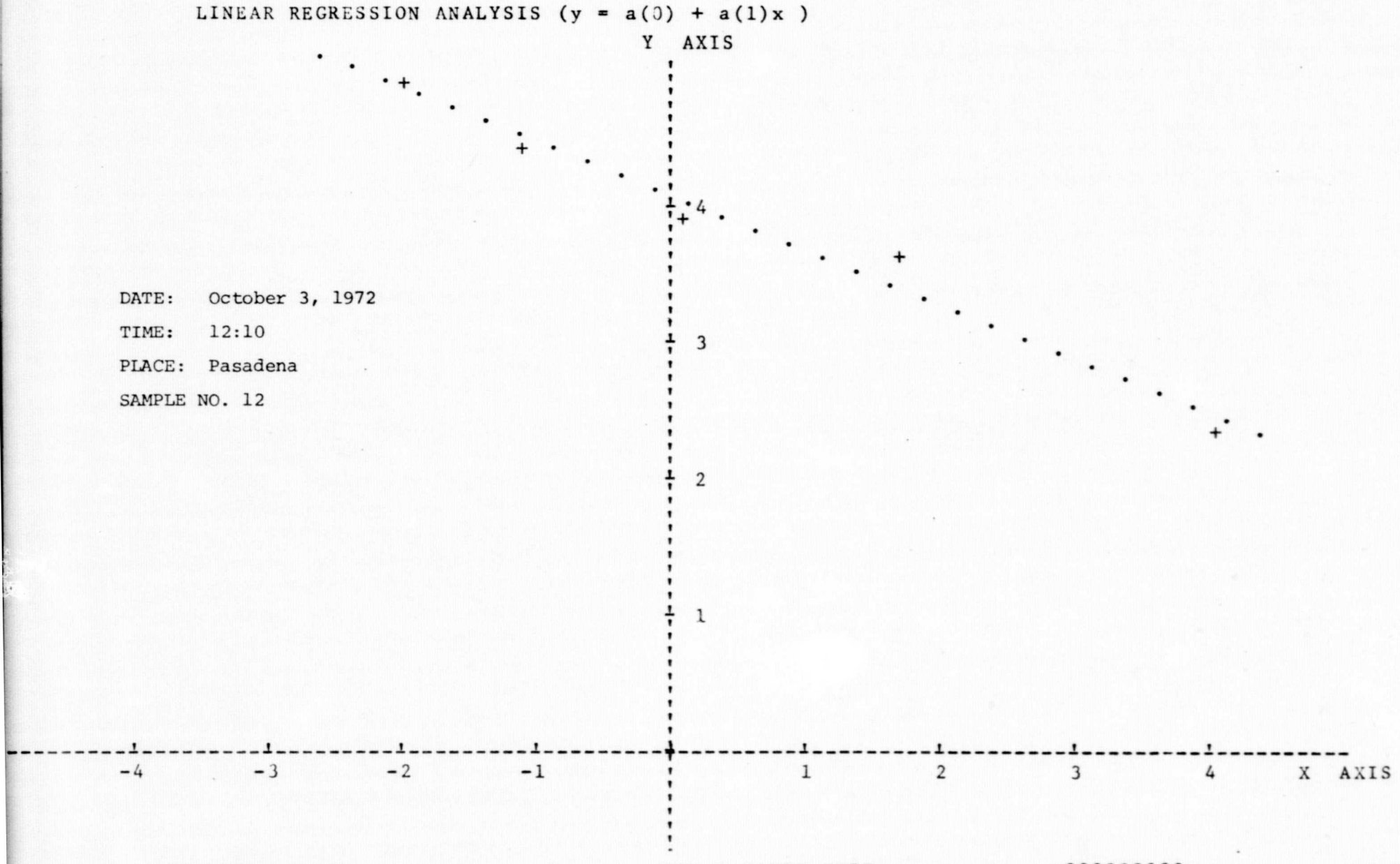

FIGURE . Particle Size Distribution

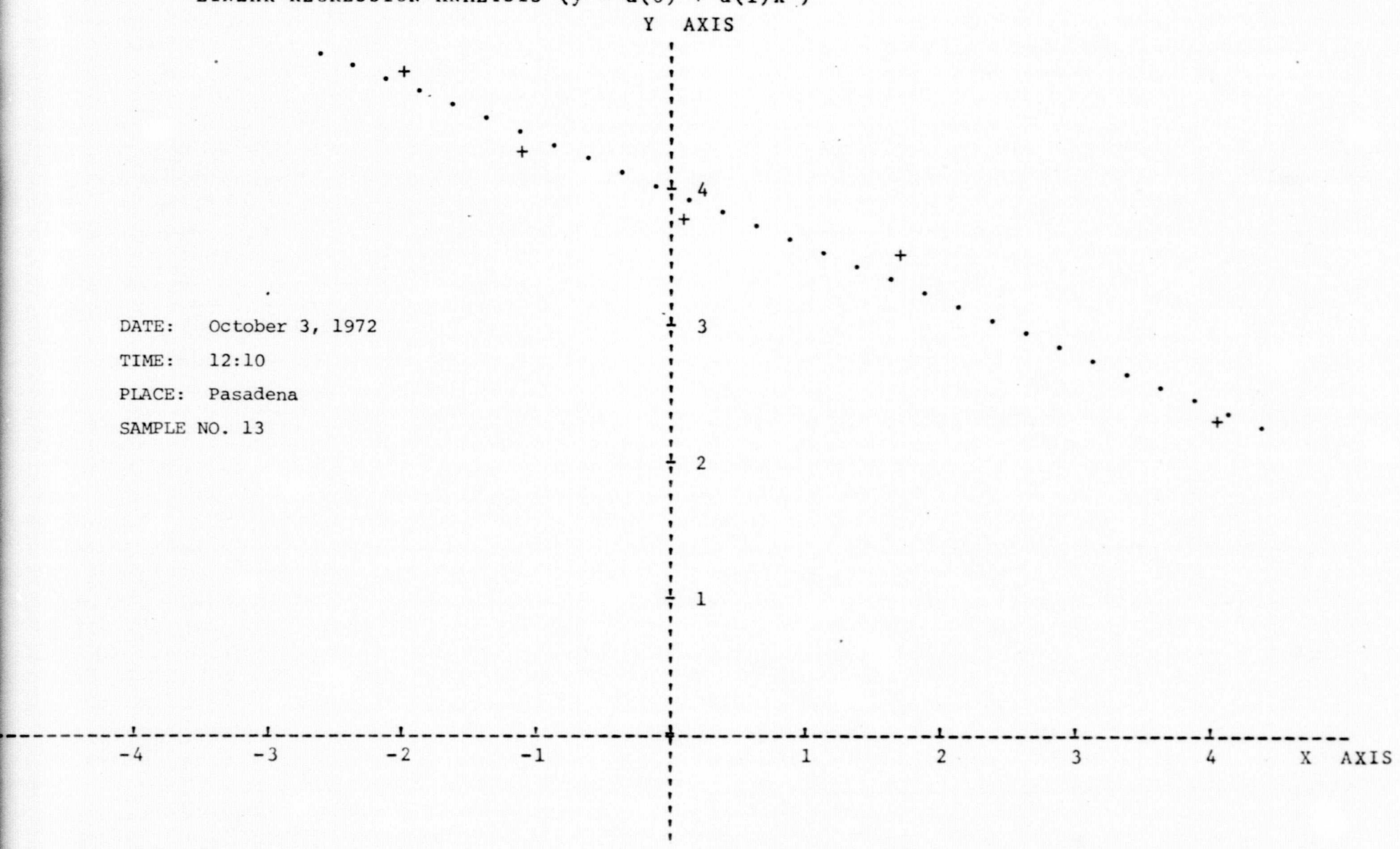

APPENDIX D: MISSION 216-175

1. Microdensitometry traces

2. Linear Regression Analyses of Particle Size Distribution

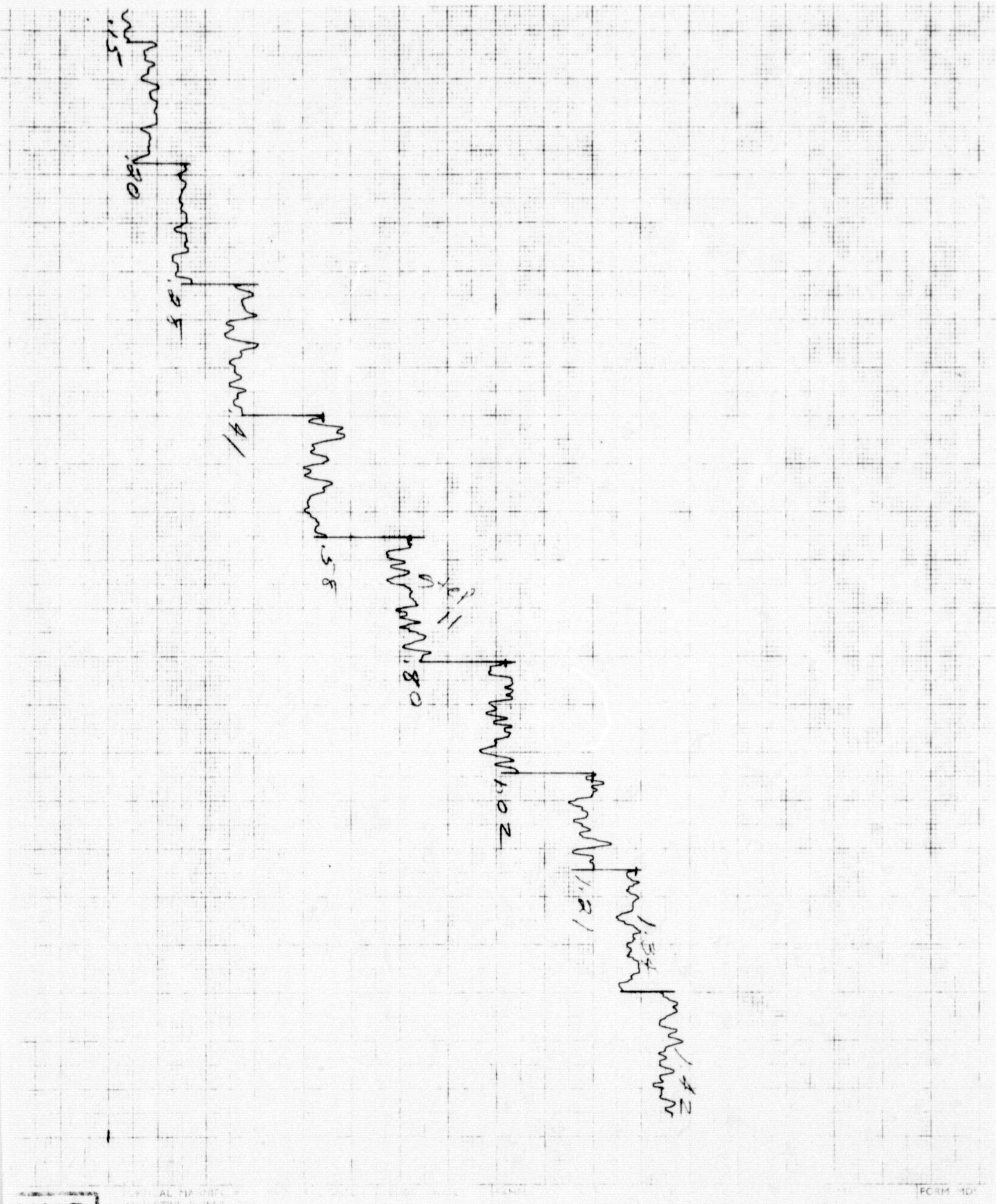

JOYCE LOEBL

RECORDING MICRODENSITOMETER

OPTICAL MAGNIFICATION

OBJECTIVE POWER

SLIT (ACTUAL)

REMARKS

For Frames 1,2 & 3
Roll 04

FORM MD

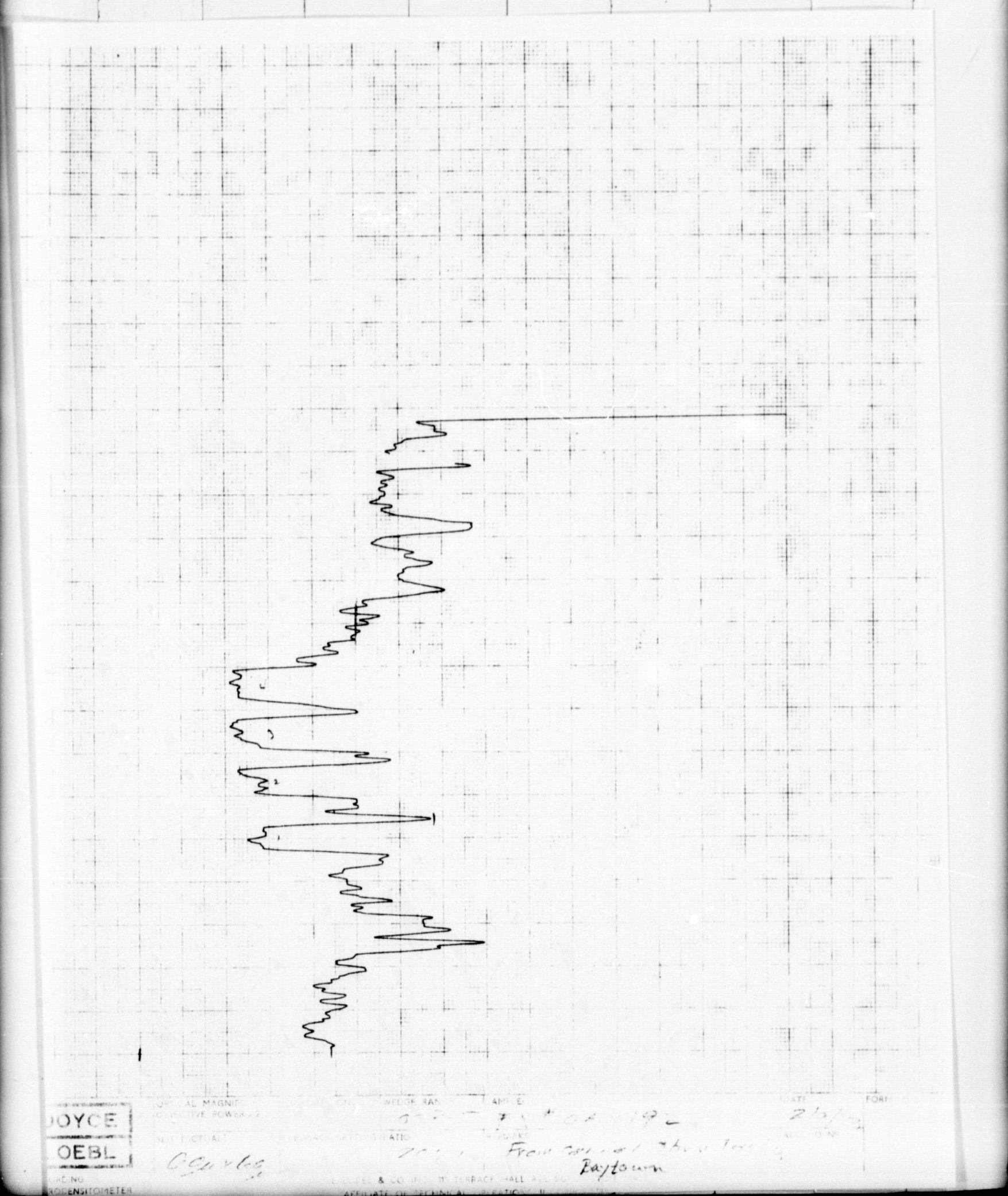

JOYCE
OEBL

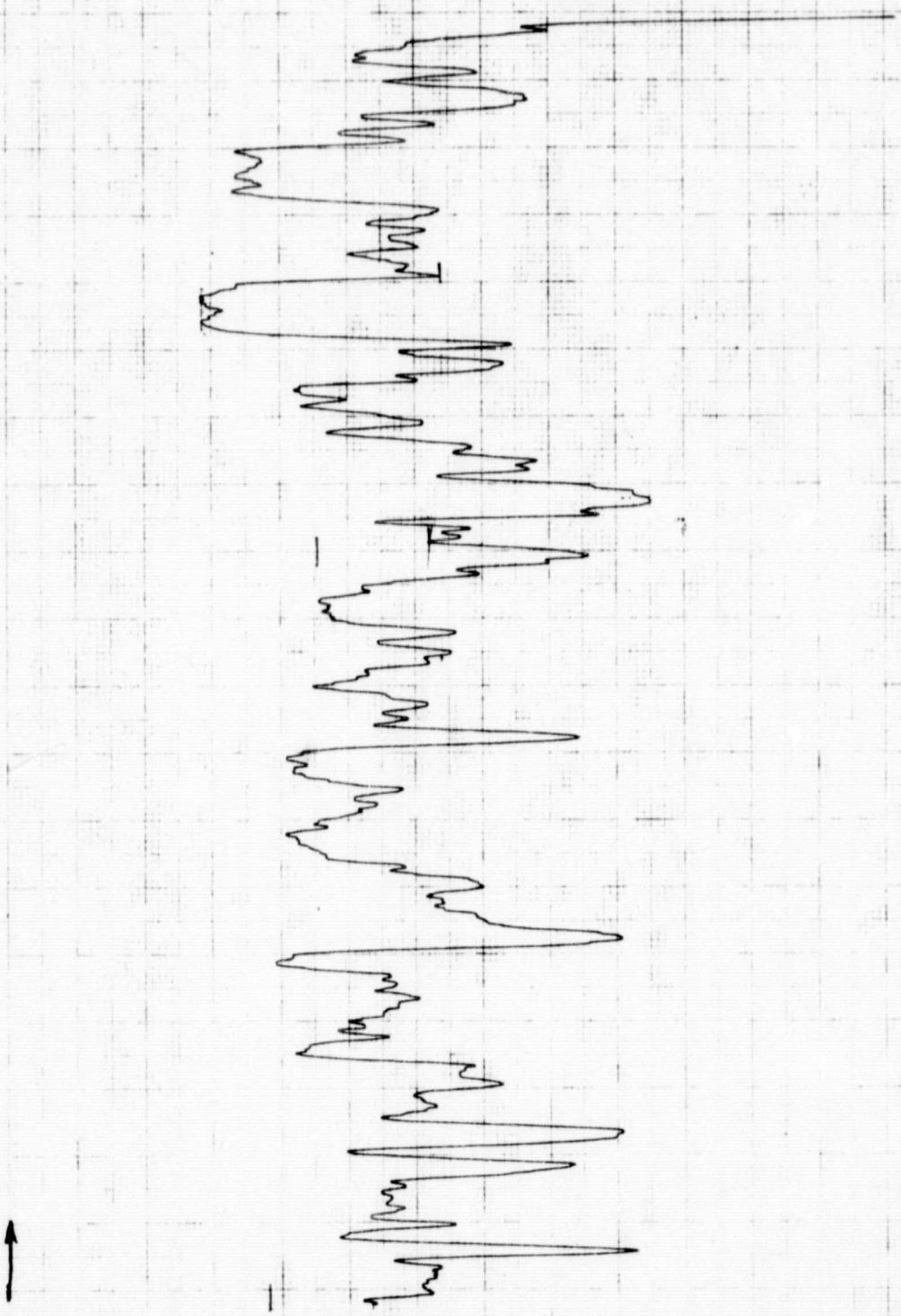

JOYCE
LOEBL
DING
DENSITOMETER

JOYCE

LOEBL

EDING

DENSITOMETER

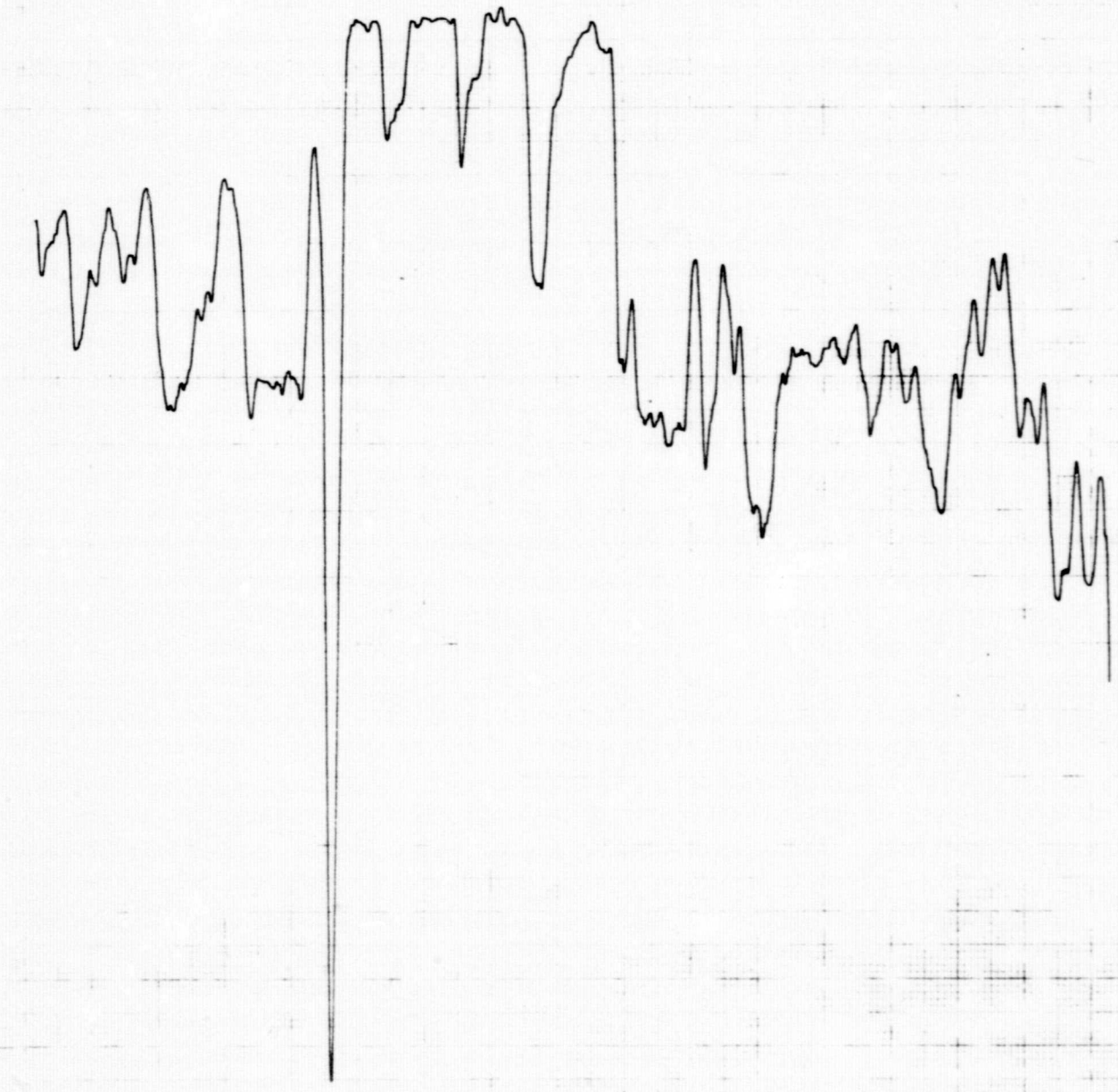

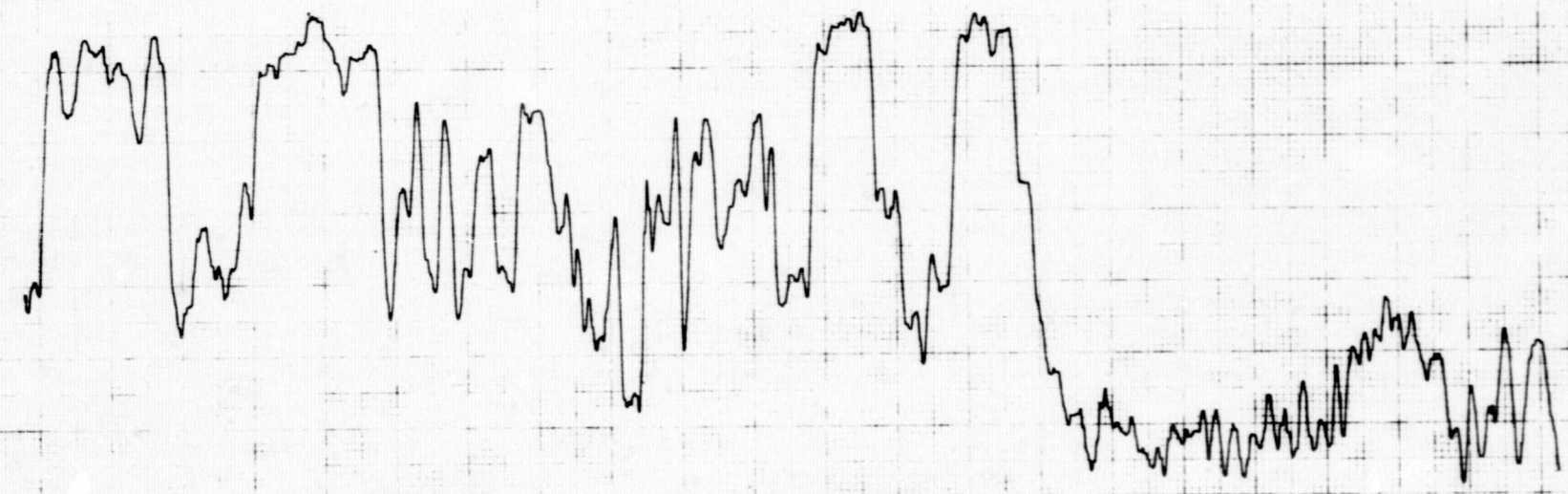

MacBeth Densitometer Measurements for density measurements on Rolls 21 and 22

Roll 21		Roll 22	
Steps	Density	Steps	Density
1- 4	1.90	1- 4	1.69
5	1.87	5	1.65
6	1.85	6	1.60
7	1.77	7	1.51
8	1.65	8	1.39
9	1.46	9	1.23
10	1.24	10	.99
11	1.00	11	.75
12	.83	12	.52
13	.67	13	.33
14	.52	14	.20
15	.40	15	.12
16	.31	16	.08
17	.22	17	.06
18	.16	18	.04
19	.12	19	.04
20	.09	20	.03
21	.07	21	.03

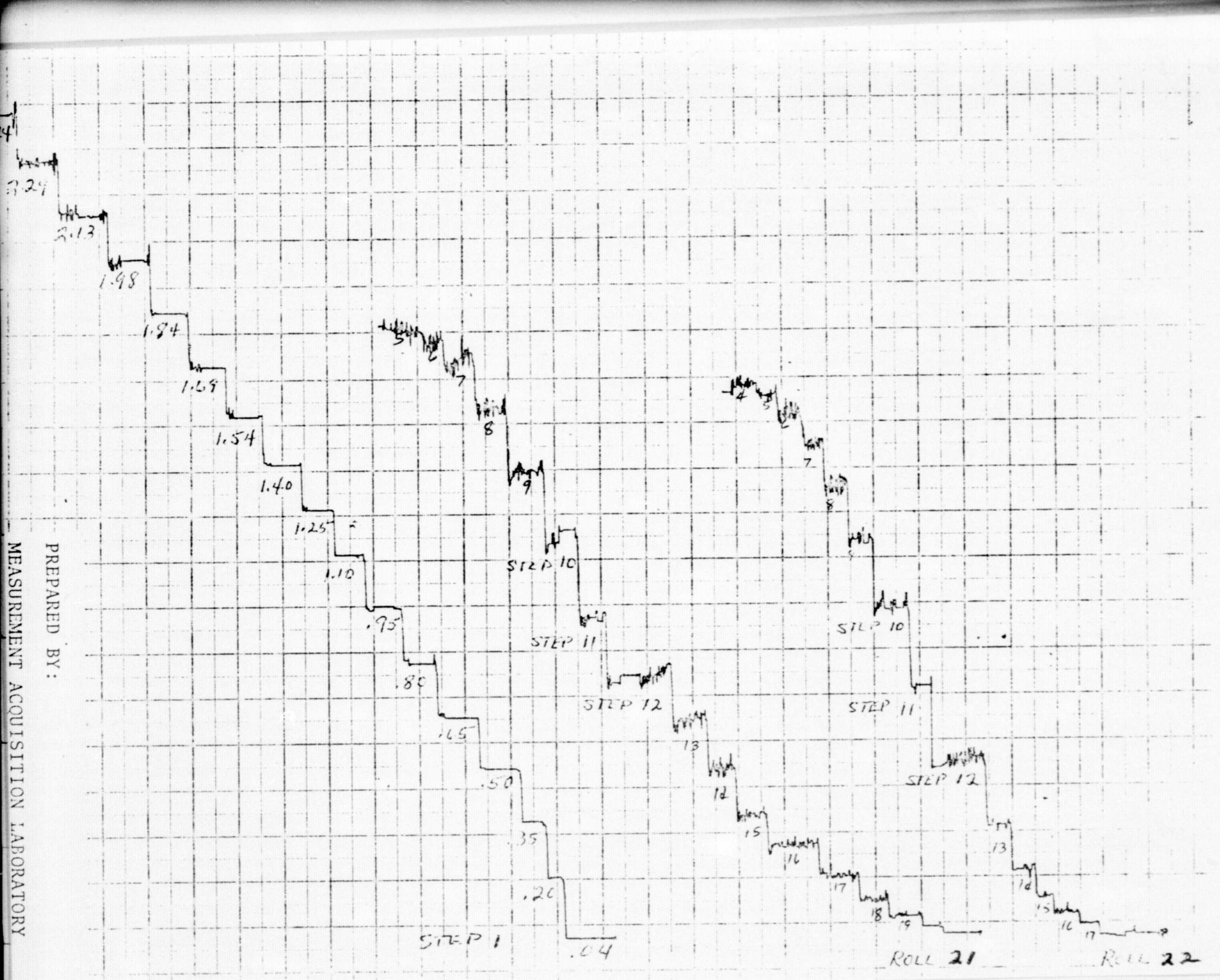

PREPARED BY:

MEASUREMENT ACQUISITION LABORATORY

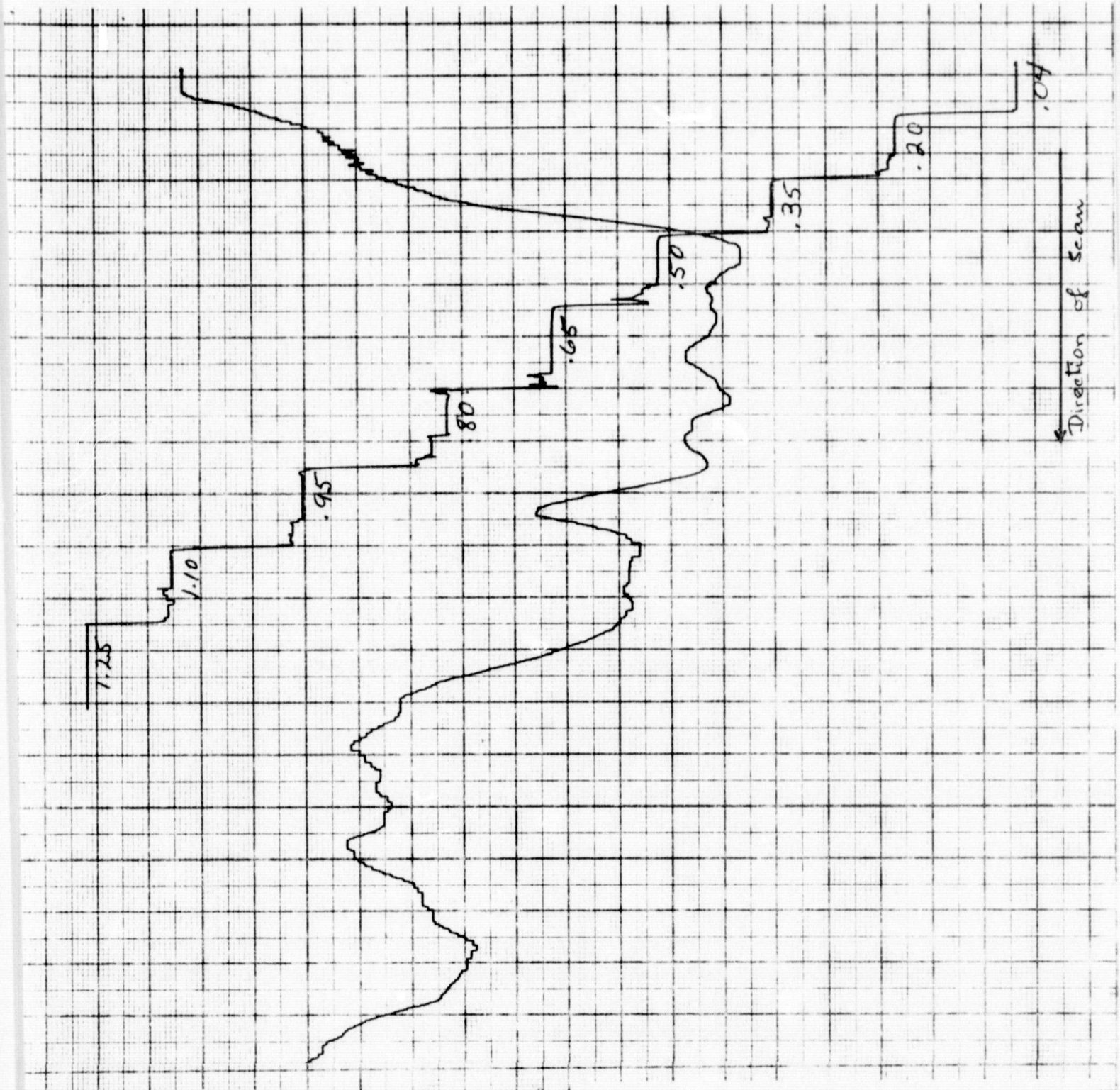

PREPARED BY:

MEASUREMENT ACQUISITION LABORATORY
DATA APPLICATIONS & PHYSICS BRANCH, EOD
NASA, LYNDON B. JOHNSON SPACE CENTER
HOUSTON, TEXAS

Effective slit width : 17 microns
" " height : 28 "

WEDGE RANGE
RATIO 200:1
SAMPLE 22-154
REMARKS
DATE 10-1-73
RECORD No. 1-67
FORM MDS

RECORDING MICRODENSITOMETER

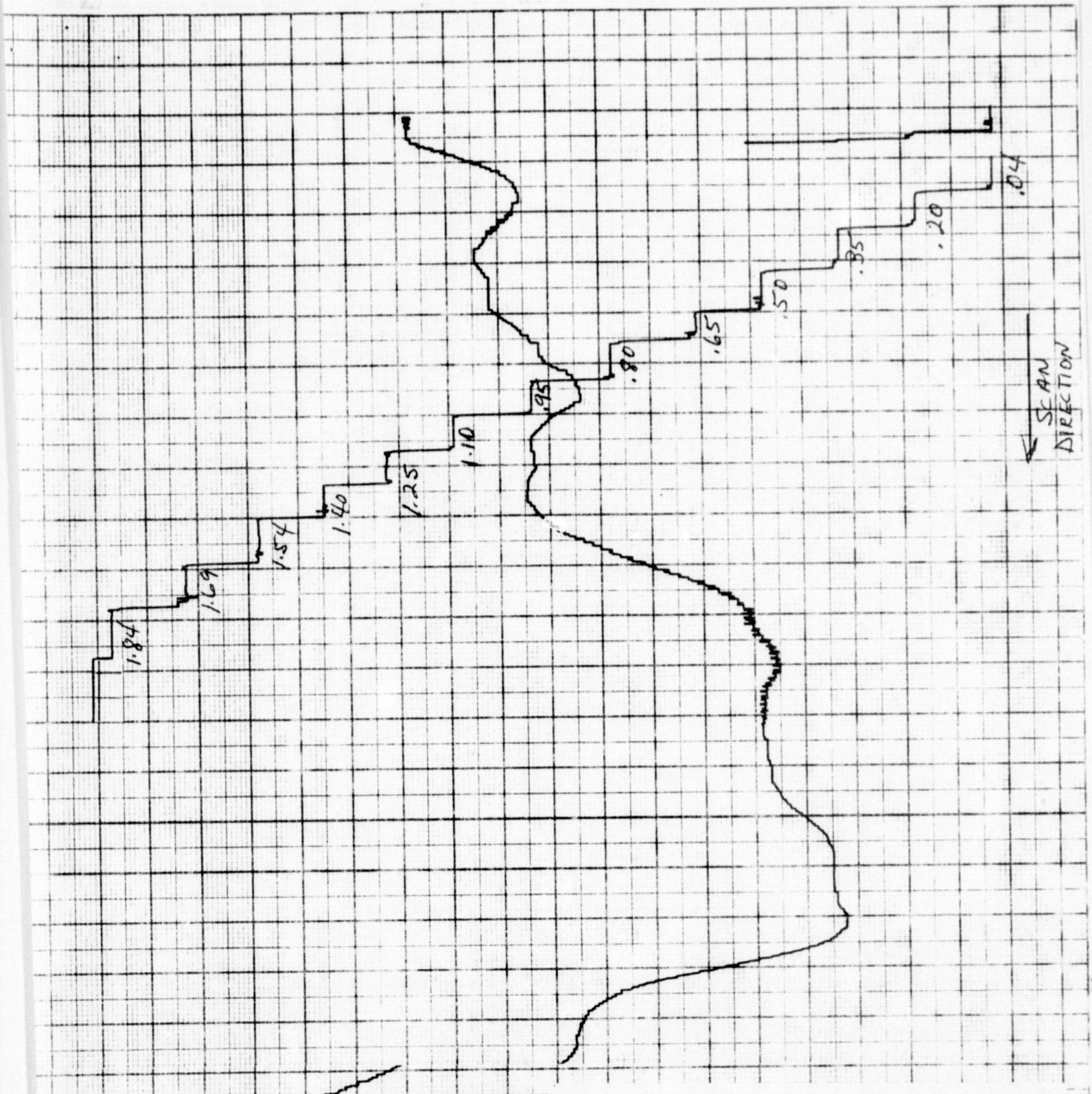

PREPARED BY:

MEASUREMENT ACQUISITION LABORATORY
DATA APPLICATIONS & PHYSICS BRANCH, EOD
NASA, LYNDON B. JOHNSON SPACE CENTER
HOUSTON, TEXAS

Effective slit width : 17 microns
" " height : "

WEDGE RANGE | SAMPLE 22-136 | DATE 10-2
RATIO 200:1 | REMARKS | RECORD No. 1-67

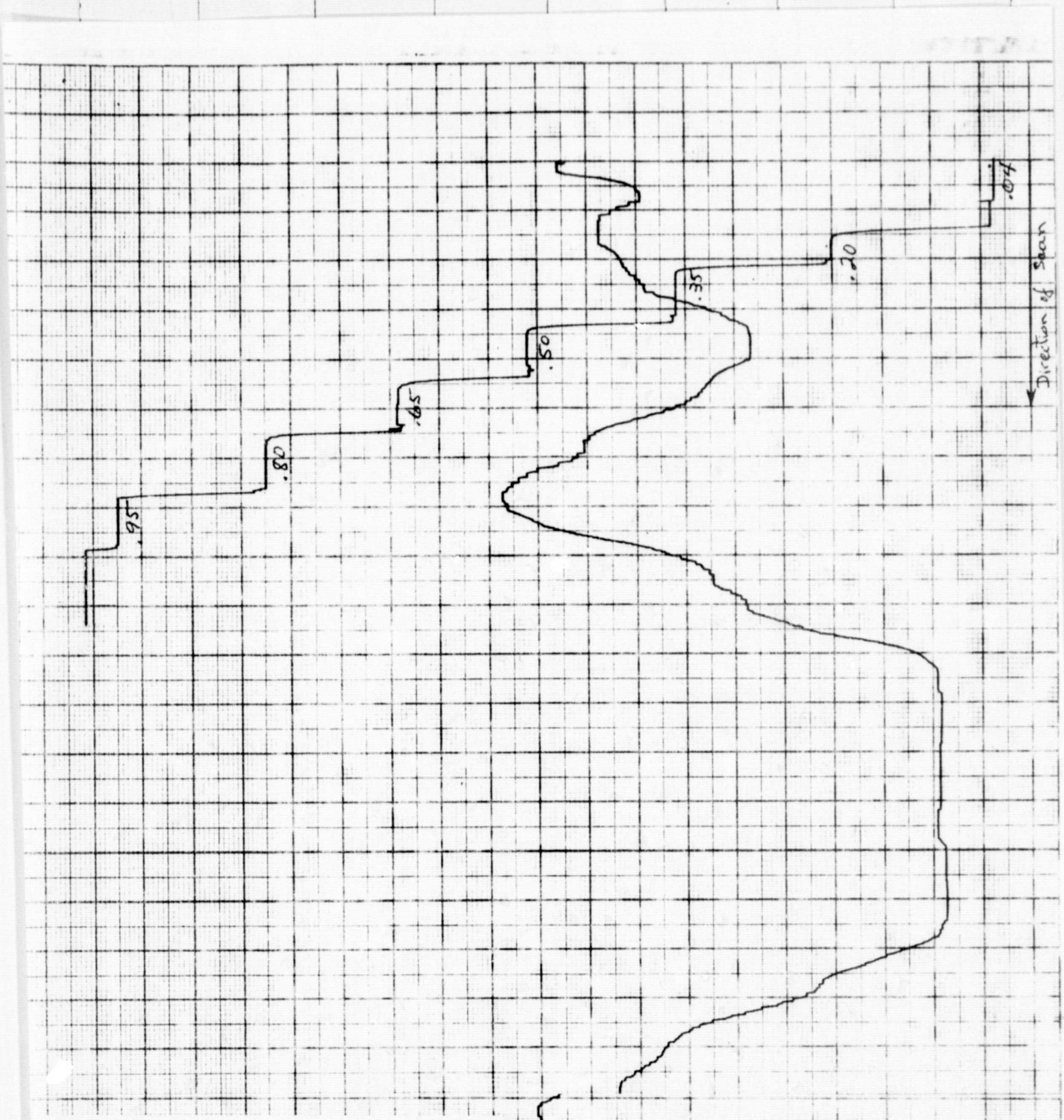

REPARED BY:

EASUREMENT ACQUISITION LABORATORY
ATA APPLICATIONS & PHYSICS BRANCH, EOD
ASA, LYNDON B. JOHNSON SPACE CENTER
OUSTON, TEXAS

Effective slit width : 17 microns
" " height : 28 "

WEDGE RANGE 21-136 DATE 10-1-73
RATIO 200:1

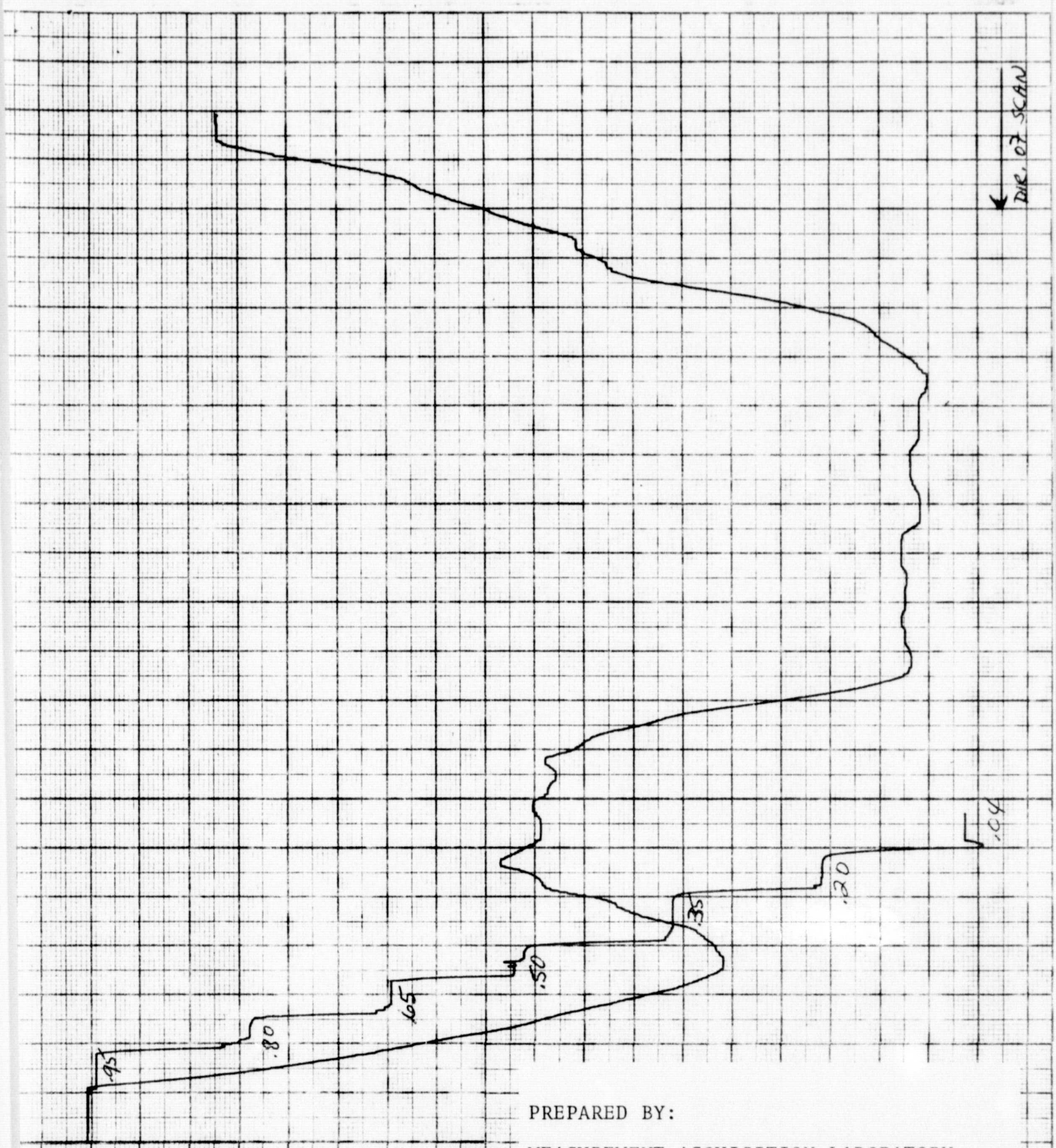

PREPARED BY:

MEASUREMENT ACQUISITION LABORATORY
DATA APPLICATIONS & PHYSICS BRANCH, EOD
NASA, LYNDON B. JOHNSON SPACE CENTER
HOUSTON, TEXAS

Effective slit width : 17 microns
" " height : 28 "

WEDGE RANGE
SAMPLE 21-154
DATE 10-2-73
RATIO 200:1
REMARKS
RECORD No 167
FORM A-105

FIGURE . Particle Size Distribution

LINEAR REGRESSION ANALYSIS (y = a(0) + a(1)x)

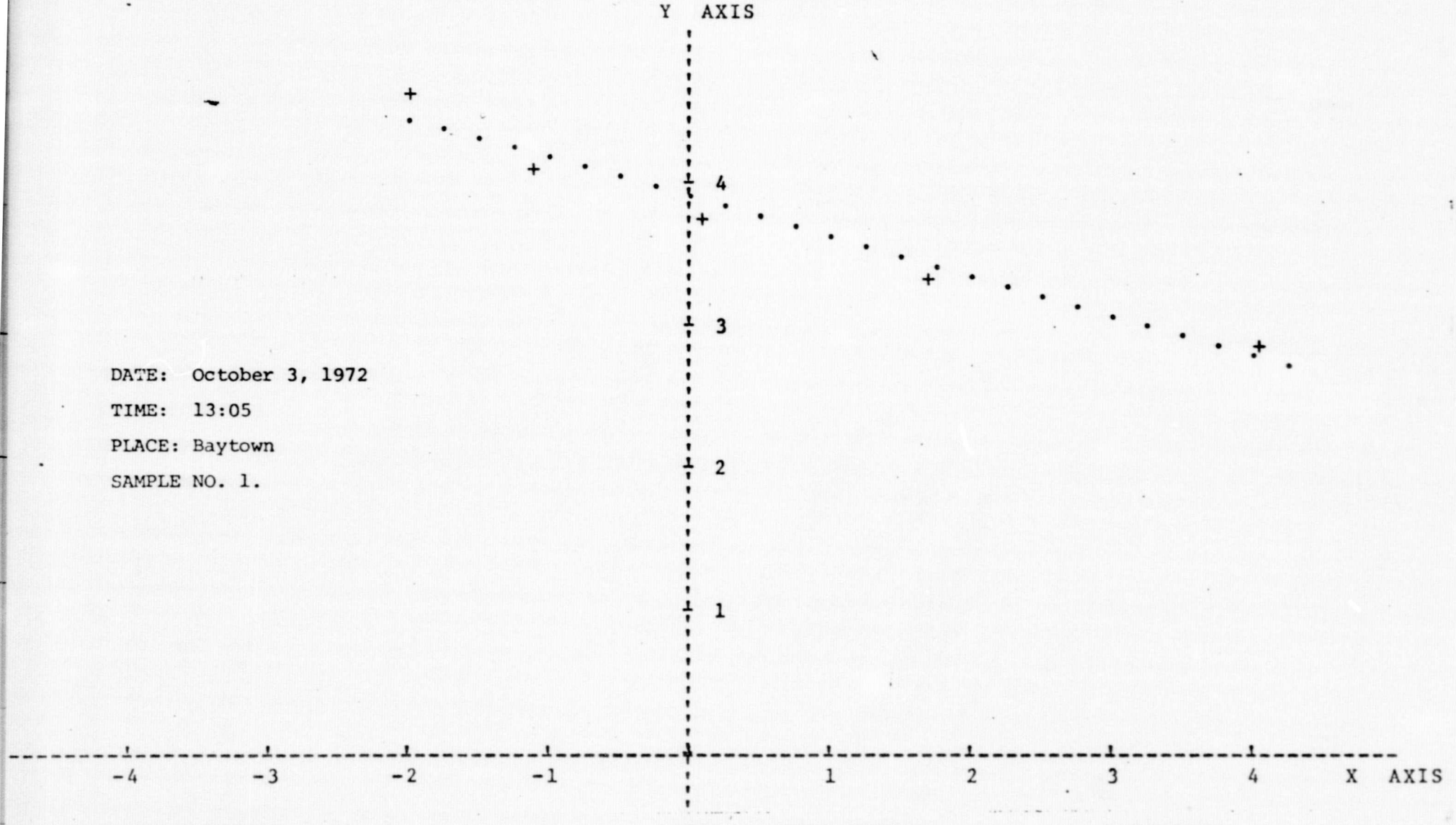

DATE: October 3, 1972

TIME: 13:05

PLACE: Baytown

SAMPLE NO. 1.

3.885797783 = a(0)
-1.388900303 = a(1)
-.979905992 = r
.121540107 = S(x,y)

ONE X AXIS UNIT = .200000000
ONE Y AXIS UNIT = 1.000000000

FIGURE . Particle Size Distribution

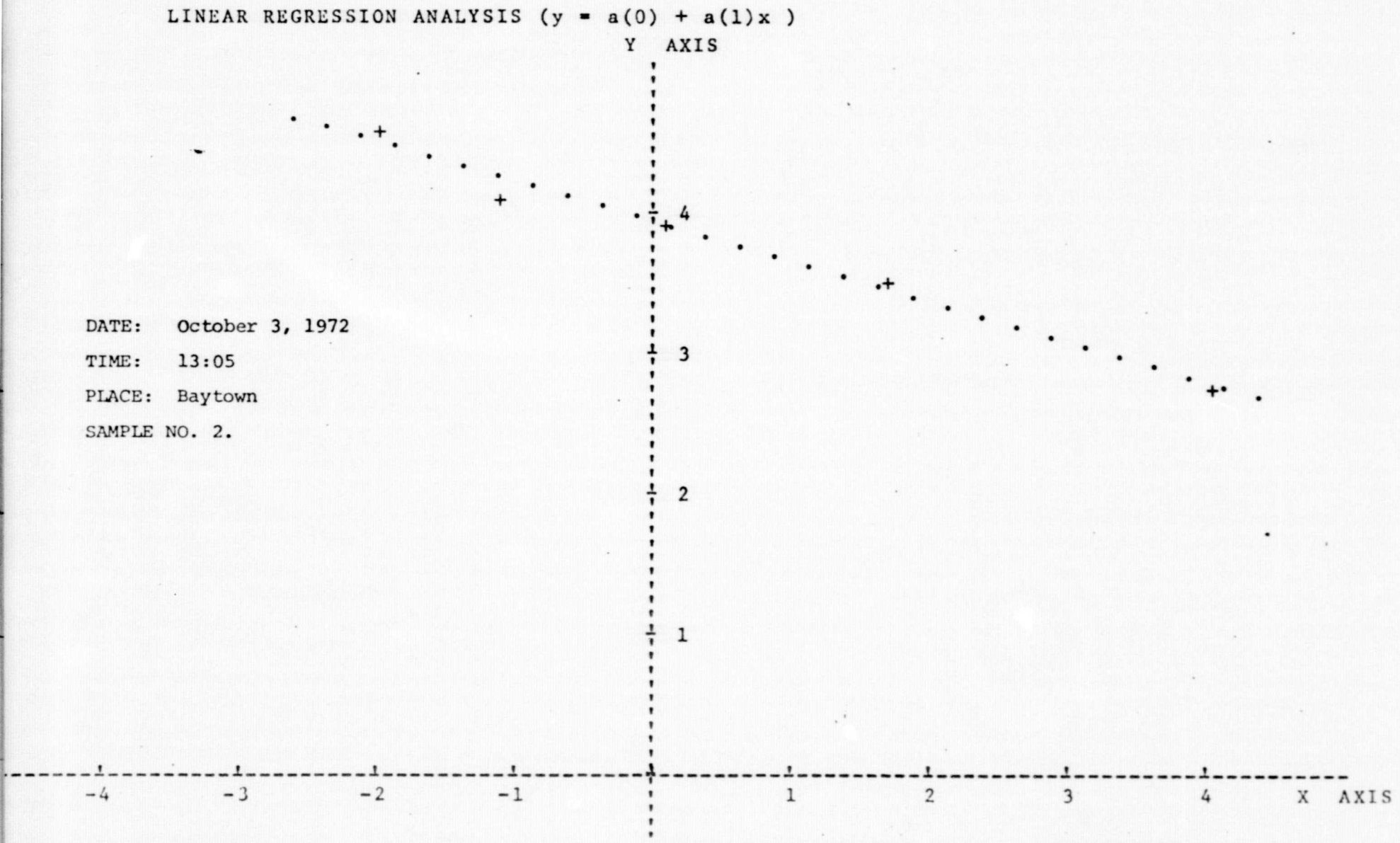

FIGURE . Particle Size Distribution

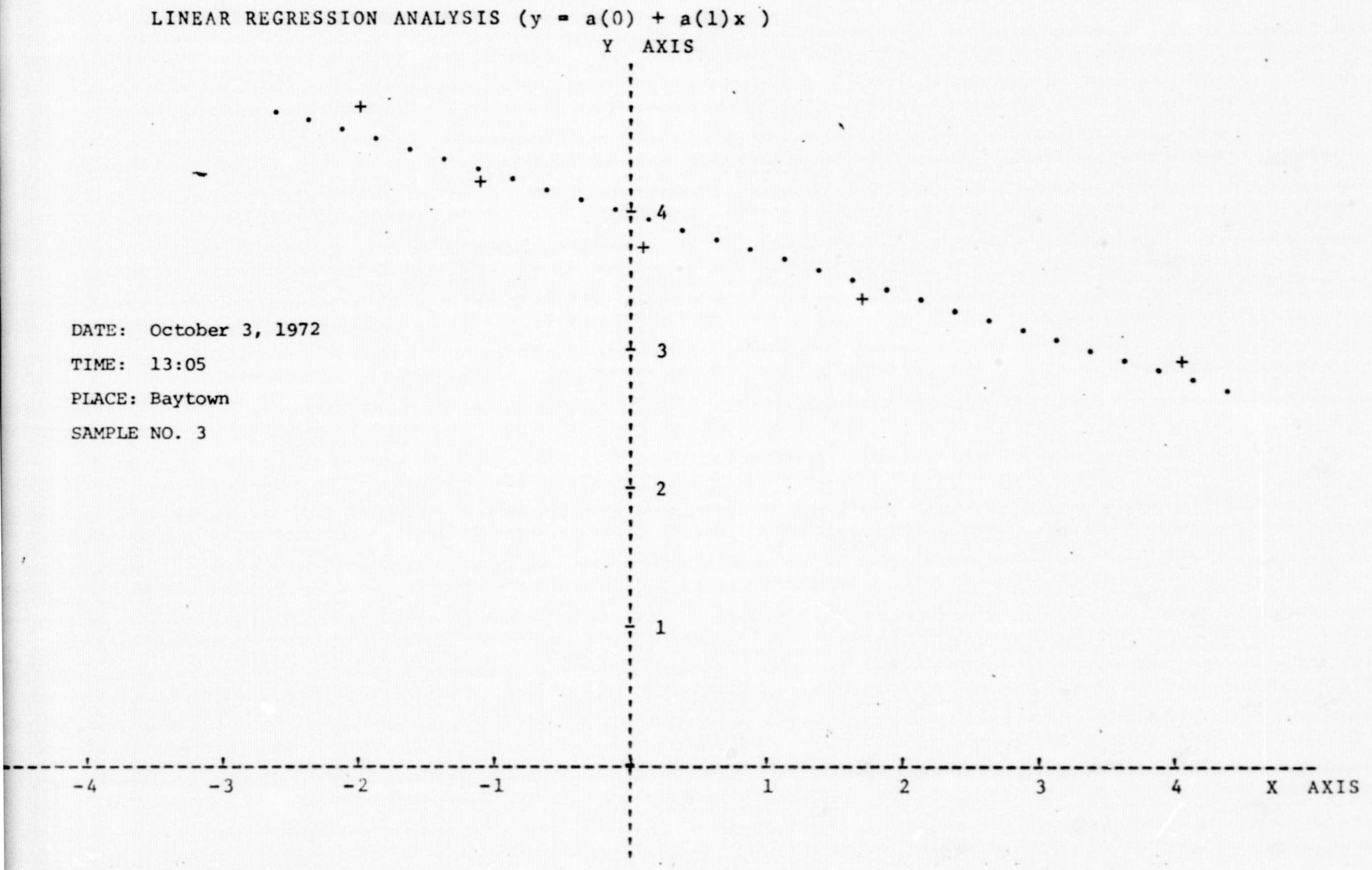

FIGURE . Particle Size Distribution

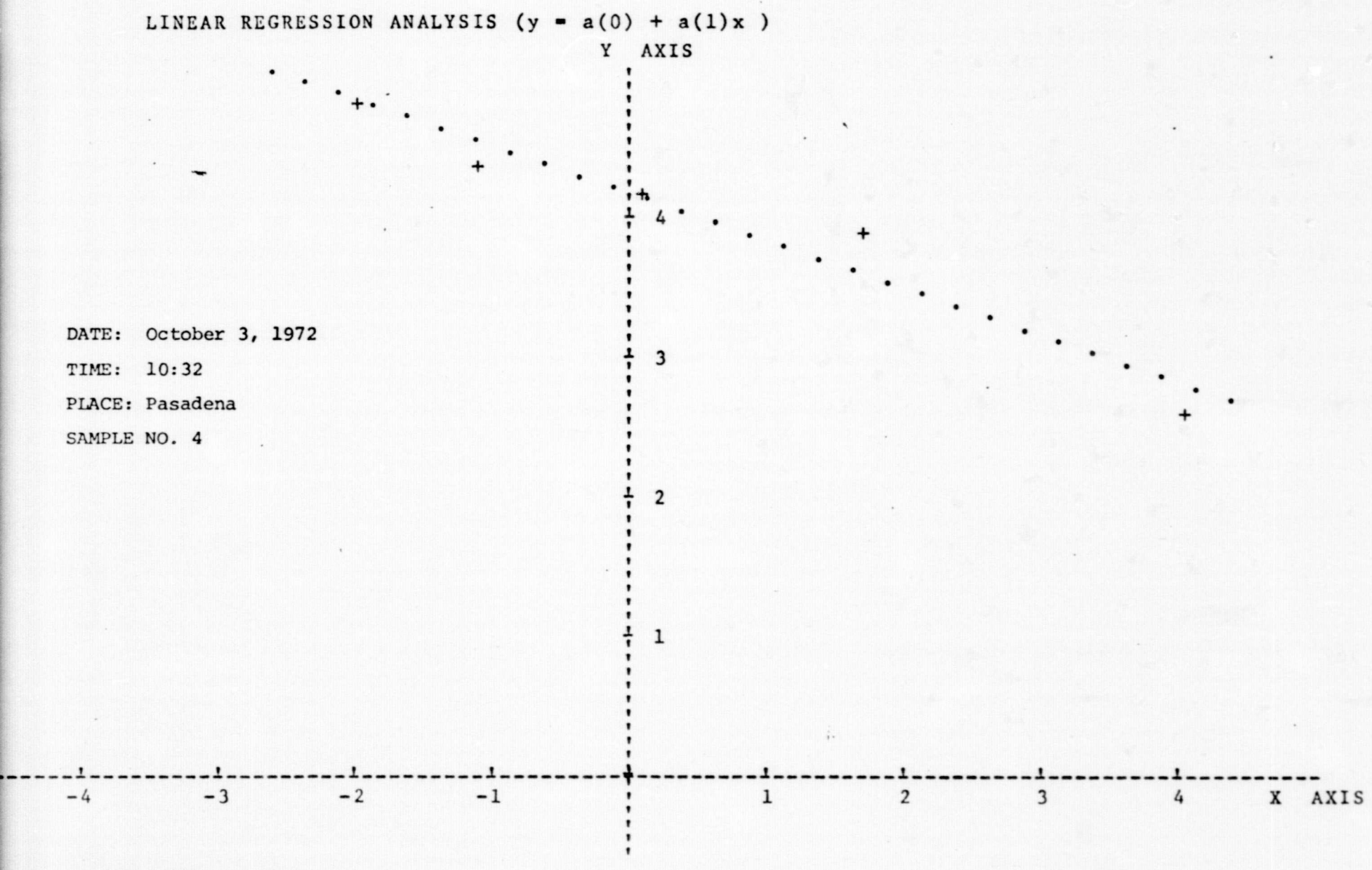

FIGURE . Particle Size Distribution

LINEAR REGRESSION ANALYSIS (y = a(0) + a(1)x)

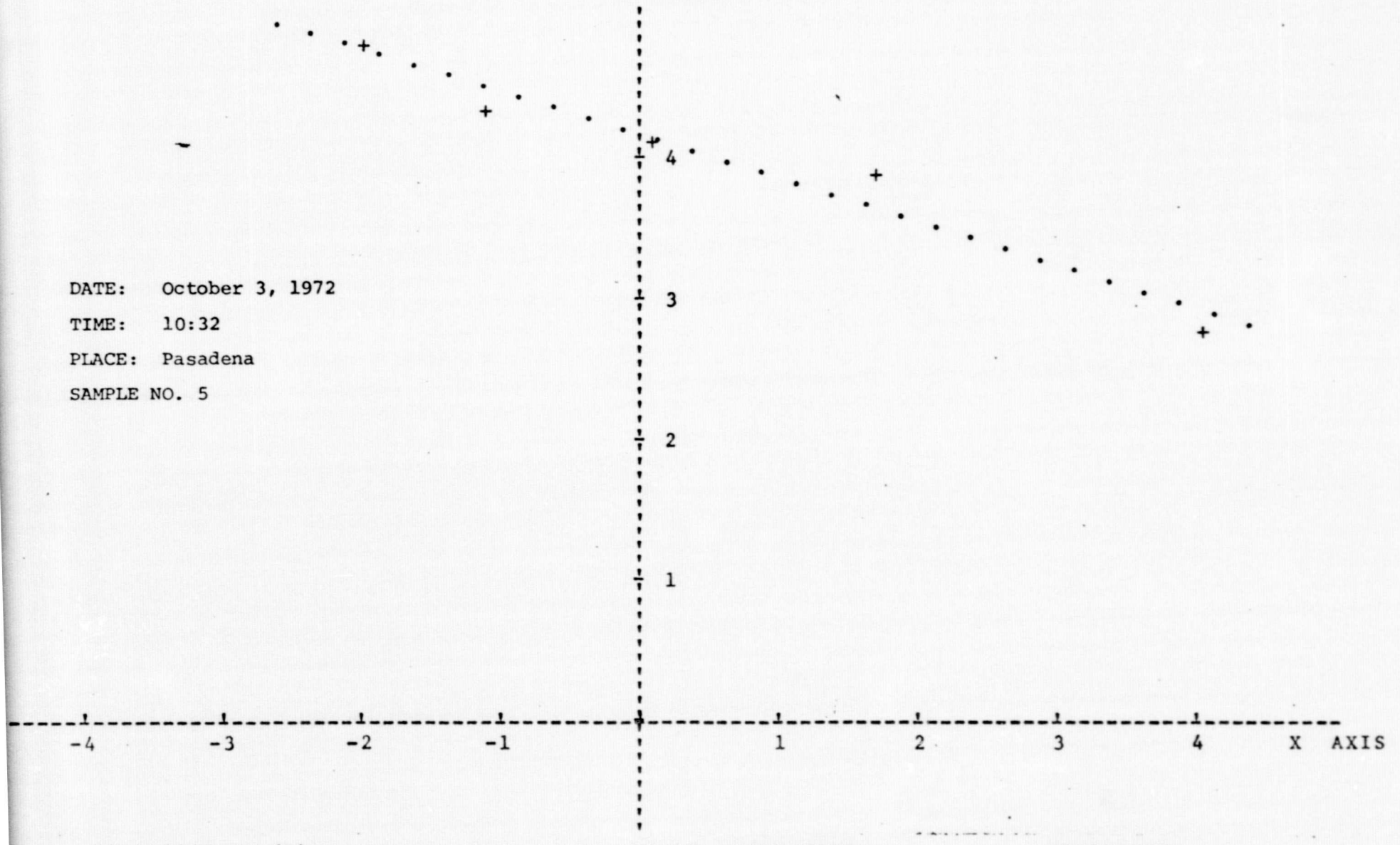

DATE: October 3, 1972

TIME: 10:32

PLACE: Pasadena

SAMPLE NO. 5

4.143516063 = a(0)
-1.534264033 = a(1)
-.975043236 = r
.150188285 = S(x.y)

ONE X AXIS UNIT = .200000000
ONE Y AXIS UNIT = 1.000000000

FIGURE . Particle Size Distribution

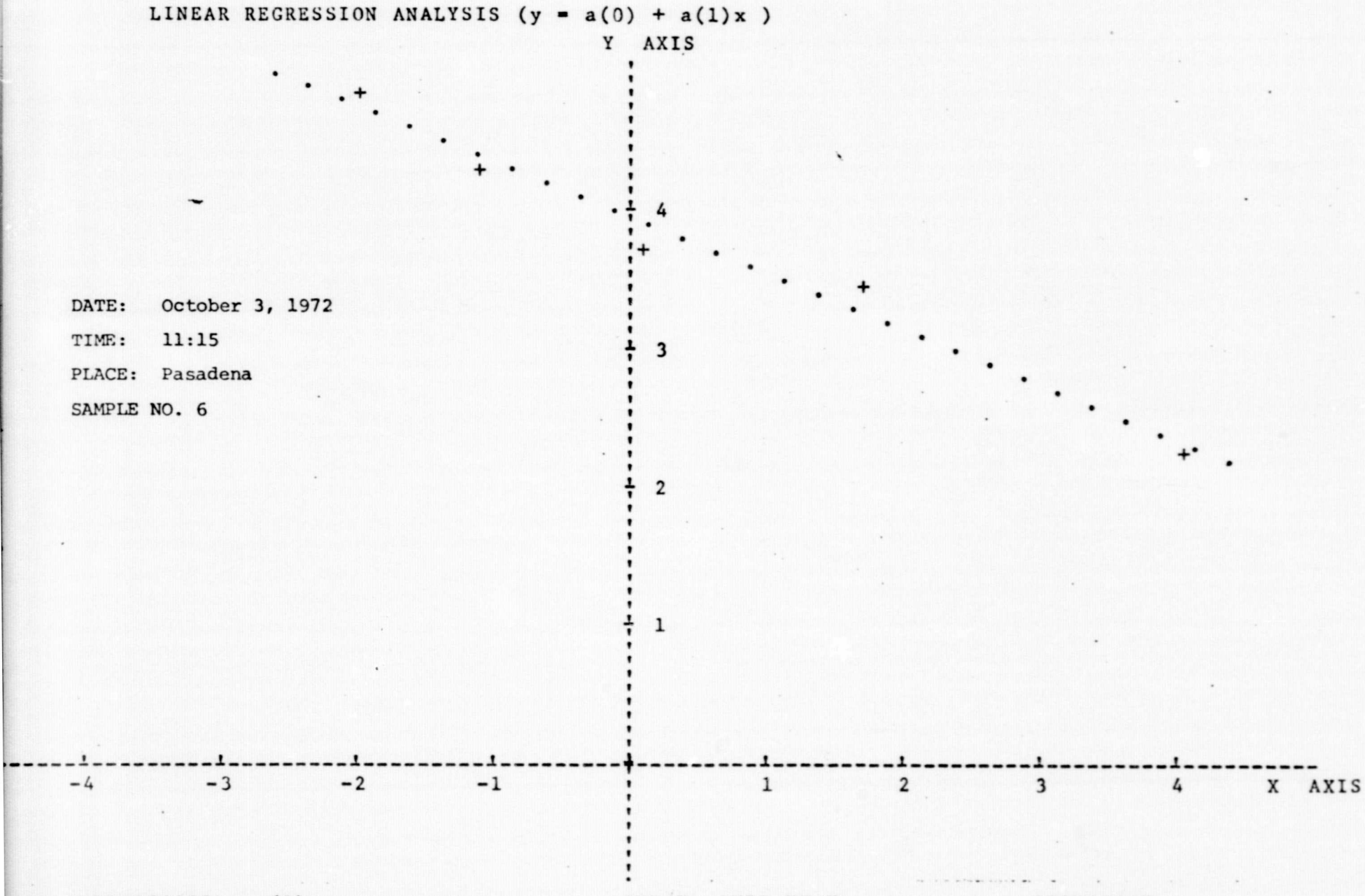

FIGURE . Particle Size Distribution

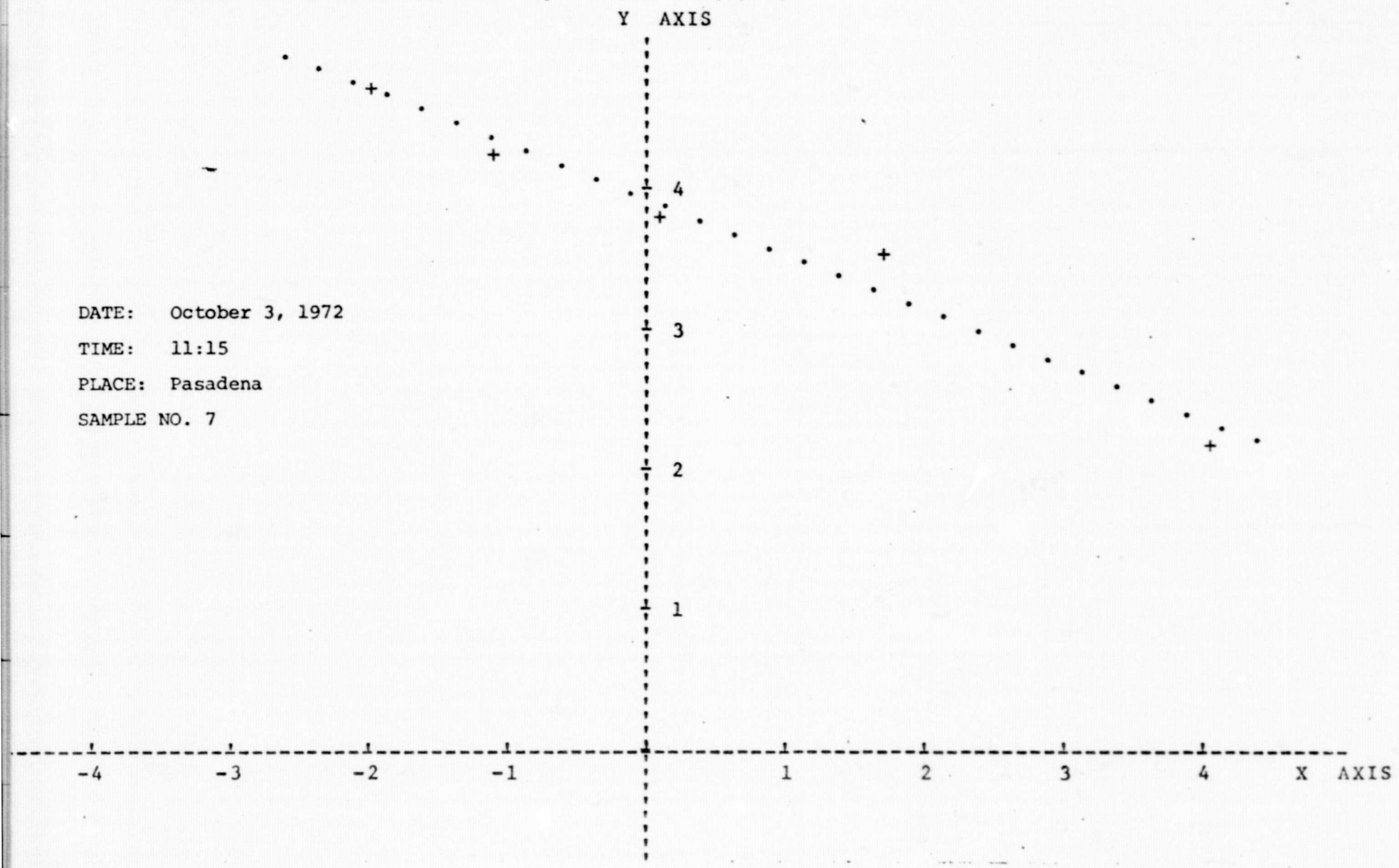

FIGURE . Particle Size Distribution

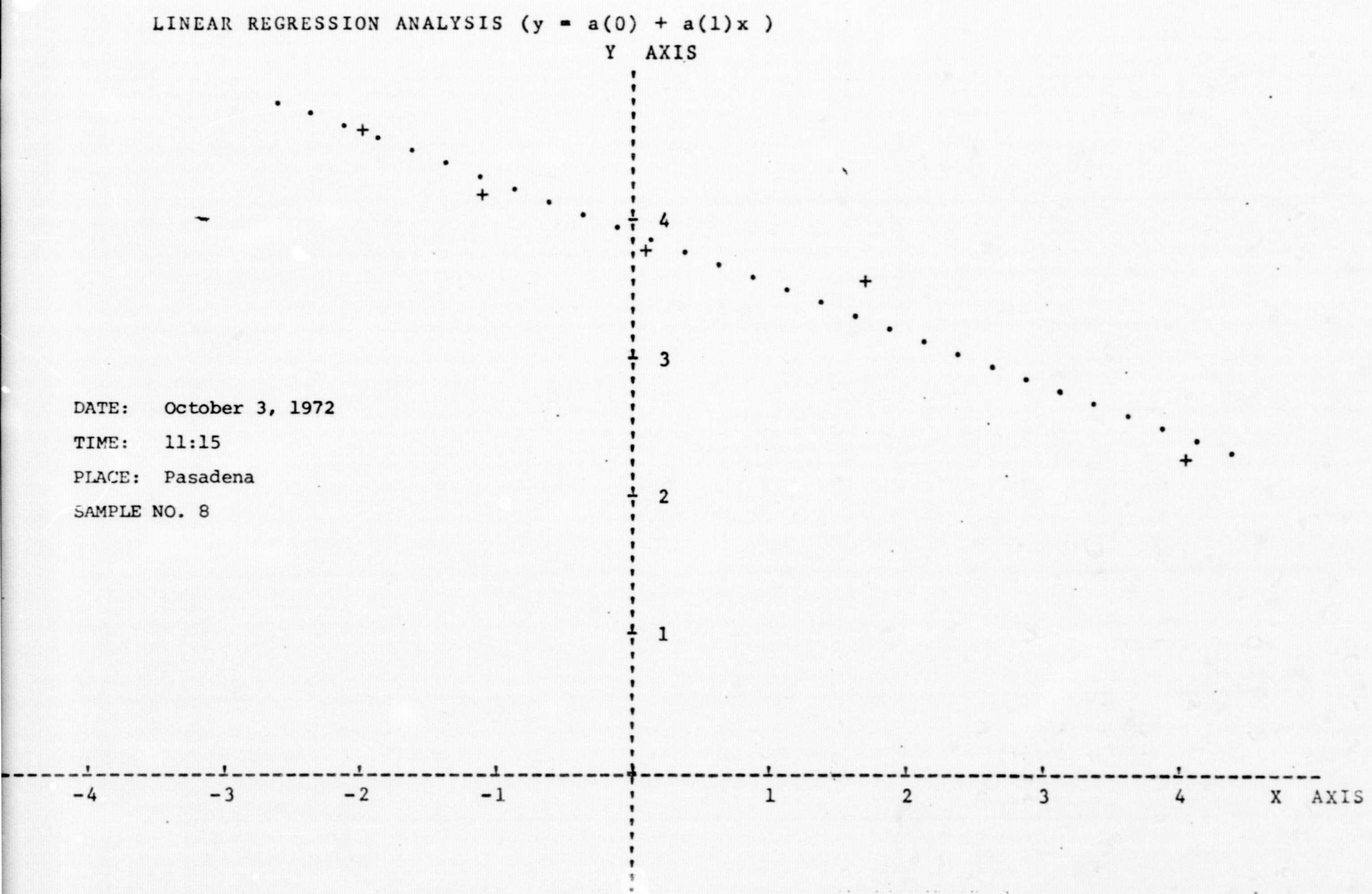

FIGURE . Particle Size Distribution

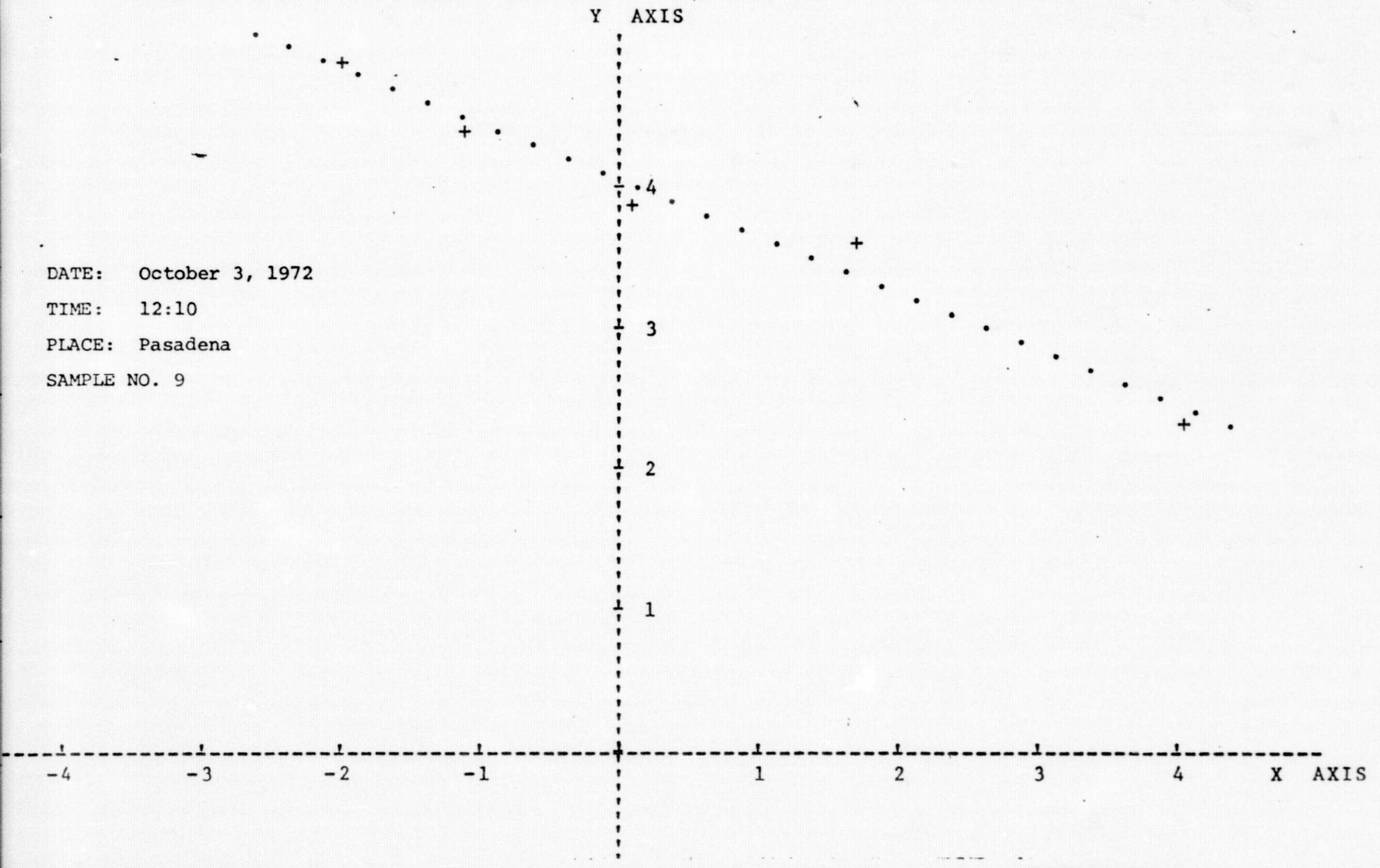

FIGURE . Particle Size Distribution

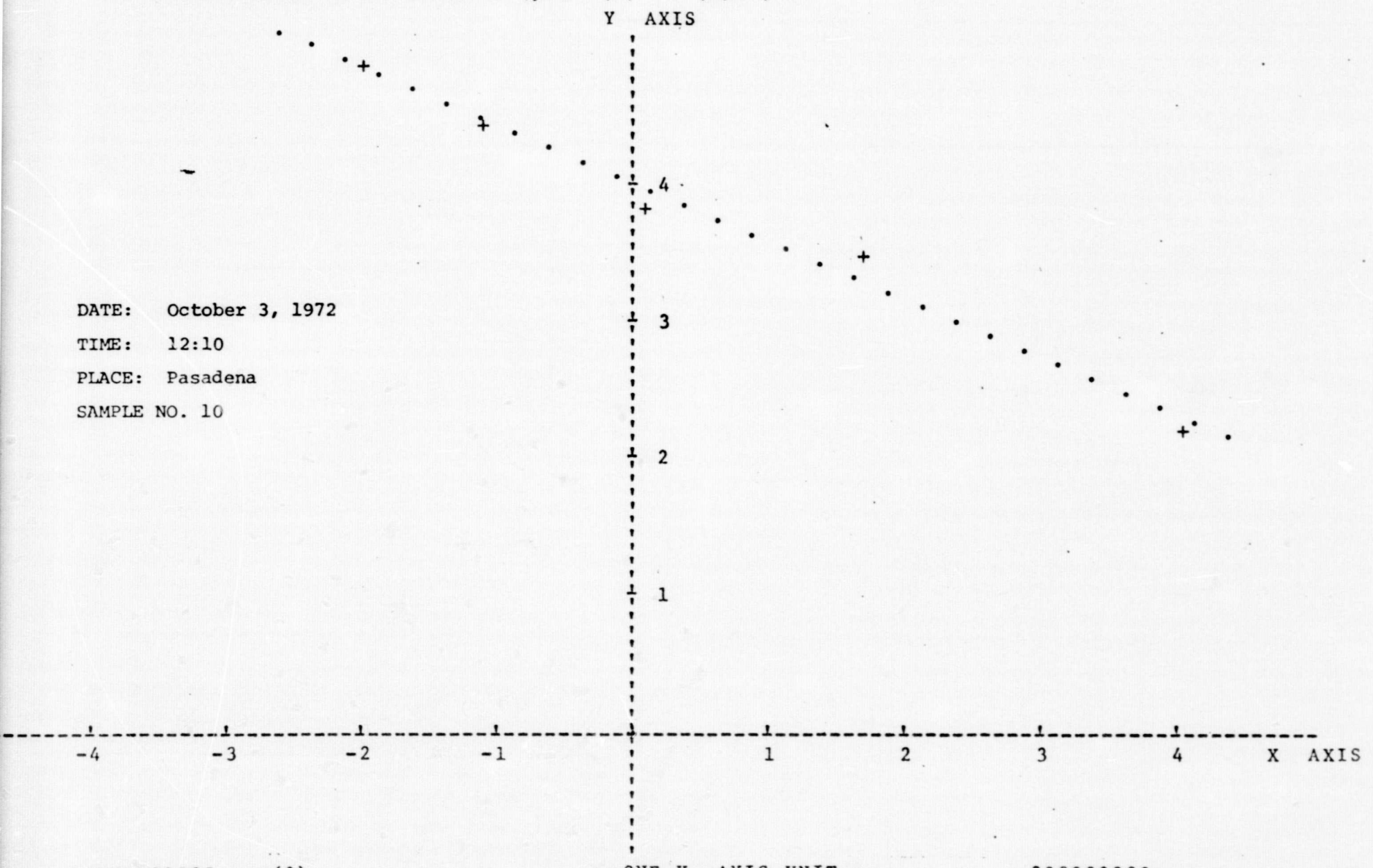

FIGURE . Particle Size Distribution

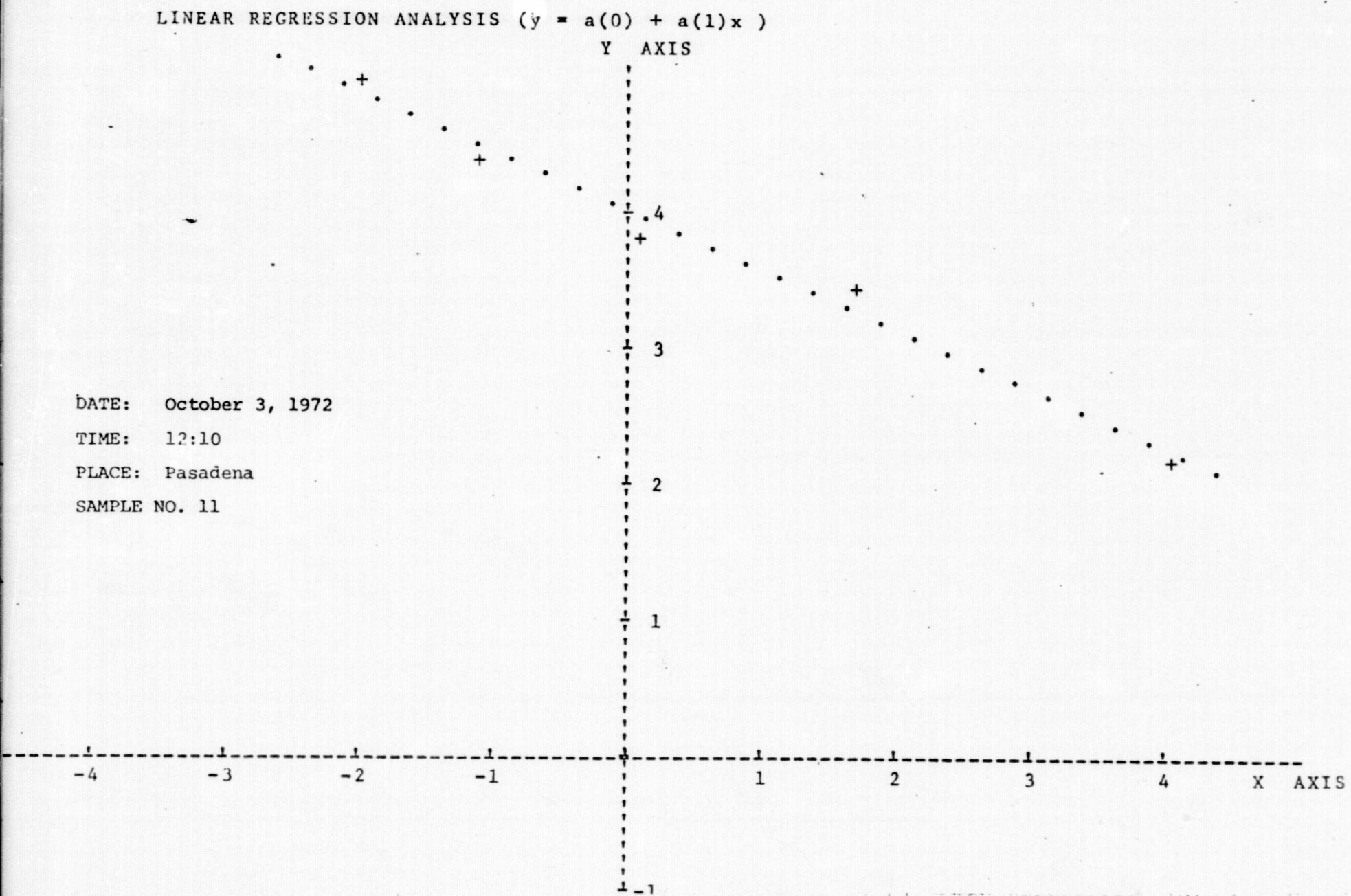

FIGURE . Particle Size Distribution

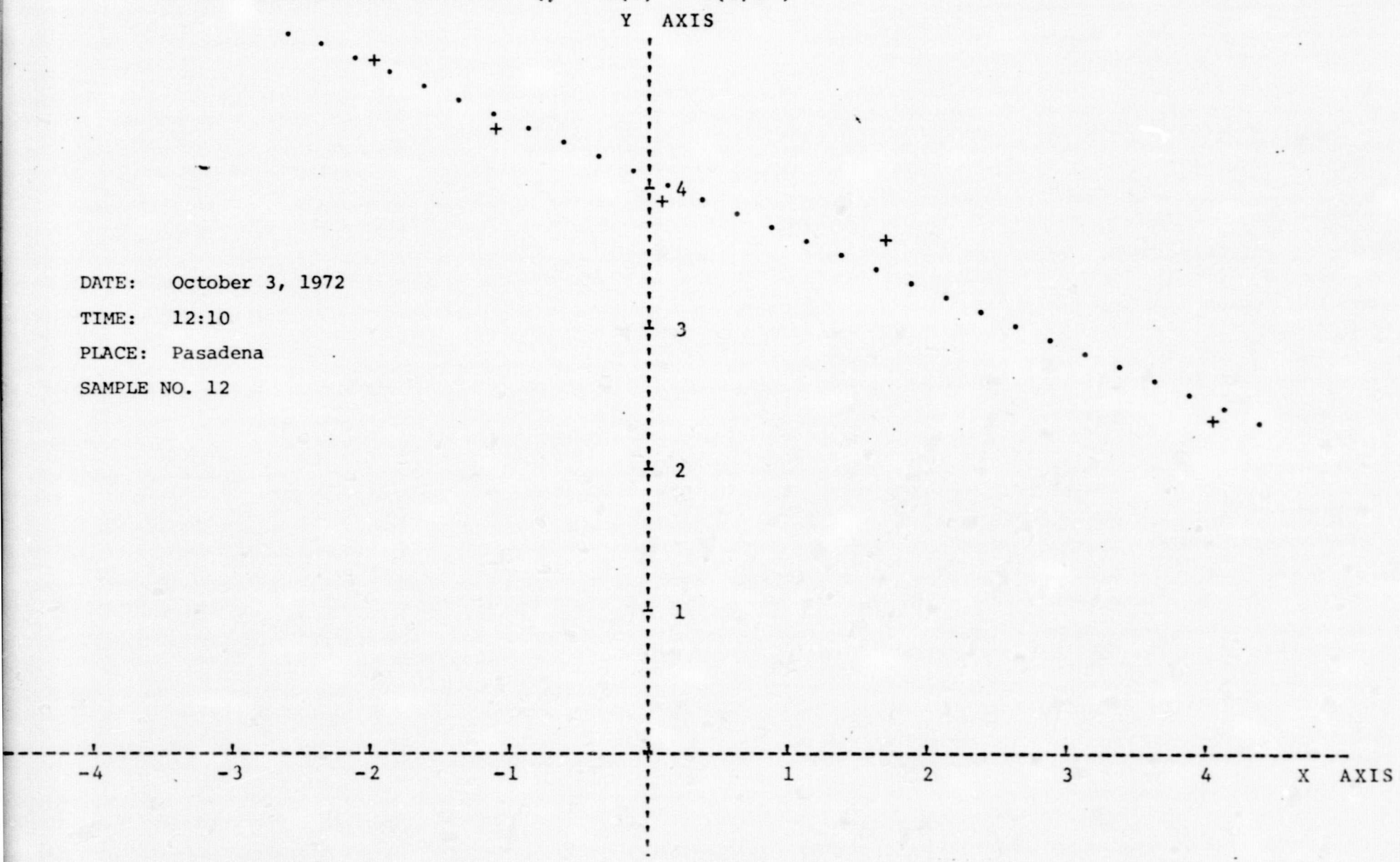

FIGURE . Particle Size Distribution

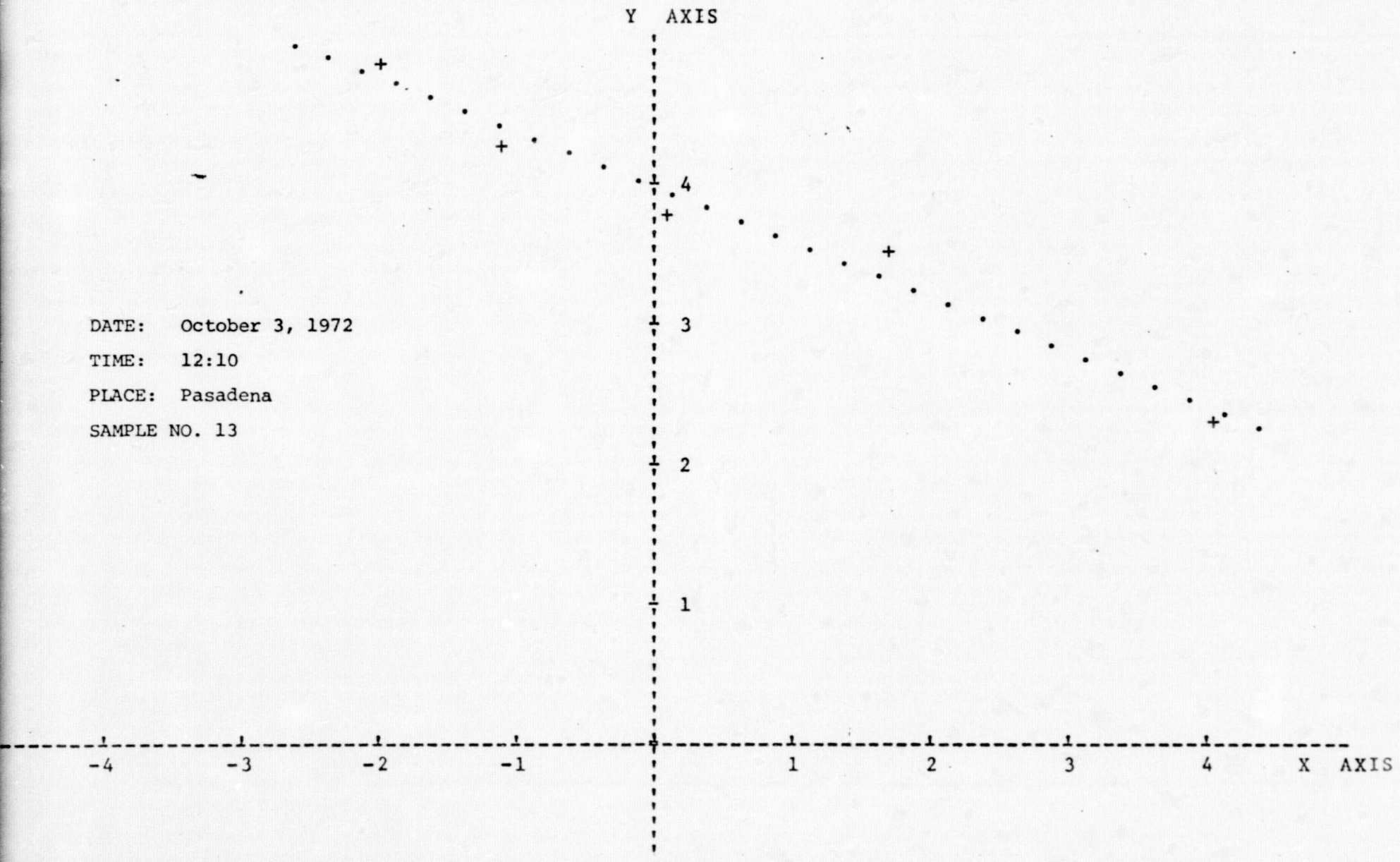

APPENDIX E

Linear Regression Analyses of Suspended Particulate Distributions
November 27, 1972.

FIGURE . Particle Size Distribution

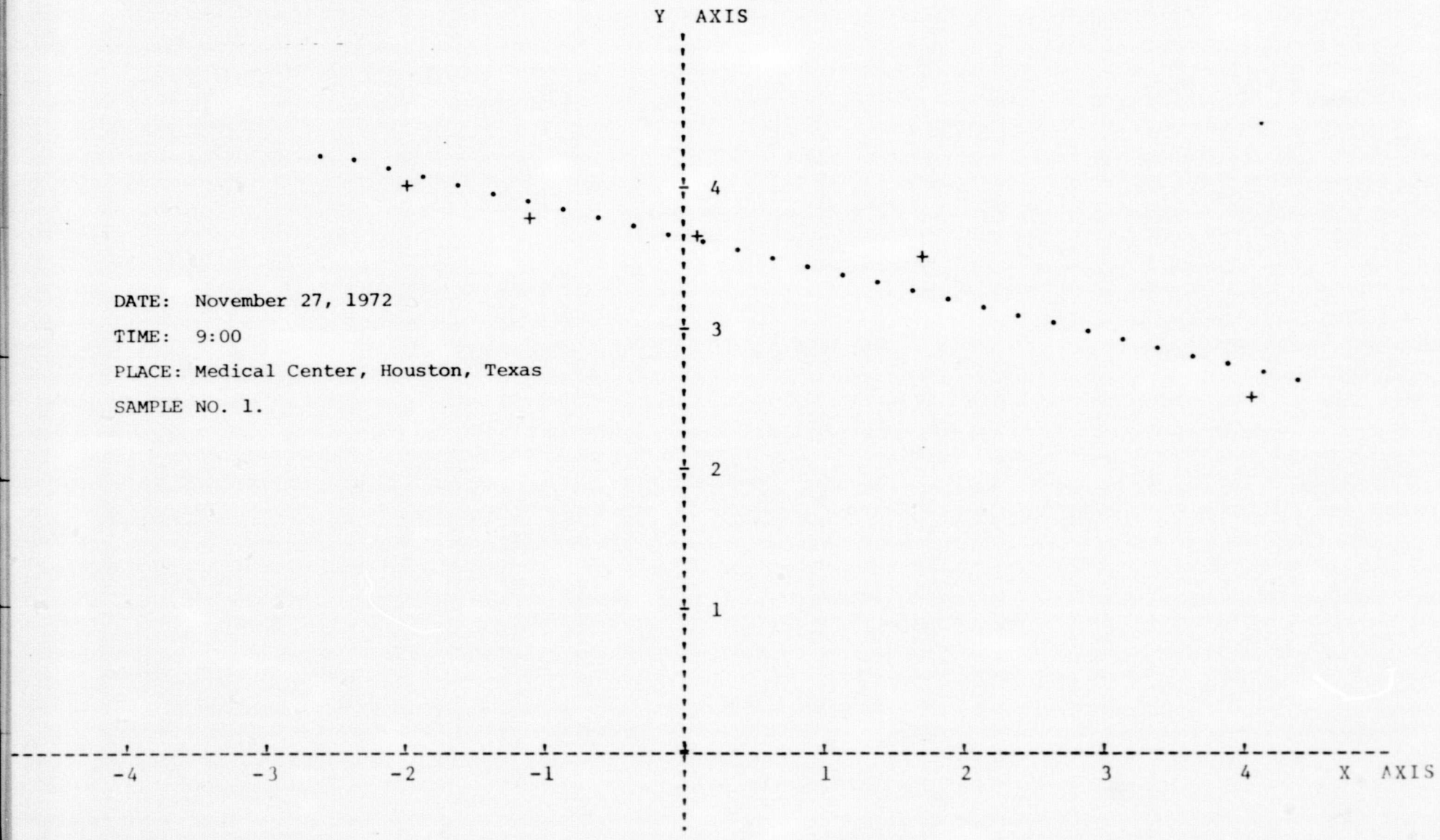

FIGURE . Particle Size Distribution

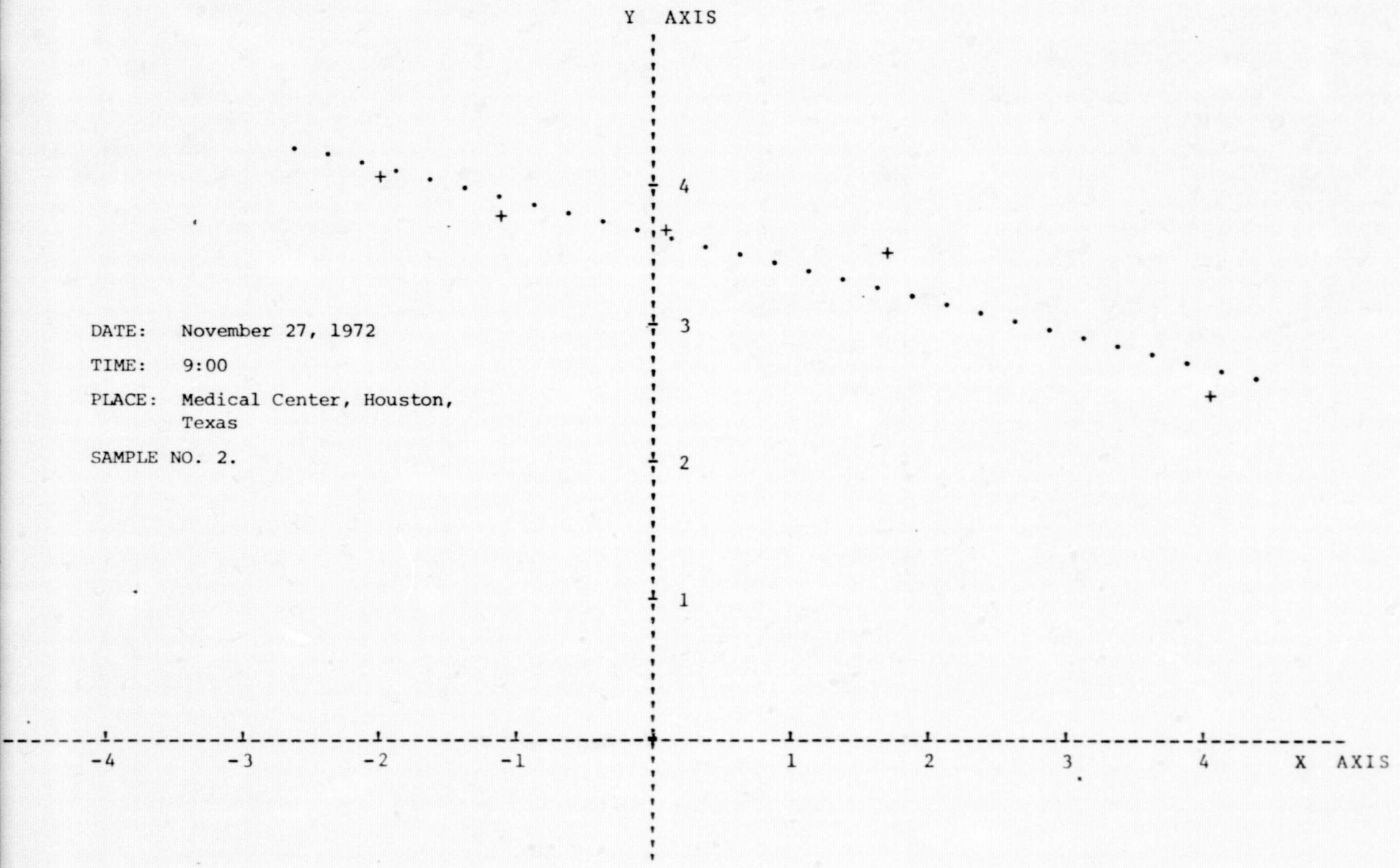

FIGURE . Particle Size Distribution

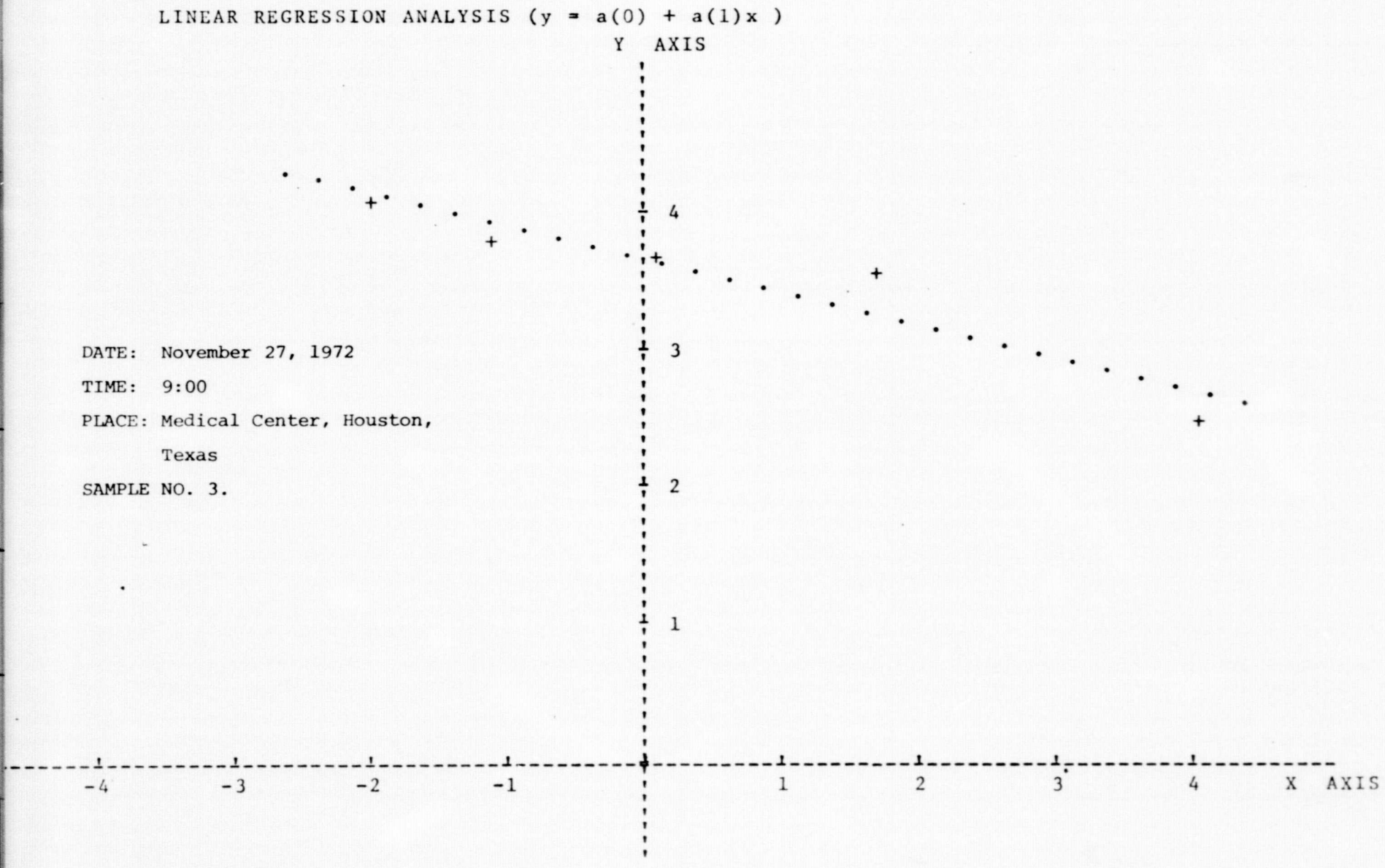

FIGURE . Particle Size Distribution

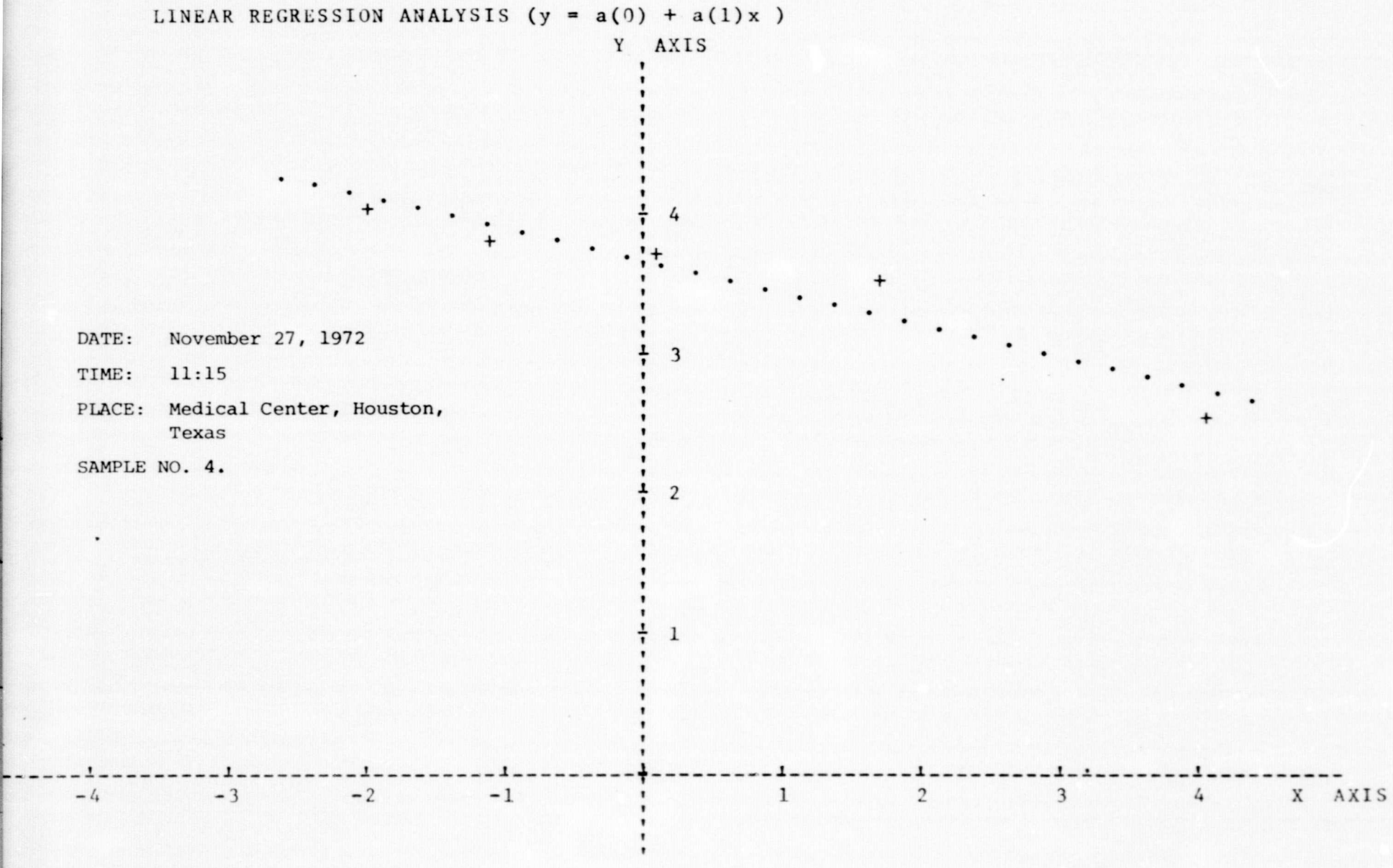

FIGURE . Particle Size Distribution

LINEAR REGRESSION ANALYSIS (y = a(0) + a(1)x)

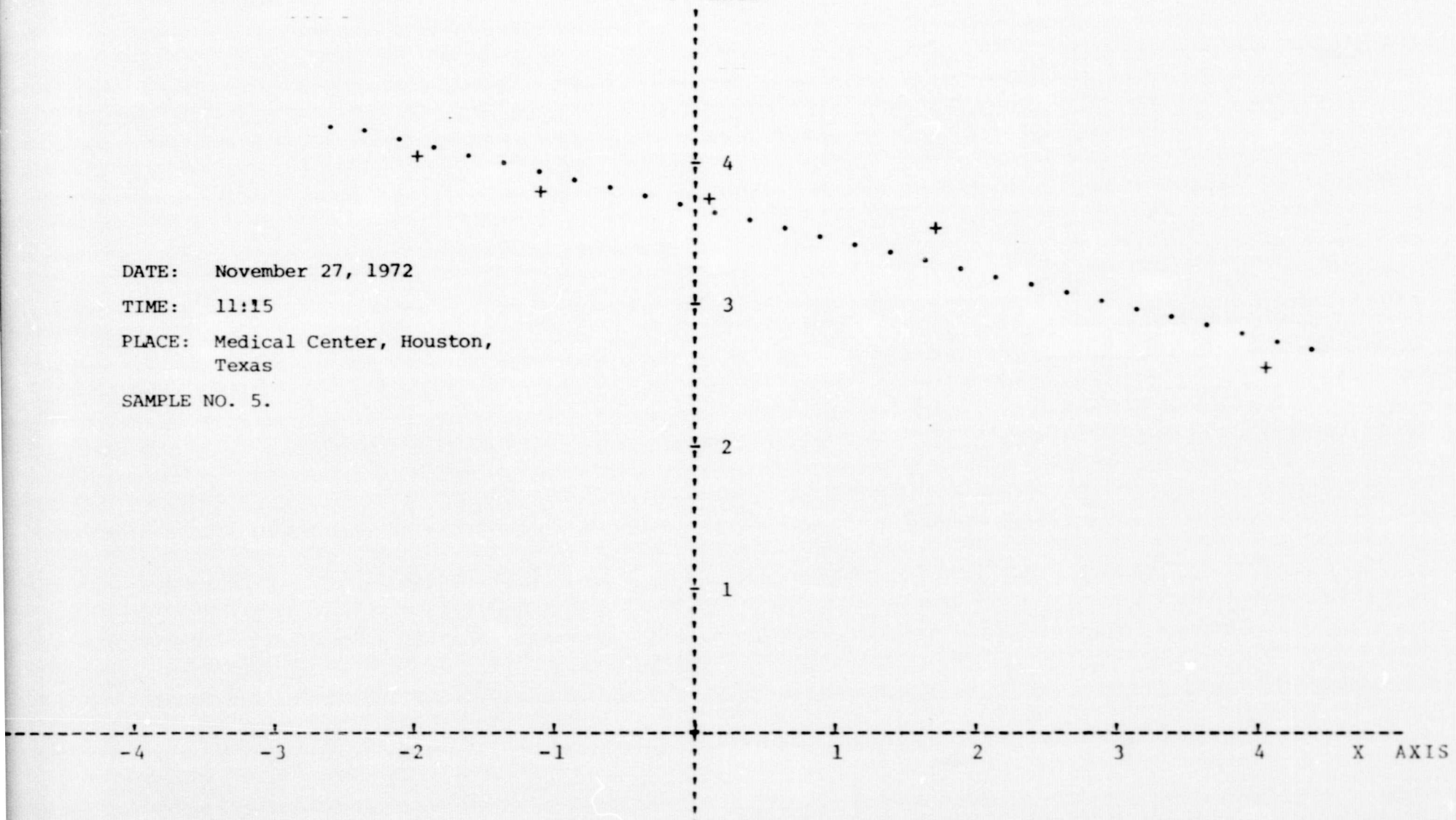

DATE: November 27, 1972

TIME: 11:15

PLACE: Medical Center, Houston, Texas

SAMPLE NO. 5.

3.659044852 = a(0)
-1.148161531 = a(1)
-.947870223 = r

ONE X AXIS UNIT = .200000000
ONE Y AXIS UNIT = 1.000000000

FIGURE . Particle Size Distribution

LINEAR REGRESSION ANALYSIS (y = a(0) + a(1)x)

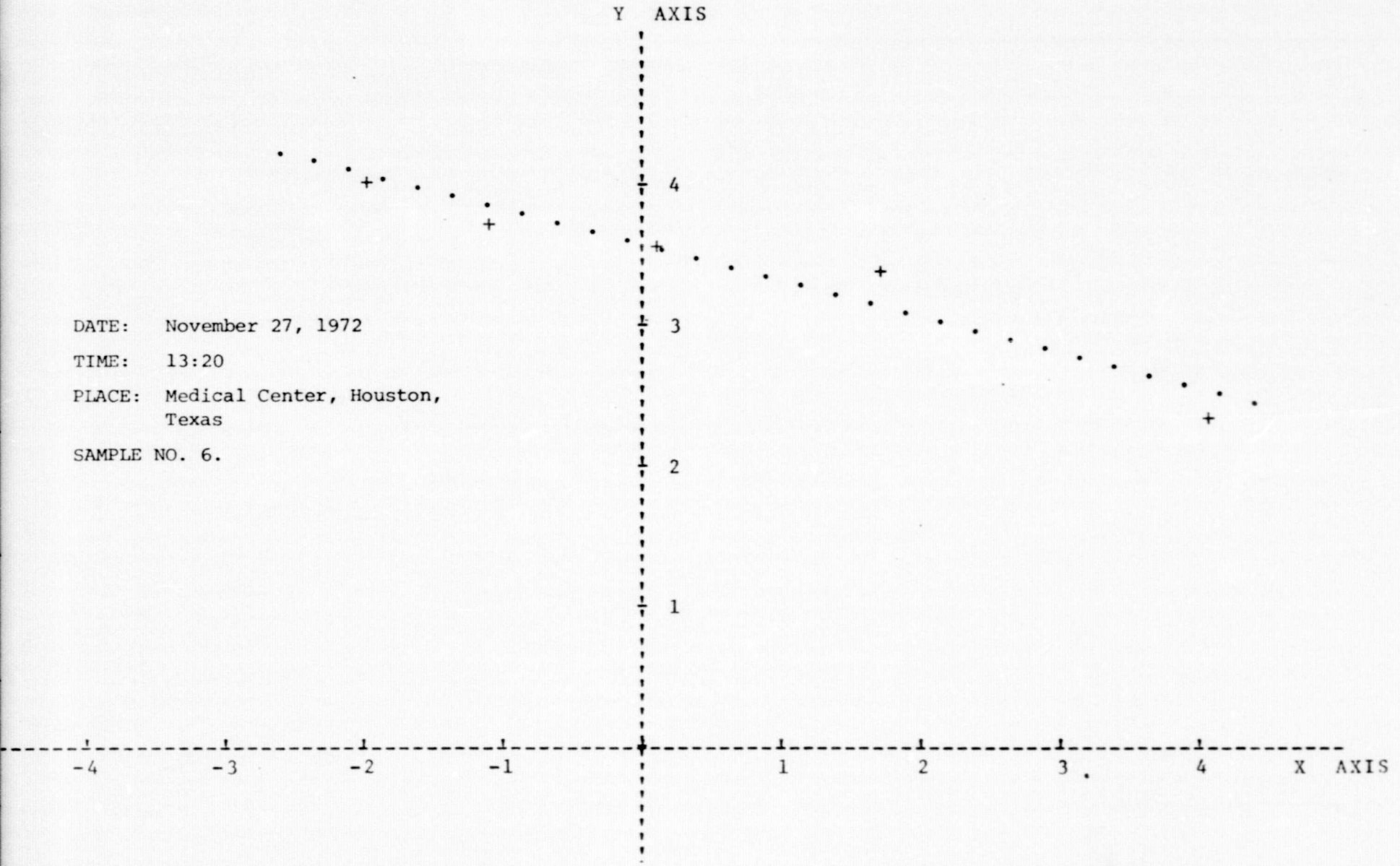

DATE: November 27, 1972

TIME: 13:20

PLACE: Medical Center, Houston, Texas

SAMPLE NO. 6.

3.541551276 = a(0)
-1.281907839 = a(1)
-.963676624 = r
.152732323 = S(x.y)

ONE X AXIS UNIT = .200000000
ONE Y AXIS UNIT = 1.000000000

FIGURE . Particle Size Distribution

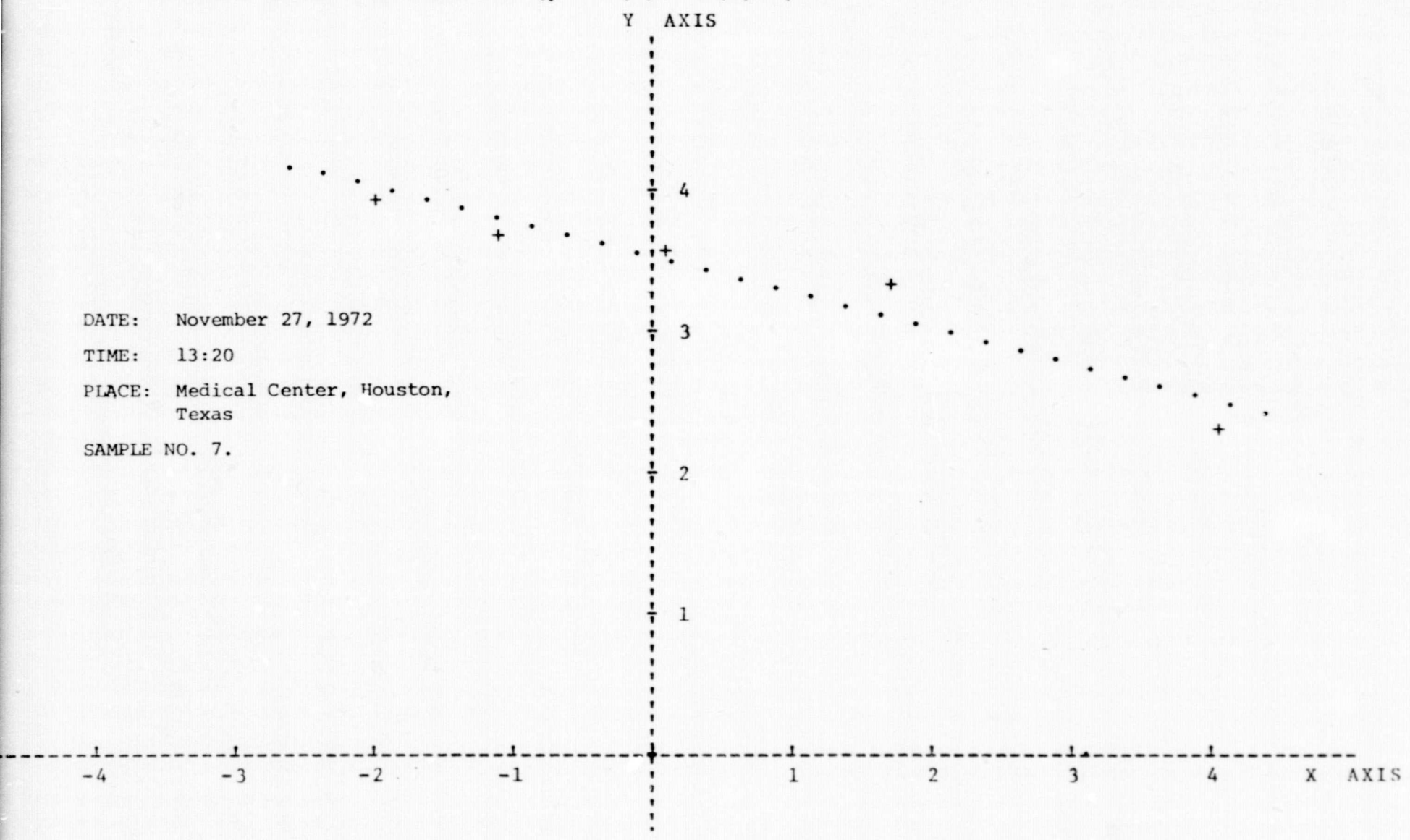

FIGURE . Particle Size Distribution

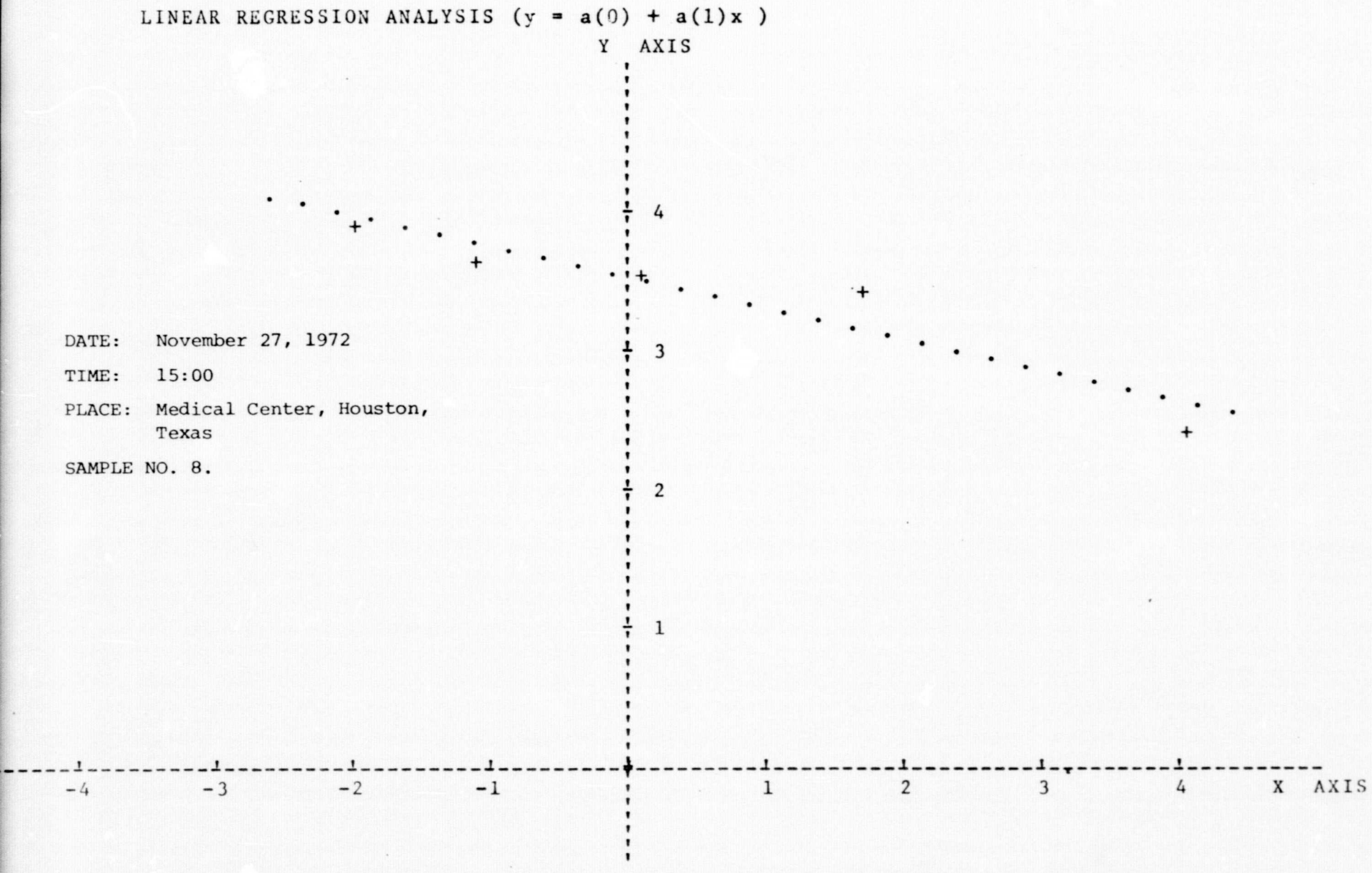

FIGURE . Particle Size Distribution

LINEAR REGRESSION ANALYSIS (y = a(0) + a(1)x)

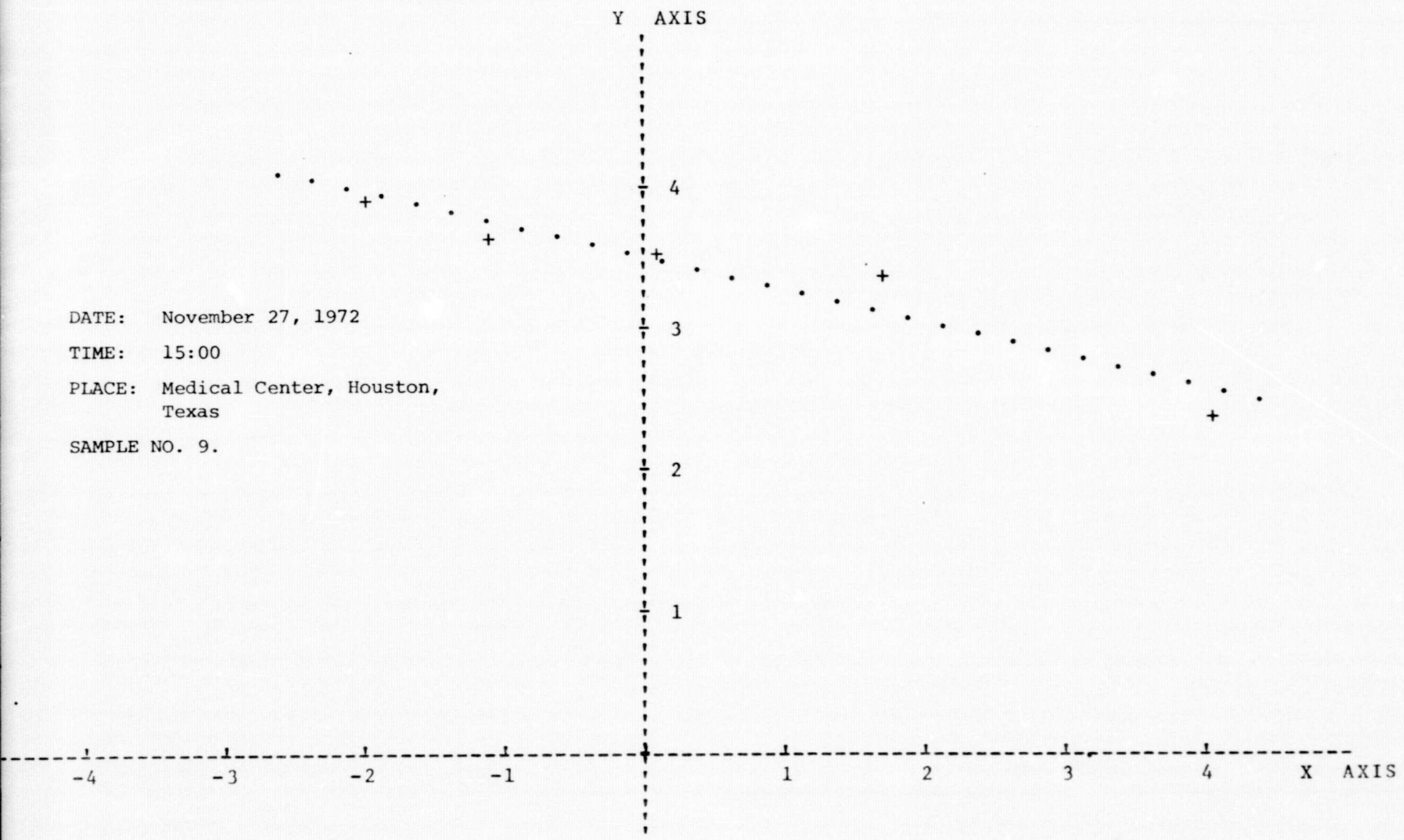

DATE: November 27, 1972

TIME: 15:00

PLACE: Medical Center, Houston, Texas

SAMPLE NO. 9.

3.486987674 = a(0)
-1.164778620 = a(1)
-.952572530 = r
.159971013 = S(x.y)

ONE X AXIS UNIT = .200000000
ONE Y AXIS UNIT = 1.000000000

APPENDIX F

Linear Regression Analyses of Suspended Particulate Distributions
April 27, 1973

FIGURE . Particle Size Distribution

LINEAR REGRESSION ANALYSIS (y = a(0) + a(1)x)

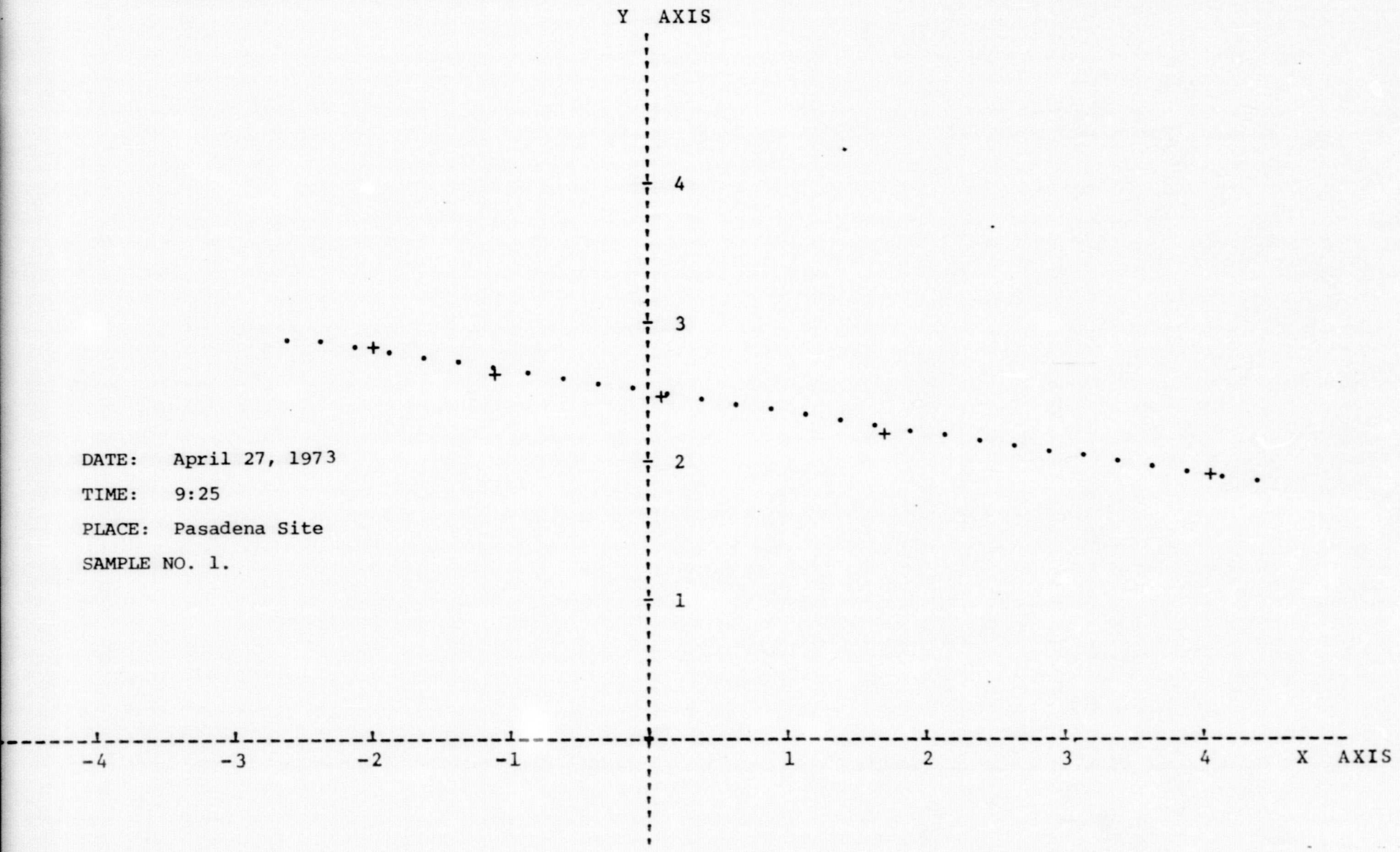

DATE: April 27, 1973

TIME: 9:25

PLACE: Pasadena Site

SAMPLE NO. 1.

4.968401751 = a(0)
-1.511927540 = a(1)
-.996284861 = r
.056185418 = S(x.y)

ONE X AXIS UNIT = .200000000
ONE Y AXIS UNIT = 2.000000000

FIGURE . Particle Size Distribution

LINEAR REGRESSION ANALYSIS (y = a(0) + a(1)x)

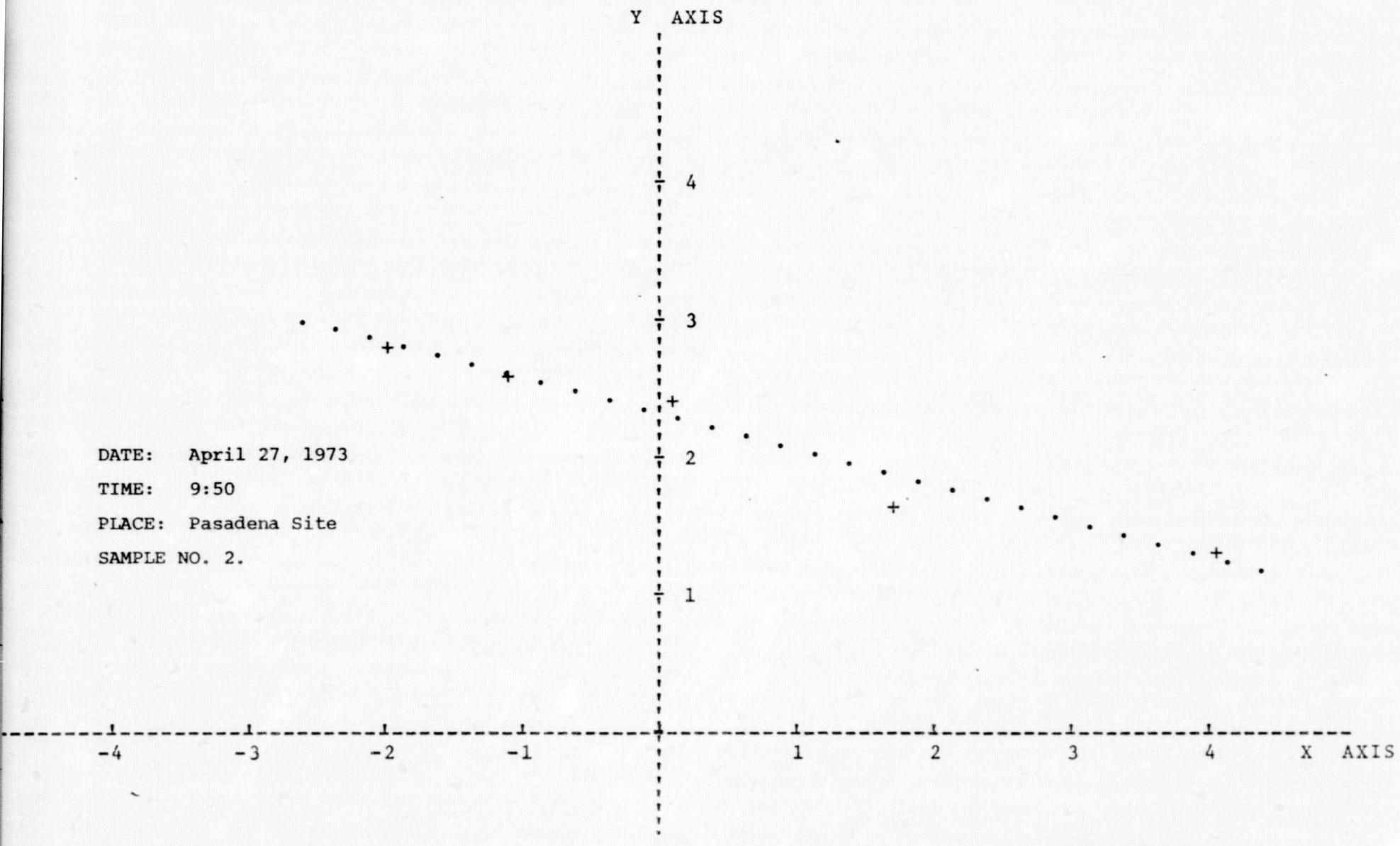

DATE: April 27, 1973

TIME: 9:50

PLACE: Pasadena Site

SAMPLE NO. 2.

4.580057930 = a(0)
-2.617834961 = a(1)
-.979442457 = r
.231791640 = S(x.y)

ONE X AXIS UNIT = .200000000
ONE Y AXIS UNIT = 2.000000000

FIGURE . Particle Size Distribution

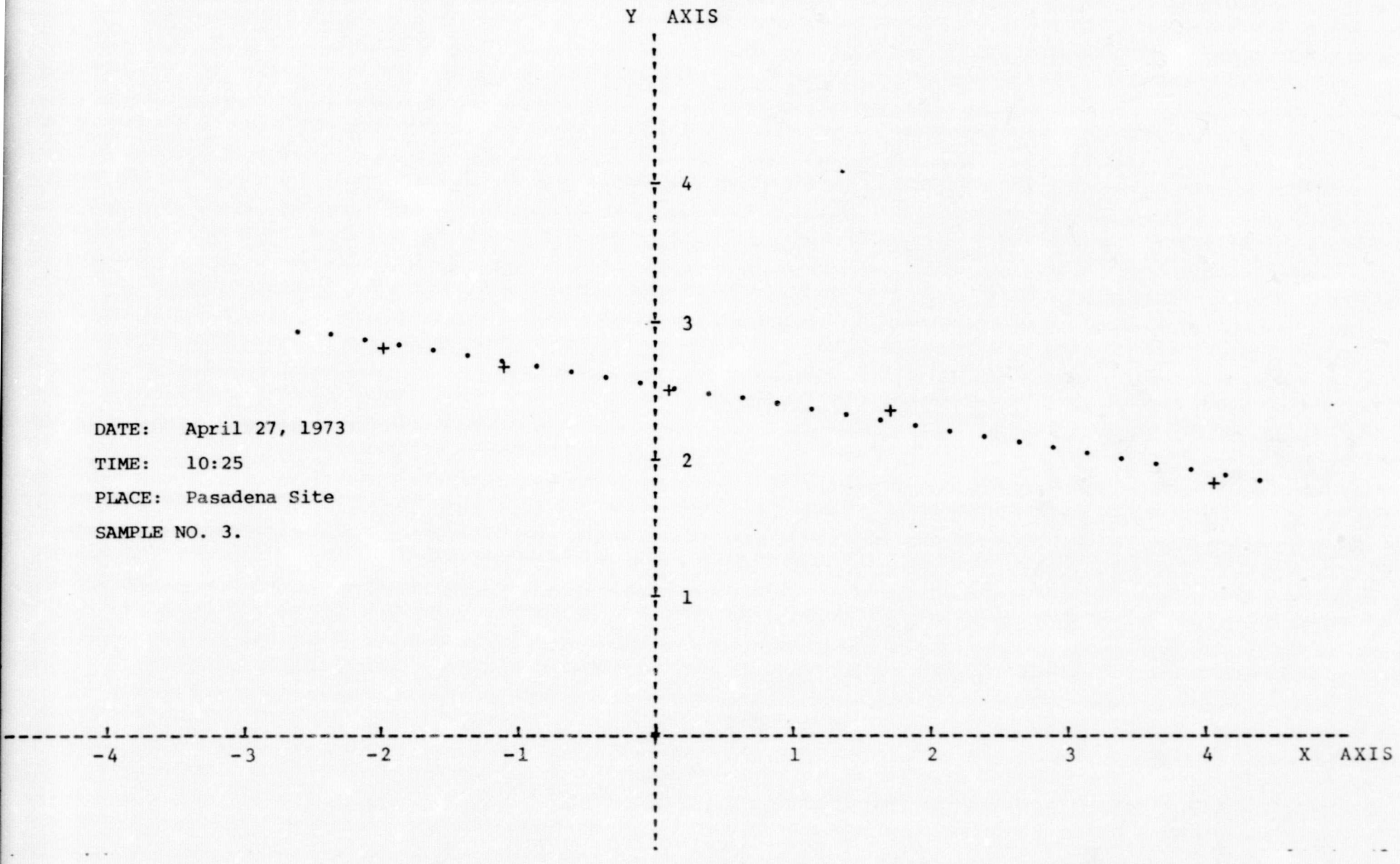

FIGURE . Particle Size Distribution

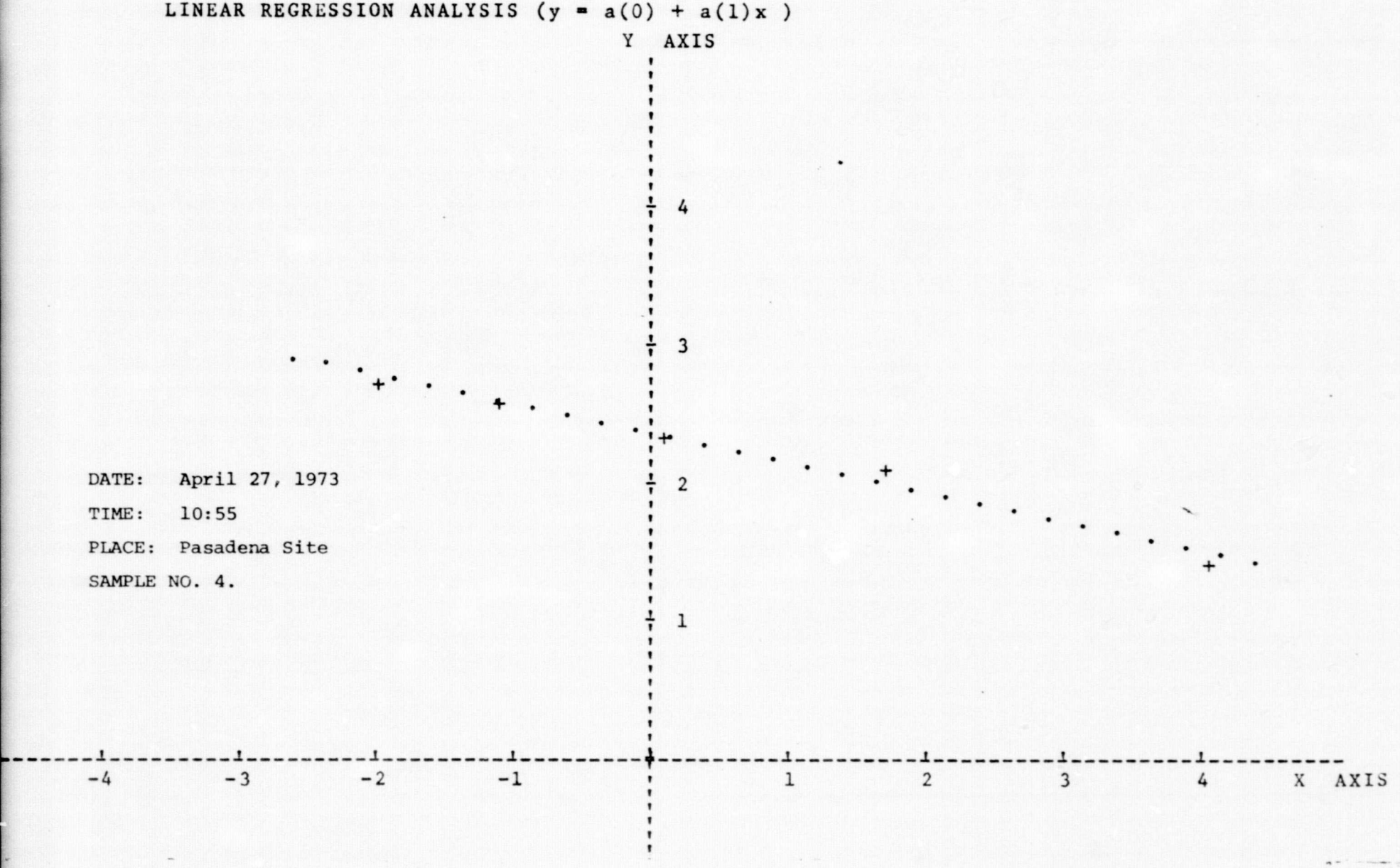

FIGURE . Particle Size Distribution

LINEAR REGRESSION ANALYSIS (y = a(0) + a(1)x)

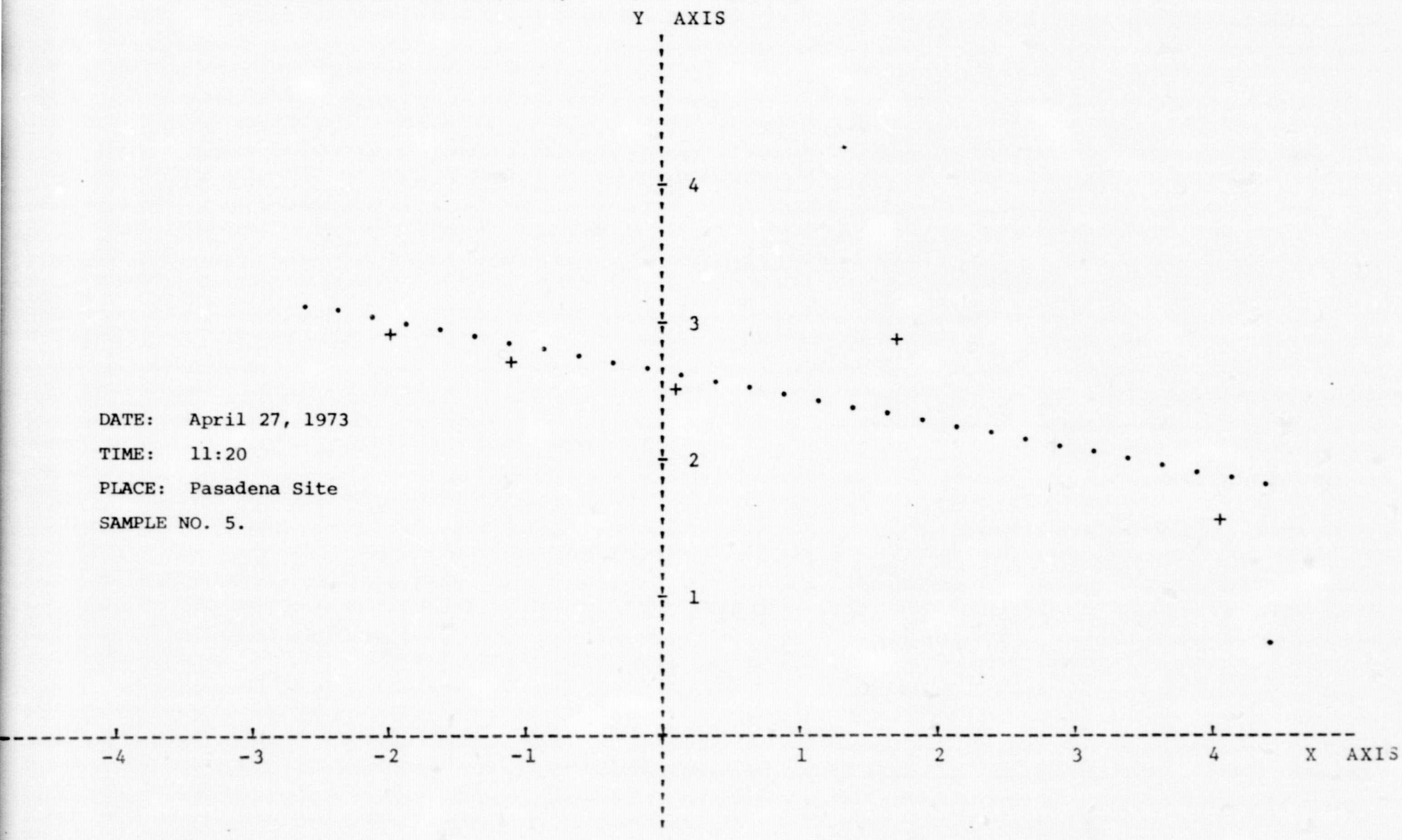

DATE: April 27, 1973

TIME: 11:20

PLACE: Pasadena Site

SAMPLE NO. 5.

5.239028348 = a(0)
-1.877865574 = a(1)
-.802827638 = r
.599542127 = S(x.y)

ONE X AXIS UNIT = .200000000
ONE Y AXIS UNIT = 2.000000000

FIGURE . Particle Size Distribution

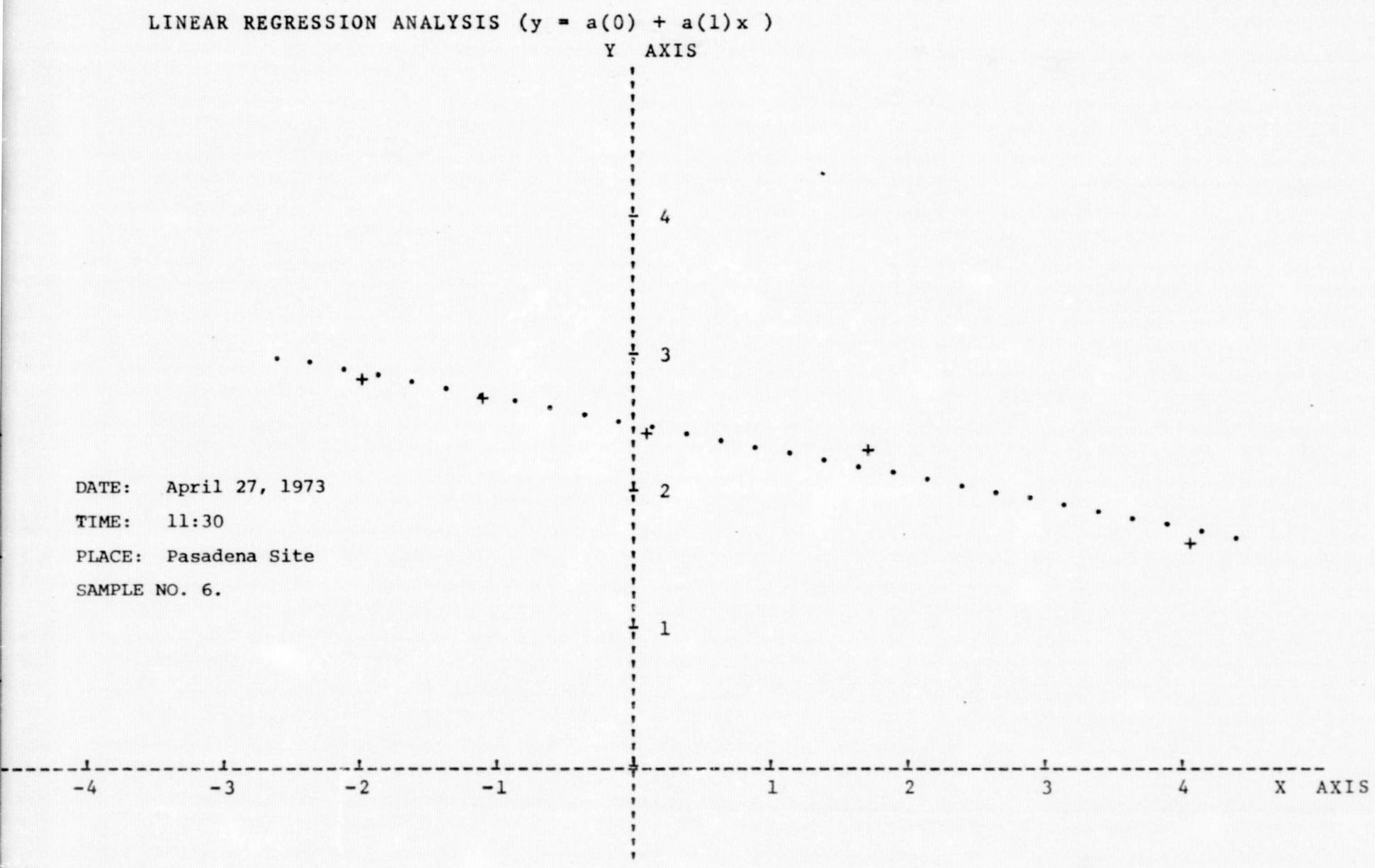

FIGURE . Particle Size Distribution

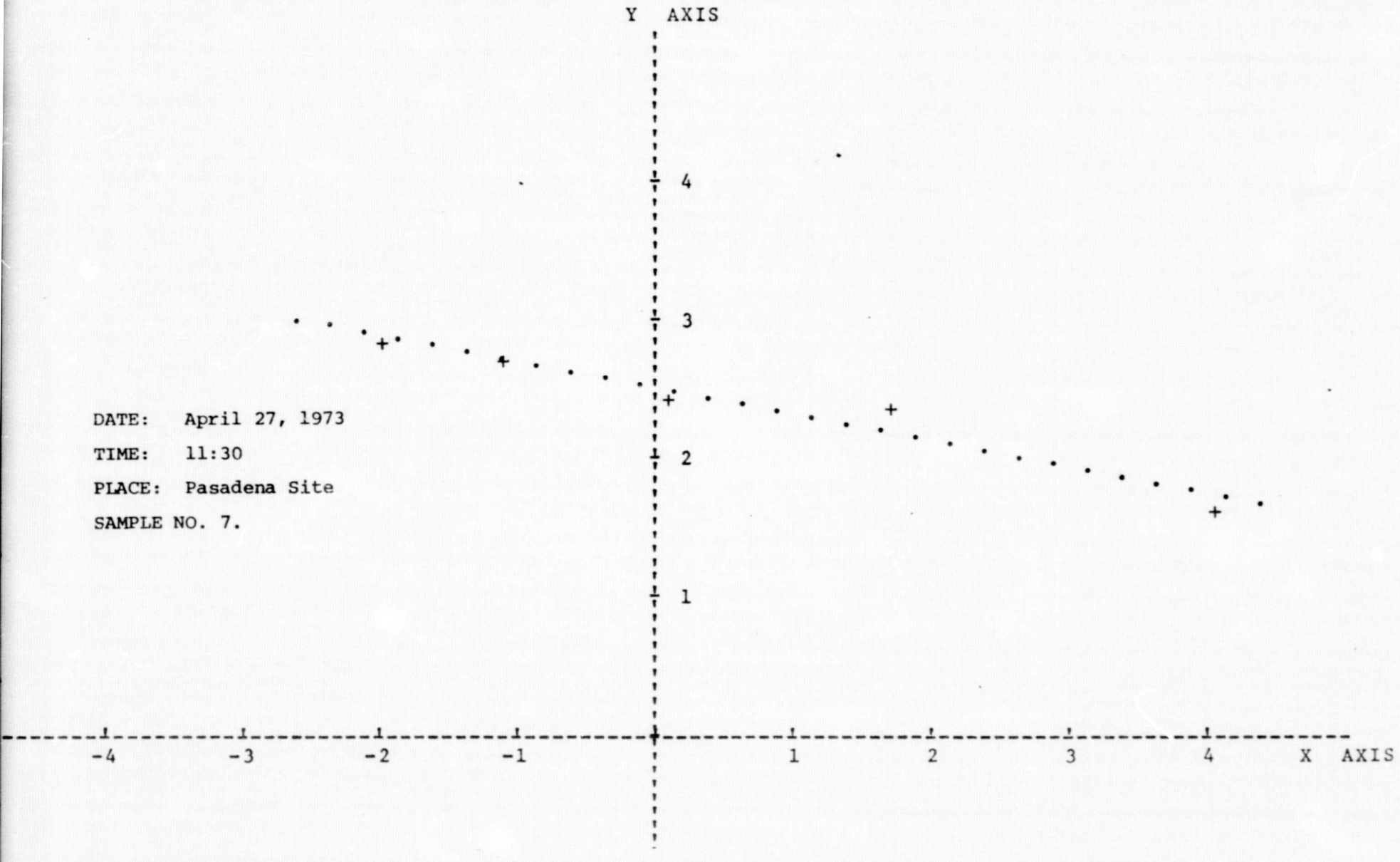

FIGURE . Particle Size Distribution

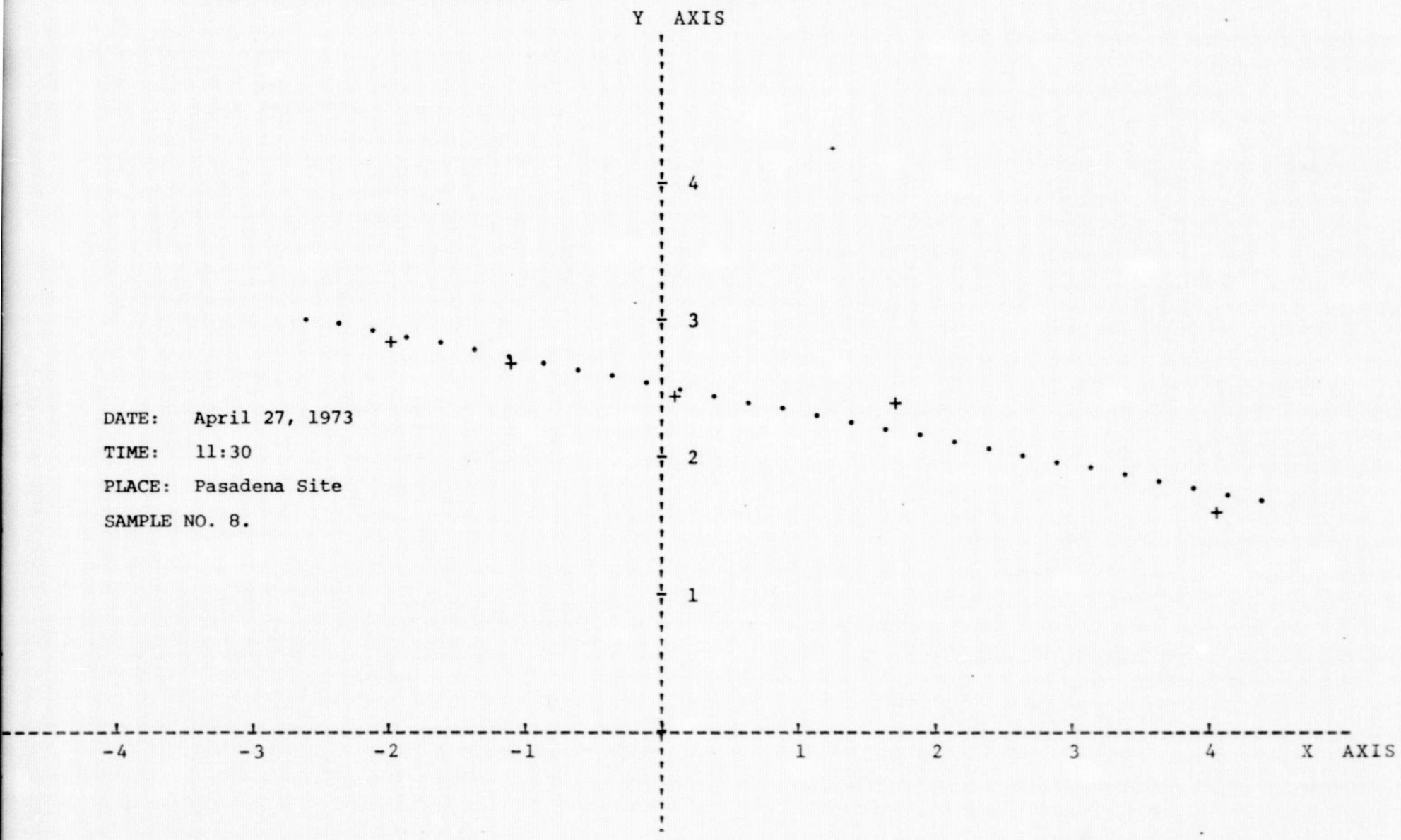

FIGURE . Particle Size Distribution

LINEAR REGRESSION ANALYSIS (y = a(0) + a(1)x)

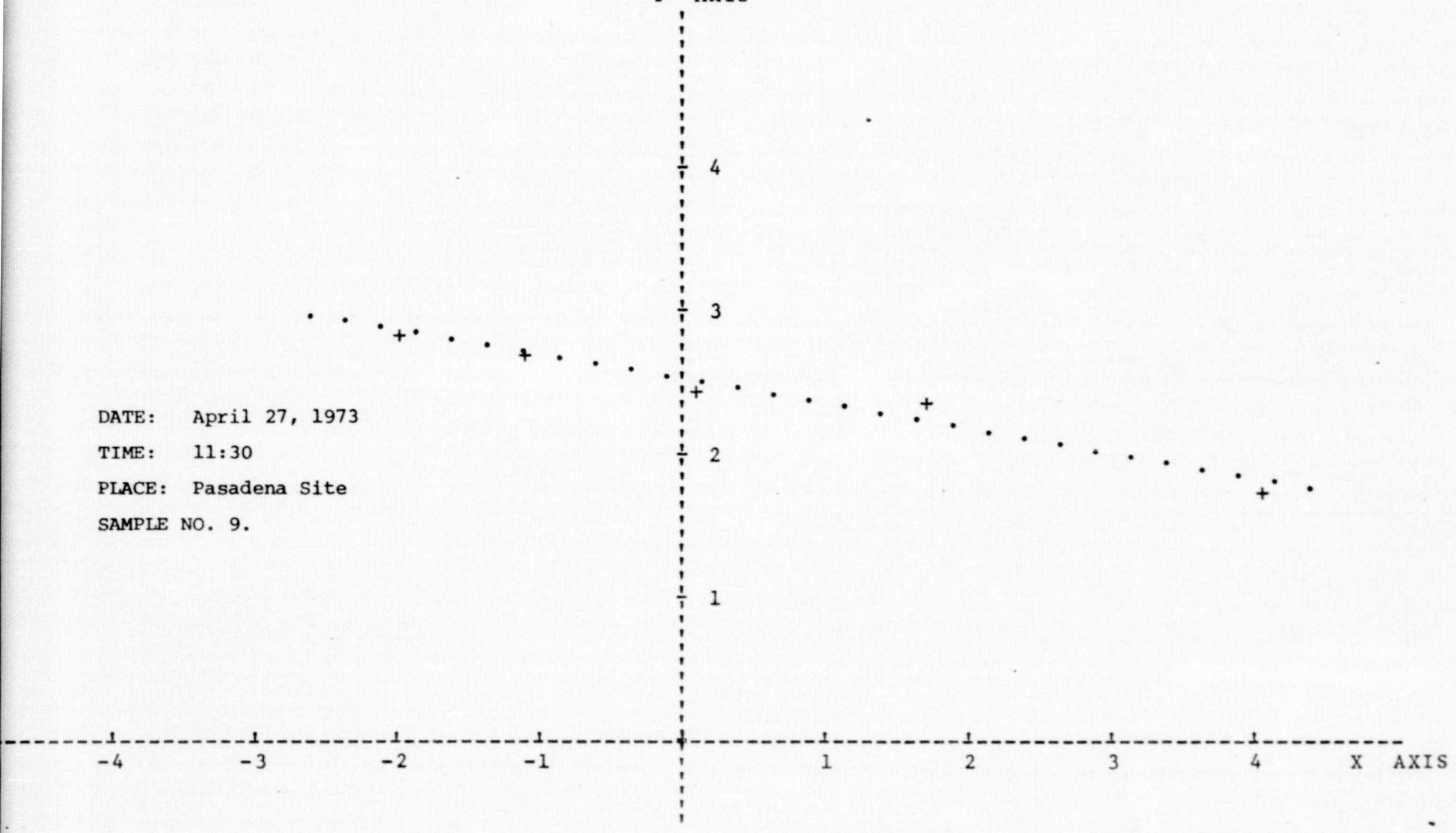

DATE: April 27, 1973

TIME: 11:30

PLACE: Pasadena Site

SAMPLE NO. 9.

4.997118272 = a(0)
-1.736027828 = a(1)
-.980278705 = r
.150458030 = S(x.y)

ONE X AXIS UNIT = .200000000
ONE Y AXIS UNIT = 2.000000000

FIGURE . Particle Size Distribution

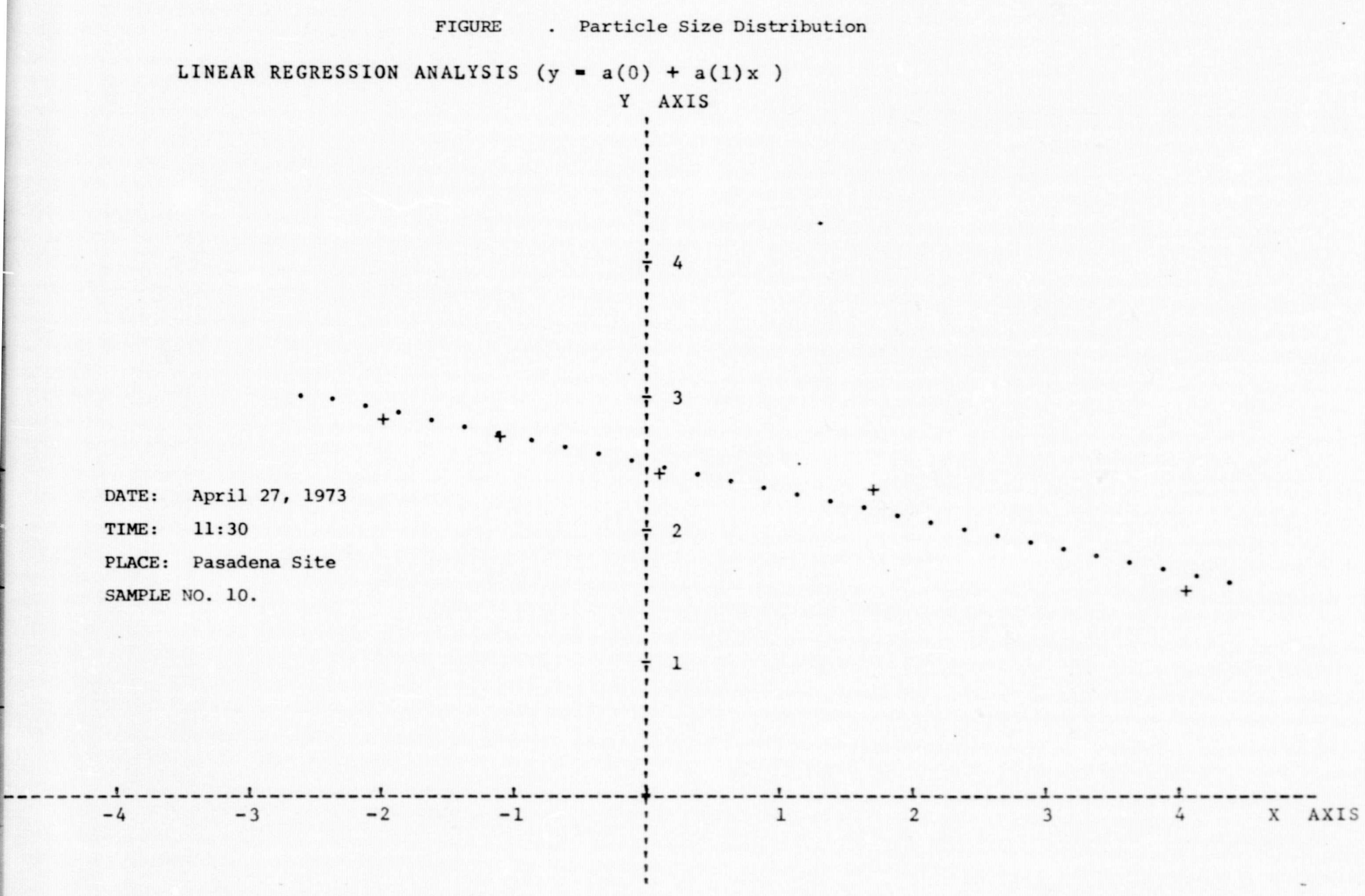

FIGURE . Particle Size Distribution

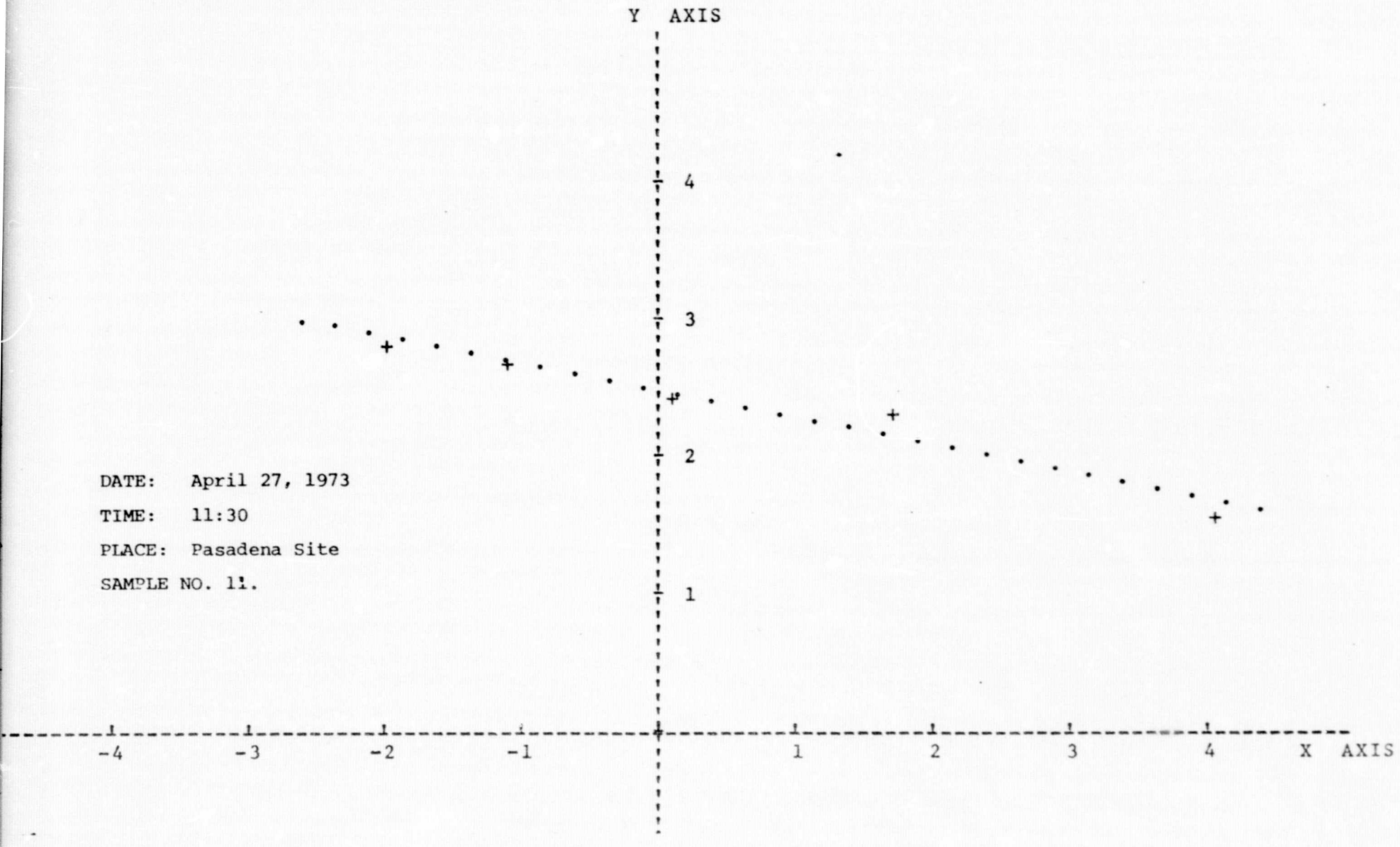

FIGURE . Particle Size Distribution

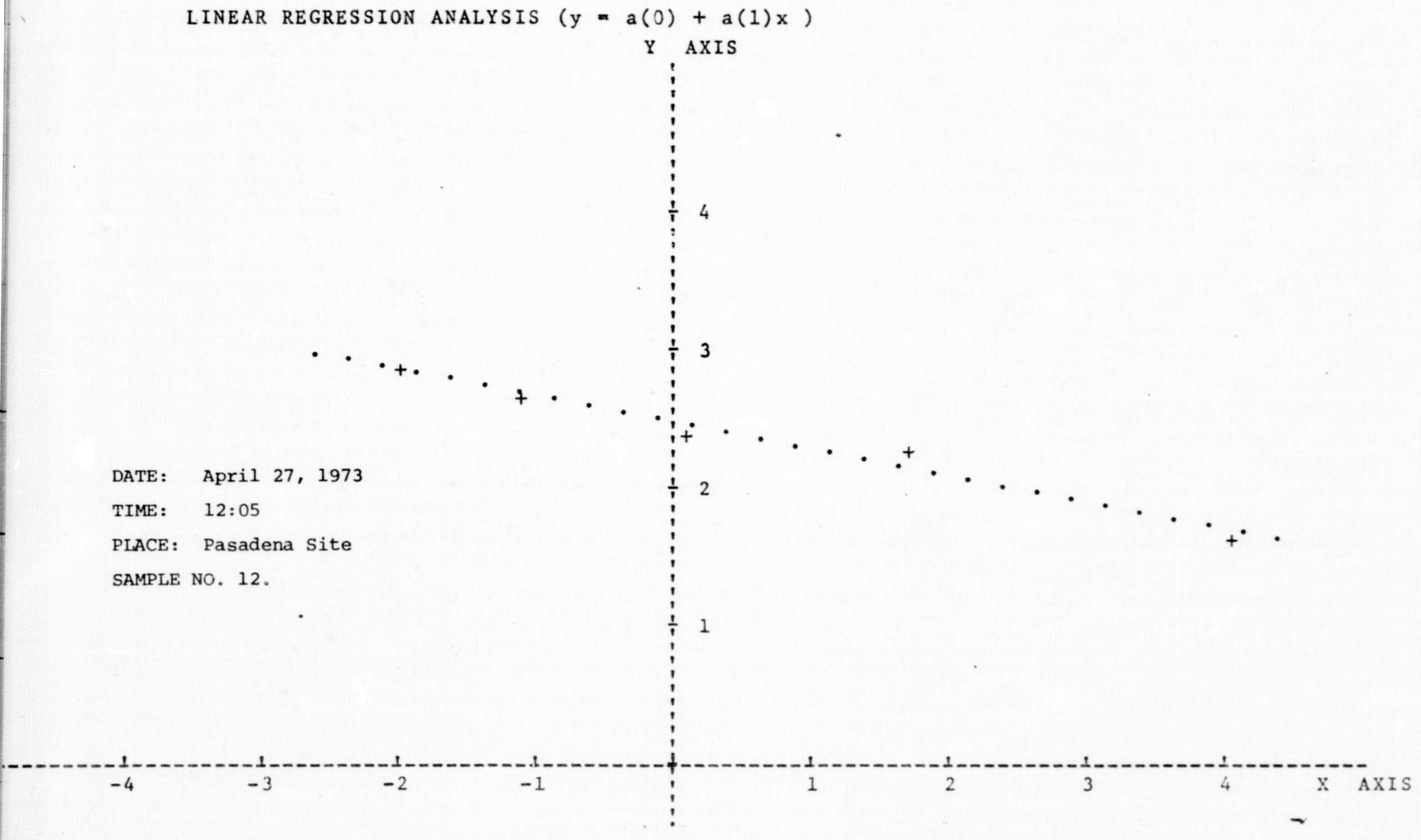

FIGURE . Particle Size Distribution

LINEAR REGRESSION ANALYSIS (y = a(0) + a(1)x)

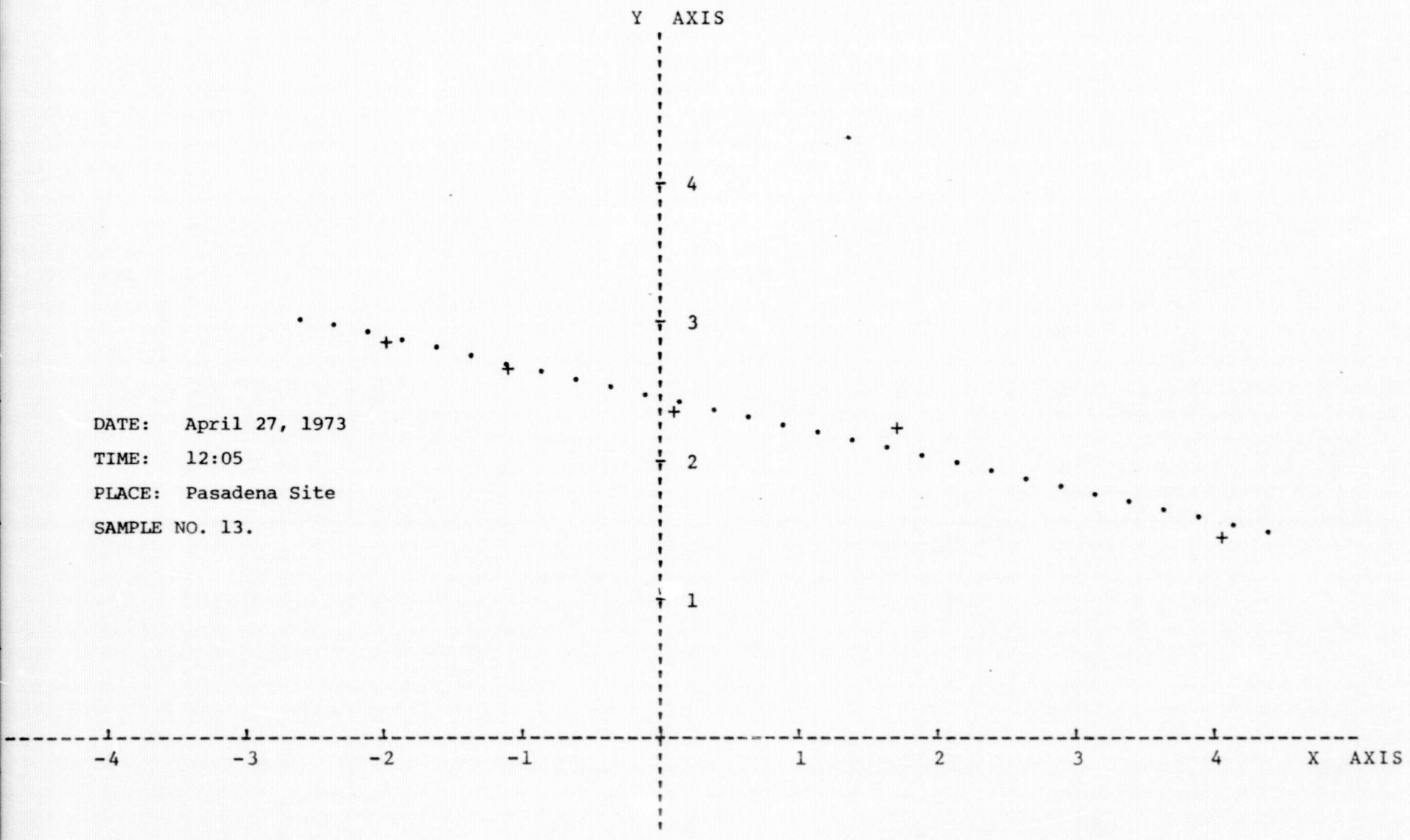

DATE: April 27, 1973

TIME: 12:05

PLACE: Pasadena Site

SAMPLE NO. 13.

4.866511629 = a(0)
-2.213254914 = a(1)
-.981296359 = r
.186657928 = S(x.y)

ONE X AXIS UNIT = .200000000
ONE Y AXIS UNIT = 2.000000000

FIGURE . Particle Size Distribution

LINEAR REGRESSION ANALYSIS (y = a(0) + a(1)x)

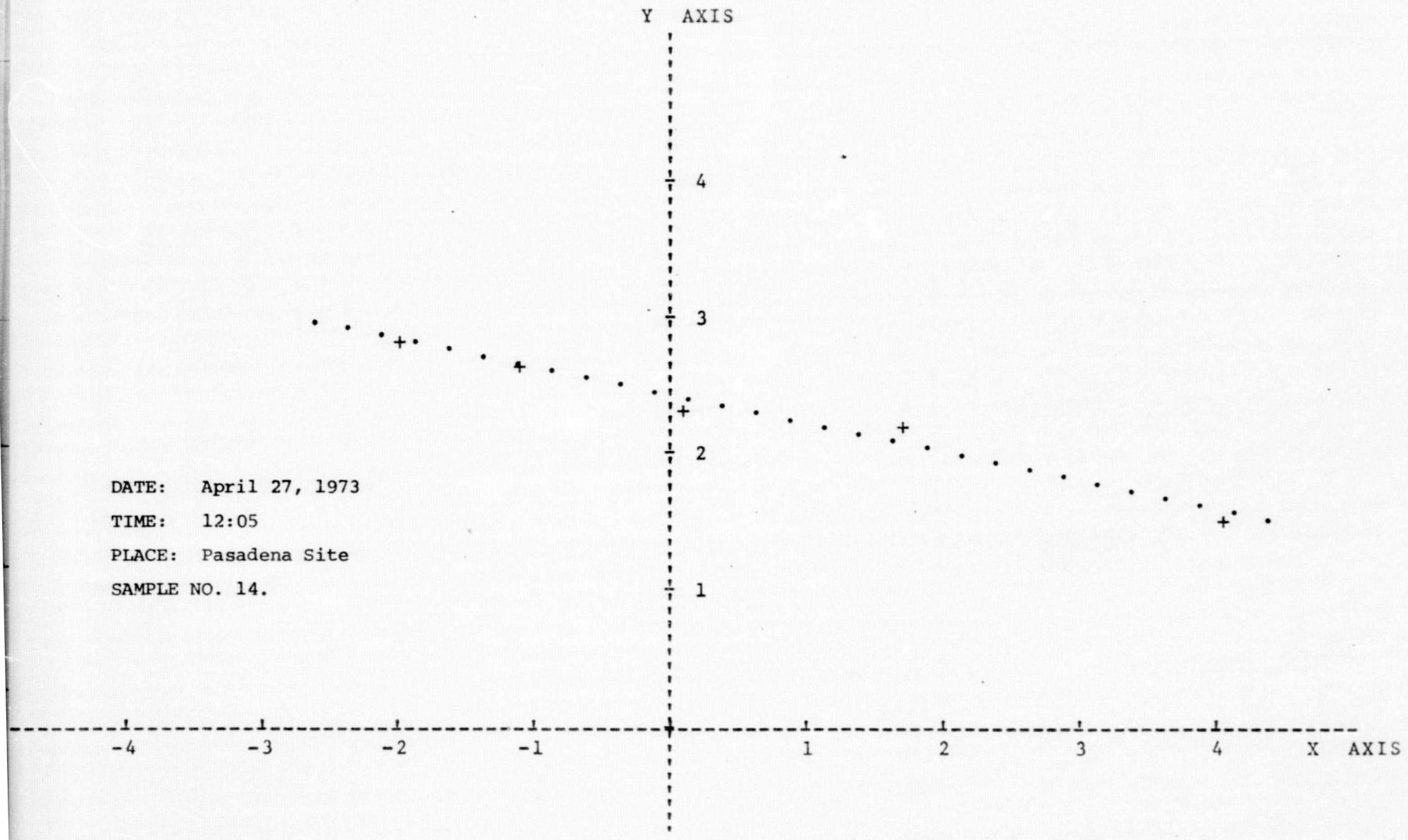

DATE: April 27, 1973

TIME: 12:05

PLACE: Pasadena Site

SAMPLE NO. 14.

4.808721456 = a(0)
-2.087316070 = a(1)
-.985898316 = r
.152316681 = S(x,y)

ONE X AXIS UNIT = .200000000
ONE Y AXIS UNIT = 2.000000000

FIGURE . Particle Size Distribution

LINEAR REGRESSION ANALYSIS (y = a(0) + a(1)x)

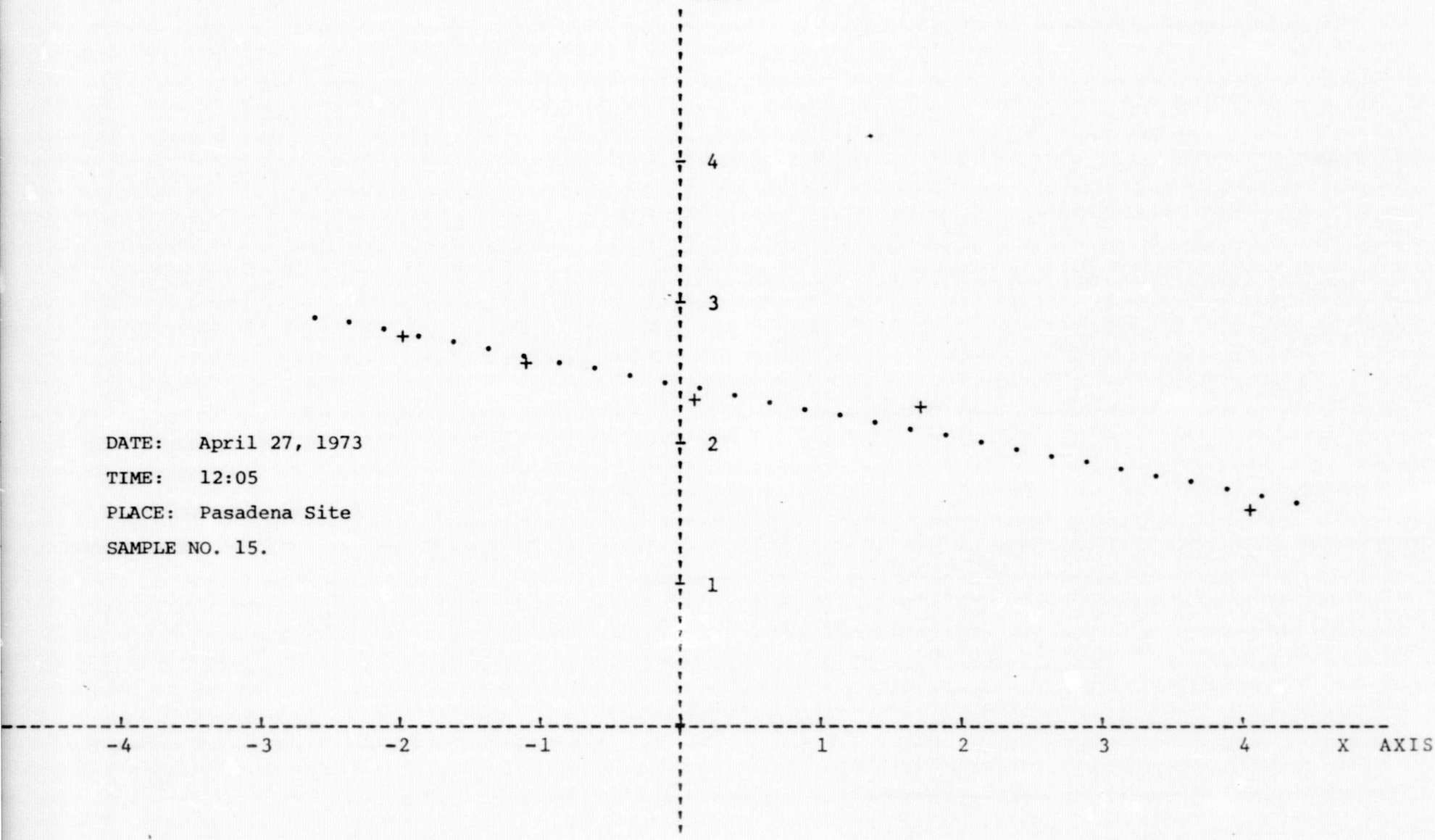

DATE: April 27, 1973

TIME: 12:05

PLACE: Pasadena Site

SAMPLE NO. 15.

4.773090600 = a(0)
-1.888118890 = a(1)
-.970784232 = r
.200637546 = S(x.y)

ONE X AXIS UNIT = .200000000
ONE Y AXIS UNIT = 2.000000000

FIGURE . Particle Size Distribution

LINEAR REGRESSION ANALYSIS (y = a(0) + a(1)x)

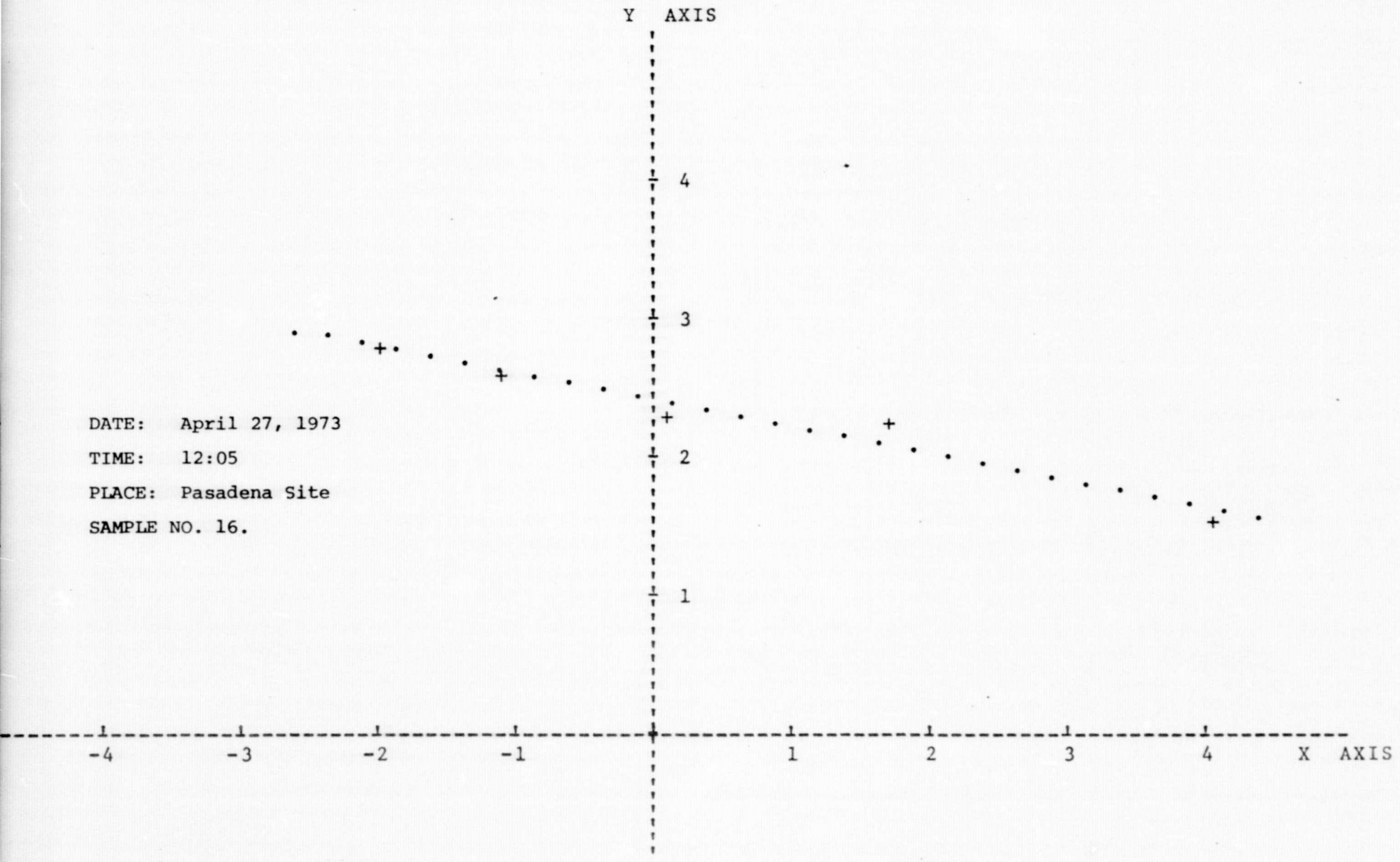

DATE: April 27, 1973

TIME: 12:05

PLACE: Pasadena Site

SAMPLE NO. 16.

4.780879320 = a(0)
-1.948900472 = a(1)
-.975369344 = r
.189478568 = S(x.y)

ONE X AXIS UNIT = .200000000
ONE Y AXIS UNIT = 2.000000000

FIGURE . Particle Size Distribution

LINEAR REGRESSION ANALYSIS (y = a(0) + a(1)x)

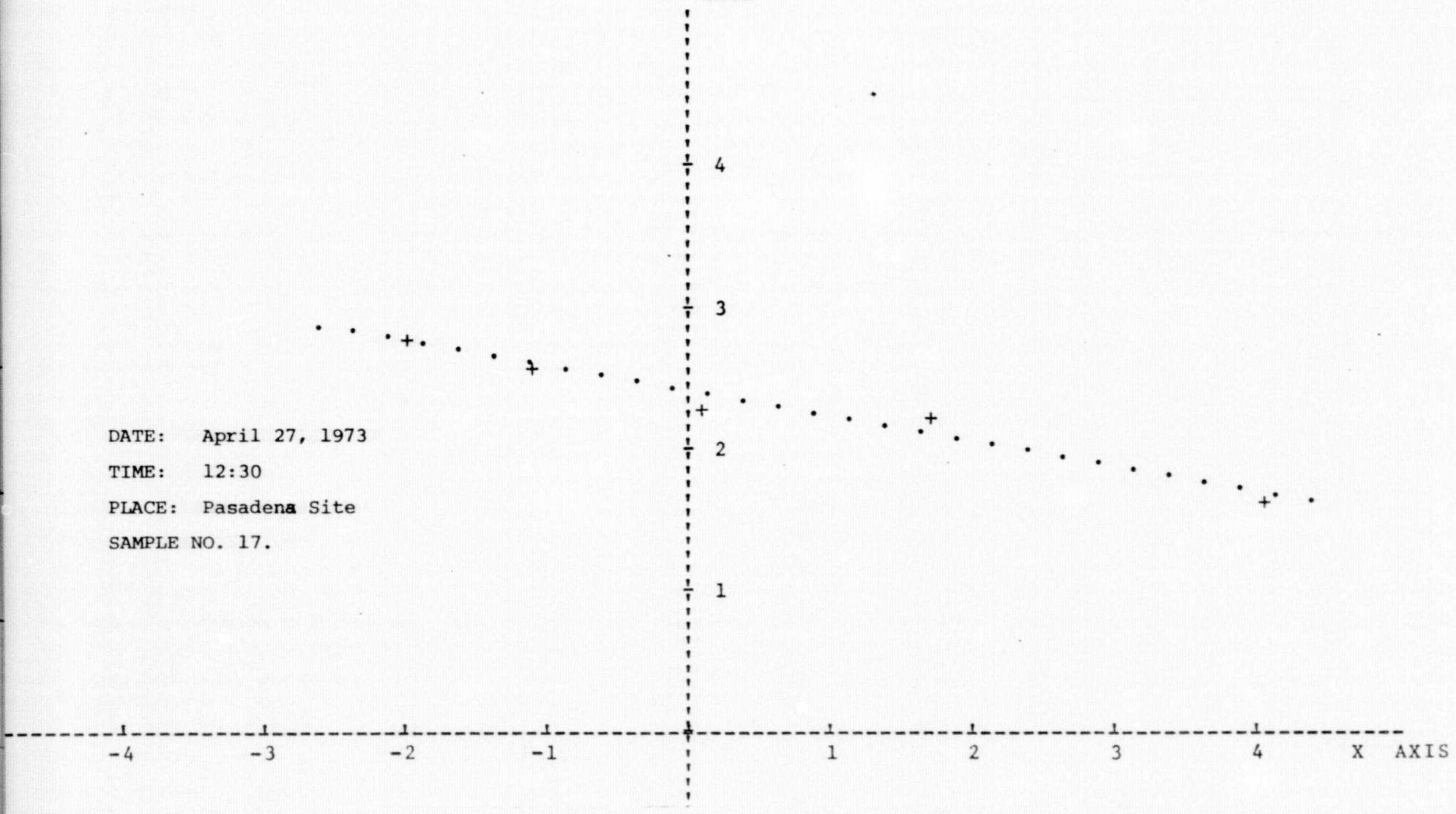

DATE: April 27, 1973

TIME: 12:30

PLACE: Pasadena Site

SAMPLE NO. 17.

4.771538444 = a(0)
-1.784055900 = a(1)
-.981810249 = r
.148321017 = S(x.y)

ONE X AXIS UNIT = .200000000
ONE Y AXIS UNIT = 2.000000000

FIGURE . Particle Size Distribution

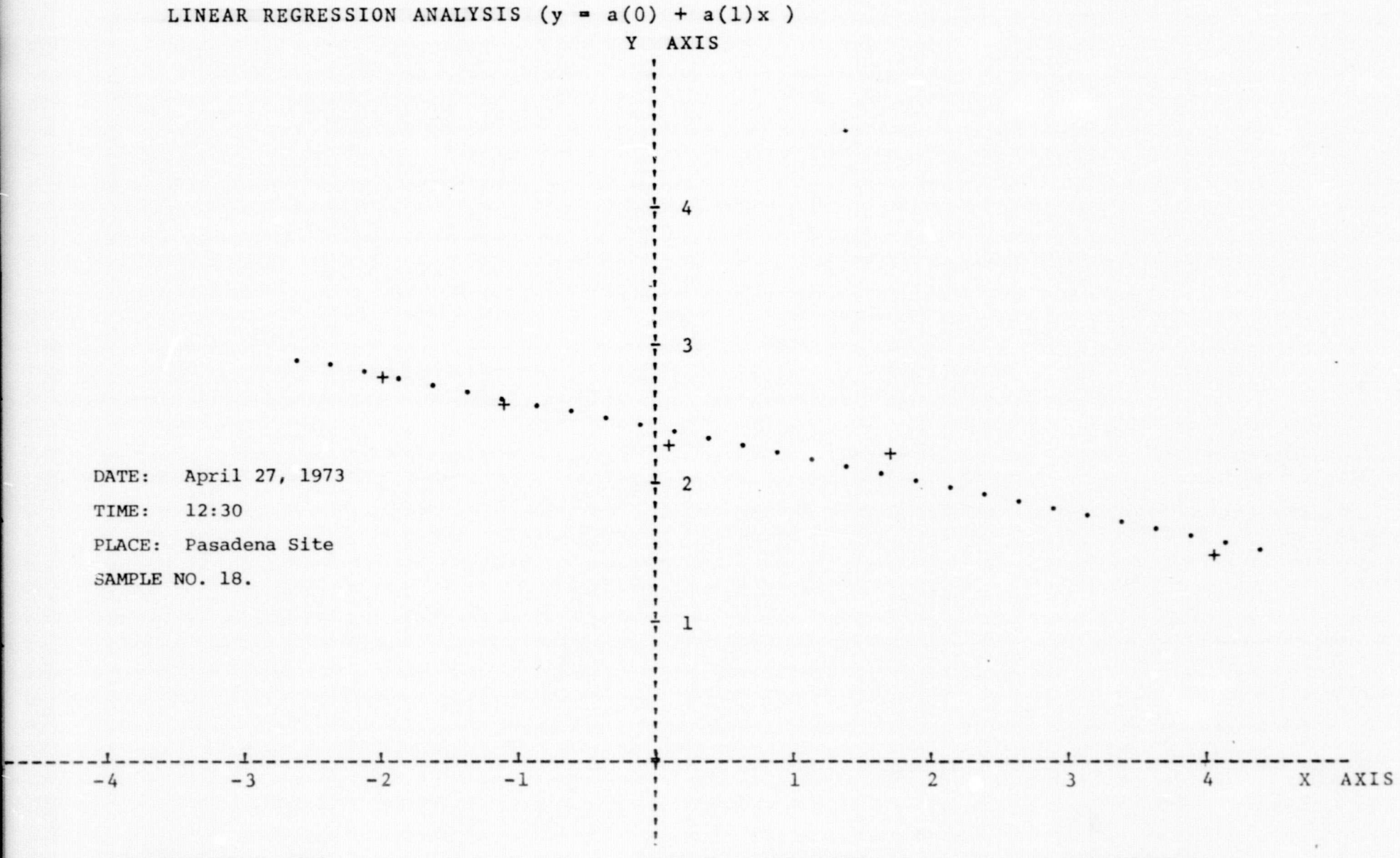

FIGURE . Particle Size Distribution

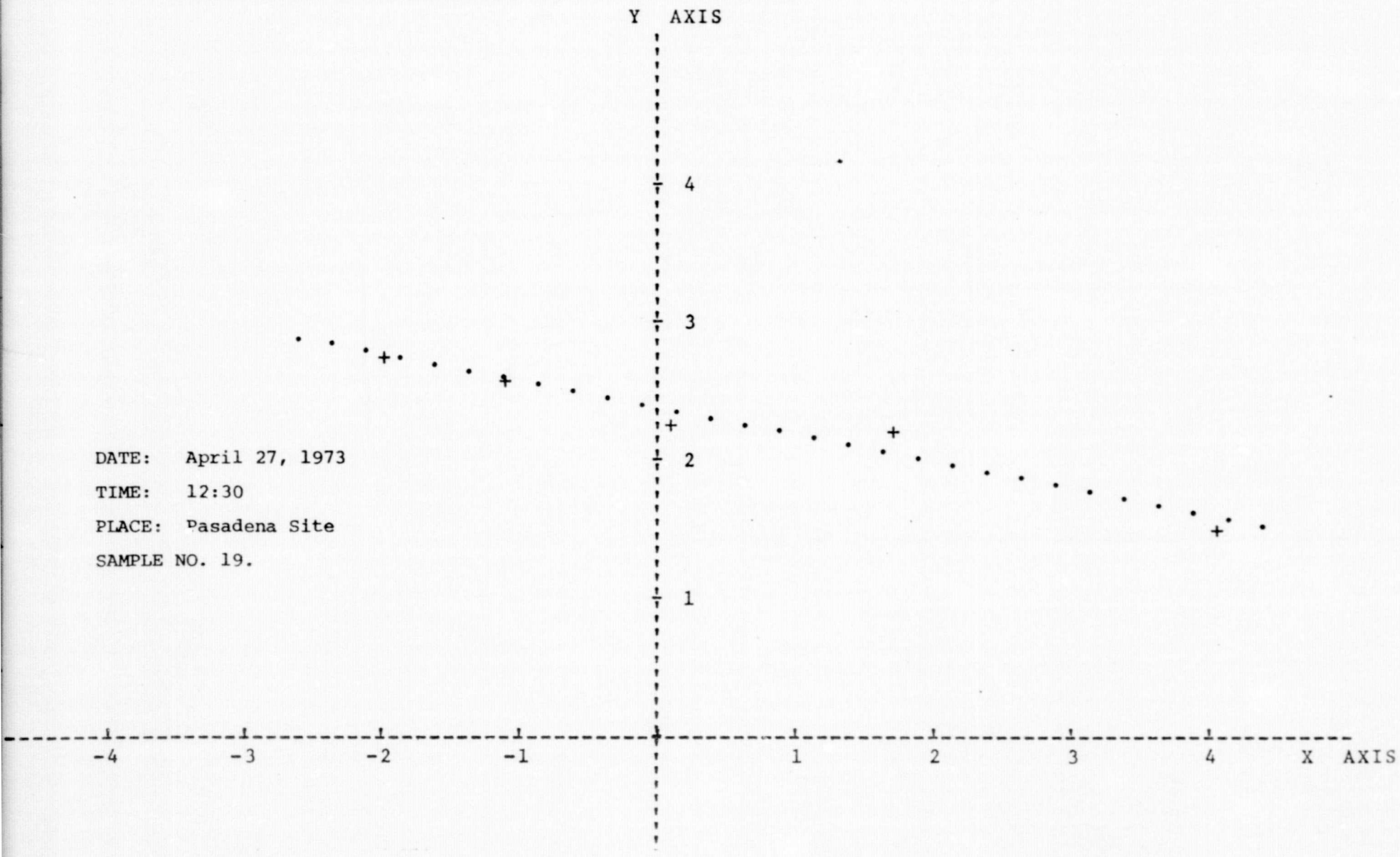

FIGURE . Particle Size Distribution

LINEAR REGRESSION ANALYSIS (y = a(0) + a(1)x)

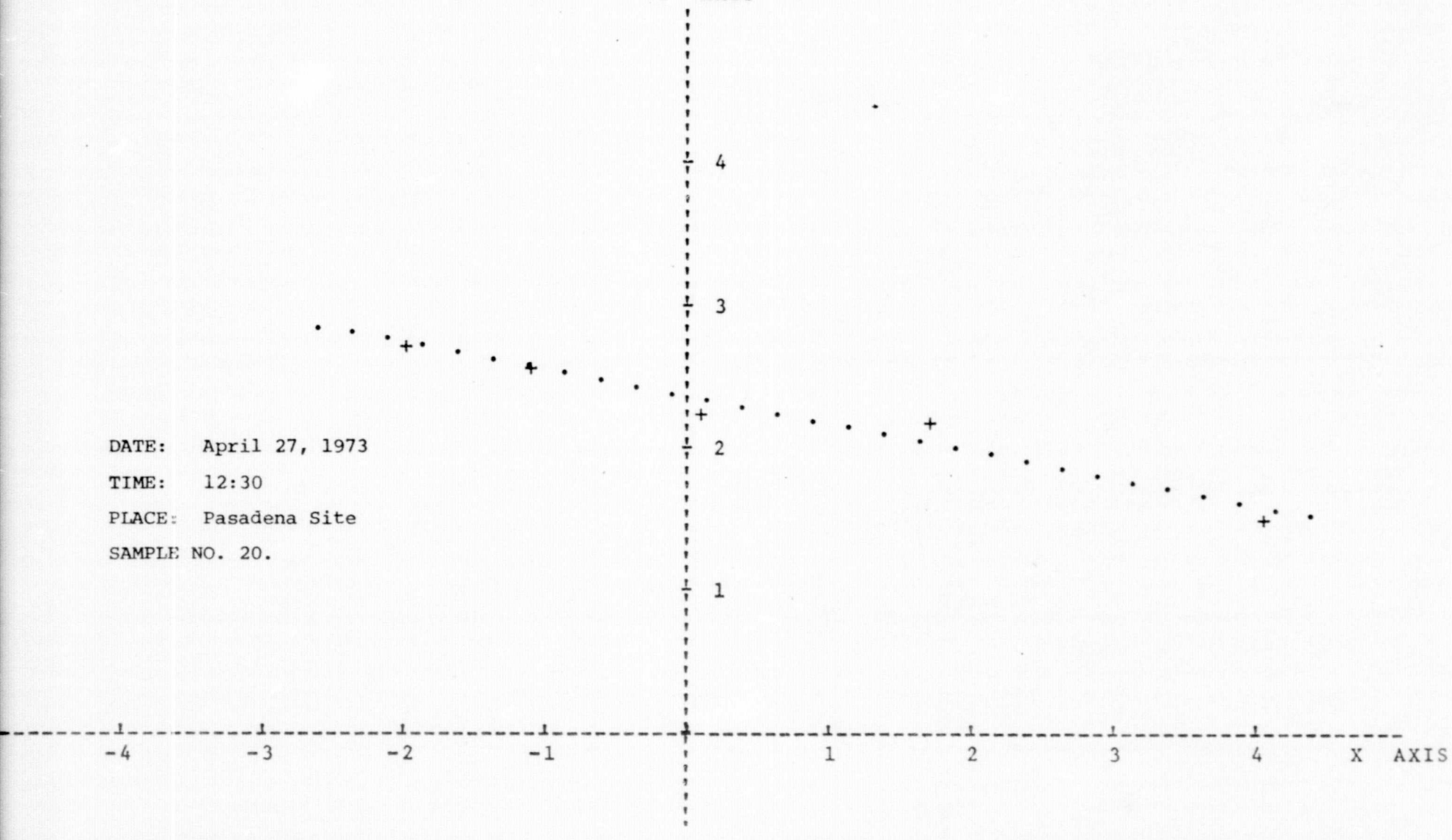

DATE: April 27, 1973

TIME: 12:30

PLACE: Pasadena Site

SAMPLE NO. 20.

4.675880215 = a(0)
-1.907227229 = a(1)
-.978724385 = r
.171890997 = S(x.y)

ONE X AXIS UNIT = .200000000
ONE Y AXIS UNIT = 2.000000000

FIGURE . Particle Size Distribution

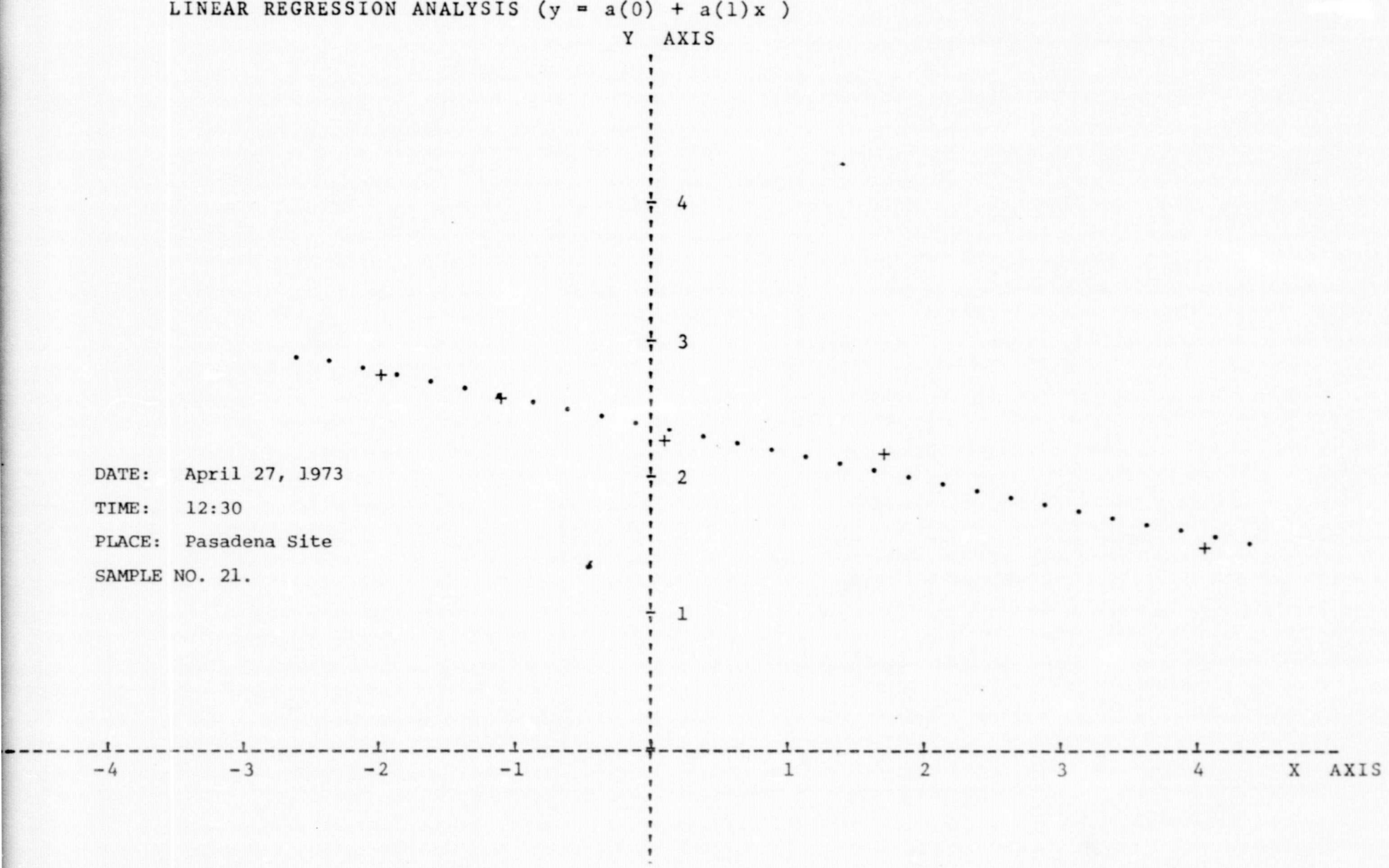

21

REFERENCES

1. AIHA Aerosol Technology Committee (1970). Guide for Respirable Mass Sampling, Amer. Industr. Hyg. Ass. J. 31:133-7.

2. Ahlquist, N.C., and R.J. Charlson (1968). Measurement of the Vertical and Horizontal Profile of Aerosol Concentrations in Urban Air with the Integrating Nephelometer, Environ. Sci. Tech. 2:363-6.

3. Ahlquist, N.C., and R.J. Charlson (1969). Measurement of Scatter, The Wavelength Dependence of Atmospheric Extinction, Atmos. Environ. 3:551-64.

4. Andersen, A.A. (1966). A Sampler for Respiratory Health Hazard Assessment, Amer. Industr. Hyg. Ass. J. 27:160.

5. Austin, Roswell W. (1964). Techniques of Measurement, Appl. Opt. 3(5):584-7.

6. Boilequ, Alerian R. (1964). Visibility: Atmospheric Properties, Appl. Opt. 5:570-81.

7. Buchen, W.E. and Charlson, R.J. (1968). Urban Haze; The Extent of Automotive Contribution, Science 159:192.

8. Bullrich, Kurt, Reiner Eiden, Ruprecht Jaenicke and Wolfram Nowak (1968). Solar Radiation Extinction, Sky Radiation, Sky Light Polarization and Aerosol Particle Total Number and Size Distribution on the Island Maui, Pure and Appl. Geophys. 69:280.

9. Cadle, Richard D. (1965). Particle Size, Reinhold Publishing Corp., New York.

10. Charlson, R.J. (1968). On the Generality of Correlation of Atmospheric Aerosol Mass Concentrations, Atmos. Environ. 2:455-64.

11. Charlson, R.J., H. Horvath and R.F. Pueschel (1967). The Direct Measurement of Atmospheric Light Scattering Coefficient for Studies of Visibility and Pollution, Atmos. Environ. 1:469-78.

12. Curcio, J.A. and G.L. Knestrick. (1958). Correlation of Atmospheric Transmission with Backscattering. J. Opt. Soc. Amer. 48(10):Oct.

13. Curcio, J.A., G.L. Knestrick and T.H. Cosden, (1958). Naval Res. Laboratory Report 5143.

14. Ettinger, H.J. and Royer, G.W. (1971). Particle Size, Visibility, and Mass Concentration in a Non-Urban Environment. Presented at the 64th Annual Meeting of the Air Pollution Control Assn., June, 1971.

15. Fenn, Robert W. (1966). Correlation Between Atmospheric Backscattering and Meteorological Visual Range, Appl. Opt. 5(2):Feb.

16. Garland, J.A. (1969). Condensation on Ammonium Sulphate Particles and Its Effect on Visibility, Atmos. Environ. 3:347-54.

17. Gordon, Jacqueline I. (1964). Optical Properties of Objects and Backgrounds, Appl. Opt. 3(5):556-62.

18. Gordon, Jacqueline I. (1964). Visual Search, Appl.Opt. 3(5):591-6.

19. Herman, B.M., S.R. Browning and R.J. Curran (1971). The Effect of Atmospheric Aerosols on Scattered Sunlight, J. Atmos. Scientist 28:419-28.

20. Horvath, Helmuth (1969). Visibility and light Scatter as a Measure for Air Pollution, Staub-Reinholt, Luft, 29:26-32.

21. Horvath, H. and Charlson, R.J. (1969). The Direct Optical Measurement of Atmospheric Air Pollution, AIHA J. 30:500-9.

22. Horvath, Robert, John G. Braithwaite, and F.C. Polcyn (1969). Effects of Atmospheric Path on Airborne Multispectral Sensors, NASA Report #1674-5-T. Institute of Science and Technology, The University of Michigan.

23. Hyzer, W.J. (1971). How Accurate Are Photographic Measurements? Res. Dev. 43-7, August.

24. Hyzer, W.J. (1971). Errors in the Data Reduction Process, Res. Dev. 75-8, October.

25. Junge, C. and E. McLaren (1971). Relationship of Cloud Nuclei Spectra to Aerosol Size Distribution and Composition. J. Atmos. Scientist 28:328-90.

26. Kattawar, G.W. and G.N. Plass (1967). Electromagnetic Scattering from Absorbing Spheres, Appl. Opt. 6:1377-.

27. Lee, Robert E. (1972). Size Distribution of Suspended Particulates in Air, Res. Dev. 18-21, June.

28. Ludwig, F.L. and Elmer Robinson (1970). Observations of Aerosols and Droplets in California Stratus. Tellus 22:94-105.

29. Lundgren, D.A. and Cooper, D.W. (1969). Effect of Humidity on Light-Scattering Methods of Measuring Particle Concentration, APCA J. 19:243-7.

30. Masaki, H. (1959). Apparent Colors of Natural Objects, Sci. Lt. Tokyo 8:67-86.

31. Masaki, H. (1960). Apparent Colors of Natural Objects, (II), Sci. Lt. Tokyo 9:39-54.

32. McClintock, Michael, T.A. Hariharan, Alden McLellan (1970). Studies on Techniques for Satellite Surveillance of Global Atmospheric Pollution. NAPCA Report #APTD-0672.

33. Meszaros, E. (1968). On the Size Distribution of Water Soluble Particles in the Atmosphere, Tellus 20:443-8.

34. Middleton, W.E.K. (1963). Vision Through the Atmosphere, Univ. of Toronto Press, Toronto.

35. Nalepka, R.F. (1970). Discrimination Techniques, Report #2264-12-F, The Inst. of Science and Technology, The Univ. of Michigan, p.188.

36. National Research Council. Committee on Remote Sensing (1970). Remote Sensing, Washington, D.C., National Academy of Sciences.

37. Noll, K.E., P.K. Mueller and M. Imada, (1968). Visibility and Aerosol Concentration in Urban Air. Atmos. Environ. 2:465-75.

38. O'Donnell, Hugh, T.L. Montgomery and M. Corn, (1970). Routine Assessment of the Particle Size-Weight Distribution of Urban Aerosols. Atmos. Environ. 4:1-7.

39. Preining, I. (1968). The Cross Sensitivities of the Royco Aerosol Photometer. PC 200, Staub 28:29-32.

40. Quenzel, H. (1970). Determination of Size Distribution of Atmospheric Aerosol Particles from Spectral Solar Radiation Measurements. J. Geophy. Res. 75:2915.

41. Rae, J.B. and J.A. Garland, (1970). A Stabilized Integrating Nephelometer for Visibility Studies, Atmos. Environ. 4:219-23.

42. Robinson, E. (1962). Effects of Air Pollution on Visibility, Air Pollution 1:220.

43. Steffens, C. (1949). Measurement of Visibility by Photographic Photometry, Ind. Eng. Chem. 41:2396.

44. Steffens, C., (1956). IN Air Pollution Handbook, P.L. Magill, F.R. Holden, and C. Ackley, eds., McGraw-Hill, New York.

45. Steffens, C. and Sylvan R. (1949). Visibility and Air Pollution Proceedings of the First National Air Pollution Symposium, Stanford Research Institute, Menlo Park, Calif., p. 103-9.

46. Taylor, John H. (1964). Use of Visual Performance Data in Visibility Prediction, Appl. Opt. 3(5):562-9.

47. Twomey, S. and H.B. Howell, (1965). The Relative Merit of White and Monochromatic Light for the Determination of Visibility by Backscattering Measurements, Appl. Opt. 4:501-6.

48. Van de Hulst, H.C. (1957). Light Scattering by Small Particles New York, Wiley, 470pp.

49. White, Carroll T. (1964). Ocular Behavior in Visual Search, Appl. Opt. 3(5):569-70.

50. Yamamoto, Ciichi and Masayuki Tanaka, (1969). Determination of Aerosol Size Distribution from Spectral Attenuation Measurements, Appl. Opt. 8:447.

51. Yates, H.W. (1970). A General Discussion of Remote Sensing of the Atmosphere, Appl. Opt. 9:1971-5.

52. Zuev, V.E. (1970). Atmospheric Transparency in the Visible and the Infrared, Israel Scientific Translation, 215p.

GLOSSARY

J, J_o = light intensities (luminous flux) before and after

x = path length

b = overall extinction coefficient

b_a^a = absorption coefficient of the aerosol

b_s^a = scattering coefficient of the aerosol

b_a^g = absorption coefficient of the gas medium

b_s^g = scattering coefficient of the gas medium

Q = decrease in luminous flux/flux incident upon particle cross-section

λ = light wavelength

r = particle radius

m = refractive index of the particle

α = cross section/wavelength, or $2\pi r/\lambda$

c = contrast

I_b = Intensity of the background luminosity

I_o = Intensity of the object (target) luminosity

E = contrast threshold, about 0.02 for people

H_o = original incident light flux

dB = amount of scattered light in volume between target or object and observer, (τ)

B_H = Brightness of the horizon (Intensity of luminous flux from the direction of the horizon)

B_o = Brightness of a black body ($B_o=0$ at $x=0$)

γ = the film constant

$C(0)$ = inherent contrast at $x=0$ when $B_o \neq 0$.

$n(r)$ = number of particles of radius r

q = a characteristic constant of the power distribution function

τ = intensity from the direction of the white object $\tau_o=I_o=J_o$

L_x = equivalent attenuation length

C_r = apparent contrast at distance x

L_v = meteorological range

M = Mass of particulates, μgm^{-3}

B = function of α and the optical properties of particles

V = visibility

X = vertical optical depth of the atmosphere

m(r) = scattering efficiency for light of wavelength λ

P(r) = density of the aerosol of radius r

r = radius of the aerosol

V = volume of the aerosol